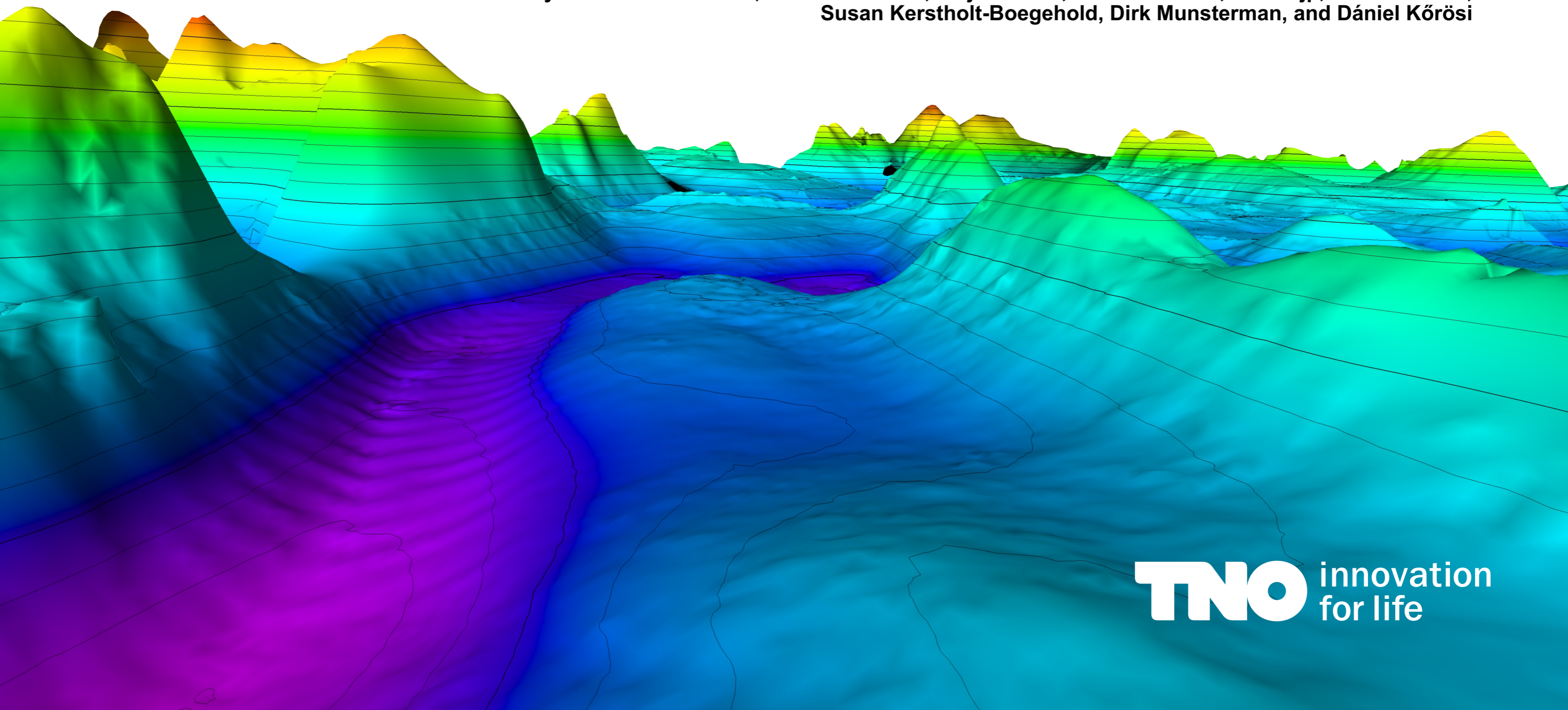# ComMa Project

Understanding Jurassic Sands of the Complex Margins of the Eastern Part of the Terschelling Basin during the Upper Jurassic and Lowermost Cretaceous

by Renaud Bouroullec, Roel Verreussel, Thijs Boxem, Geert de Bruin, Mart Zijp, Nico Janssen, Susan Kerstholt-Boegehold, Dirk Munsterman, and Dániel Kőrösi

TNO innovation for life

COMMA Project

Understanding Jurassic Sands of the Complex Margins of the eastern part of the Terschelling Basin during the Upper Jurassic and Lowermost Cretaceous

30.11.2016

Renaud Bouroullec, Roel Verreussel, Thijs Boxem, Geert de Bruin, Mart Zijp, Susan Kerstholt-Boegehold, Nico Janssen, Dirk Munsterman, Pantelis Karamitopoulos and Stefan Peeters

In the COMMA Project we investigated the Upper Jurassic and Lower Cretaceous in the Terschelling Basin located in the Dutch offshore. The main aim of the project is to provide new insights on the regional and local stratigraphic, depositional and syn-depositional settings within the basin, with a special focus on the margins of the basin where poorly understood sand accumulations may be present.

Despite having numerous known reservoirs, the Upper Jurassic and Lower Cretaceous stratigraphic interval still holds key remaining questions regarding its depositional environments and the preservation of sandy strata. The correlation of these strata across the basin, and locally on the neighboring platforms, requires new analysis and insights that this project offers. The study area encompasses three main structural provinces, 1) the Terschelling Basin, 2) its surrounding platforms (the Schill Grund Platform to the north; the Ameland Block to the west; and the Friesland Platform to the south) and 3) the Dutch Central Graben to the west.

The main stratigraphic interval of interest is the Upper Jurassic and Lower Cretaceous, which is divided into three sequences (Sequences 1, 2 and 3) that contain sand-rich reservoir intervals such as the Lower, Middle and Upper Graben Formations, the Friese Front Formation, the Terschelling Sandstone Member and the Scruff Greensand Formation. In the Terschelling Basin the main reservoir intervals present are the latter two that are part of Sequence 2 (for the Terschelling Sandstone Member) and Sequence 3 (for the Scruff Greensand Formation). Note that a third sandy interval, the Noordvaarder Member, is also observed in the northern part of the Terschelling Basin in Sequence 2.

This project includes biostratigraphic, stratigraphic and structural analysis of subsurface data including cores, cuttings, wireline logs and seismic data. The project started in December 2015 and lasted until November 2016. The present report summarizes and compiles the results obtained by the TNO Basin Analysis Team. It describes the multidisciplinary approach that was used to analyze the complex interplays between the depositional systems, active structures and paleotopographic reliefs.

1) The palynological analysis gave new constrain to better understand the depositional environments and the climatic variations during the Late Jurassic-Early Cretaceous in the study area. These new palynological analyses help refining the chronostratigraphic controls of the sediments encountered at the locations of thirteen wells. These results were extremely valuable in constraining the regional stratigraphic correlations within such structurally complex basins that were affected by various tectonic events and growth structures (salt diapirs and active faults).

2) The tectonic analysis was carried out using 2D and 3D seismic analysis. Four seismic horizons where interpreted in the Terschelling basin as well as faults and salt structures (pillows, roller, diapirs, walls and welds). Isochore maps were produced to better understand the growth stratigraphy and the timing of active structures. Particular attention was given to the basin margins, the transitional zones between the Basin and its surrounding platforms.

3) The stratigraphic correlation of key surfaces and intervals (including the new biostratigraphic results) was achieved by correlating numerous wells along regional transects that were also used for regional seismic transects analysis. This combined approach allows to better constrain the structural and paleotopographic variabilities between wells. This approach permits a robust stratigraphic analysis that includes seismically-controlled regional and local unconformities, that were often previously missed or underestimated, as well as better constrain on the complex interplays between active structures (salt bodies and faults) and syn-tectonically influenced depositional systems.

The results obtained from the combination and integration of these various analytical techniques are used to produce a new stratigraphic, tectono-stratigraphic and paleogeographic models for the Upper Jurassic and Lower Cretaceous in the Terschelling Basin. This project strongly improved the understanding of the Upper Jurassic and Lower Cretaceous in the Terschelling Basin by providing a calibrated tectono-stratigraphic framework based on modern concepts of sequence stratigraphy and syn-depositional tectonic models. The use of regional seismic and well correlation panels helped to better constrain the main depositional systems (Terschelling Sandstone Member, Noordvaarder Member and Scruff Greensand Formation) identified in the study area as well as their varying preservation potential within and outside the Basin. The new paleogeographic maps give a clear picture of the paleo-coastlines trajectories, their changes through time and the interplay between multiple sediment sources and depositional systems.

1

Content

Recommendations on reading and accessing information in this report:

1) The report is built in a graphically heaving format with some figures that, locally, display small fonts and graphic details, For full appreciation of these graphics we recommend to use the digital version of this report in which the high resolution graphics are preserved and accessible.

2) There is a lot of cross referencing between chapters to avoid repetitions of figures and the reader will require to often turn few pages back and forth to follow some of the discussions.

3) The detailed core interpretation as well as the compiled seismic and correlation panels are displayed as single pages in the Appendices. These documents may be printed as stand alone A0 format posters.

1

INTRODUCTION

1.1 Research goals

- To better understand and predict the distribution and stratigraphic architecture of Upper Jurassic to Lower Cretaceous reservoir sands in the Terschelling basin (TB)
- To decrease uncertainties related to the occurrence and spatial distribution (lateral and vertical trends) of these sandstones as well as their preservation potential in the basin axis and along the basin margins.
- To build stratigraphic and tectono-stratigraphic and paleogeographic models based on new biostratigraphic, lithofacies, sequence stratigraphic and structural information.

1.2 Objectives

The main objective of this project is to build a new stratigraphic framework for the Upper Jurassic and Lower Cretaceous in the TB by:

- obtaining new time lines from palynological information to better constrained the local and regional correlation between wells,
- analyzing the structural framework of the basin and its surrounding platforms by seismically characterizing the salt structures, syn-depositional faults and basin margins, and
- correlating key stratigraphic intervals throughout the study area using standard well correlation techniques combined with seismic interpretation along the same sections.

This project, in opposite to its predecessor (FOCUS Project, Bouroullec et al., 2016) does include substantive seismic mapping with time structure maps and isochore maps complied. No attribute mapping was carried out in this project but will be used in a upcoming follow up project (MAXIM Project, TNO, 2017).

1.3 Study area

The study area includes focuses on the TB but several surrounding areas are also investigated (Fig. 1.1), including:

- the southeastern part of the Dutch Central Graben (DCG): blocks F15, F18, L02 and L05;
- the Schill Grund High (SGH): blocks G10, G11, G13, G14, G16, G17;
- the western part of the Ameland Block (AB): blocks M05, M07 and M08;
- the Friesland Platform (FP): blocks M07, M10, L08, L09 and L12;
- the northern part of the Vilelannd Basin (VB): Block L12 and L15)

1.4 Stratigraphic interval of interest

Three sandy stratigraphic intervals were originally proposed as main investigation targets for this project (see Fig. 1.2):
:

- Late Jurassic Terschelling Sandstone Mb: Early Tithonian (or Early/Middle Volgian) in age. Aggradational, barrier sandstones, parallel to the palaeo-shore lines.
- Late Jurassic Noordvaarder Mb: Early Tithonian (or Early/Middle Volgian) in age. Shallow marine sand-rich deposits.
- Late Jurassic/Early Cretaceous Scruff Greensand Fm./ Scruff Spiculite Mb.: Late Tithonian to Berriasian (Middle Volgian to Ryazanian) in age. Aggradational, shoreface, wide spread distribution.

These intervals are part of stratigraphic sequences studied in Munsterman et al. (2012) and Bouroullec et al., (2116) which set the stage for the present project. Each one of these sequences were deposited within a different stage of the basin's evolution (Verreussel et al., in prep).The project focuses on these three sandy intervals but also extends to all stratigraphic units (of the Upper Jurassic to Lower Cretaceous in the study area.
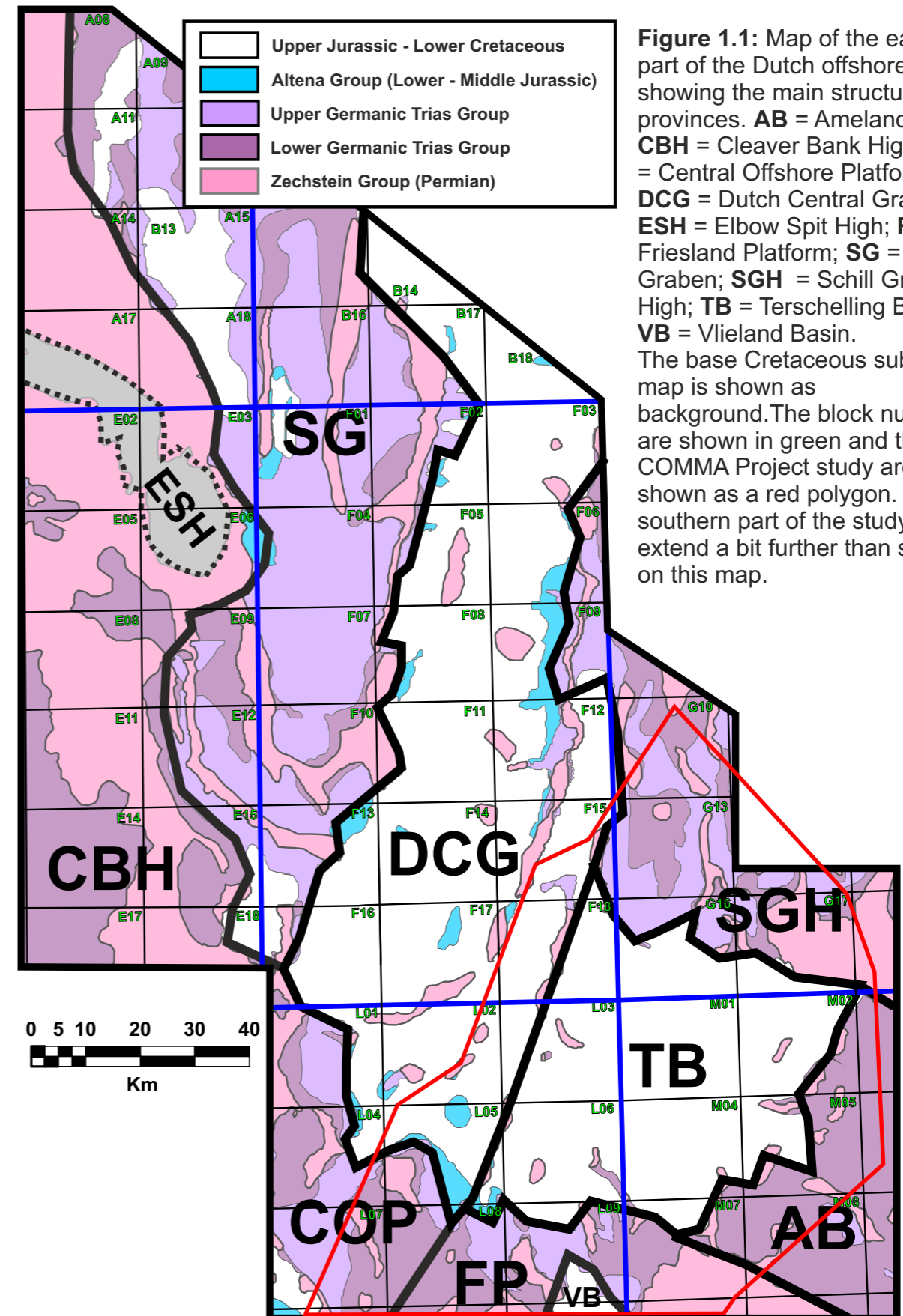
Figure 1.1: Map of the eastern part of the Dutch offshore showing the main structural provinces. **AB** = Ameland Block; **CBH** = Cleaver Bank High; **COP** = Central Offshore Platform; **DCG** = Dutch Central Graben; **ESH** = Elbow Spit High; **FP** = Friesland Platform; **SG** = Step Graben; **SGH** = Schill Grund High; **TB** = Terschelling Basin; **VB** = Vlieland Basin. The base Cretaceous subcrop map is shown as background.The block numbers are shown in green and the COMMA Project study area is shown as a red polygon. The southern part of the study area extend a bit further than shown on this map.

Legend:
- Upper Jurassic - Lower Cretaceous
- Altena Group (Lower - Middle Jurassic)
- Upper Germanic Trias Group
- Lower Germanic Trias Group
- Zechstein Group (Permian)

0 5 10 20 30 40 Km

Figure 1.2: Stratigraphic framework of the uppermost Middle Jurassic - Lower Cretaceous in the Terschelling Basin, Dutch Central Graben and Step Graben in the Dutch offshore.
The sand-rich intervals are shown as yellow polygons, with dark yellow polygons for regional depositional systems and light yellow for locally derived depositional systems (e.g. Noordvaarder Mb.). Fluvial, delta plain and esturarine/lagoonal claystones are shown in green. Marine claystones are shown in blue. Unconformities are shown as red lines and maximum flooding surfaces as blue lines. The three Middle Graben Formation coals are shown as three black lines. Densiplicatum Climate Shift shown as a light blue line. Dash black line show the lithostratigraphic limits if some of the upper Sequence 1 formations. Sandy units A-E refer to five sandy units in the Friese Front Fm. in the L02, F18, F17 and B14 areas. From Bouroullec et al. (2016)
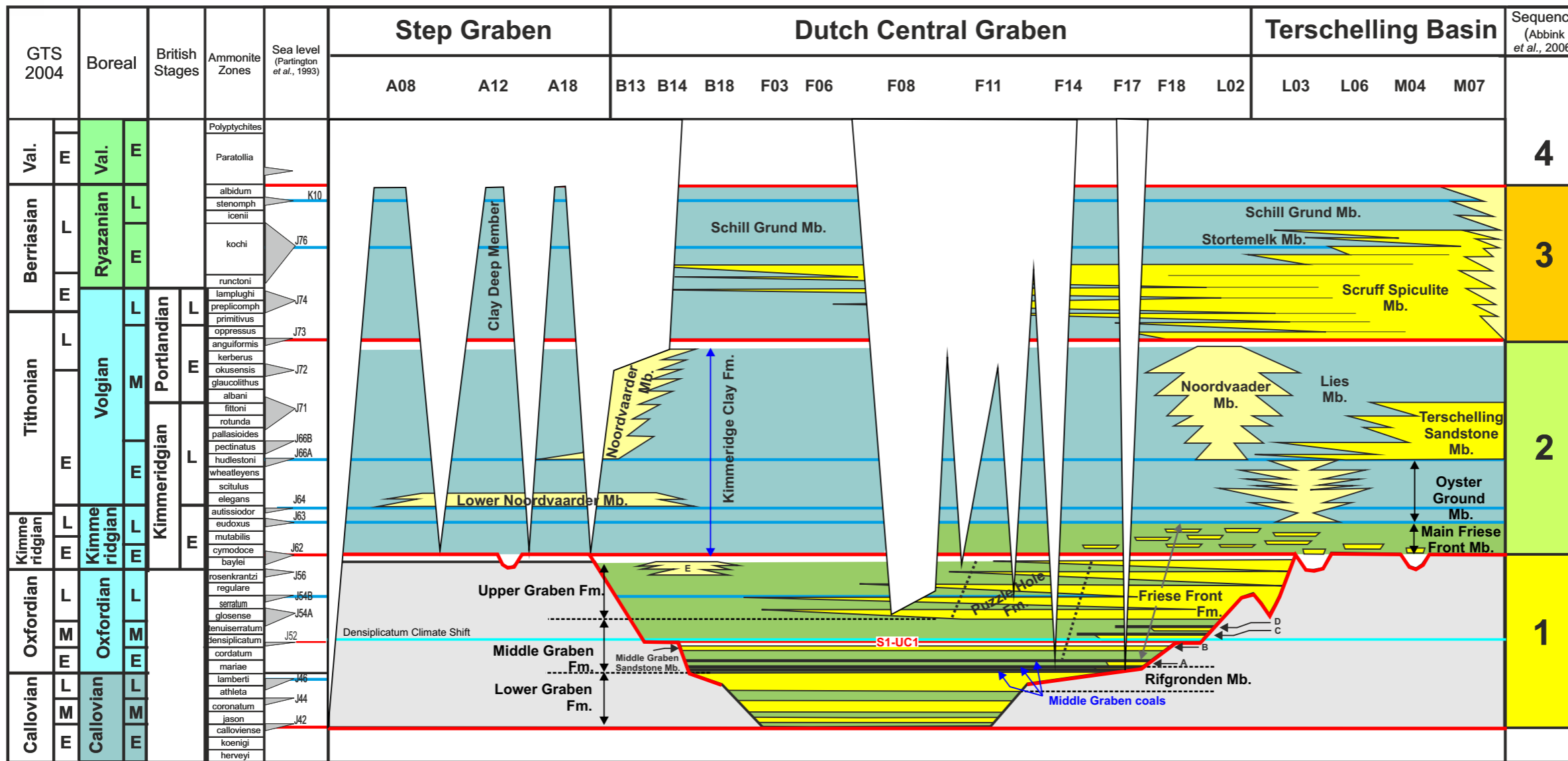
1.5   Project core research team

Renaud Bouroullec	Senior Geologist (TNO)	Lead Scientist: Seismic interpretation, stratigraphic correlation, structural analysis and final integretation
Roel Verreussel	Senior Geologist (TNO)	Biostratigraphy, stratigraphic correlation and final integration
Thijs Boxem	Geologist (TNO)	Project Manager
Geert de Bruin	Geologist (TNO)	Seismic interpretation
Mart Zijp	Geologist (TNO)	Seismic interpretation
Susan Kerstholt-Boegehold	Analyst (TNO)	Biostratigraphic interpretation
Nico Janssen	Analyst (TNO)	Rock sample processing
Dirk Munsterman	Senior Geologist (TNO)	Biostratigraphic interpretation
Pantelis Karamitopoulos	Junior Geologist (TNO)	Seismic interpretation
Dániel Kőrösi	MSc. student (Utrecht Uni.)	Internship project at TNO linked to this project (Appendix A4 for manuscript)

1.6   Acknowledgments

8

2

GEOLOGICAL SETTING

The geological setting of the study area is complex since it involves several extensional, compressional and strike-slip deformation phases during the Meso-Cenozoic (Figure 2.1). The deposition settings encountered in the Upper Jurassic and Lower Cretaceous interval vary greatly and include continental, shallow marine to open marine depositional systems that are studied in the present project.

In this chapter we summarize key published geological information regarding the Mesozoic tectonic evolution and stratigraphy. The third part of this chapter summarizes the existing stratigraphic information of three sequences deposited within the study area during the Upper Jurassic and Lower Cretaceous.

2.1 Overview of the tectonic evolution of the study area and greater North Sea Region during the Mesozoic

The Mesozoic tectonic evolution of the studied part of the Dutch offshore has been summarized in several publications (Herngreen and Wong, 1989; van Adrichem *et al.,* 1997; de Jager, 2007; Geluk, 2007; Wong, 2007; Rosendaal *et al.*, 2014). It is important to place this tectonic evolution into a larger regional west-european context and various key publications are instrumental in that respect (e.g. the extensive work of Ziegler; the Millennium and Southern Permian Basin atlases).

During the Triassic and Jurassic the structural setting of the Netherlands changed from a single extensional basinal configuration (the Southern Permian Basin) to a series of smaller, fault-bounded basins and highs (De Jager, 2007). Two main tectonic events shaped the North Sea Basin during the Mesozoic: 1) the break-up of Pangea and the associated rifting during most of the Mesozoic, and 2) the closure of the Tethys Ocean/Alpine collision and the associated inversion tectonics during the late Mesozoic (culminating later during the Cenozoic).

A brief summary of the tectonic activity during the Mesozoic is presented below, with information regarding the overall North Sea region as well as specific information regarding the study area.

A) Early Triassic

The start of rifting during the Early Triassic was related to the break-up of Pangea in the proto-Atlantic between Greenland and the Fennoscandia High (Lott *et al.*, 2010). The southward propagation of the rift system toward the North Sea can be traced down into the northern part of the study area, breaching the Mid North Sea–Ringkøbing-Fyn High, with more prominent extensional faulting in the Northern part of the North Sea than in the study area (Zeigler, 1990b; Roberts *et al.,* 1995; Coward *et al.*, 2003).

Farther south, into the study area as well as in the North German Basin, the subsidence (mainly thermal in origin) was uniform, with Buntsandstein and Muschelkalk reflectors apparently unaffected by syn-depositional faulting (Ziegler, 1990a; Hoffmann & Stiewe, 1994; Geluk, 2007). The Dutch Central Graben subsided faster during the Bundsandstein depositional cycle than the platform areas (Terschelling and Vlieland basins) but not as rapidly as the Horn and Glückstadt Grabens farther to the east.

B) Middle Triassic

In response to continued thermal subsidence, the Muschelkalk strata were deposited over a wider area than the Bundsandstein series and onlap onto paleo-highs such as the London-Brabant and Bohemian massifs (Pharaoh *et al.,* 2010). Differential subsidence of the Central, Horn and Glückstadt grabens is reflected in synsedimentary faulting and increased thicknesses of Muschelkalk strata compared to areas outside the grabens (Geluk, 2005 and 2007).

Triassic sequences thicken into the newly-formed Dutch Central Graben and Broad Fourteens Basin (Fig. 2.2). The Zechstein salt was mobilized at this time with piercing salt domes and rim-synclines developing in later stages (De Jager, 2007).
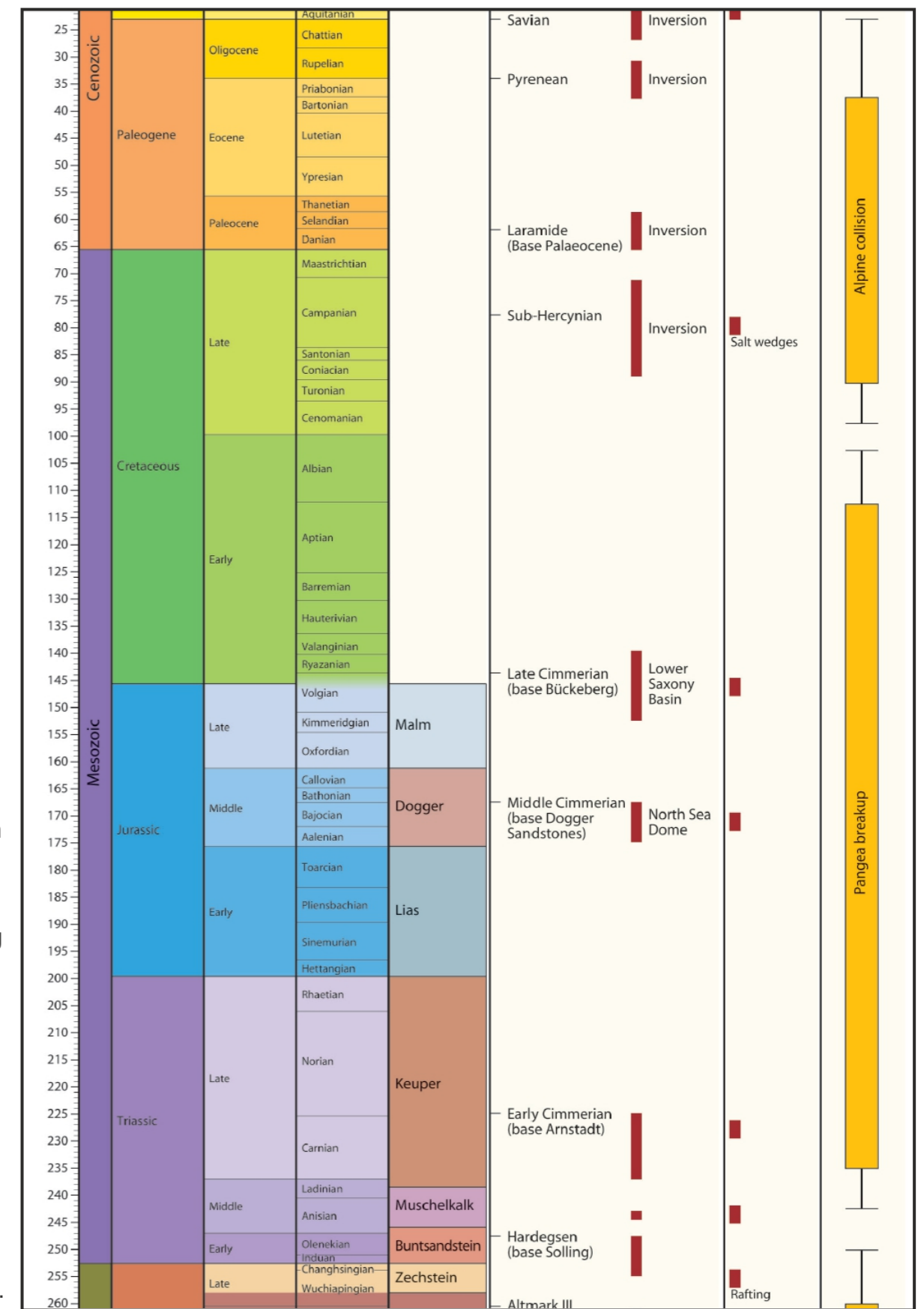

Figure 2.1: Main tectonic episodes and halokinetic episodes during the Mesozoic and Paleogene in the Southern Permian Basin (Pharaoh *et al.*, 2010).

C) Late Triassic

The North Atlantic rift system propagated southward into the Central Atlantic area (Fig. 2.2). Contemporaneous, uplift of the flanks of the rift is indicated by the increased clastic influx into the Southern Permian Basin from northern sources (Ziegler, 1988 and 1990a). In response to continued counter-clockwise rotation of Pangea, the Souther Permian Basin moved to latitudes of 30 to 40 degree N by Late Triassic times. In the Southern North Sea, the direction of extension was E-W during the Late Triassic (Pharaoh et al. 2010). The North Sea, Horn and Glückstadt grabens remained active during this period, with very minor associated volcanic activity (Ziegler, 1990a).

Stratigraphic sequences deposited during this period thicken northwards into the Dutch Central Graben and Broad Fourteens Basins, the only regions with active faulting. The faults affecting the Upper Triassic were produced by dextral transtension (Van Hoorn, 1987).The increased sediment loading upon the thick Zechstein salt in the northern Dutch offshore sector, triggered piercing of salt diapirs and the development of rim-synclines (Pharaoh et al., 2010). It is important to notice that some salt structures extruded onto the basin floor to form large allochthonous overhangs onlapped by uppermost Triassic deposits (Krzywiec, 2004).

D) Early Jurassic

The North Atlantic rift propagated southwards into the Central Atlantic, with crustal separation achieved toward the end of the Early Jurassic. There seems to have been very little Early Jurassic rifting in the northern North Sea. The palaeogeography indicates infilling of the passively subsiding Triassic–Lower Jurassic rift (Coward et al., 2003). Continued regional thermal subsidence of the Northern and Southern Permian basins during the Rhaetian and Hettangian, combined with a eustatic sea-level rise, controlled the development of a wide, open-marine basin. Clastics were shed into this broad, regionally subsiding basin from the Fennoscandian Shield, East European Platform and Bohemian Massif. Stagnant-water stratification led to the deposition of the Posidonia Shale Formation during the Toarcian, the principal source rock for the oil provinces of the southern North Sea and northern Germany (Ziegler, 1990a).

The Lower Jurassic series was later deeply truncated in the central North Sea during Mid- to Late Jurassic times. Nevertheless, it appears that the Early Jurassic was a period of relative tectonic quiescence, with faulting largely restricted to the Dutch Central Graben and locally to the Broad Fourteens Basin. The Cleaver Bank and Schill Grund Highs remained stable areas during much of the Early Jurassic and probably accumulated sediments hundreds of metres thick (Pharaoh et al., 2010).

E) Middle Jurassic

The most important event during this period is the uplift of the central North Sea area that started towards the end of the Aalenian, presumably in response to the impingement of a transient mantle plume on the lithosphere, which continued during the Bajocian and Bathonian (Ziegler, 1990a; Underhill & Partington, 1993; Surlyk & Ineson, 2003). Development of this large thermal dome (700 × 1000 km), caused deep truncation of Lower Jurassic and even Triassic sediments and the development of the regional Mid Cimmerian Unconformity (also referred as the Intra-Aalenian Unconformity by Underhill and Partington,1993) in the central North Sea area (Fig. 2.3). This regional uplift closed the existing seaway, separating the Arctic Seas from the Tethys and Atlantic Oceans (Ziegler,1988 and 1990a). Crustal extension across the North Sea rift system persisted during the uplift of this thermal dome as shown by continued fault-controlled subsidence of the Viking Graben, the subsidence of deep half-grabens containing continental series in the Central Graben, and continued tectonic activity in the array of transtensional basins along the southern margin of the Southern Permian Basin (Ziegler, 1990a). Three major rift systems were active in the Netherlands during Mid to Late Jurassic (Figures 2.4 and 2.5): 1) the N-S oriented Dutch Central Graben-Vlieland Basin system, 2) the E-W oriented Lower Saxony Basin system, and 3) the NW-SE oriented Ruhr Valley Graben, West and Central Netherlands Basins, and Broad Fourteens Basin (extending to the UK to the Sole Pit Basin).

By late Mid-Jurassic times, the Central North Sea Dome had subsided sufficiently for open-marine conditions to be restored in the North Sea. Sedimentation resumed variably during the Callovian or Late Jurassic in areas uplifted during Mid-Jurassic times (Ziegler 1990a).

It is important to notice that the London-Brabant Massif was also uplifted during Mid-Jurassic times, its Triassic and Upper Paleozoic cover was removed to expose the Lower Carboniferous core. Fission-track data suggest that a thickness of 3000 m of sediments was removed (Van den Haute & Vercoutere, 1990).

BCB Bristol Channel Basin
EISB East Irish Sea Basin
JB Jeanne d'Arc Basin
LB Lusitania Basin
MNH Mid North Sea High
RFH Rinkøbing-Fyn High
TEL Trans-European Lineament
WeB Wessex Basin
WSB West Shetland Basin

Diagram a
- Shallow-marine shales
- Shelf carbonates and shales
- Shelf carbonates
- Coastal-margin deposits
- Nonmarine sediments
- Emergent area
- Volcanics
- Feather edge
- Normal fault
- Caledonian basement structure

Diagrams b and c
- Oceanic crust
- Continental crust
- Mountain belt related to plate convergence
- Muschelkalk salts
- Keuper salts
- Bunter salt
- Zechstein salt
- Edge of Permian basins
- Salt diapirs
- Triassic marine incursion direction
- Permian marine incursion direction
- Relative plate movement
- Spreading ridge
- Subduction zone
- Normal fault
- C Cimmerian mountain belt
- SEF South-East France Basin

Figure 2.2: Triassic times in the North Sea Region. a) Palinspastic maps. b) Global views. c) Distribution of the basins and structures. From Coward et al., 2003.

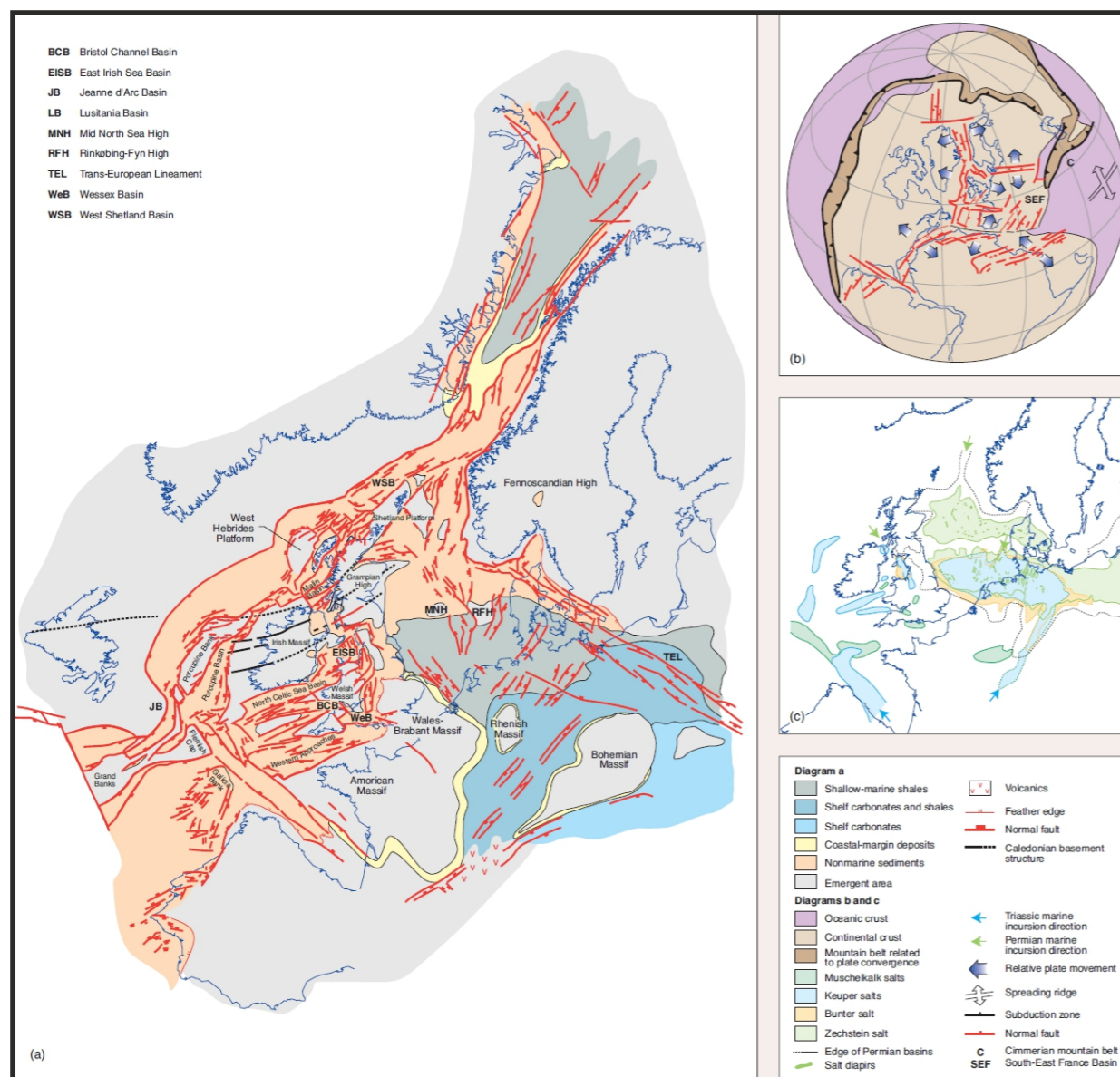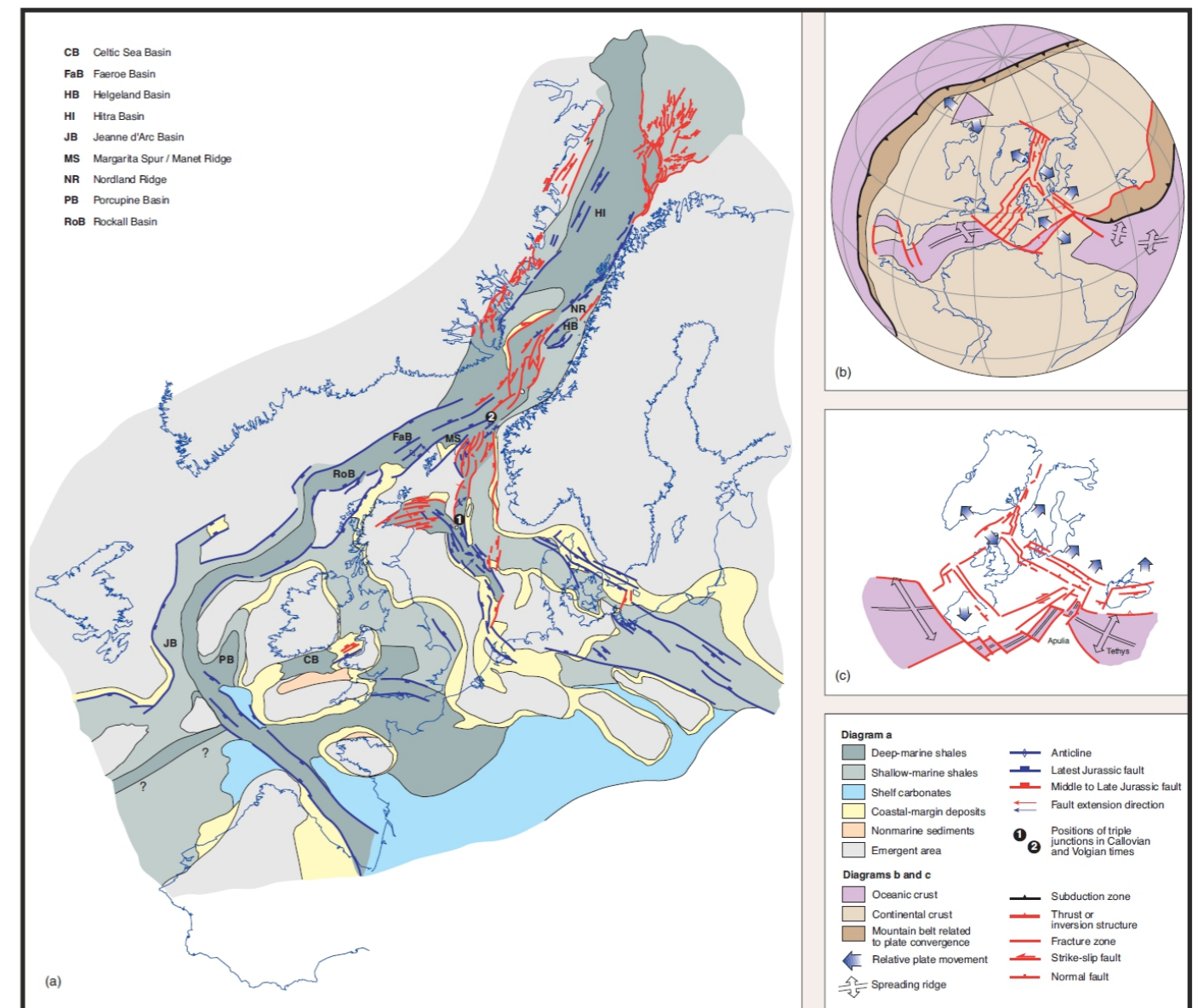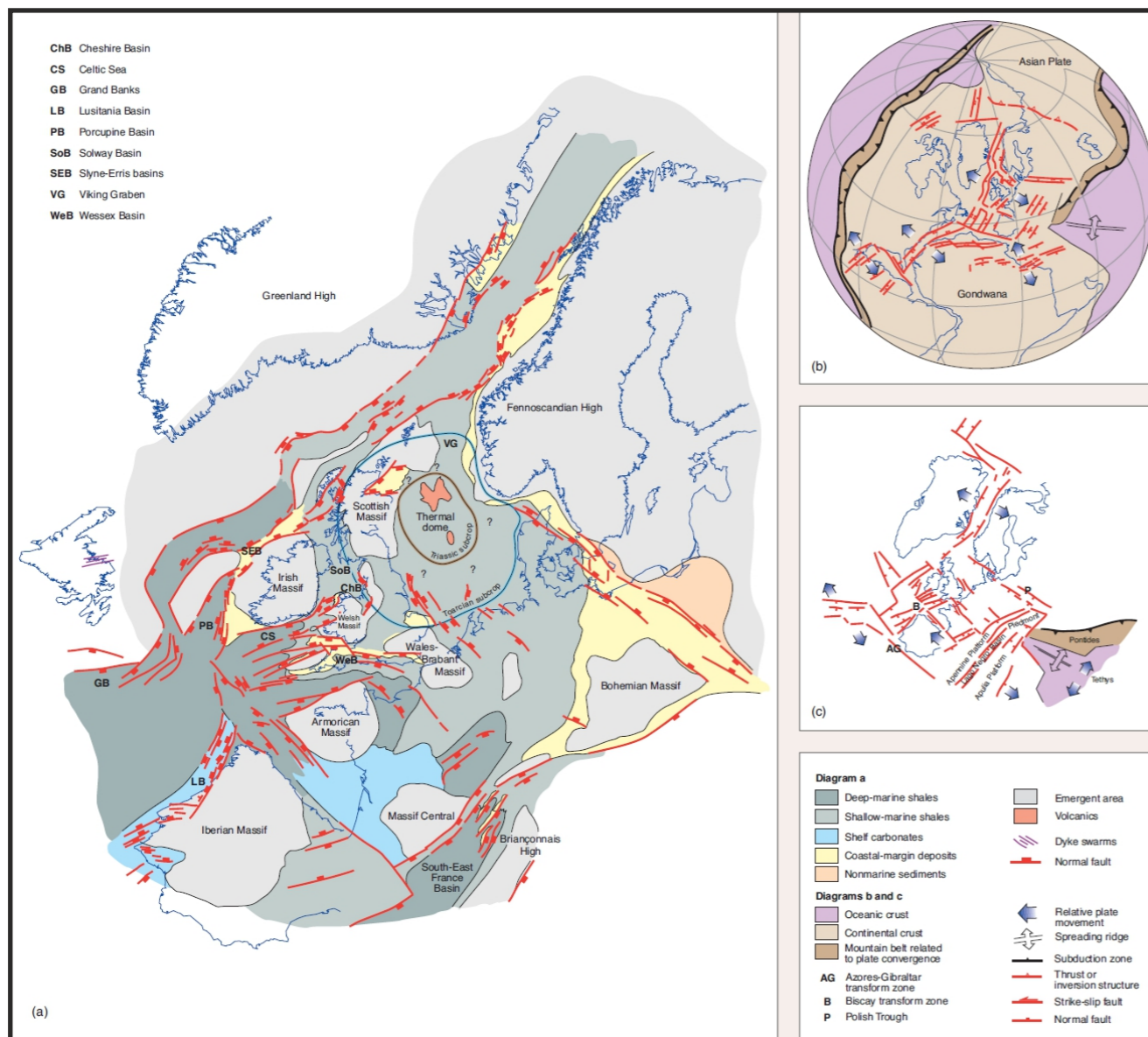**Figure 2.3:** Mid-Jurassic times in the North Sea Region. a) Palinspastic maps. b) Global views. c) Distribution of the basins and structures. From Coward *et al.*, 2003.

Figure 2.4: Late Jurassic times in the North Sea Region. a) Palinspastic maps. b) Global views. c) Distribution of the basins and main structures. From Coward *et al.*, 2003.

F) Late Jurassic to Early Cretaceous

Accelerated crustal extension across the North Sea rift system resulting in NW trending transtensional basins to form along the southern margin of the Southern Permian Basin (Figures 2.4, 2.5 and 2.6). This rifting phase allowed large areas to be exposed and subsequently eroded. During the Late Jurassic and Early Cretaceous transtensional subsidence occurred within northwest-oriented basins but also transpressional uplift of narrow highs along the southern margin of the Southern Permian Basin. The main tectonic elements of the Dutch sub-surface developed during the Late Jurassic and Early Cretaceous, comprising the late Cimmerian rift pulses. Extensional faulting and subsidence accelerated in the northerly trending Dutch Central Graben (Heybroek, 1975; Schroot, 1991).

A eustatic sea-level lowstand at the Jurassic-Cretaceous transition, combined with stress-induced deflection of the lithosphere, led to earliest Cretaceous emergence and erosion of large parts of western and central Europe (Ziegler, 1990a). Crustal extension across the North Sea graben system gradually decreased during the Early Cretaceous and essentially ended during the Aptian to Albian (Ziegler, 1990a; Torsvik *et al.*, 2002; Coward *et al.*, 2003).

In the Dutch sector, thick fluviolacustrine to shallow-marine sequences accumulated in the Dutch Central Graben during Late Jurassic and Early Cretaceous times. Volgian to Ryazanian shales are kerogenous in the northern Dutch Central Graben (Herngreen & Wong, 1989). In the southern part of the graben, the provenance of clastic sediments was the Cleaver Bank-Broad Fourteens High, which was uplifted during Callovian times. Adjacent highs such as the Friesland Platform were uplifted and eroded at the same time. The Schill Grund High formed a stable platform area on the eastern flank of the Dutch Central Graben.
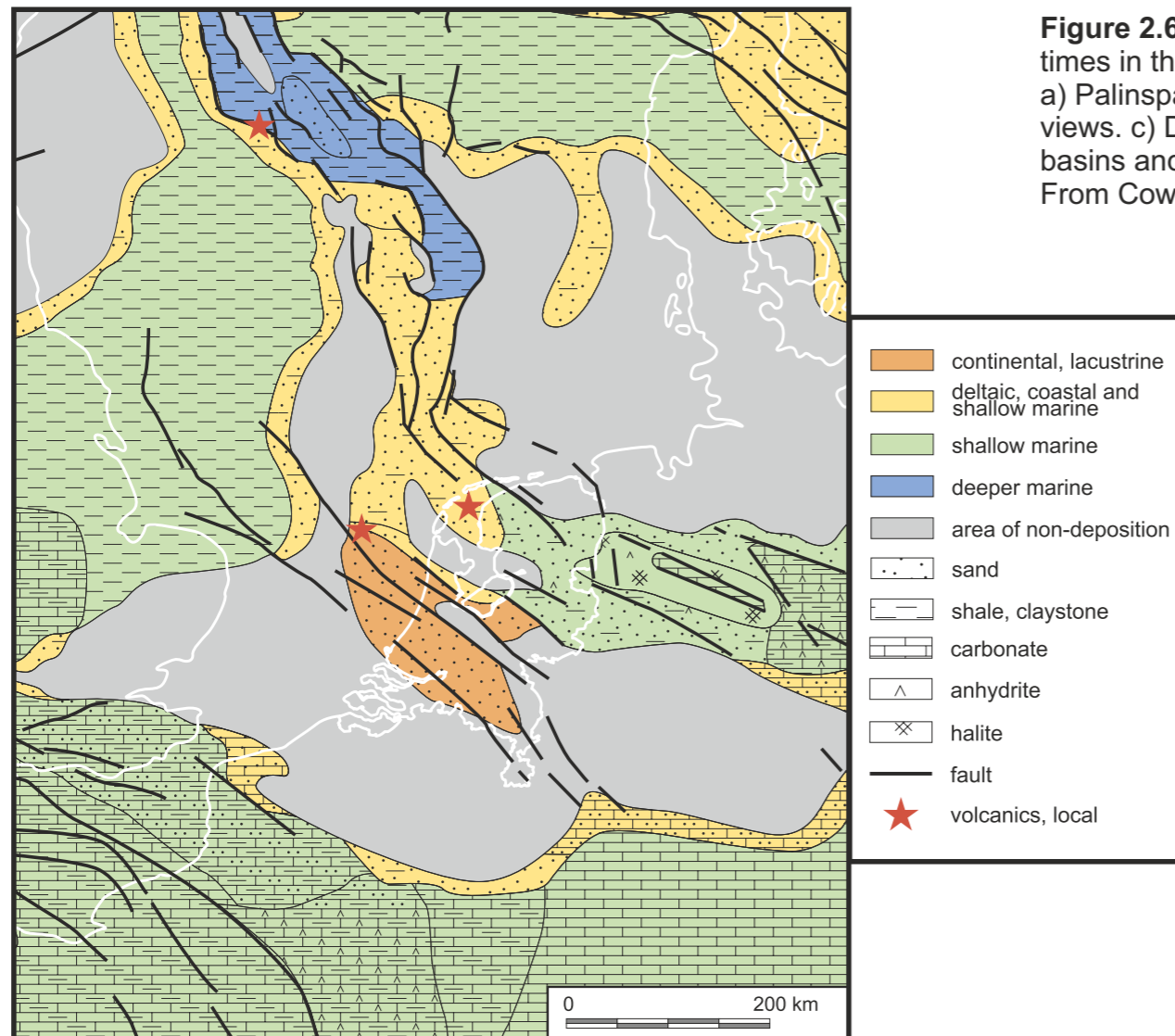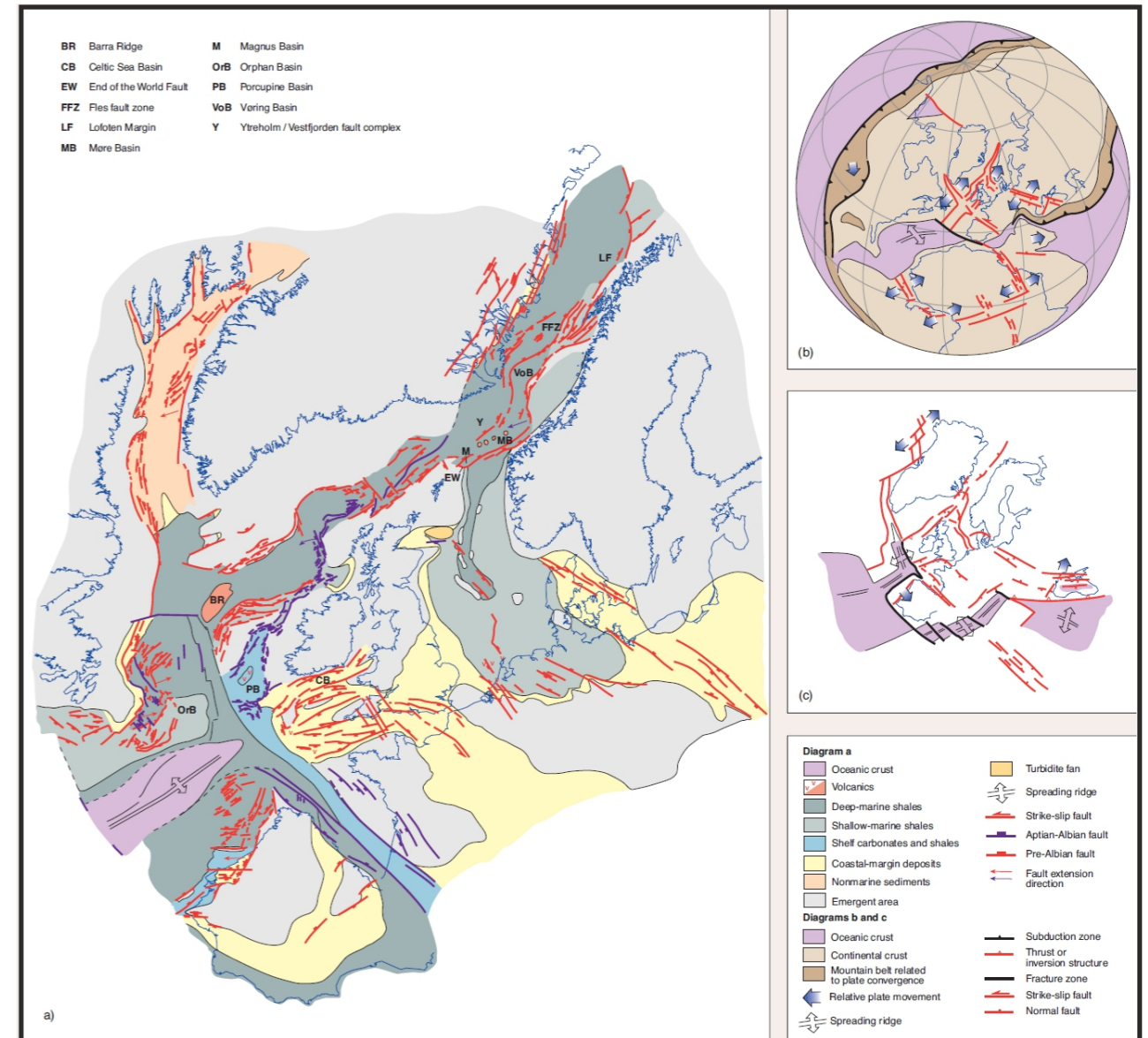
Figure 2.5: Paleogeographic map of the Netherlands and adjacent areas during the Kimmeridgian-Tithonian. Present day shorelines shown as white lines (after Ziegler, 1990; modified from Wong, 2007).

Legend:
- continental, lacustrine
- deltaic, coastal and shallow marine
- shallow marine
- deeper marine
- area of non-deposition
- sand
- shale, claystone
- carbonate
- anhydrite
- halite
- fault
- volcanics, local

0   200 km

Figure 2.6: Early Cretaceous times in the North Sea Region. a) Palinspastic maps. b) Global views. c) Distribution of the basins and main structures. From Coward *et al.*, 2003.

BR	Barra Ridge	M	Magnus Basin
CB	Celtic Sea Basin	OrB	Orphan Basin
EW	End of the World Fault	PB	Porcupine Basin
FFZ	Fles fault zone	VoB	Vøring Basin
LF	Lofoten Margin	Y	Ytreholm / Vestfjorden fault complex
MB	Møre Basin		

Diagram a
- Oceanic crust
- Volcanics
- Deep-marine shales
- Shallow-marine shales
- Shelf carbonates and shales
- Coastal-margin deposits
- Nonmarine sediments
- Emergent area
- Turbidite fan
- Spreading ridge
- Strike-slip fault
- Aptian-Albian fault
- Pre-Albian fault
- Fault extension direction

Diagrams b and c
- Oceanic crust
- Continental crust
- Mountain belt related to plate convergence
- Relative plate movement
- Spreading ridge
- Subduction zone
- Thrust or inversion structure
- Fracture zone
- Strike-slip fault
- Normal fault

The Step Graben and Terschelling Basin subsided more slowly than the Central Graben during the Late Jurassic and accumulated thinner sequences. Salt walls developed along the main bounding faults of the Dutch Central Graben. Late Jurassic uplift of the Friesland Platform resulted in erosion down to Lower Triassic and, locally, to Zechstein levels. Basin-controlling faults accommodated the east–west extension in the Central Graben. However, due to the complex reactivation history, unambiguous evidence of dextral transtensional displacement is only available locally, for example, in the Rifgronden Fault Zone between the Terschelling Basin and the Schill Grund High (De Jager, 2007).

During Callovian to Oxfordian times, the uplift of structural highs such as the Broad Fourteens and Friesland highs shed clastics into the adjacent rapidly subsiding basins. The Zuidwal alkaline volcanic complex (Kimmeridgian) developed during the late Kimmerian rifting phase. In the Terschelling Basin, tectonic events were slightly delayed compared to the Dutch Central Graben; uplift occurred before the end of the Mid-Jurassic and a thin, younger, Upper Jurassic sequence rests on the Triassic, whereas the Lower Cretaceous sequence is thicker than in the Central Graben.

The Cleaver Bank High and Schill Grund High, which were platforms during much of Triassic to Early Jurassic times, were uplifted and eroded during the mid- to late Kimmerian rifting phases. Upper Jurassic and Lower Cretaceous syn-rift strata are consequently missing from these highs, where Triassic and Permian strata are unconformably overlain by thin post-rift Lower Cretaceous and thicker Upper Cretaceous rocks (De Jager, 2007). Hundreds of metres of Triassic to Middle Jurassic sediments were probably removed from these highs. The thick Rijnland Group (latest Ryazanian to Albian) succession, comprising mainly fine-grained clastics, was subsequently deposited across a large open-marine basin. (Pharaoh *et al.*, 2010).

G) Mid- to Late Cretaceous

The North Sea rift system became inactive and the North Atlantic Ocean started to open with rifting concentrated on areas between Europe and Greenland (Ziegler 1988 and 1990a). The Neo Tethys Ocean opened to the south of Europe during the Mid-Cretaceous and starting to close during the Late Cretaceous due to the convergence between the African and Eurasian plates (Ziegler, 1990a).

Regional thermal subsidence of the North Sea Basin started during the Hauterivian and Barremian in combination with gradually rising sea levels, and by Aptian-Albian times the southern Permian Basin was a vast shallow-marine basin. Transgression and thermal subsidence occurred during the Albian to Turonian. During the Late Cretaceous, this basin further expanded to reach its maximum extent in response to thermal subsidence and sea-level rise to about 100-200 m above the present-day level. The Upper Cretaceous Chalk series is up to 2000 m thick in the basin (Ziegler, 1990a).

In the southern Permian Basin, inversion tectonics due to the Alpine collision affected basement blocks during the late Turonian and intensified during the Senonian and the Paleocene (Ziegler, 1990a). This inversion was heterogenous with strain localized in narrow zones separated by undeformed regions (Pharaoh *et al.*, 2010). Inversion also produced decoupling on Zechstein salt and thin-skinned tectonics. The NW trend of early inverted basins and transpressional fault reactivation indicates N to NE oriented compressional stresses (Kley & Voigt, 2008).

2.2 Overview of structural elements affecting the study area since the Triassic

A) Strike slip deformation

The dominant NW-SE fault set in the Netherlands such as the Hantum and Rifgronden Fault Zones, probably dates back to the Caledonian orogeny when Laurentia and Avalonia collided (De Jager, 2007). Several of this early NW-SE faults were reactivated during the Permian (George and Berry, 1993 and 1997; Glennie, 1998; De Jager, 2007) as well as less prominent conjugate NE-SW to NNE-SSW oriented fault set which is the second most common fault set in the Dutch subsurface (Ziegler, 1988 and 1990). Reactivation of some of these NW-SE oriented structures also occurred during the Meso-Cenozoic.

In the study area the Rifgronden and Hantum Fault Zones are present. The Rifgronden Fault Zone is a WNW-ESE trending fault zone is the northern margin of the Terschelling Basin. This fault zone shows dextral offsets (De Jager 2007). The Hantum Fault Zone is a WNW-ESE oriented fault zone is the southern boundary of the Terschelling Basin. The Hantum Fault Zone extends southeastward and forms the western boundary of the Lauwerszee Trough. In the study area faults in the Hantum Fault Zone show vertical offsets at the base of the Zechstein Group of up to 1500 m (De Jager 2007). Different phases of fault activation and reactivation were identified. The old Hantum Fault Zone have been active since the Late Carboniferous, and was reactivated multiple times during the Triassic and Late Jurassic. The Rifgronden Fault zone may be a similar repeatedly reactivated fault zone (De Jager 2007).

B) Rifting

- Active rifting started in the north of the study area in the **Early Triassic** (e.g. Central and Horn Grabens) but only reached the study area in the Mid-Triassic. The Dutch Central Graben subsided slightly faster than adjacent platforms (Terschelling and Vlieland Basins) but not as rapidly as the Grabens farther east in Germany and Denmark. No rift-shoulder uplift has been documented during this period.

- During the **Mid-Triassic** the Dutch Central Graben and the Broad Fourteens Basin started to subside with Zechstein salt becoming mobile along bounding faults (Remmelts, 1995).

- During the **Late Triassic** the differential subsidence persisted between the basins and their shoulders. Locally, transtentional dextral strike slip structures (including flower structures) are involved (Van Hoom, 1987). Zechstein salt was also mobilized during this period.

- Rifting was still possibly active during the **Early Jurassic** in the Dutch Central Graben but little evidence of active faulting is observed in the Southern Permian Basin, especially in the study area where tectonic activity is focused in the Dutch Central Graben.

- The rift evolution during the **Mid-Jurassic** is broadly unknown due to the Central North Sea-related uplift that eroded all of the Middle Jurassic deposits in the study area. The erosion locally denudated the Dutch Central Graben down to the Carboniferous level such as in the northern part of the Cleaver Bank High. The exact amount of eroded strata on the eastern shoulder of the Dutch Central Graben is unknown, The Step Graben and the Terschelling Basin were also uplifted and erosion cut down to Lower Jurassic and Triassic levels (Van Hoorn, 1987). The Horn Graben became inactive during the Middle Jurassic.

- The rifting during the **Late Jurassic** and Early Cretaceous is dominantly expressed as wrench tectonics with NW-oriented transtensional basin subsidence and transpressional uplift of narrow zones. The main rifting pulses (Kimmerian rift pulses) in the study area occurred during this period. The Schill Grund High was a stable platform area and the Step Graben and Terschelling Basin subsided but relatively less than the Dutch Central Graben. Late Jurassic uplift of the Friesland Platform resulted in erosion down to Lower Triassic and, locally, to Zechstein levels. There are evidences of local dextral transtensional displacement in the Rifgronden Fault Zone between the Terschelling Basin and the Schill Grund High (De Jager, 2007). The Zuidwal alkaline volcanic complex (Kimmeridgian) developed during the late Kimmerian rifting phase. In the Terschelling Basin, tectonic events were slightly delayed relative to the Dutch Central Graben; uplift occurred before the end of the Mid-Jurassic and a thin, younger, Upper Jurassic sequence rests on the Triassic, whereas the Lower Cretaceous sequence is thicker than in the Dutch Central Graben (Doornenbal and Stevenson, 2010). The Cleaver Bank High and Schill Grund High were uplifted and eroded during the mid- to late Kimmerian rifting phases. Therefore, Upper Jurassic and Lower Cretaceous strata are often missing on these highs, where Triassic and Permian strata are unconformably overlain by thin post-rift Lower Cretaceous and thicker Upper Cretaceous rocks (De Jager, 2007).
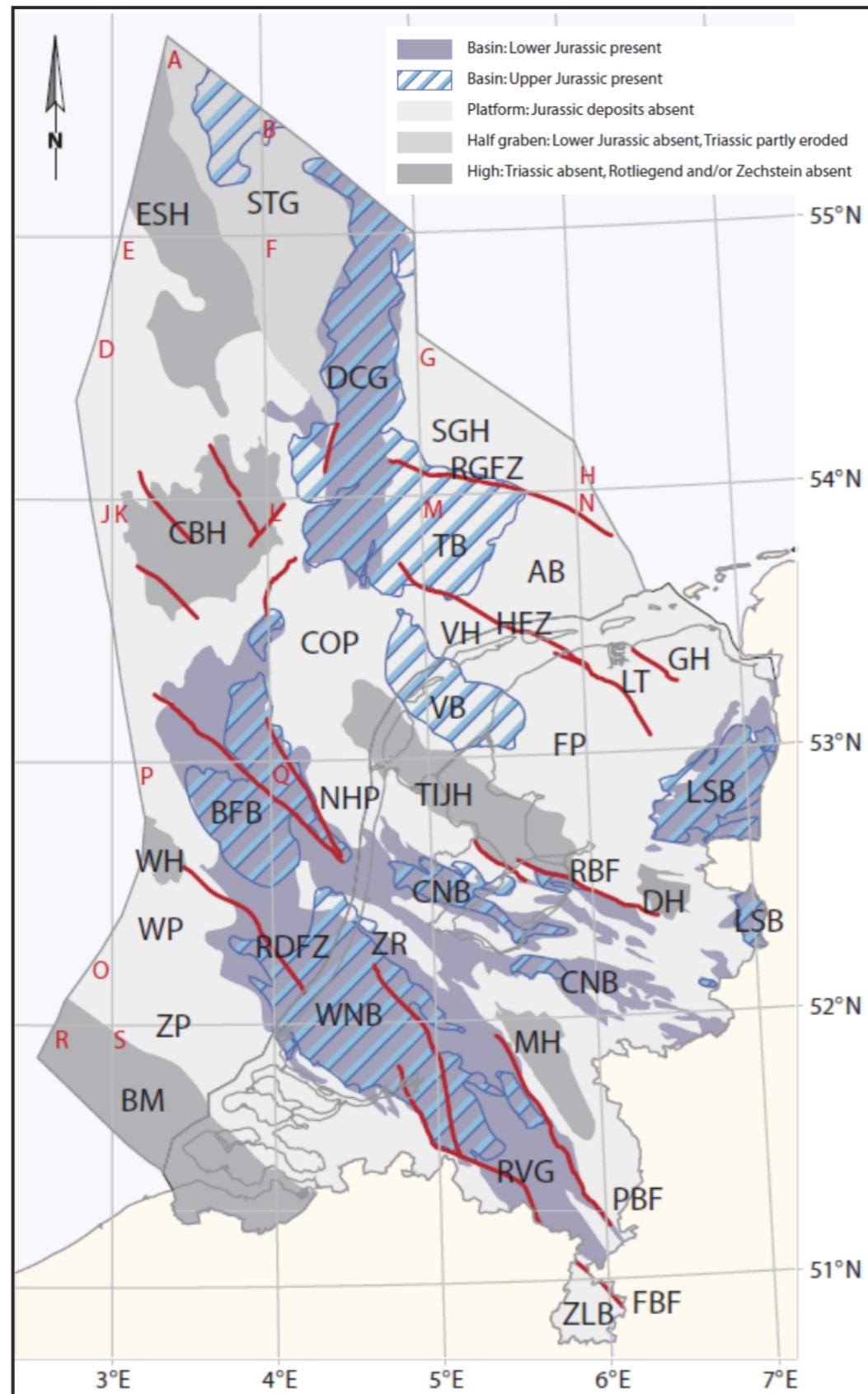
Figure 2.7: Late Jurassic-Early Cretaceous structural elements in the Netherlands. Adapted from Duin *et al.* (2006).

C) Salt tectonics

The presence of Zechstein salt that was deposited during the Late Permian had a pronounced influence on the subsequent evolution of the North Sea Basin, beginning with its effects on Triassic sedimentation patterns.

The partitioning of the Southern Permian Basin into several basins and highs during the Triassic and Jurassic was accentuated by the intense salt tectonics, primarily along fault-bounded basin margins (Wong, 2007). Basin compartmentalization and minibasin formation were associated with salt withdrawal in much of the Dutch Central Graben. These basins are often bounded by listric growth faults. Mid-Triassic minibasins subsided into the Zechstein salt over much of the central North Sea.

Differential loading was important for minibasin development near sediment entry points, and thin-skinned extension on the platforms was balanced by basement extension in the central axis of the basin. Along the edges of the Triassic fault basins, the faults are commonly soft-linked and offset through the Zechstein salt (Pharao*h et al.*, 2010).

During the Mid-Triassic, thin-skinned normal faults formed on autochthonous Zechstein salt and large salt swells formed. Piercing salt bodies and rim-synclines developed later (Jager, 2007). With increased differential subsidence between the subsiding basins and their shoulders, salt bodies increasingly mobilized upward from the previously formed salt swells and initiated large rim-synclines.In the study area the salt bodies are located mainly along the basin margin and a few in the basin itself (Fig. 2.8). The salt bodies are either salt diapirs or salt walls with a SSW/NNE preferential orientation.
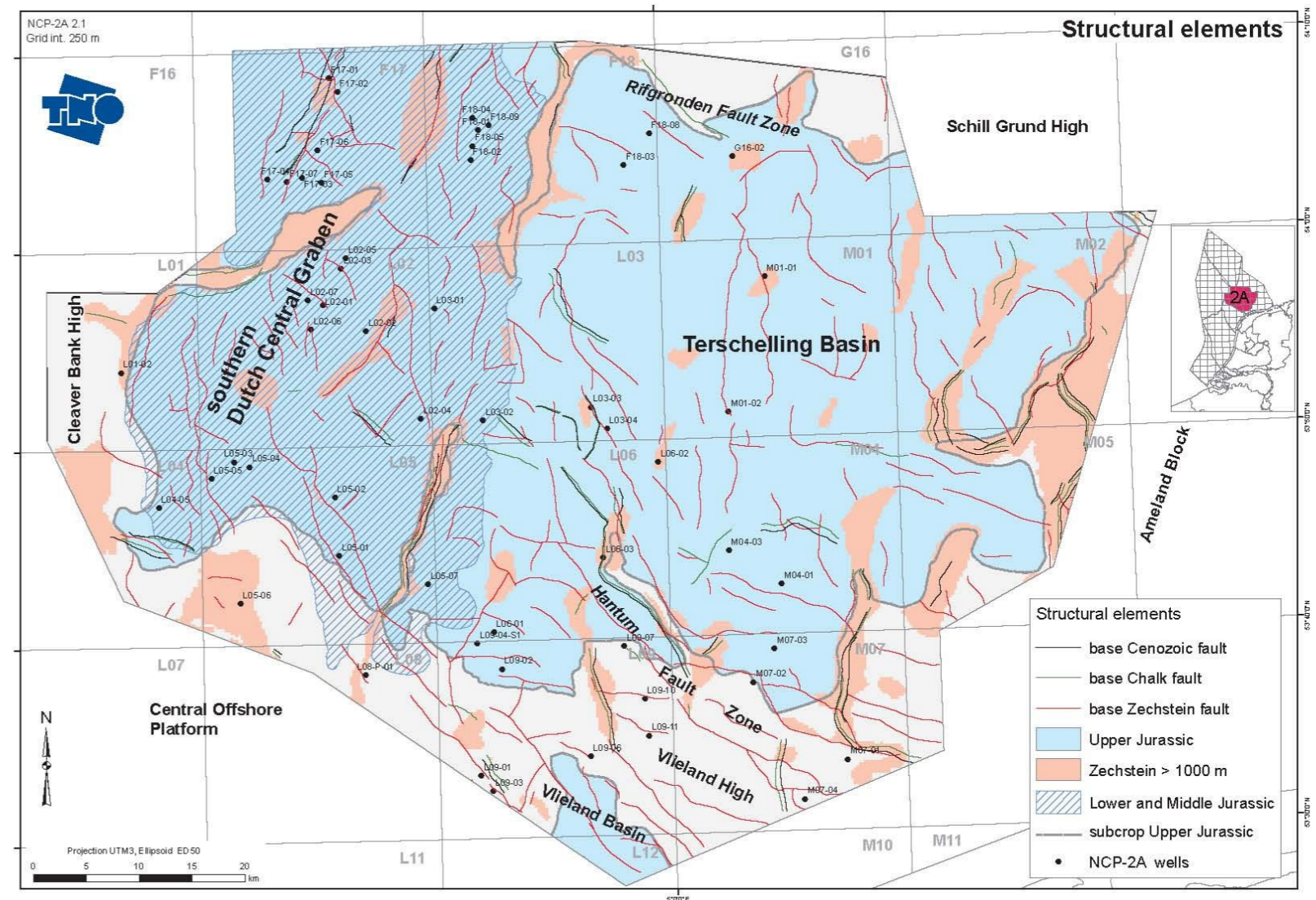

Figure 2.8: Main structural element of the Terschelling Basin and surrounding areas. From Verweij and Witmans (2009)

2.3 Overview of the stratigraphy of the Upper Jurassic and Lower Cretaceous in the study area and in surrounding regions of the southern North Sea

The Upper Jurassic to Lower Cretaceous interval is composed of four groups (Schieland, Scruff, Niedersaksen and Rijnland Groups). Three of these groups are present within the study area, the Schieland, Scruff and Rijnland Groups. The first two groups (Schieland and Scruff Groups) are studied in detail in this project. Their strata were deposited on top of the Lower to Middle Jurassic Altena Group, mainly consisting of argillaceous sediments (including the well known Posidonia Shale Formation) with intercalation of calcareous units.

The sedimentary in filling of basins and adjacent regions in the Upper Jurassic – Lower Cretaceous is predominantly controlled by the structural evolution of the region (Figures 2.7 and 2.8).

A) Sequence 1

In the Callovian, rifting resumed and continued until the Early Cretaceous (Valanginian). At first, this rifting was oriented E-W and influenced the axis of the DCG and further to the southwest the Broad Fourteens Basin (BFB). Deposits of this phase are referred to as Sequence 1 by Abbink *et al.* (2006) and as Graben Axis in Verreussel *et al.* (in prep.) (Figure 2.9). These deposits are primaraly deposited in the DCG and in the western part of the TB. This sequence comprises the Lower Graben Fm., Puzzle Hole Fm. and Friese Front Fm. sands and coals. During the Kimmeridgian, a dramatic change in structural setting and structural style occurred.

B) Sequence 2

The direction of the extension regime changed from E-W to SW-NE. Numerous old NW-SE oriented lineaments and structures become rejuvenated, resulting in the opening of peripheral basins such as the Terschelling Basin, the Step Graben, and also lead to major basin development in the Broad Fourteens Basin. In some parts of the DCG, the opposite occurs: uplift and erosion. Most of the uplift and erosion in the DCG can be ascribed to salt movement. Salt is withdrawn from some parts (e.g. the F11 rim syncline), resulting in the formation of turtle structures (e.g. the F03-FB condensate Field) and diapirs (e.g. the F17-18 salt structure) in other part. This interval is referred to as Sequence 2 in Abbink *et al.* (2006) and Peripheral Basins in Verreussel *et al.* (in prep.) (Fig. 2.9). This phase provided accommodation space for siliciclastic deposits with hydrocarbon reservoir potential (non-marine Schieland Group and Scruff Group) in the peripheral basins. Towards the end of the phase, fault activity and salt movement reached a peak.

C) Sequence 3

During this third phase, adjacent platforms like the Schill Grund Platform and the Cleaver Bank High were flooded. In the Dutch Central Graben area, large accumulations of sandstone of the Scruff Greensand Fm. are associated with this phase. In the Danish Central Graben area, highly condensed organic-rich mudstones are associated with this phase. This phase, occurring around the Jurassic-Cretaceous boundary is referred to as Sequence 3 in Abbink *et al.* (2006) and as Adjacent Plateaus in Verreussel *et al.* (in prep.) (Fig. 2.9). Sequences 2 and 3 are relatively thick in the peripheral basins compared to the DCG. In the Broad Fourteen Basin, deposition continued in the axial region, whereas renewed tectonic activity in the Ryazanian led to major erosion on its margins.

At the end of the Ryazanian the rifting came to an halt. Fault activity in the DCG-area gradually ceased and the younger marine sandstones and shales of the Rijnland Group effectively cover the former graben and platform areas in the north of the Dutch offshore. As the basins continued to (thermally) differentially subside, characterizing **Sequence 4** (not analyzed in this project), the coastal Vlieland Sandstone and the Vlieland Claystone Formation were deposited.

2.4 Overview of the depositional environments of the Upper Jurassic and Lower Cretaceous in the study area (from Munsterman *et al.*, 2012 and Bouroullec et al., 2016)

A) Sequence 1

This sequence is rarely observed in the study area (Terschelling Basin) where it consists only of its younger interval of the Friese Front Formation (and specifically the Main Friese Front Member). The Lower Graben, Middle Graben, Upper Graben and Puzzle Hole Formations are not present in the study area but are observed farther west and north within the Dutch Central Graben and its surrounding platforms.

Friese Front Formation: Alternating claystones, siltstones, sandstones and some minor coal. Non-marine (coastal) delta plain to lagoonal deposits.

B) Sequence 2

Kimmeridge Clay Formation: The sediments of the Kimmeridge Clay Fm. were deposited in an outer shelf setting. Dolomitic beds and structureless organic matter (SOM) indicate times of decreased input of clastics and stagnant water conditions due to a stratified water column. The higher frequency of dolomitic beds and SOM in the northern realm reflects a slightly deeper environment .

Oyster Ground Member: Claystones, non- to slightly silty. Lithology, fossils, lignite and regional palaeogeography suggest that the Oyster Ground Member was deposited in restricted lagoon-like conditions with washover deposits. The monotypical thin-walled shell assemblages confirm a restricted marine setting.

Terschelling Sandstone Member: Fine- to medium-grained sandstone (occasionally up to coarse sand and gravel), well to poorly sorted. In most cases, e.g. in wells L06-02, L06-03 and M01-01, the sediments of this member are interpreted to be deposited as a barrier island complex, including shoreface to foreshore and washover fans environments, protecting the restricted marine (lagoonal) setting of the Oyster Ground.

Noordvaarder Member: Well-sorted, greenish-grey, slightly argillaceous, occasionally calcite cemented, glauconitic sandstones. The sands were deposited in a shallow marine environment, ranging from offshore to lower shore face.

Lies Member: Bioturbated silty to sandy claystones. The sediments are considered to be deposited in the offshore/shelf environment.

C) Sequence 3

Scruff Spiculite Member: Light green-grey, fine-grained, glauconitic and slightly argillaceous intensely bioturbated sandstones. The sediments of this formation were deposited in a (offshore to) shoreface environment. Facies change laterally from relatively clean 'bioclastic' sandstone to an argillaceous sandstone reflecting the position of the depositional area on the basin floor topography (Abbink *et al.*, 2006). A semi-enclosed shallow marine environment is envisaged.

Stortemelk Member: Fine- to very fine-grained, argillaceous sandstones with intense bioturbation. Shoreface to offshore.

Clay Deep Member: Grey to black claystone. Deposited in a shelf environment. Basin circulation stagnated which resulted in dysoxic to anoxic basin-floor conditions and in the deposition of bituminous claystones.

Schill Grund Member: Olive-grey to grey-brown claystones. Open-marine shelf conditions prevail. The slightly or non-bituminous nature of the sediments indicate near-normally oxygenated basin-floor circumstances.
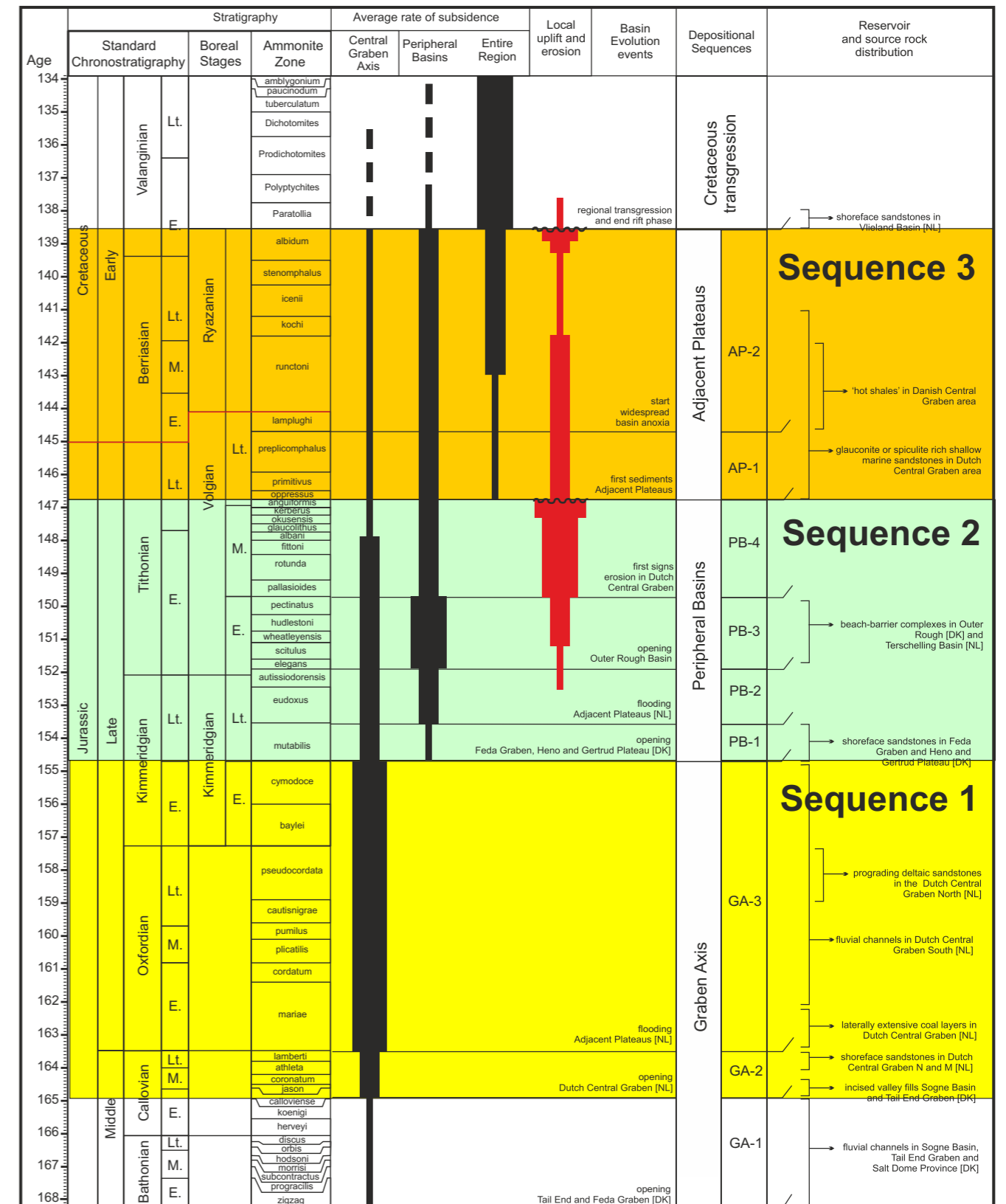

Figure 2.9: Schematic representation of the Late Jurassic to Early Cretaceous basin evolution of the Central Graben area from Denmark, Germany and The Netherlands (from Verreussel *et al.*, in prep.).

3

DATABASE & METHODOLOGY

Several analytical techniques were used for the COMMA project: 1) 3D seismic horizon and fault interpretation, 2) itime thickness mapping, 3) palynological analysis, 4) stratigraphic correlation, 5) tectono-stratigraphic analysis and 6) lithofacies mapping.
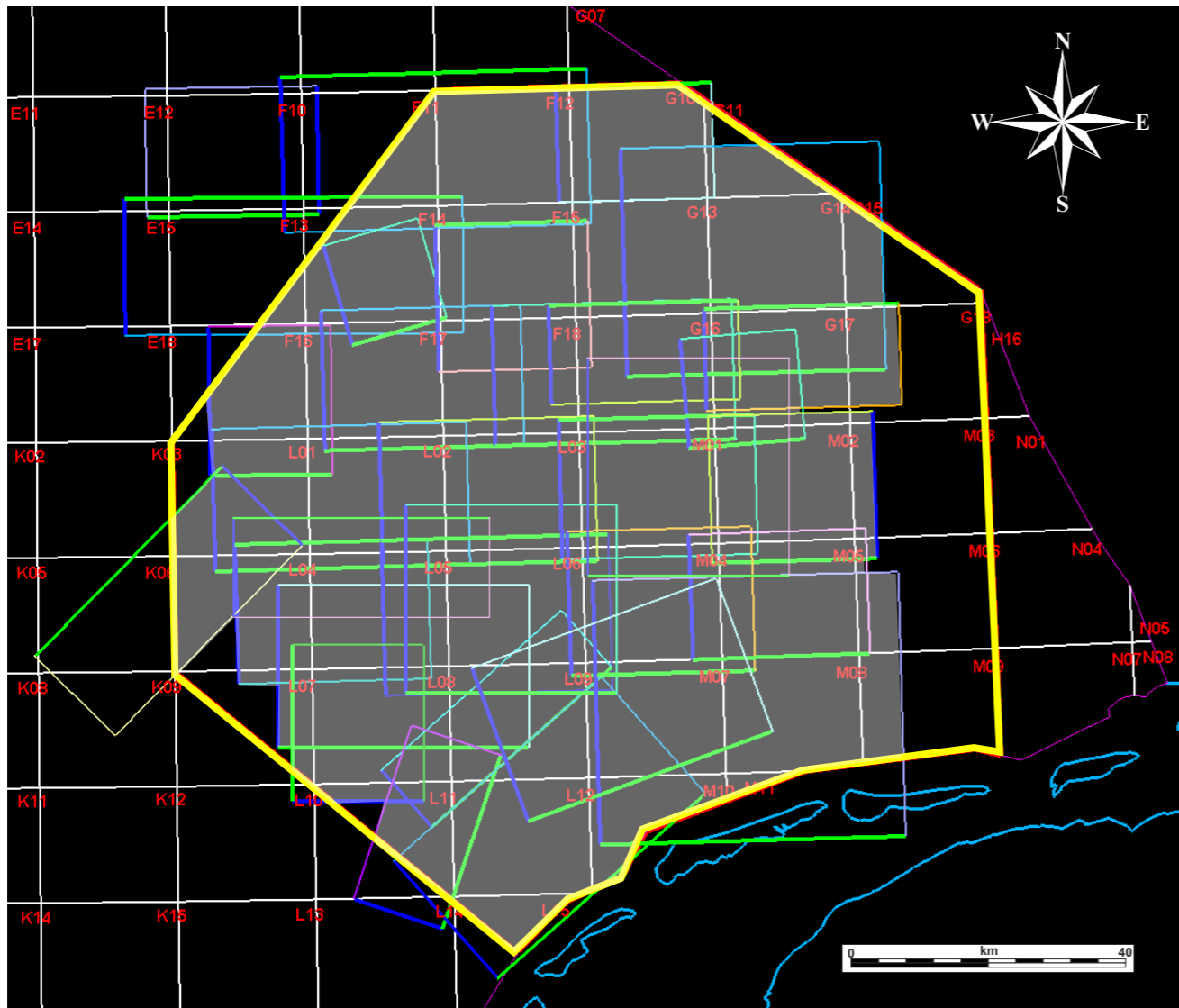
The database used consist of:

Well data
- 228 wells in the petrel project, of which 103 are time-depth converted.
- A total of 85 wells are displayed in this report, 66 of which have Upper Jurassic-Lowermost Cretaceous strata.
- 54 wells were used in this project either for palynological analysis or for the stratigraphic correlation.

Seismic data
- Thirty two 3D seismic cubes (Fig. 3.1.1) and twelve 2D seismic surveys present in the study area.
- Out of this database, a total of twenty two 3D seismic cubes and three 2D seismic survey were used systematically for mapping purposes (Fig. 3.1.2)

Palynological data
- Anonymized legacy information from twenty two (22) wells is used to correlate from well to well in this study. The information is derived from previous business-to-business projects and is not disclosed in this study.
- Thirteen (13) wells are either newly analyzed, or are additional analyses are carried out, or is re-interpreted entirely to accommodate the for the current TNO zonation scheme.

Figure 3.1.1: 3D seismic surveys located within the study area (yellow polygon). Grey polygon shows the zone within the study area that is covered by 3D data. Only the eastern part of the study area (blocks G18, M03, M06 and M09) are not covered with 3D data.
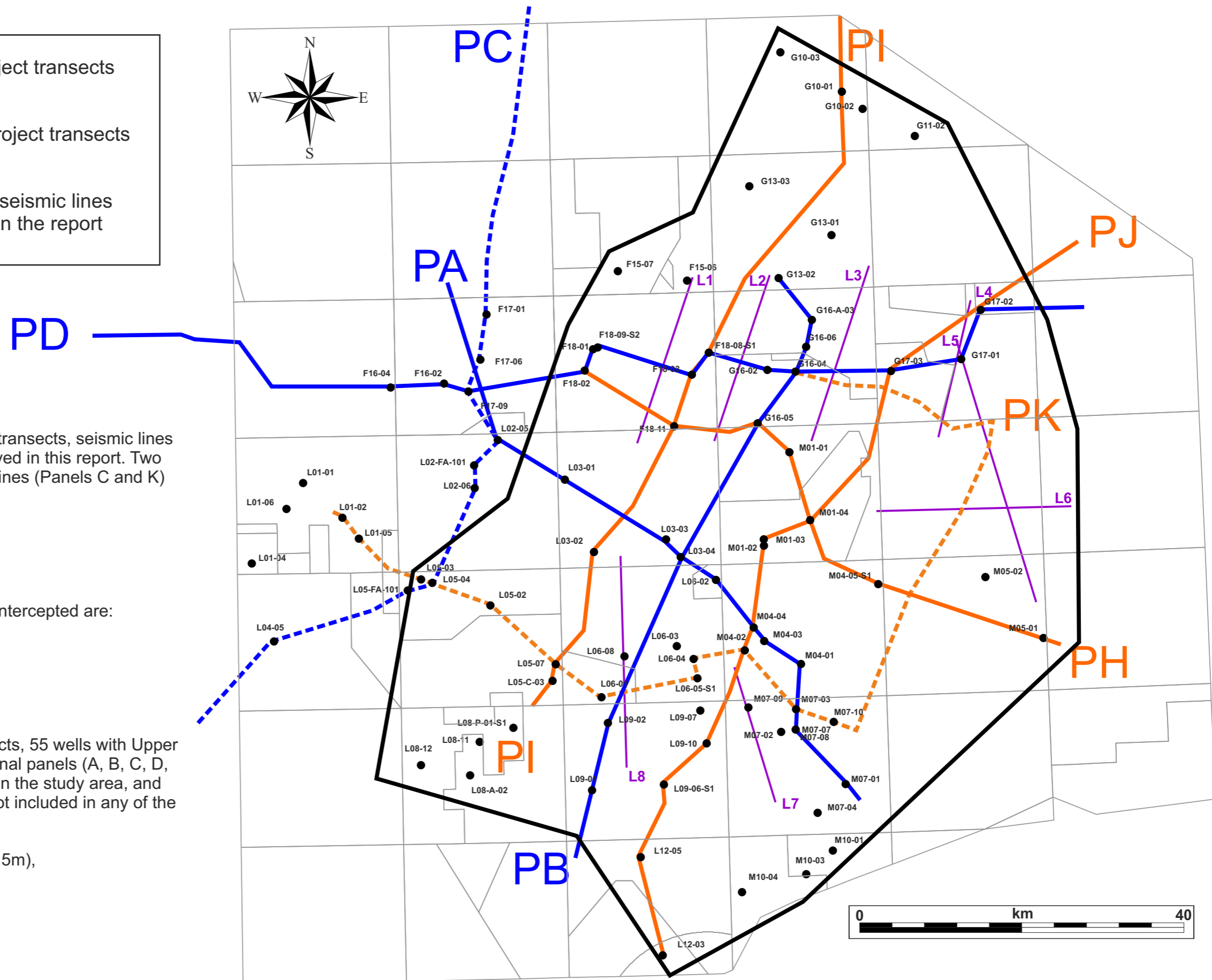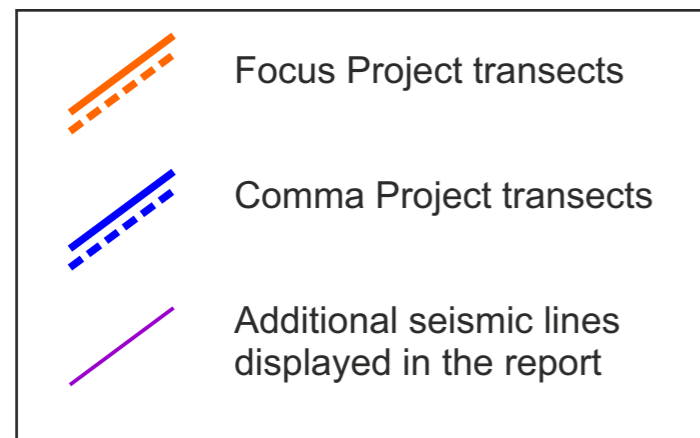
	Wells	S1	S2	S3	S4
3D surveys	F06				■
	F17-F18	■			■
	F18-G16		■	■	■
	G13_G14_G16_G17				■
	G16				■
	L06_L05_L09				■
	L06_L05_L09				■
	L01_L02				■
	L03-L02		■	■	■
	L05				■
	L06-L05		■	■	■
	L09		■	■	
	L11				■
	L06-big_2005				■
	M09_broken				■
	M01		■		■
	M02			■	■
	M04		■	■	■
	M05		■	■	■
	M07-M08_M05				■
	M07-L09		■	■	■
	Seismic_ONE		■	■	■
2D surveys	SNST-83				■
	SNST-87				■
	E_F_2D				■
	Focus panels	■			
	Comma panels	■	■	■	■

Figure 3.1.2: List of 3D and 2D seismic surveys used for mapping of the base of sequences 1, 2, 3 and 4.

Figure 3.1.3: Map showing the seismic transects, seismic lines and wells used in the project and displayed in this report. Two of the transects are showed as dashed lines (Panels C and K) to make their trajectories easier to see.

The panels length and number of wells intercepted are:
- **Panel H:** 90 km long, 7 wells
- **Panel I:** 109 km long, 8 wells
- **Panel J:** 130 km long, 11 wells
- **Panel K:** 165 km long, 15 wells

Between the FOCUS and Comma Projects, 55 wells with Upper Jurassic-age strata are included in regional panels (A, B, C, D, H, I, J, K panels). Only 11 wells located in the study area, and having Upper Jurassic-age strata, are not included in any of the panels. They are wells

- G11-02 (only 10m), G13-01 (only 5m),
- F15-06, F15-07,
- L06-03, L06-08,
- M07-02, M07-09, M07-10,
- M10-03, M10-04.

TNO innovation for life

For the COMMA project, four seismic and stratigraphic correlation panels (H, I, J and K panels) have been constructed to illustrate the Upper Jurassic structural and stratigraphic geometry for the Terschelling Basin and surrounding areas (Fig. 3.1.3). These panels are complementary to the correlation panels A, B and D, that were compiled in the FOCUS project. Below, wells are listed that have been included in the COMMA Project. New palynological analyses have been carried out on 12 wells. Legacy palynological data of 23 other wells were re-interpreted to accommodate for the TNO zonation.

Seismic panels

█ Well occurrence in panels

Biostratigraphy

▮ Legacy data (FOCUS and other)

▮ New analyses (COMMA)

CO — Core samples

SWC — Side-wall core samples

CU — Cuttings samples

Core

▮ Cored section in Upper Jurassic

Well	FOCUS E	B	D	COMMA H	I	J	K	Biostrat	Core	Subcrop	Cored section
F18-01			X					CO	●	ATAL	ÇÇÖ Ï ĠĠÏ
F18-02			X	X				CO; CU		ATAL	8m SLCF
F18-03					X			CU		RNKP	
F18-08-S1			X							RNMUU	
F18-09-S1			X					CO; SWC	●	ATAL	58m SLCF
F18-11				X	X					RNKP	
G10-01				X	X			CU	●	Z	17m top Z
G13-01		X						CO	●	Z	24m SGGS
G13-02		X								Z	
G16-02			X							Z	
G16-04		X	X				X	CU		RNKP	
G16-05		X	X					CU		RNKPL	
G16-06-S1			X					CO	●	Z	40m Z caprock
G17-01			X							Z3	
G17-02			X							Z3	
G17-03			X			X		CU		RBSHM	
L01-02							X			RNMUU	
L01-05							X	CU		ATWD	
L02-05	X							CU		ATWD	
L03-01	X				X			CO; SWC		ATAL	20m SGGS; 10m SGKO
L03-02					X					ATAL	
L03-03	X								●	Z	15m top SGSKO
L03-04	X	X						CU		RNKPR	
L05-02								CO; CU		ATAL	17m SGGS
L05-03								CO; CU		ATAL	25m SLCF
L05-04								CO; CU		ATPO	65m SLCF; 15m ATPO
L05-07					X			CO; CU		ATAL	12m SGGS
L05-C-03					X					ATAL (20m); RNM	
L06-01							X	SWC		RNKPS	
L06-02	X							CO; SWC	●	Z	35m SGGS; 40m SGSKT
L06-03		X						CO	●	Z	16m SGGS; 13m SGSKT; 21m SLCF
L06-05-S1						X				RNKP	
L09-01		X								Z	
L09-02		X						CO; SWC	●	RN	17m SGGS
L09-04							X	CU		RNRO	
L09-06-S1						X				RNMUL	
L09-10						X				RNKP	
L12-03						X		SWC; CU		RBSH	
L12-05						X		SWC		Z2	
M01-01				X				CO; SWC	●	Z	10m SGKT
M01-02						X				RNKPL	
M01-03								CU		RNKPL	
M01-04				X						RNKP	
M04-01	X							CU		RNKP	
M04-02						X			●	RNKPD	12m SGSKT, 4m SGSKO
M04-03	X							CU		RNKP	
M04-04	X					X		CU		RNKPL	
M04-05-S1				X			X	CU		RNSO	
M05-01				X				CU		RBSH	
M07-01	X									Z	
M07-03	X						X	CO; CU	●	RNM	16m SGGS
M07-07	X						X	CO; CU	●	RBSH	54m SGGS
M07-08								CO	●	Z	107m SGGS

Figure 3.1.4: Wells used in the Focus and Comma projects,

K	Zechstein Group	
RN	Upper Germanic Trias Group	
RNKP	Keuper Fm	Keuper Fm
RNKPU	Upper Keuper Claystone Mb	Keuper Fm
RNKPD	Dolomitic Keuper Mb	Keuper Fm
RNKPR	Red Keuper Claystone Mb	Keuper Fm
RNKPE	Red Keuper Evaporite Mb	Keuper Fm
RNKPM	Middle Keuper Claystone Mb	Keuper Fm
RNKPS	Main Keuper Evaporite Mb	Keuper Fm
RNKPL	Lower Keuper Claystone Mb	
RNM	Muschelkalk Fm	Muschelkalk Fm
RNMUU	Upper Muschelkalk Mb	Muschelkalk Fm
RNMUA	Middle Muschelkalk Marl Mb	Muschelkalk Fm
RNMUE	Muschelkalk Evaporite Mb	Muschelkalk Fm
RNMUL	Lower Muschelkalk Mb	
RNRO	Röt Fm	
RNSO	Solling Fm	
RB	Lower Germanic Trias Group	
RBMH	Hardegsen Fm	
RBMD	Detfurth Fm	
RBMV	Volpriehausen Fm	
RBSH	Lower Buntsandstein Fm	
RBSHR	Rogenstein Mb	Lower Buntsandstein Fm
RBSHM	Main Claystone Mb	Lower Buntsandstein Fm
AT	Altena Group	
ATWD	Werkendam Fm	
ATPO	Posidonia Fm	
ATAL	Aalburg Fm	
SG	Scruff Group	
SGSK	Skylge Fm	
SGSKT	Terschelling Sandstone Mb	Skylge Fm
SGSKO	Oysterground Claystone Mb	Skylge Fm
SGSKN	Noordvaarder Mb	Skylge Fm
SGSKL	Lies Mb	Skylge Fm
SGGS	Scruff Greensand Fm	
SL	Schieland Group	
SLCF	Friese Front Fm	

Figure 3.1.5: Subcrop formations underneath Upper Jurassic interval

23

A)   Principles and application

Palynologists study acid-resistant organic matter from sedimentary rocks. Organic matter is classified into palynomorphs, organic microfossils within a certain size range, and palynodebris, all other organic material such as plant-tissue, wood fragments, structureless organic matter, and so on. The combination of palynomorphs and palynodebris is called palynofacies. Within the palynomorph category, two groups are considered the most important: the dinoflagellate cysts, or dinocysts, and the pollen and spores, or sporomorphs. Because palynology straddles both the marine and the terrestrial realm, it is ideally suited for the study of shallow- to non-marine sedimentary rocks.

Palynodebris: depositional environment

Amorphous Organic Matter (AOM)

Wood

Pediastrum (freshwater algae)

Palynology

Dinoflagellate cysts: marine signal
> Sea Surface Temperature
> Productivity
> Salinity / fresh-water influence
> Age dating

Impagidinium multiplexum

Pollen and spores: terrestrial signal
> Climate
> Distance from shore
> Depositional facies
> Age dating

Grimsdalea magnaclavata

Figure 3.2.1: Principles and application of palynological analysis.

B)   Workflow

The organic matter is extracted from the rock by a standard laboratory processing procedure. During the first step, the sedimentary rock is crushed and treated with HCl to digest the carbonate. After that, the mineral bonds of the silicates are destroyed by applying HF, which releases the acid-resistant organic matter. The organic residue is then concentrated by sieving over a 7 micron mesh. The organic matter particles larger than 7 micron are brought on a glass slide, fixed by a mounting medium such as glycerine jelly, and covered by a thin glass cover slip.

The result is called a palynological preparation or slide. Its content is studied using a transmitted light microscope with magnifications varying between 100 and 1000 microns. The microfossils such as dinoflagellate cysts and pollen and spores are identified on species level and counted. The occurrences of the different species are displayed on distribution charts. These charts are the basic modules for the age and palaeoenvironmental interpretation.
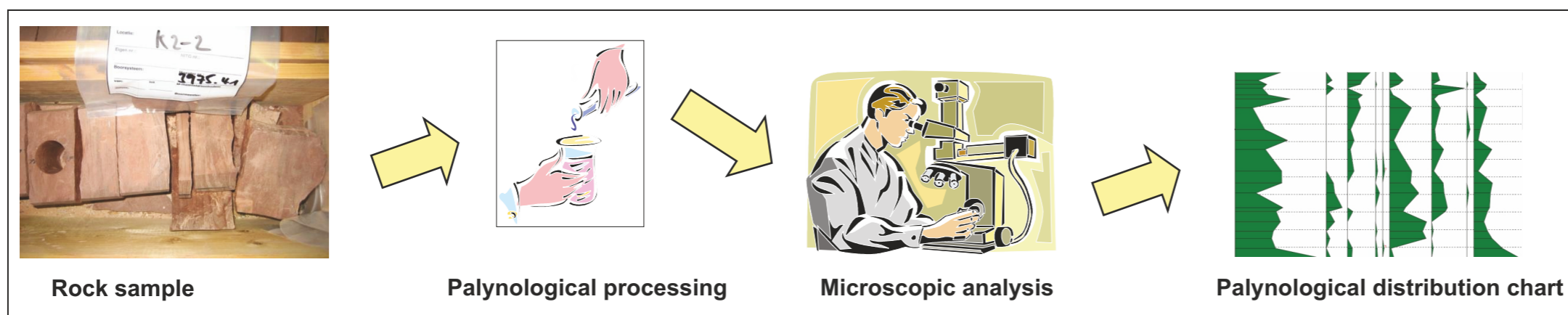
Figure 3.2.2: Typical workflow for palynological analysis: sample selection, processing, microscopy and distribution charts.

Rock sample   **Palynological processing**   **Microscopic analysis**   **Palynological distribution chart**

C)   Age assessments

The TNO zonation has been compiled over the past ten years and is based on palynological data from a vast number of exploration wells in the Dutch offshore. The four main zones defined in the TNO zonation line up with the four sequences that are defined to describe the basin evolution (see Chapter 2). The TNO zonation is based on the LODs (Last Occurrence Datum) and FODs (First Occurrence Datum) of palynomorphs. The correlation to the international chronostratigraphic standard is achieved through comparison with key references such as Abbink

(1998), Abbink *et al.* (2006), Bucefalo Palliani *et al.* (2002), Bucefalo Palliani & Riding (2000), Costa and Davey (1992), Davey (1979;1982), Duxbury *et al.* (1999), Heilmann-Clausen (1985), Herngreen *et al.* (1989, 2000), Koppelhus & Nielsen (1994), Partington *et al.* (1993a; b), Powell (1992), Riding and Thomas (1992) and Riding *et al.* (1999). The international geological timescale of Gradstein *et al.* (2012) is followed.
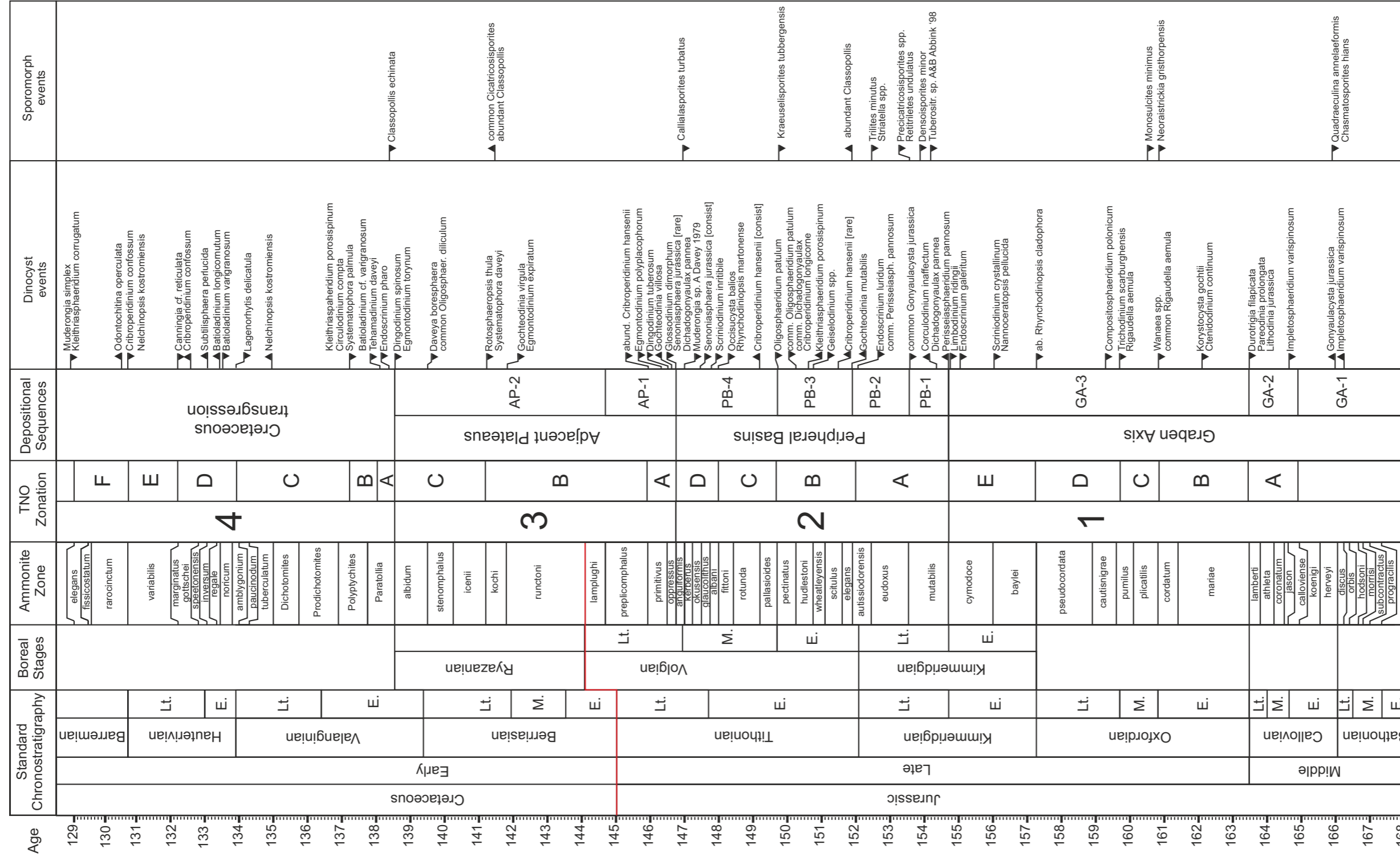
Figure 3.2.3: TNO zonation.
The zonation is based on both dinoflagellate cyst and pollen and spore events. For the chronostratigraphic calibration, GTS 2012 is used (Grandstein et al., 2012). The oldest Jurassic deposits at the base of the "Late Jurassic rift phase", in the Central Graben area are Early to Middle Callovian, correlating to TNO Subzone 1A.

D) Palaeoenvironmental interpretation

The palaeoenvironmental interpretations based on palynology can not be compared one-on-one with the facies interpretations based on the core descriptions. Where the paleoenvironmental constraints from the core descriptions are based on *in-situ* features, such as ichnofossils or sedimentary structure, the palaeoenvironmental interpretations from the palynological analyses are biased by taphonomical processes, such as selectional preservation and transport. Therefore, a schematic representation of depositional environments is made where both worlds meet (Fig. 3.2.4). The palaeoenvironmental interpretation resulting from the palynological analysis are based on a couple of general assumptions, which are listed below.

Open marine
Dominance of dinoflagellate cysts indicates open marine environments, in particular when the dinoflagellate cyst assemblages are highly diverse (many species).

Restricted marine
Dinoflagellate cyst associations of the type High Dominance – Low Diversity indicate a restricted marine environment, such as a lagoon, embayment or estuary.

Non-marine
Absence or near-absence of dinoflagellate cysts generally indicates non-marine or marginal marine environments.

Transgression
An increase in the ratio between dinoflagellate cysts and pollen and spores indicates a sea level rise.

Regression
A decrease in the ratio between dinoflagellate cysts and pollen and spores indicates a sea level fall.

Low energy conditions
Excellent physical preservation of palynomorphs and other organic matter particles may indicate low energy conditions such as for instance a lagoon or a lake.

High energy conditions
Poor physical preservation of palynomorphs may indicate high energy conditions such as for instance a river channel, basin floor fan or a beach.

Figure 3.2.4: Depositional environments. An array of depositional environments in the marine, continental and transitional realm is displayed. At the base of the scheme, the extent of the depositional environments inferred from palynolpgical analysis are compared with the detailed depositional setting, as can be inferred for instance from core description analysis.

26

E)   Reworking and caving

Fossils, like palynomorphs, typically occur in specific stratigraphic intervals. For example fossil remains of dinosaurs may occur in the Jurassic and the Cretaceous, but not in the Paleogene, because dinosaurs became extinct at the Cretaceous-Paleogene boundary. Reworking refers to fossils that first have been eroded from old layers and subsequently deposited in younger layers. When, for instance, dinosaur bones occur in Paleogene strata, then these occurrences are due to reworking. In the case of dinosaur bones, the chances of fossil bones surviving erosion is quite unlikely, but small palynomorphs are less vulnerable and therefore easily reworked into younger sediments.

Caving is phenomenon that is related to the process of taking cuttings samples during drilling. When a well is drilled, mud flows down the drill string to the drill bit. The rotating drill bit produces clippings when cutting through the rock layers. The drill clippings, or cuttings, are taken up hole by the drill mud and are successively collected in troughs. During the way up the borehole, pieces from the side of the hole break off (cave) and are also taken up in the mud flow. These pieces from younger layers then end up in the cuttings sample from an older layer. Only the well transects that are sealed off by a casing cannot contribute to the mud flow.
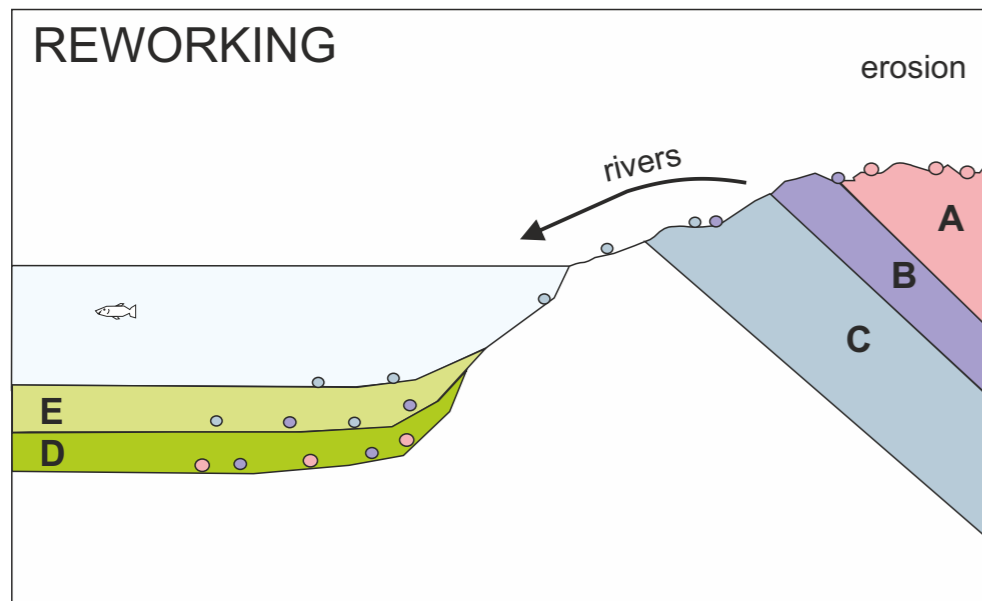
Figure 3.2.5: Reworking explained: old strata A, B and C are eroded and material from it is transported by rivers into the sea. In the sea, the reworked material from A, B and C becomes incorporated in the younger sediment layers D and E.
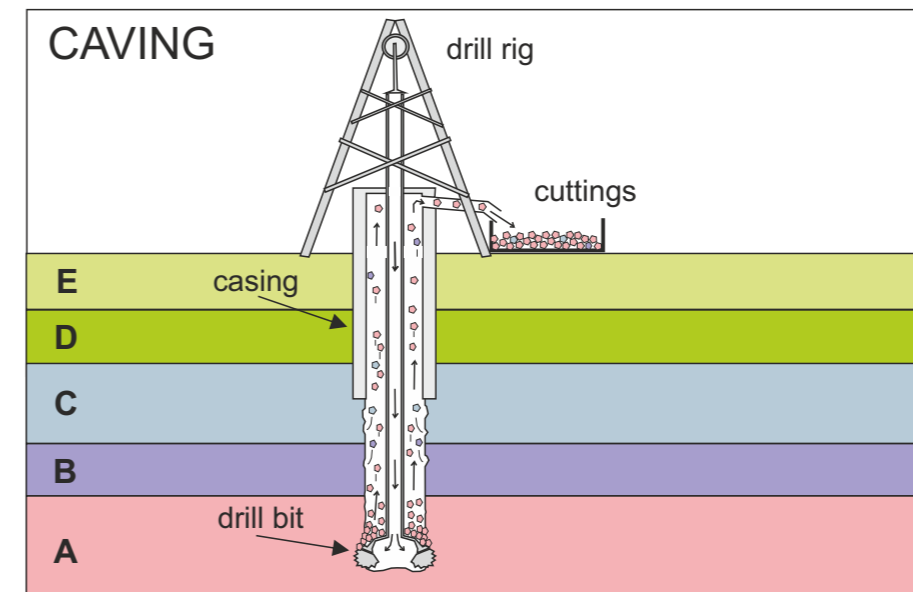
Figure 3.2.6: Caving explained: the drill bit cuts clippings from layer A, which are taken up by the mud stream. During its way up hole, the drill mud picks up pieces of younger layers B and C from the wall of the borehole. Layers D and E are sealed off from the mud stream by a casing.
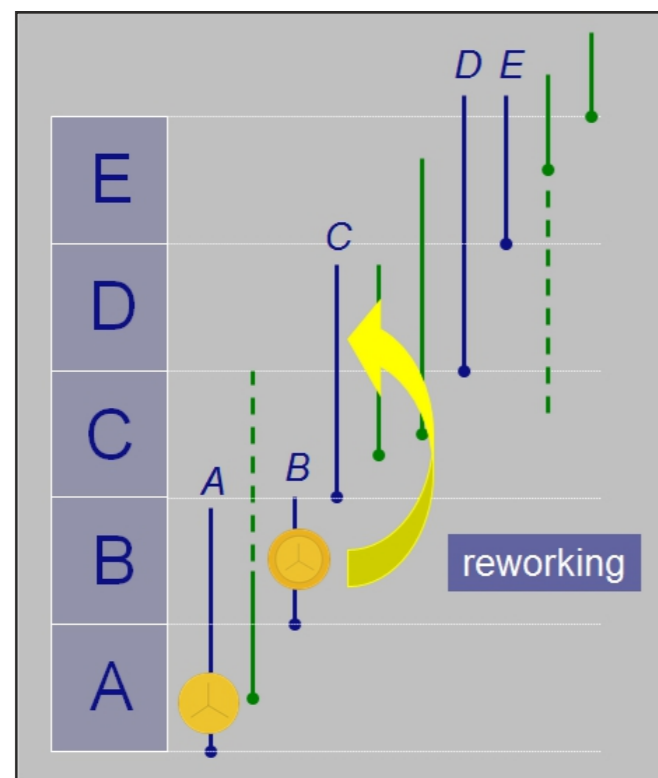
Figure 3.2.7: Reworking explained: pollen and spores with a stratigraphic range limited to layers A or B, end up in younger layers D and E via erosion and transport by rivers.
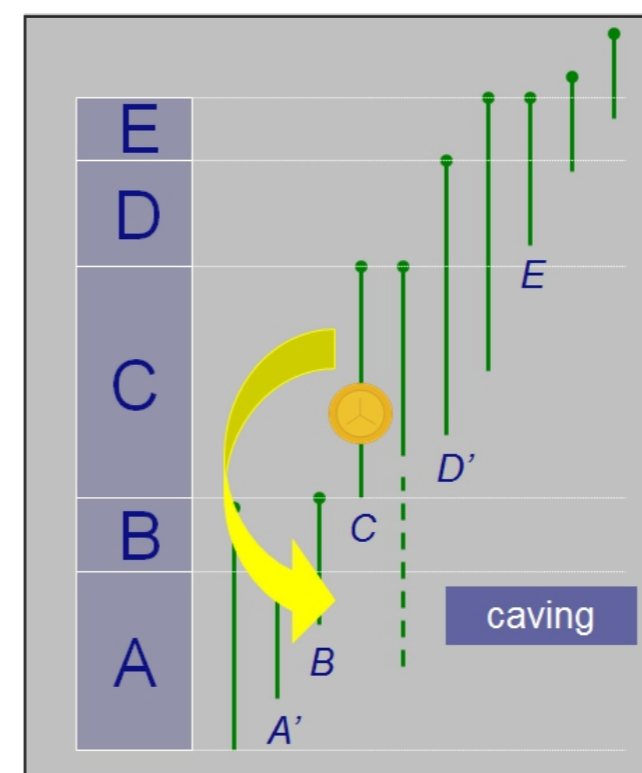
Figure 3.2.8: Caving explained: cuttings samples from layer A are contaminated by palynomorphs from layer C.

The main focus of the seismic analysis is threefold. First, a series regional scale seismic transects were constructed to cover all of the Terschelling Basin and surrounding platforms. Four regional seismic sections (H to K) have been constructed using a combination of 2D and 3D seismic lines (see location map, Fig. 3.1.3). On each of these seismic panels, key seismic horizons (see below) and structures (faults, salt welds and salt bodies) were interpreted in Petrel and exported to a drafting package for edits. starting out with correlation between the available wells in the areaBelow is the list of horizons and structures interpreted.

A) Horizons

Eight main horizons, have been interpreted on seven 2D regional transects as well as in several additional seismic sections. These horizons have been calibrated on well data.

- Base of Zechstein,
- Top of Zechstein : Including salt bodies, either connected to the autochthonous salt or disconnected as allochthonous salt diapirs. The salt feeders (or stems) were also interpreted, as well as salt welds,
- Base of Upper Triassic (base Upper Trias Germanic Group),
- Base of Sequence 1 of the Upper Jurassic,
- Base of Sequence 2 of the Upper Jurassic,
- Base of Sequence 3 of the Upper Jurassic,
- Base of Rijnland Group, and
- Base of Chalk Group.

Three horizon were interpreted in 3D across the TB. These horizons have been calibrated on well data.

- Base of Sequence 2,
- Base o Sequence 3,
- Top of Sequence 3.

Note that the base of Sequence 2 is stratigraphically younger on the eastern side of the study area where it consists of the base of the Skylge Formation. In the western side of the study area this horizon corresponds to the base of the Main Friese Front Member. For this reason, the seismic interpretation for this horizon was handle differently. First two individual seismic horizons where interpreted in those two subregions. In a second stage those horizons were merged into one horizon for base of Sequence 2. Where the two original horizons overlaps, the deepest one (base of Friese Front Member) was selected.

B) Faults

Normal and reverse faults where identified at the base Zechstein and throughout the post Zechstein sections. Particular attention was paid to faults intercepting the Upper Triassic to Cretaceous interval, and especially for the faults that show evidence of syn-depositional activity during the Late Jurassic and the Early Cretaceous.

C) Salt features

Zechstein salt features such as salt pillows, rollers, diapirs, walls, welds and feeders have been identified in the study area. Specific mapping of salt bodies along the Terschelling Basin margins and within the basin itself have been carried out during to better understand the relationship between active structures and the stratigraphy. Particular attention was spent on the salt bodies that were affecting the geometry and architecture of Upper Jurassic and Lowermost Cretaceous strata in the form of stratigraphic thinning, thickening, terminations characteristics (see below). Salt that affected the Upper Jurassic and Lowermost Cretaceous but did not pierce higher, were also identified.

D) Stratal termination interpretation

In addition to the interpretation of key horizons and structures, stratal terminations were identified and mapped within the Upper Jurassic Sequences 2 and 3. These include truncations, onlaps and downlaps, which are represented as black half arrows on the interpreted seismic panels.

E) Seismic flattening technique

Each interpreted regional seismic sections was also flatten onto the top of Sequence 3 to be able to have a more realistic display of the depositional geometry at the end of the Late Jurassic. This technique, is purely using vertical shifts and, therefore, is not perfect (it does not take into account time-depth variations nor horizontal movements) and does not replace a real structural restoration approach. Still this technique allows to observe more easily relevant stratigraphic geometries in basins where post-deposition deformation are prominent. It also permits to better evaluate subtle stratigraphic thickness variation and stratal terminations by correcting for post-depositional folding and faulting. For these flattened sections, the main Upper Jurassic horizons, faults active during the Late Jurassic and salt bodies present within the Upper Jurassic were interpreted. Stratal terminations were also added to highlight the main unconformities, onlaps and downlaps associated with key horizons.

In association with the regional seismic sections, regional stratigraphic correlations were constructed using the same wells shown in the corresponding seismic panels. The stratigraphic correlations are carried out for Upper Jurassic Sequences 1, 2 and 3.The stratigraphic correlations were carried out exclusively for the Upper Jurassic, and include key surfaces and lithostratigraphic units listed below :

Sequence 1:
Stratigraphic Marker S1 (base of Sequence 1)
In the TB this surface corresponds to the base of Main Friese Front Mb. The surface is the Mid Cimmerian Unconformity.

Sequence 2:
Stratigraphic Marker S2 (base of Sequence 2)
This horizon is either the base of the Friese Front Mb in the SE part of the study area, or the base of the Skylge Fm (Stratigraphic Marker A) in the rest of the TB.
Stratigraphic Marker A
This marker correspond to the base of the Oyster Ground Mb and the Skylge Fm.
Stratigraphic Marker B
This marker is an intra Oyster Ground Mb marker.
Stratigraphic Marker C
This marker correspond to the bases of the Terschelling Sandstone and the Noordvaardwer Mbs.
Stratigraphic Marker D
This marker is an intra Terschelling Sandstone and Noordvaardwer Mbs marker, and locally the top of the Terschelling Sandstone Mb.
Stratigraphic Marker F
This marker is an intra Noordvaarder Mb marker, and locally the top of the Terschelling Sandstone Mb.

Sequence 3:
Base of Sequence 3
This horizon, referred as Stratigraphic Marker G, is the base the Scruff Greensand Fm.
Stratigraphic Marker J
This marker is an intra Scruff Greensand Fm marker.
Stratigraphic Marker J20
This marker is an intra Scruff Greensand Fm marker and locally the base of the Lutine Fm.
Stratigraphic Marker L
This marker is an intra Scruff Greensand Fm marker and locally the base of the Lutine Fm.
Stratigraphic Marker M
This marker is the top of Sequence 3, the top of the Scruff Greensand and Lutine Fms.

Since some of this lithostratigraphic subdivisions are locally lateral and time equivalent of each other (e.g. Terschelling Sandstone Mb. transitions northward to the Lies Mb. within the TB), correlation heavily relies on age determination to identify primary correlation units. For work we used previously acquired palynological data (previous TNO reports) and new palynological data acquired in this study.

Standard well log correlation was applied using mainly GR and Sonic curves to correlate lithological variations between and within stratigraphic units. The main sandy intervals were highlighted for each well and correlated from well top when possible. Locally, this exercise is quite easy and strait forward.

In addition to the palynological, other correlation techniques were used. The stratigraphic correlations greatly benefit from having the seismic section equivalents (including flattened versions) that give additional and valuable information regarding the stratal geometry between wells, such as:
- Stratal thickening and thinning,
- Stratal pinch outs and drapes,
- Identification of truncations, onlaps and downlaps for top and base of Sequences 1, 2 and 3, as well as internally in these sequences,
- Presence of syn-depositional faults that locally affect the thickness of stratigraphic units,
- Presence of salt bodies that were active during deposition of given stratigraphic units.
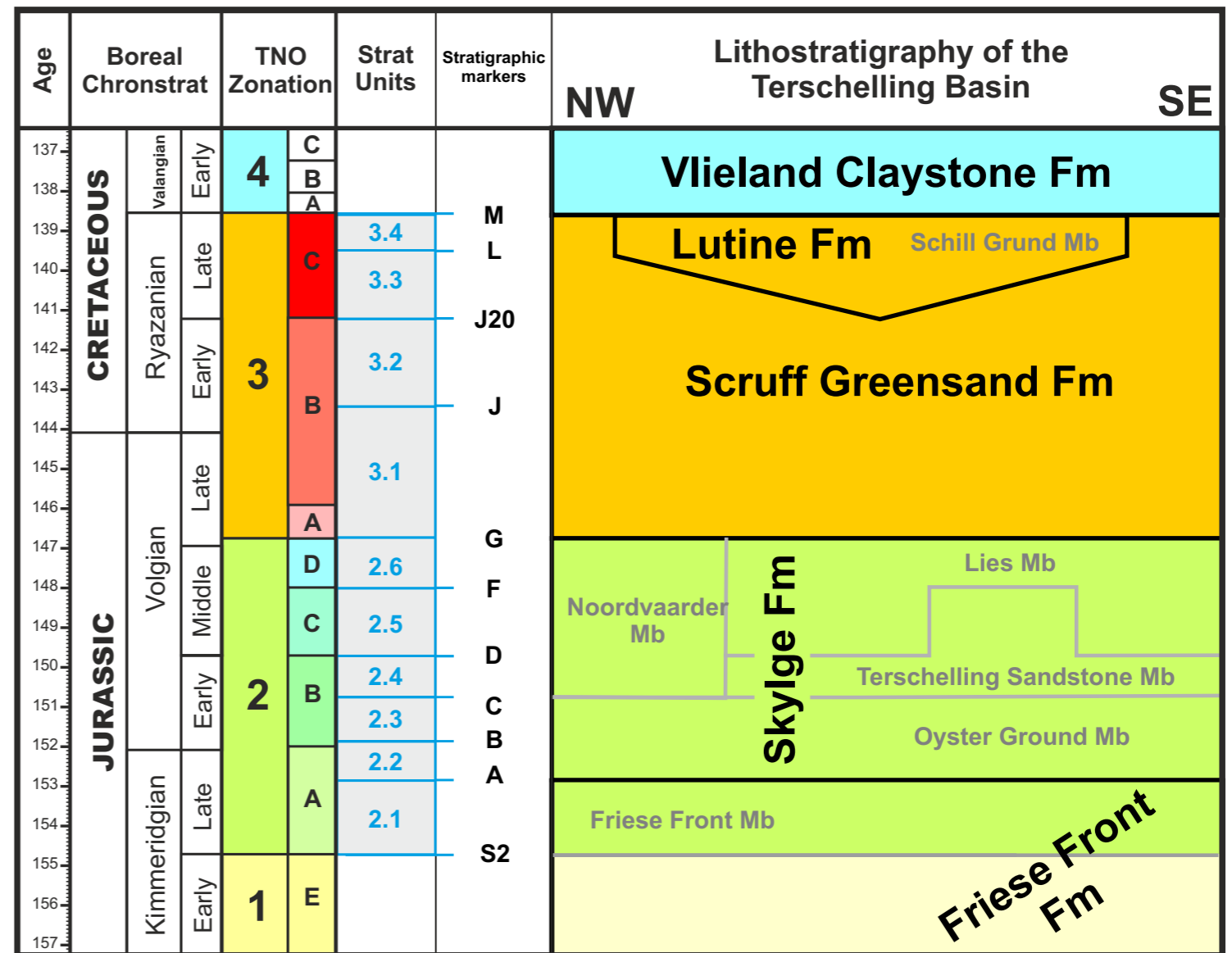
Figure 3.4.1: Chronostratigraphy and lithostratigraphy of the terschelling Basin used in this study. Note the stratigraphic markers (e.g. A, B or J20) that are also displayed in the regional stratigraphic correlations panels in this reports. Those markers bound stratigraphic units (e.g. 2.1 or 3.3).

Compared with its predecessor (the FOCUS Project of TNO, Bouroullec et *al.*, 2016), the Comma Project has included several mapping activity from a seismic perspective (time structure and time thickness mapping) to a well perspective (electrofacies/lithofacies mapping).

A)   Seismic mapping

After the seismic interpretation was completed using both 2D and 3D data (see Appendix A1), surfaces are created using convergent interpolation on a 100x100 m grid. The outline of each surface is manually set for the griding. Each time structure map is presented in the Chapter 4.2. After creating of the three surfaces for base Sequence 2, 3 and top of Sequence 3 (also referred as base Sequence 4), true stratigraphic thickness maps are created, results of these can be seen in Chapter 4.2.

B)   Isopach mapping

The thickness of each stratigraphic unit, defined at the well locations, is used to construct isopach maps for each unit. The time thickness maps derived from the seismic interpretation are used to add intra-well thickness trends in the isopach maps. Time thickness maps of Sequence 2

was used for Units 2.1 to 2.6 and Sequence 3 for Units 3.1 to 3.4.

C)   Lithofacies mapping

The addition to several intra-sequence markers (e.g. A, B or J20) allowed to define correletable stratigraphic units (e.g Units 2.1, 2.2 or 3.1) across the TB. By defining several types of lithofacies in the well database (Fig. 3.5.1), we produced ten lithofacies maps that are described in the discussion chapter (Chapter 4).

Seven lithofacies have been defined based of net-to-gross evaluation, using Gamma Ray and Sonic log information, between successive stratigraphic markers.
- Massive sandstone
- Massive sandstone (Noordvaarder Mb specific type)
- Massive mudstone
- Heterolithic lithofacies with 0 to 15% sand
- Heterolithic lithofacies with 15 to 40% sand
- Heterolithic lithofacies with 40 to 75% sand
- Heterolithic lithofacies with 75 to 100% sand

Figure 3.5.1 shows an example of lithofacies definition for three wells.
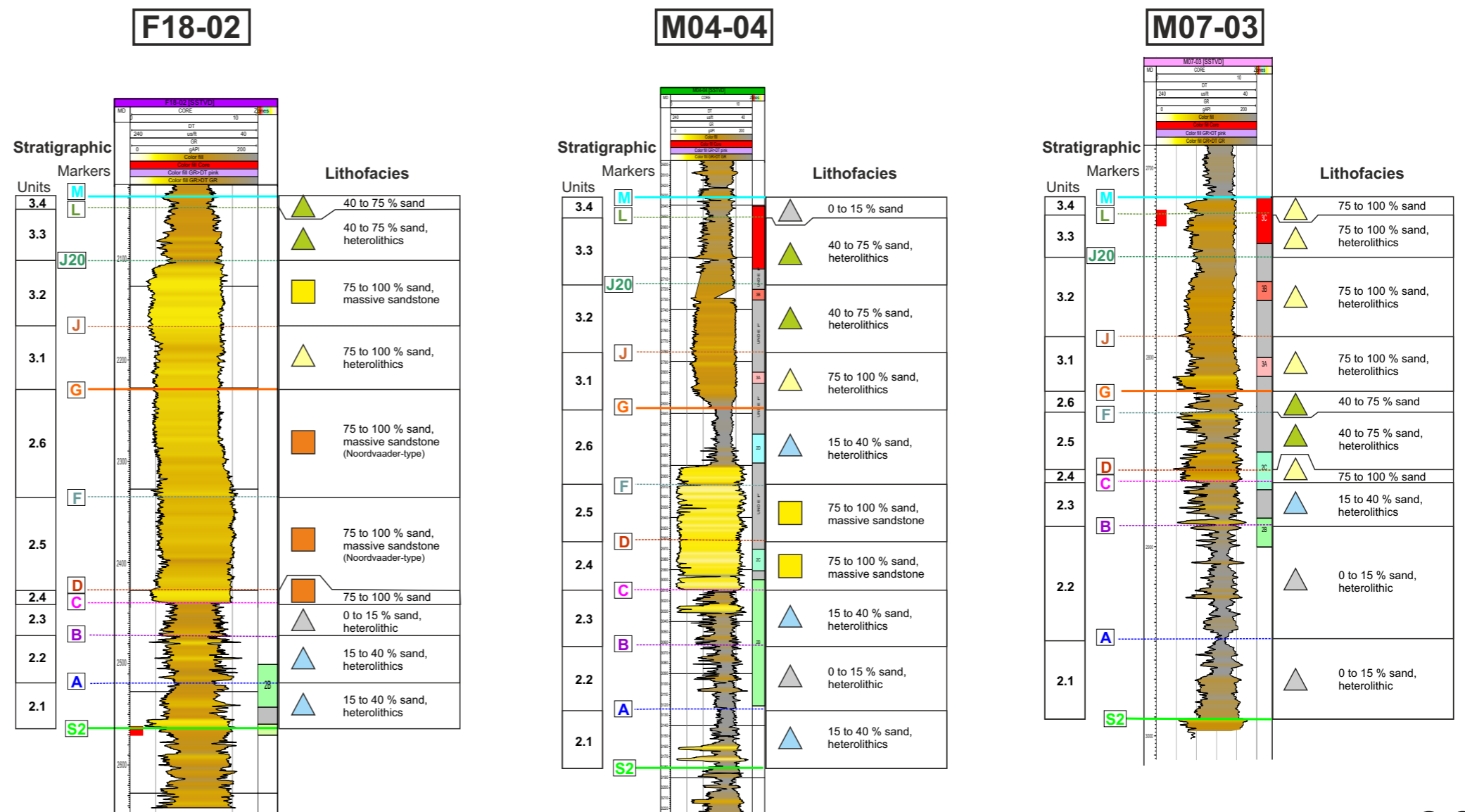
Figure 3.5.1: Example of lithofacies types for three of the wells studied. Note that each lithofacies is defined for each stratigraphic unit between two stratigraphic markers.

TNO innovation for life

The palynological results of 13 wells are displayed in summary diagrams (see Figure 4.1.1). The summary diagrams include: 1) a column with the measured depth along hole, 2) a column with the Gamma Log (from 0 to 300 API) and Sonic log (from 240 to 40 µS), 3) a column with the samples analyzed or reinterpreted for palynology, and 4) a column with zonal assignemnts (TNO zonation). The column with the samples provides information on the reliability of the interpretation. Core samples represent the best quality possible, side-wall core samples are second best, and cuttings samples represent the lowest quality. The tops and bases of zones and subzones are - per definition - linked to samples. Barren samples are 'flagged' with a blue square in the samples column. Note that the zonal assignments are based on the occurrences of fossil remains of organisms, such as dinocysts and pollen and spores. These occurrences depend on a number of variables, and should be interpreted with great care. The limits of confidence of the interpretations are discussed in the explanatory captions of the summary diagrams.

J ÑÖ	TNO Subzone	Top	Base
F18-03	4A	2412.00	2445.00
F18-03	3C	2454.00	2505.00
F18-03	3B	2520.00	2559.00
F18-03	3A	2571.00	2604.00
F18-03	2D	2631.00	2631.00
F18-03	2C	2640.00	2811.00
F18-03	2B?	2841.00	2841.00
F18-09-S1	3B	2290.00	2320.00
F18-09-S1	3A	2340.00	2340.00
F18-09-S1	2D	2395.00	2540.00
F18-09-S1	2C	2559.00	2684.60
F18-09-S1	2B	2684.70	2731.00
F18-09-S1	2A	2760.00	2880.00
F18-09-S1	PRECAL	2890.00	2921.00
G16-04	3C	3126.00	3159.00
G16-04	3B	3177.00	3195.00
G16-04	3A	3213.00	3231.00
G16-04	ND	3243.00	3253.00
G16-04	2D	3255.00	3255.00
G16-04	2C	3264.00	3309.00
G16-04	2B	3315.00	3342.00
G16-04	2A	3348.00	3372.00
G16-04	ND	3384.00	3384.00
G16-05	4A	2615.00	2615.00
G16-05	3C	2625.00	2680.00
G16-05	3B	2690.00	2740.00
G16-05	3A	2750.00	2750.00
G16-05	2D	2770.00	2770.00
G16-05	2B base	2940.00	2940.00
G16-05	2A	2960.00	2970.00
L06-02	3B	2245.36	2281.30
L06-02	3A	2289.50	2312.00
L06-02	2D	2326.00	2413.00
L06-02	2C	2432.00	2445.00
L06-02	2B	2465.00	2540.00
L06-02	2A	2594.00	2714.00
L06-03	3B	2028.90	2037.80
L06-03	3A	2041.55	2044.57
L06-03	2C	2082.00	2107.93
L06-03	2B	2109.70	2242.00
L06-03	2A	2256.50	2314.74

Well	TNO Subzone	Top	Base
L09-02	4D	2740.00	2850.00
L09-02	4B	2870.00	2920.00
L09-02	3C	2928.00	2970.00
L09-02	3B	2974.00	2995.00
L09-02	3A	3000.00	3024.00
L09-02	2D	3030.00	3034.00
L09-02	2B	3037.50	3047.00
L09-04	4B	3150.00	3162.00
L09-04	4A	3168.00	3168.00
L09-04	3C	3180.00	3182.00
L09-04	3B	3231.00	3231.00
L09-04	TRIASSIC	3243.00	3243.00
L12-03	3A	2358.00	2366.00
L12-03	2C	2374.00	2412.50
L12-03	2B	2425.00	2425.00
L12-05	3B - 3C	2578.50	2578.50
L12-05	2C	2589.50	2596.50
L12-05	ND	2605.00	2605.00
L12-05	2A	2612.50	2612.50
L12-05	1E - 2A	2620.50	2636.50
L12-05	ND	2639.50	2639.50
L12-05	1C	2648.20	2652.00
L12-05	1B	2653.00	2656.50
M01-01	2 D Top	2177.00	2256.00
M01-01	2 C Top	2272.00	2277.00
M01-01	2 B Top	2288.35	2351.00
M01-01	2 A Top	2357.00	2386.00
M04-05-ST	4B	2925.00	2965.00
M04-05-ST	4A	2975.00	2975.00
M04-05-ST	3C	2985.00	3040.00
M04-05-ST	3B	3060.00	3130.00
M04-05-ST	3A	3140.00	3160.00
M04-05-ST	ND	3180.00	3180.00
M04-05-ST	2D	3200.00	3200.00
M04-05-ST	ND	3210.00	3366.00
M07-07	4A	3935.30	3938.70
M07-07	3C	3939.75	3966.75
M07-07	3B	3969.65	3988.15
M07-07	3A	3997.00	4003.00
M07-07	2C	4012.00	4012.00
M07-07	2B	4018.00	4063.00
M07-07	2A	4072.00	4123.00
M07-07	1E - 2A	4141.00	4171.00

Table 4.1.1: Summary of results
Tabulated listing of the assignments of theTNO Subzones per well. Depths are in meters along hole.

Figure 4.1.1: Summary of results
The palynological results of well M01-01 show a complete Zone 2, including all Subzones. The base of the Terschelling Sandstone Member (Strat. marker C) coincides with Suzbone B. The sandy incursion of strat. marker F correlates to the middle of Subzone 2D. Note that a small section of Sequence 1 is present. This is inferred from the seismic. See insert map below for location

33
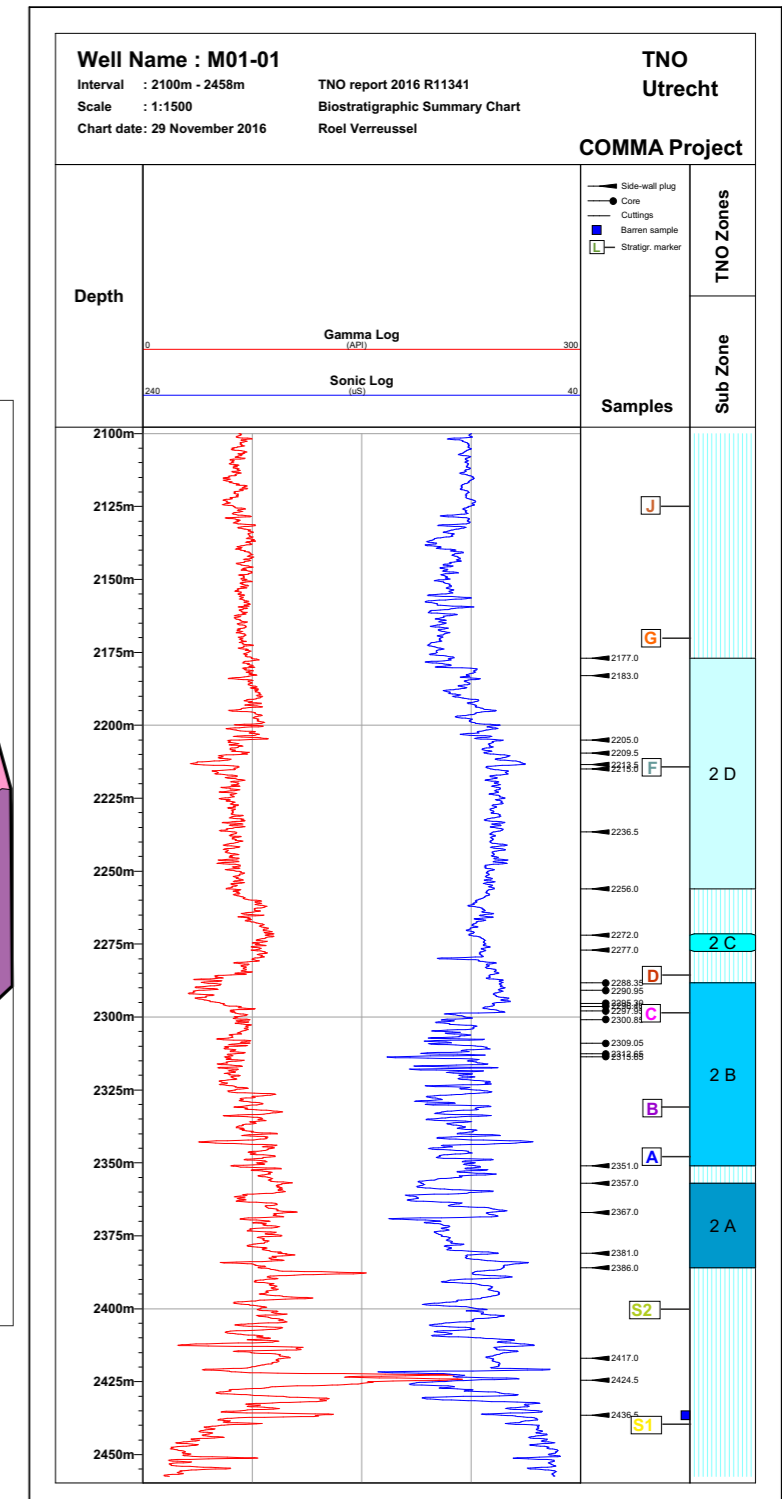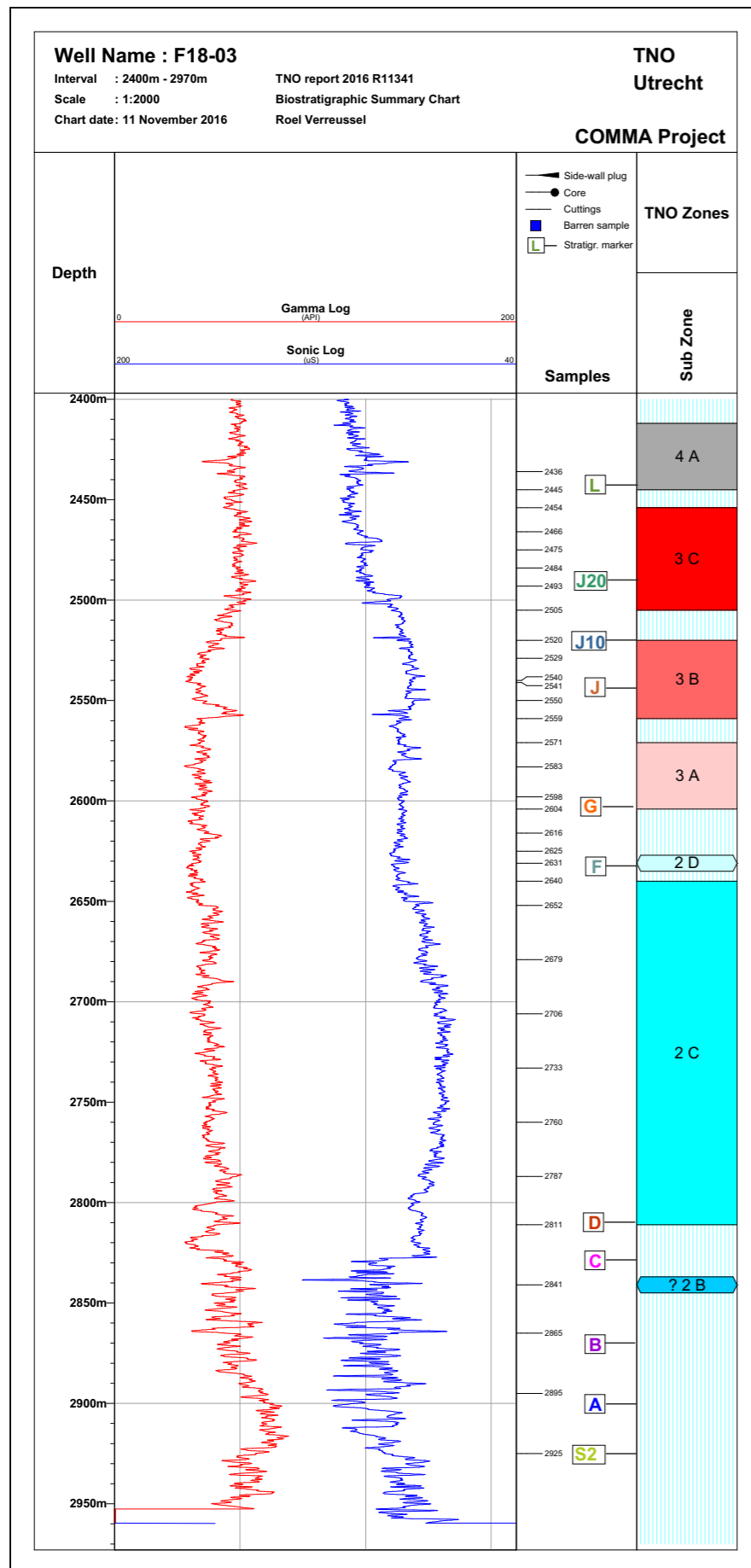
Fig. 4.1.2: Palynological results of F18-03

Although only cuttings samples are analysed, the sample resolution is high, and therefore the results are satisfying. Most noteworthy is the inconspicuous base of Sequence 3. The base of Sequence 3 is well established between 2604m and 2631m, and it is probably closer to 2604m than to 2631m, because of the sudden decrease in the relative amount of the dinocyst species *Cribroperidinium hansenii*. It is important to realize that in the F18 area, the Noordvaarder Mb grades into the Scruff Greensand Fm without a clear break and/or expression in the wireline logs. The palynological assemblages of the Lutine Fm (roughly corresonding to Subzone 3C) and the Scruff Greensand Fm (Subzones 3A and 3B) are rich and diverse compared to those of the Skylge Fm (corresponding to Subzones 2D, 2C and 2B).
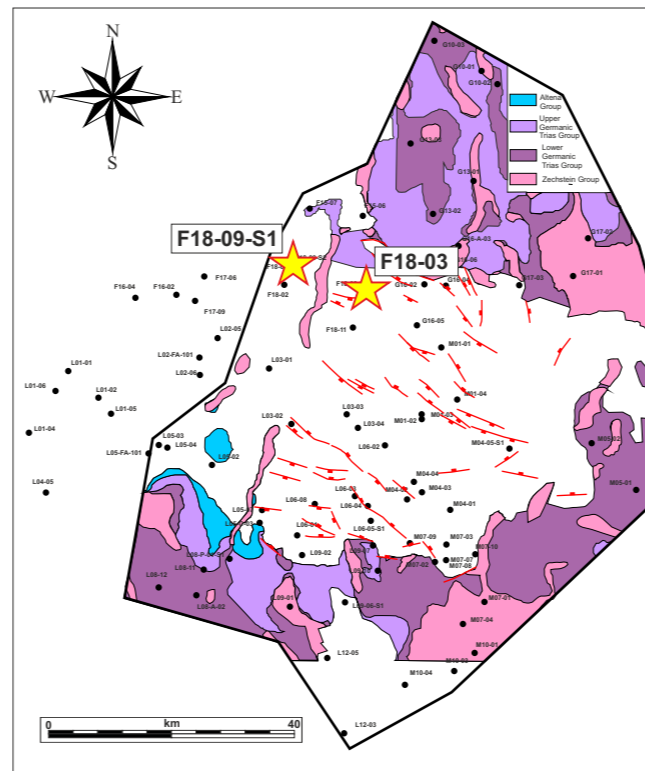
Fig. 4.1.3: Palynological results of F18-09-S1

Despite the large amount of core and side-wall core samples, the palynological results are disappointing: many samples are barren or nearly so. Nevertheless, the base of Sequence 3 (between 2345m and 2395m) is again inconspicuous, in the middle of a sandy sequence. The tops of Subzone 2C and 2B are 'delayed', the tops are too low because of the poor recovery. The base of the Noordvaarder always incepts within Subzone 2B. Note that abundant freshwater palynomorphs are recorded in the fine-grained sample 2632mCO, which is probably indicating lacustrine conditions.

34

Well Name : G16-04

Interval : 3100m - 3400m
Scale : 1:1500
Chart date: 02 November 2016

TNO report 2016 R11341
Biostratigraphic Summary Chart
Roel Verreussel

TNO Utrecht

COMMA project

Depth

Side-wall plug
Core
Cuttings
Barren sample
Stratigr. marker

Gamma Log (API) 0 — 300
Sonic Log (uS) 240 — 40

TNO Zones

Samples

Zone
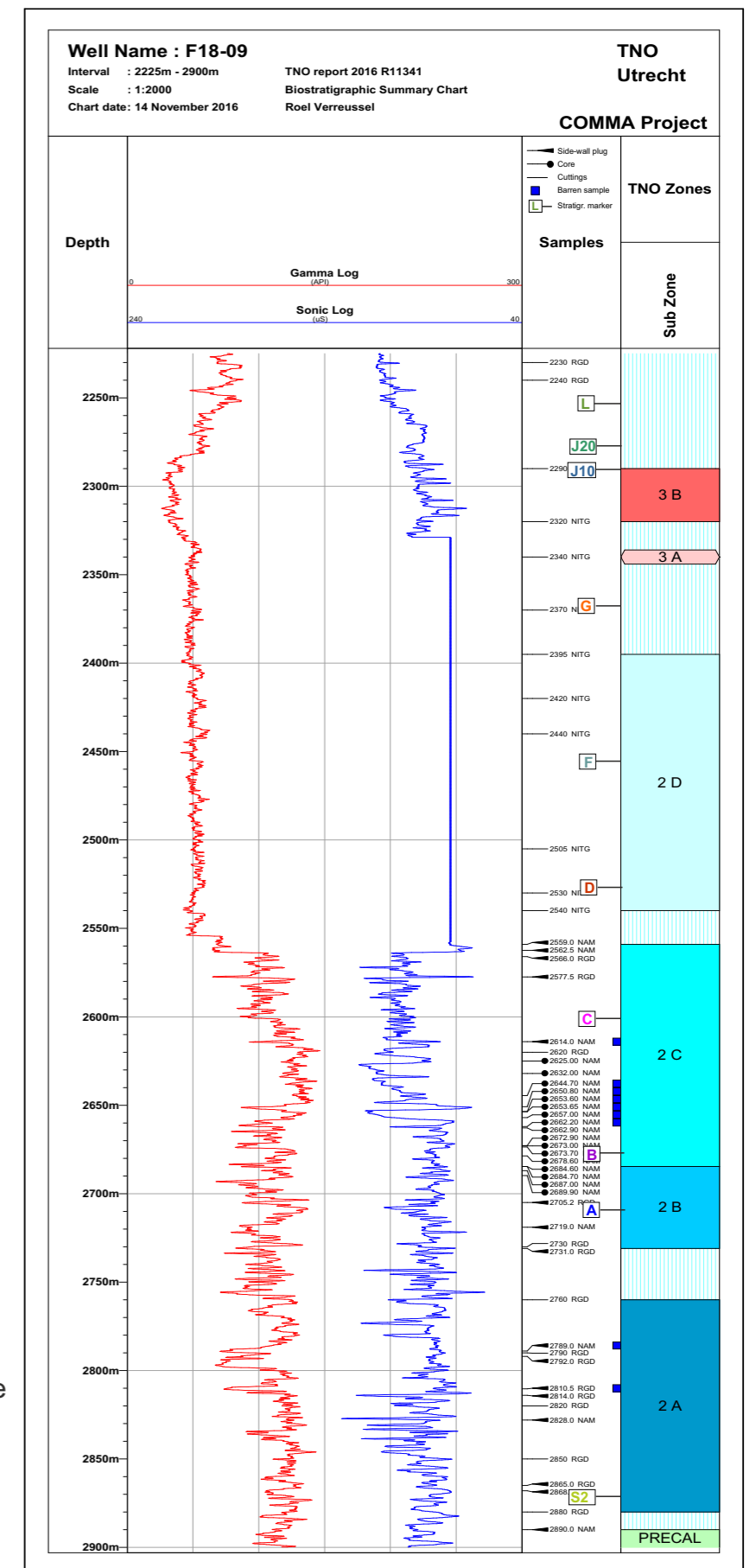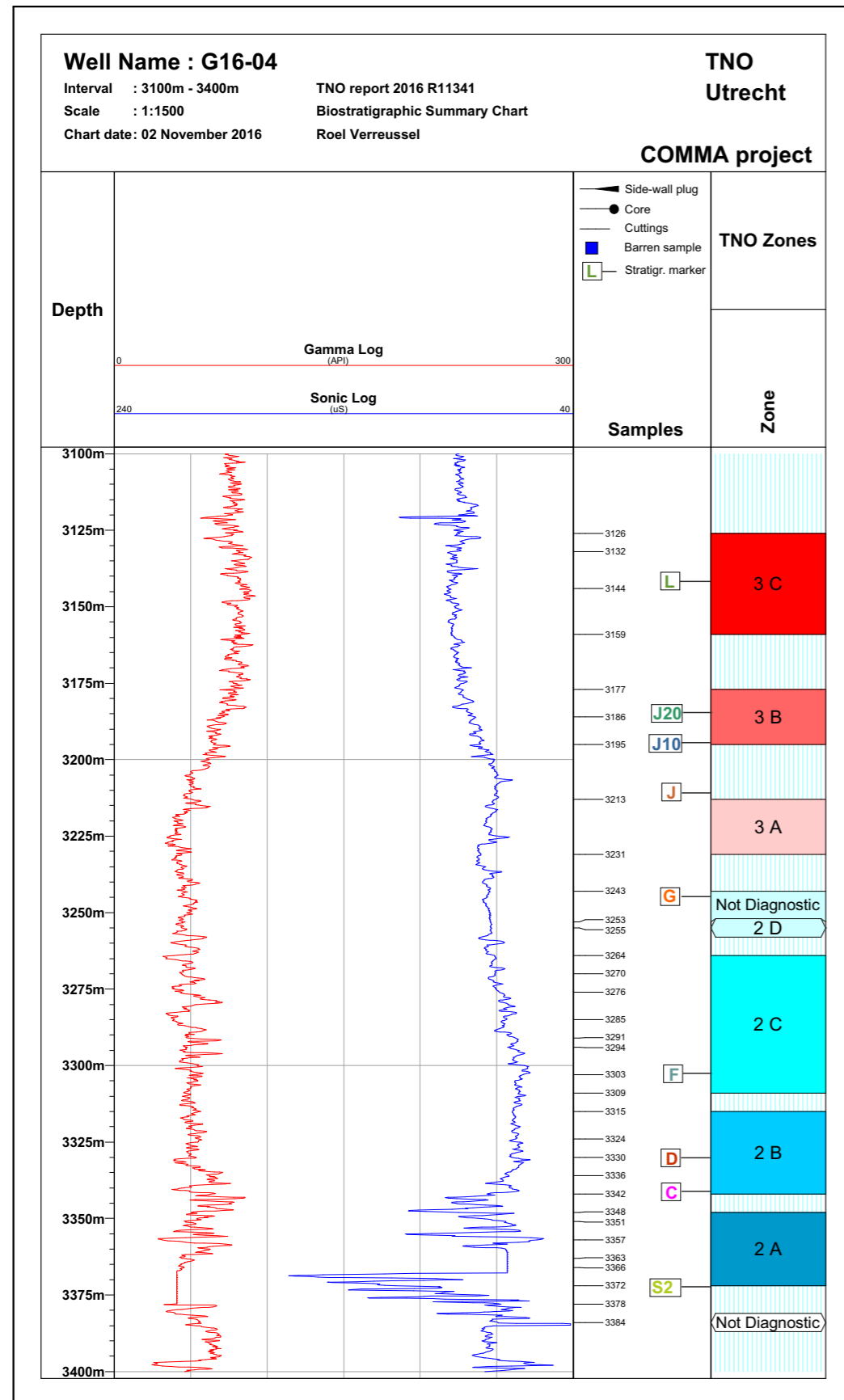
Fig. 4.1.4: Palynological results of G16-04
Only cuttings samples are analysed but the sample resolution is high. The base of Sequence 3 is - again - transitional and it is difficult to detect a change in the GR or DT. The base of the Noordvaarber Mb lies in Subzone 2B. The GR and DT signature of the base of the Noordvaarder is displaying a typical 'pulsating' character, that can be observed in F18-03 as well. The Noordvaarder (Subzones 2D, 2C and 2B) is marine, but the diversity of the dinocyst assemblages is low. Subzone 3C is very muddy. See insert map for location.
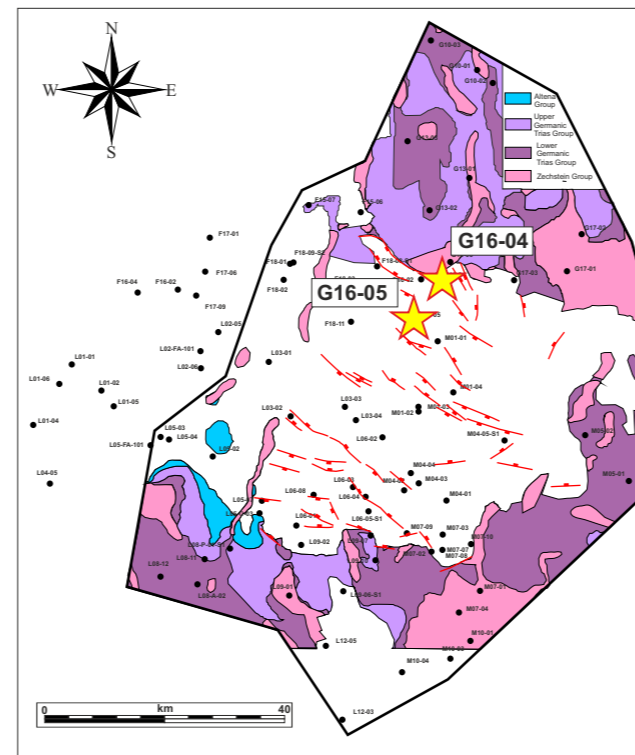
Fig. 4.1.5: Palynological results of G16-05
The cuttings samples are not fully analysed but scanned quickly for marker species. Like in well G16-04, Subzone 3C is very muddy. The Skylge Fm (Subzones 2A, 2B, 2C and 2D) shows an intermediate character between a typical "Noordvaarder" style (e.g. G16-04) and a typical "Terschelling Sandstone" style (e.g. L06-02). See insert map for location.

Well Name : G16-05

Interval : 2580m - 3000m
Scale : 1:1500
Chart date: 11 November 2016

TNO report 2016 R11341
Biostratigraphic Summary Chart
Roel Verreussel

TNO Utrecht

COMMA Project

Depth

Gamma Log (API) 0 — 300
Sonic Log (uS) 240 — 40

TNO Zones

Sub Zone

Events

Top of Tehamadinium daveyi
Top of Endoscrinium pharo, Top of Batioladinium cf. varigranosum, Top of aff. Daveya boresphaera
Top of Rotosphaeropsis thula
Top of Systematophora daveyi
acme Cribroperidinium hansenii
Top of Dichadogonyaulax pannea, Top of Dingodinium tuberosum
Base of common Classopollis
Top of common Perinopollenites spp.
Top of Densoisporites minor

35

Fig. 4.1.6: Palynological results of M07-07
The additional analyses performed on the cuttings samples revealed an almost complete Sequence 2. A small hiatus is present between the base of the Scruff (Subzone 3A) and the Terschelling Sandstone (Subzone 2C and the top of 2B). Sedimentary log descriptions of the cored section 3989m - 3936m indicate lower shoreface environments, which is corroborated by the palynological analyses. See insert map for location.
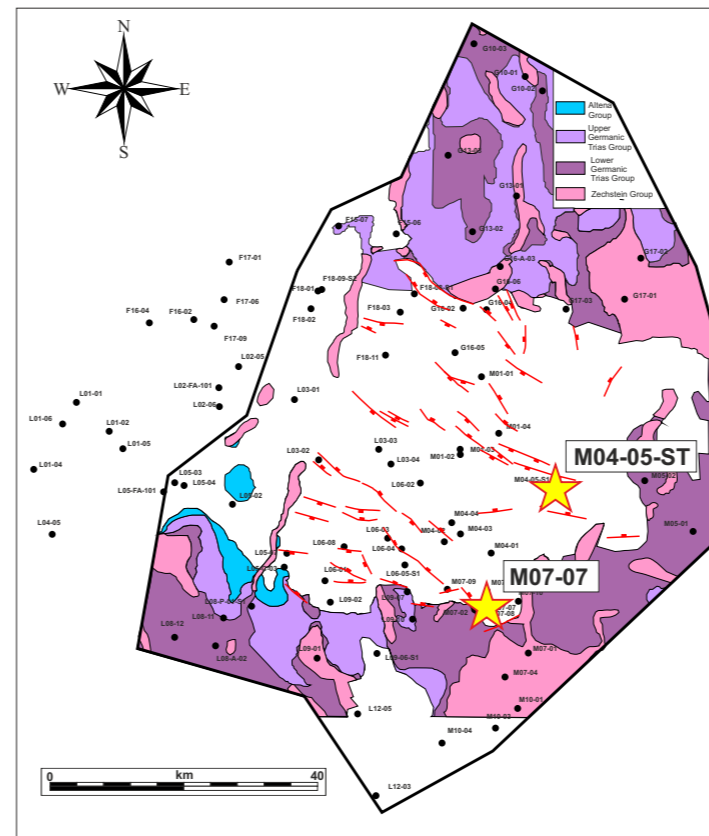
Fig. 4.1.7: Palynological results of M04-05-ST
The Scruff Greensand Fm is very thick in this well and a rapidly coarsening upward base, followed by a very slow and gradual fining upward part. Note the 'kick' in the wireline log at 3018m. This feature is observed in several wells in the Terschelling Basin and probably represents sea level variation. See insert map for location.

Well Name : L06-03
Interval : 1950m - 2360m
Scale : 1:1500
Chart date: 15 November 2016
TNO report 2016 R11341
Biostratigraphic Summary Chart
Roel Verreussel
TNO Utrecht
COMMA Project
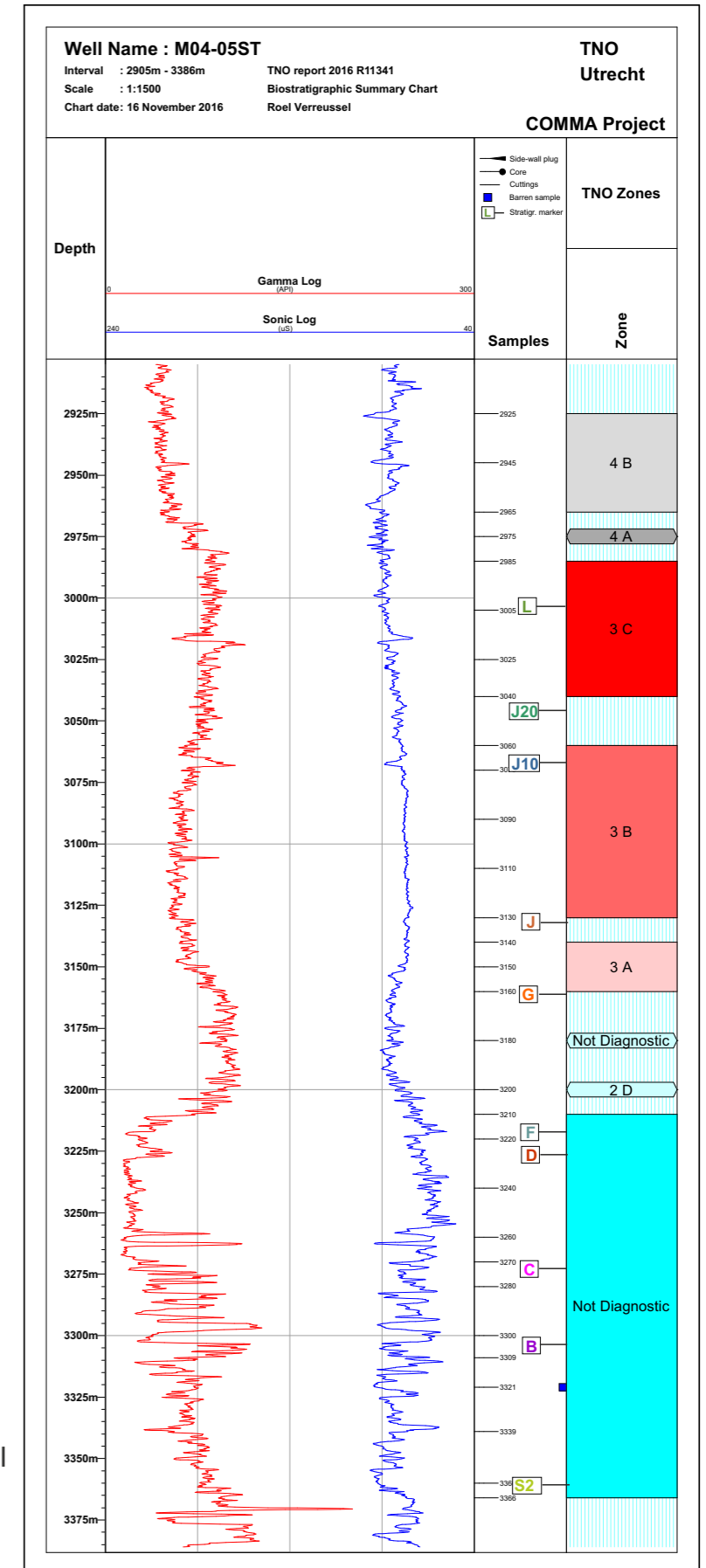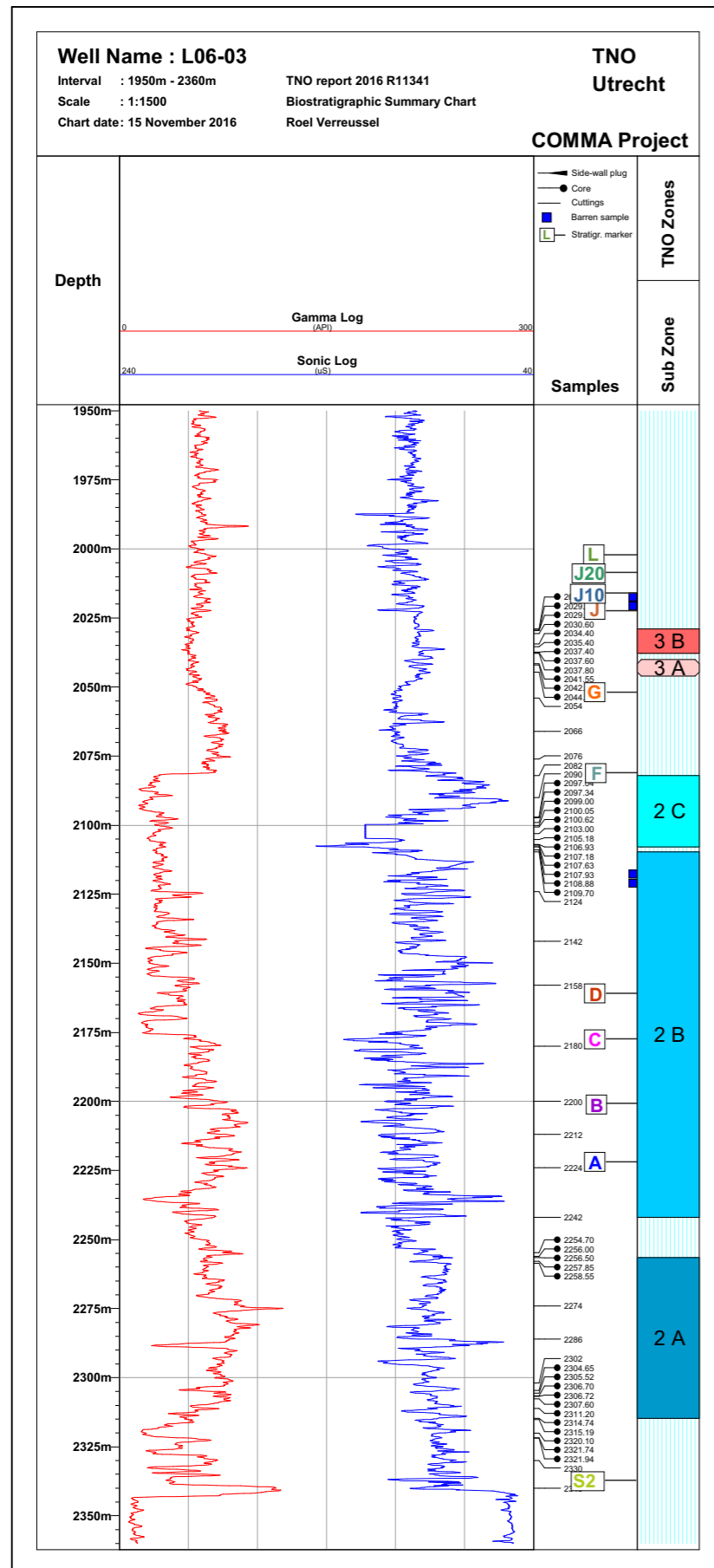
Fig. 4.1.8: Palynological results of L06-03

Cored sections are present in the Scruff Greensand Fm, in the Terschelling Sandstone Mb and in the Friese Front Fm. Sedimentary log descriptions of the cored interval 2095m - 2111m (FOCUS Report, Bouroullec et *al.*, 2016) indicate a transition from back-barrier washover fans (2111m - 2100.75m) to lower shoreface (2100.75m - 2097.5m) to upper shoreface (2097.5m - 2095m). This well nicely exemplifies the amalgamated type of Terschelling Sandstone Mb, typical for a broad ESE - WNW oriented belt. The upper part of the Terschelling Sandstone Mb is of Middle Volgian age (Subzone 2C), the lower part is of Early Volgian age (Subzone 2B). The upper part correlates with the shaly interval 2415m - 2460m of well L06-02. Note that the Scruff Greensand Fm is relatively thin and that the GR values are relatively high, due to the glauconite content. Also note that the occurrences of the euryhaline dinocyst species *Subtilisphaera paeminosa,* in the cored intervals 2254m - 2258m and 2304m - 2314m, indicate (weak) marine influence in the Friese Front Fm. Late Volgian index ammonites have been recovered from the cored Scruff Greensand interval (Abbink et al., 2001). See insert map for location.
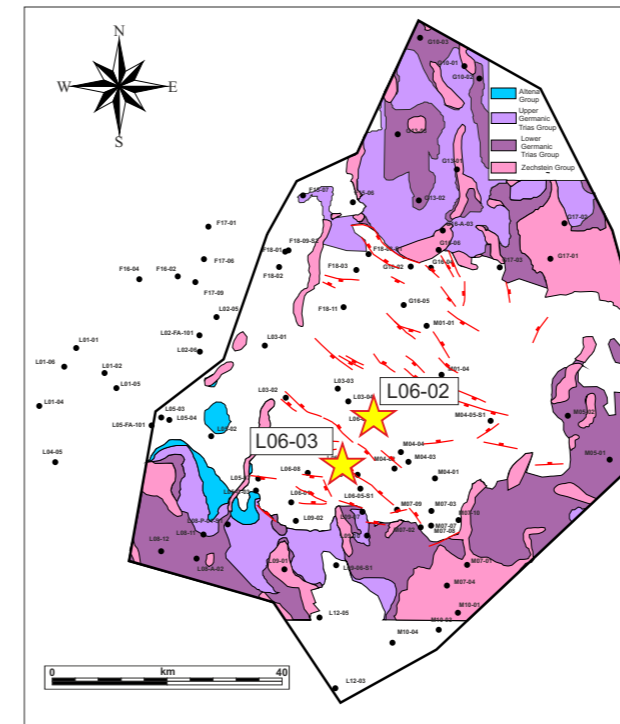
Fig. 4.1.9: Palynological results of L06-02

Cored sections are present in the Scruff Greensand Fm and in the Terschelling Sandstone Mb. Sedimentary log descriptions of the cored interval 2504m - 2464m indicate a transition from lower shoreface (2504m - 2497m), to tidal inlet and shoreface (2497m - 2474m), to tidal channels and lagoons (23474m - 2464m). Lagoonal environments for the top of the Terschelling Sandstone are also inferred from the palynological results. The Scruff Greensand is deposited in an offshore, lower shoreface environment (FOCUS Report, Bouroullec et *al.*, 2016). Early Ryazanian and Late Volgian index ammonite species have been recovered from the cored Scruff Greensand interval (Abbink et al., 2001). See insert map for location.

Well Name : L06-02
Interval : 2180m - 2744m
Scale : 1:2000
Chart date: 15 November 2016
TNO report 2016 R11341
Biostratigraphic Summary Chart
Roel Verreussel
TNO Utrecht
COMMA Project
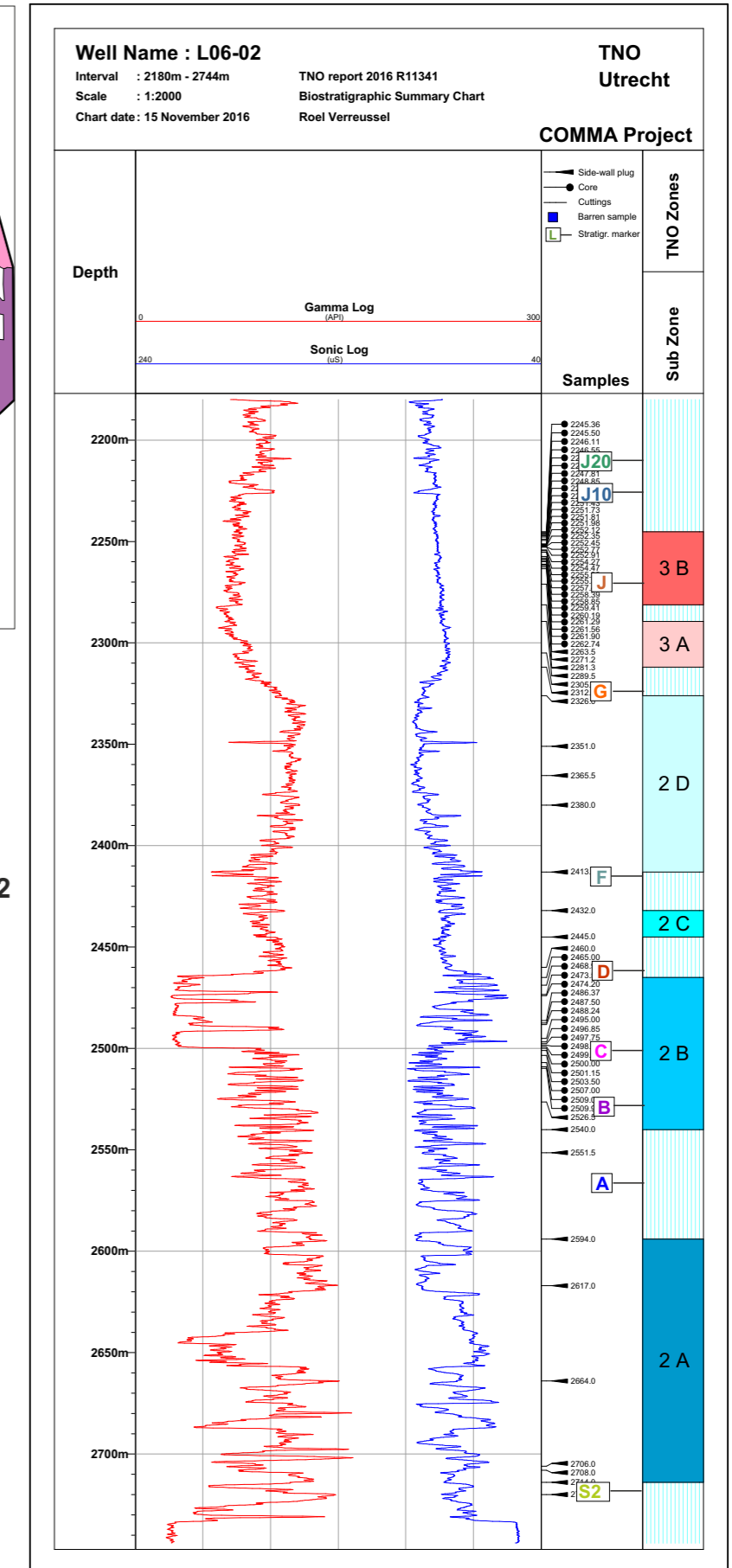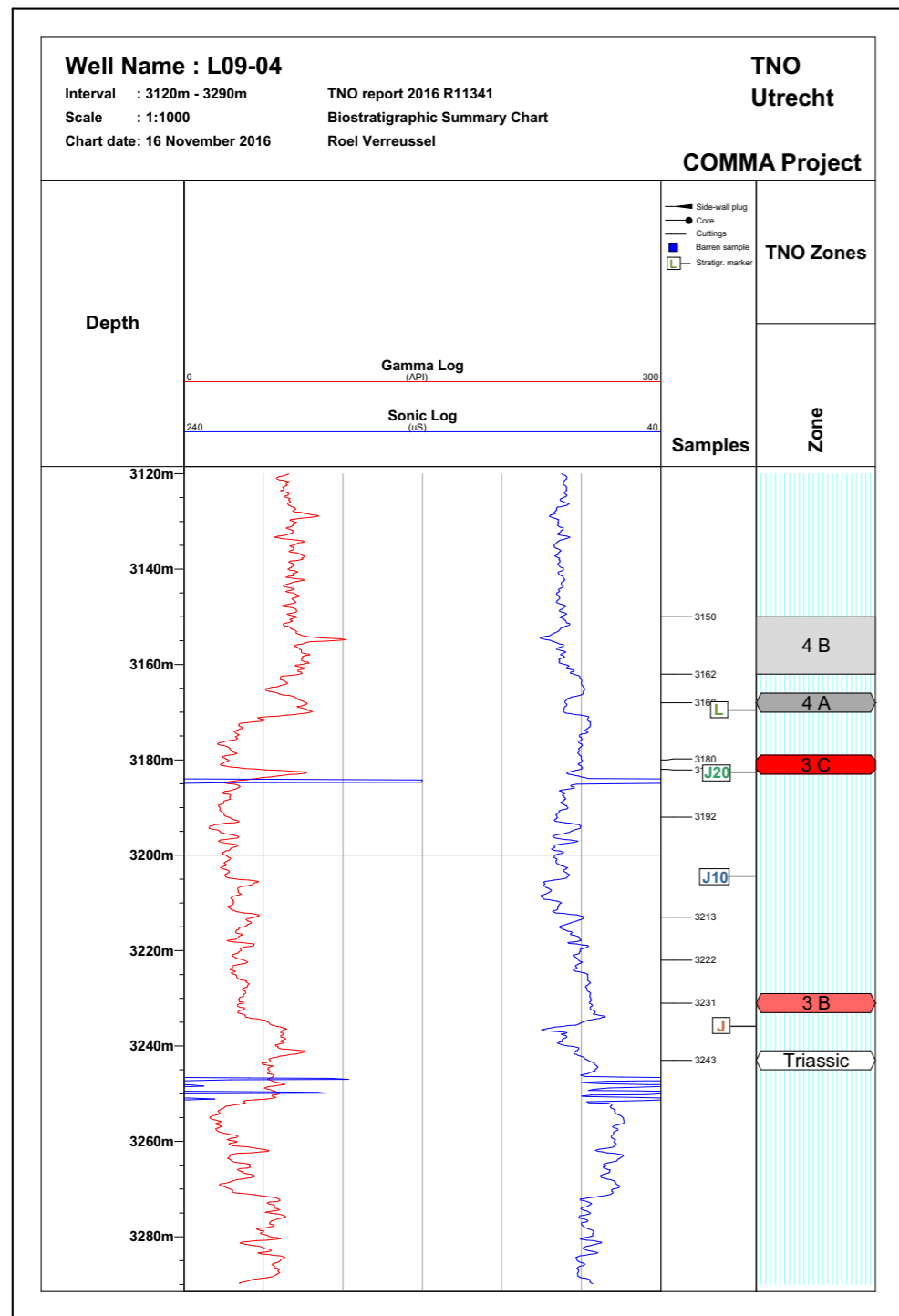
Fig. 4.1.10: Palynological results of L09-04
Only a few cuttings samples are studied. The results indicate a 65m thick stack of Sequence 3 (Scruff Greensand Fm). The base of Sequence 3, Subzone 3A is lacking. Nevertheless, it is obvious that active subsidence took place at this site during most of the Ryazanian. The Scruff Greensand remains sandy all the way to the top, probably indicating shoreface environments throughout. See insert map for location.
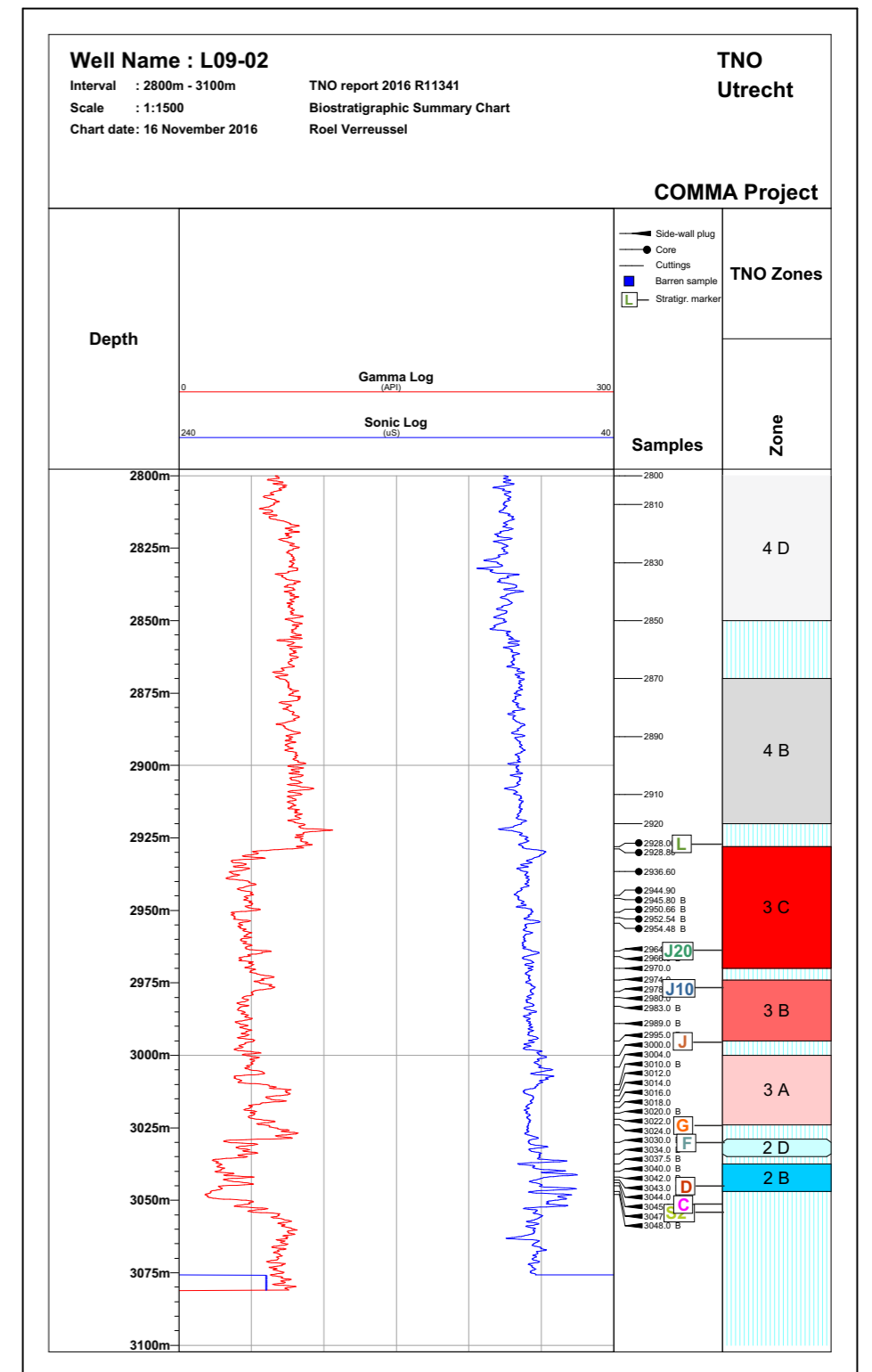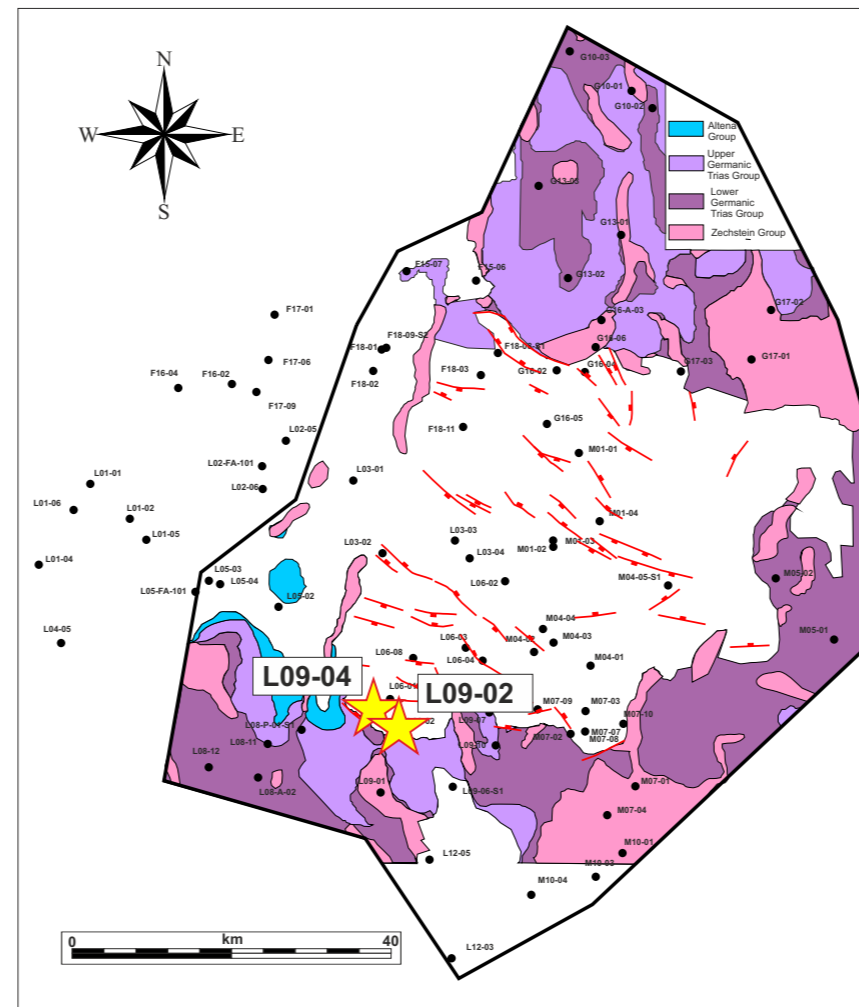
Fig. 4.1.11: Palynological results of L09-02
A cored section is present in the upper part of the Scruff Greensand Fm and many side-wall core samples in the lower part of the Scruff Greensand and in the Terschelling Sandstone Mb. The entire Sequence 3 is represented, Subzones 3A, 3B and 3C. Below the Scruff Greensand, a 20 meters thick Terschelling Sandstone interval is present, with no fine-grained clastics in between. The base of the Scruff Greensand is an almost symmetrical coarsening upward - fining upward unit of approximately 15 meters. See insert map for location.

38
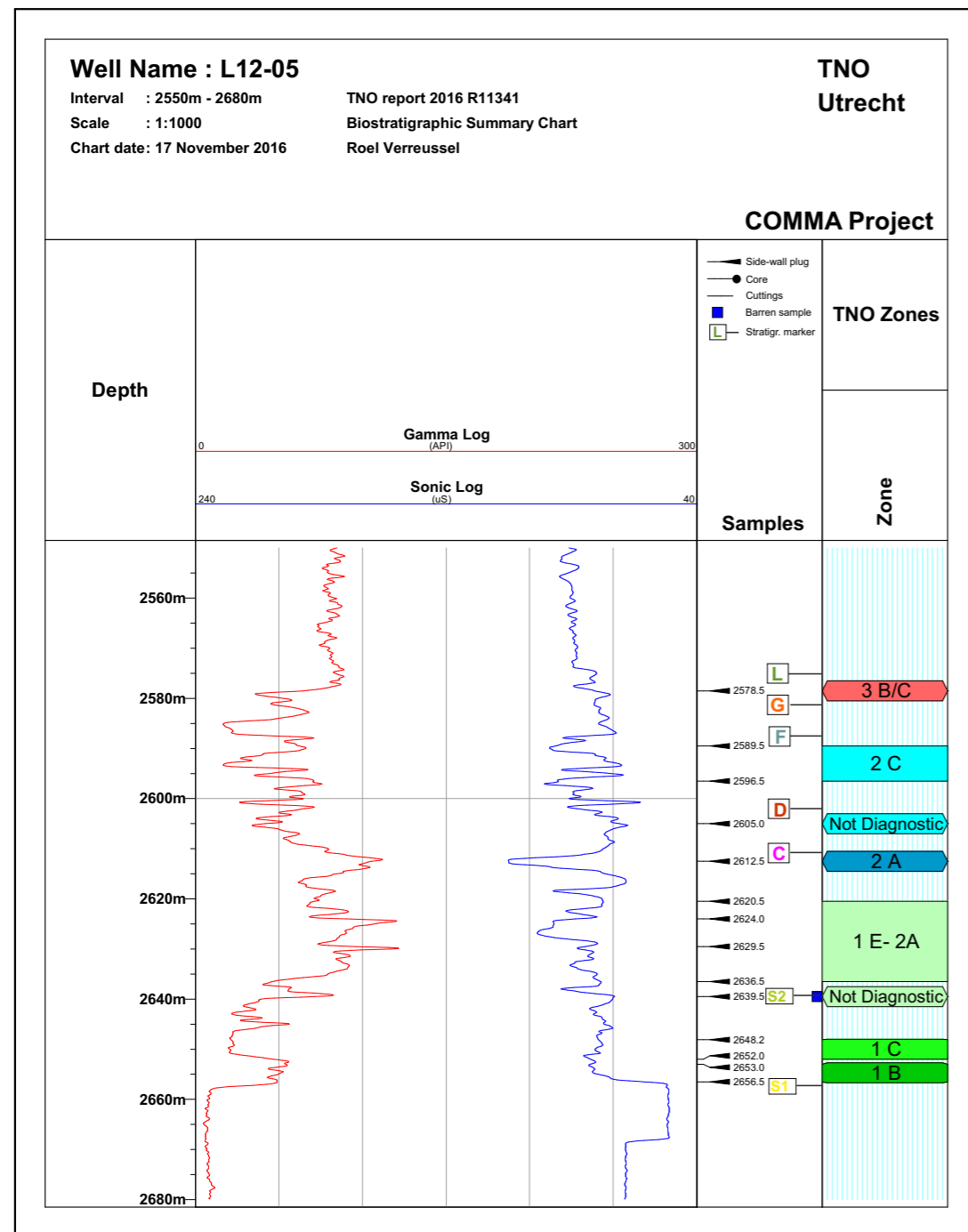
Fig. 4.1.12: Palynological results of L12-05
L12-05 is interesting because it contains a caprock section on top of a salt diapir. The side-wall core samples provide a reliable age interpretation. The base of the caprock section could be assigned to Subzone 1B and is marine. Marine sediments of the same age are also encountered in the caprock of the G16A field on the Schill Grund Plateau. This implies that during the Late Callovian or Early Oxfordian the sea extended across much of the Hantum Fault Zone and Schill Grund Plateau. Another marine transgression is recorded in the interval 2589.5m - 2596.5m, correlating to the upper part of the Terschelling Sandstone Mb in the Terschelling Basin. See insert map for location.
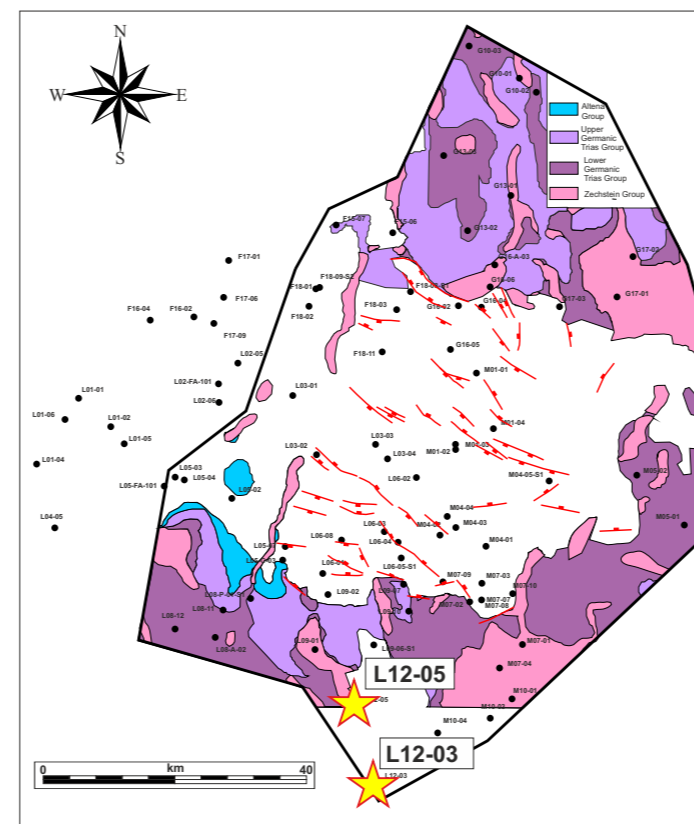
Fig. 4.1.13: Palynological results of L12-03
Only a couple of side-wall core samples are studied. Nevertheless, the results provide interesting information on the age of the interval 2375m - 2425m. The relatively 'clean' sand at the base of that interval (2425m - 2417m) is assigned to Subzone B, probably indicating that the sand correlates with the base of the Terschelling Sandstone Mb. The coarsening upward interval above the sand (2417m - 2375m) is assigned to Subzone 2C, indicating that this part correlates with the upper part of the Terschelling Sandstone Mb. See insert map for location.
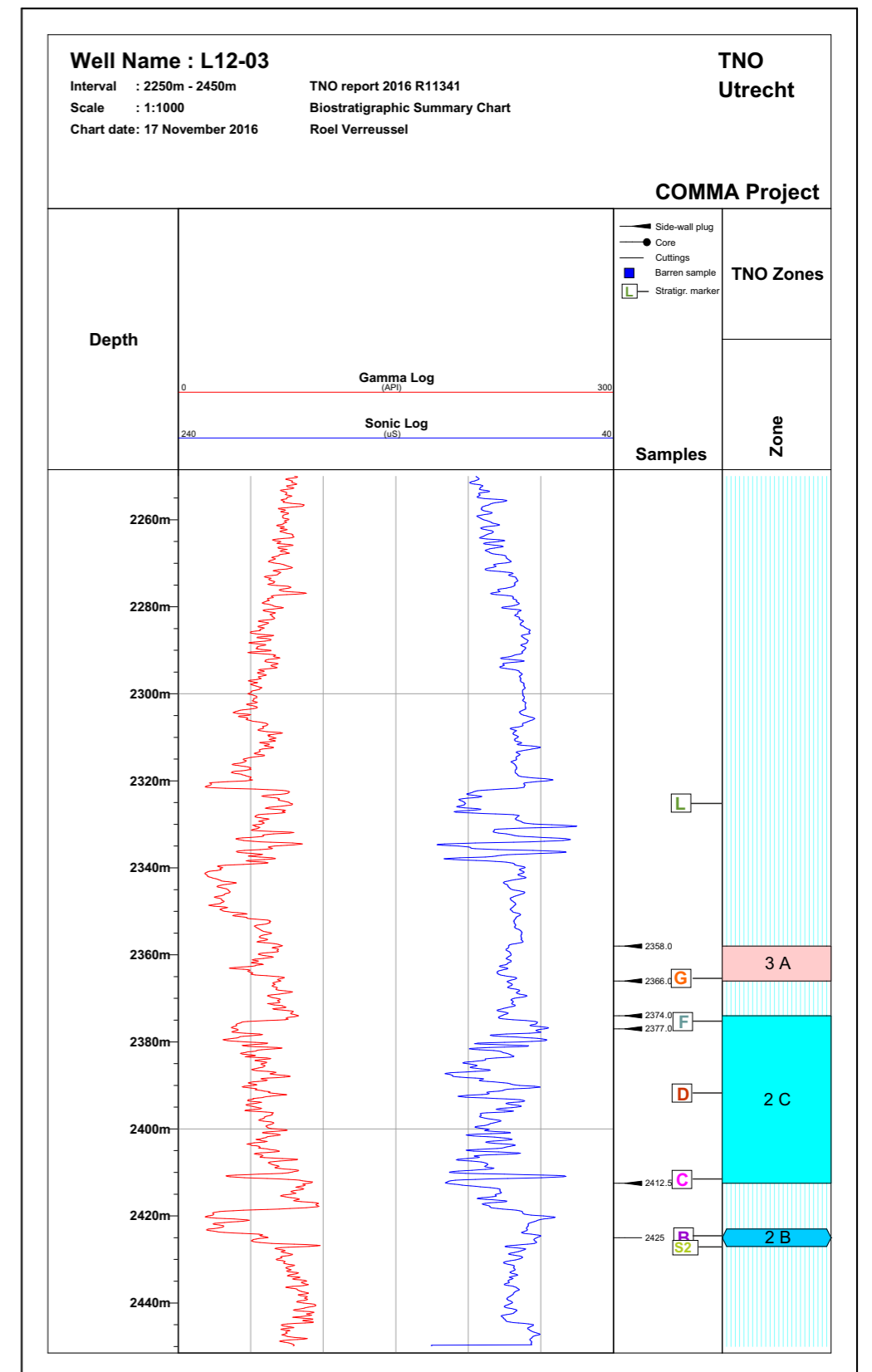
To characterize the Upper Jurassic - Lowermost Cretaceous in the Terschelling Basin (TB), a seismic analysis was performed using 2D and 3D seismic data. Three Upper Jurassic and Lowermost Cretaceous horizons were correlated in 3D across the TB. The time structures maps and time thickness maps are presented in this chapter as well as four regional 2D seismic panels. The structural analysis was also conducted with the mapping of (1) the base Rijnland Group subcrop, 2) salt features, 3) syn-depositional faults active during the Late Jurassic and Ryazanian.

The seismic interpretation and the mapping of three key surfaces (S2, S3 and S4) was done in parallel with a structural analysis that focused on salt features (autochthonous and allochthonous) as well as syn-depositional faults that where interpreted as being active during the period of interest (Upper Jurassic to Lowermost Cretaceous). In this section the results of these analysis are shown in the form of summary maps for 1) the base Rijnland Group subcrop map (Fig. 4.2.7); 2) the salt bodies (Fig. 4.2.8); 3) the syn-depositional fault map (Fig. 4.2.9); 4) the time structure map pf the base Sequence 2 (Fig. 4.2.10), 5) the time structure map the base Sequence 3 (Fig. 4.2.11); 6) the time structure map the top of Sequence 3 (Fig. 4.2.12); 7) the time thickness map of Sequence 2 (Fig. 4.2.13); and 8) the time thickness map of Sequence 3 (Fig. 4.2.14).

A) Regional seismic transects

Four regional seismic panels (Panels H, I, J and K) have been constructed and interpreted in this study (Fig. 4.2.3 - 4.2.7). They were selected to better illustrate the geometry and tectono-stratigraphy of Upper Jurassic - Lowermost Cretaceous. Three of those panels cross-cut the basin in NNE-SSW (Panels I and J) and NNW-SSE (Panel H) trends and one (Panel K) was selected to illustrate the basin margins specifically, by circling the basin along its north, east and south margins. Note that the same transects are also used for the stratigraphic correlations presented in Section 4.3. The complete panel displays (including interpreted seismic section, flatten seismic section and stratigraphic correlation) are shown in Appendix A2. Below is the list of wells that are included for each panel:
- Panel H: F18-02, F18-11, G16-05, M01-01, M01-04, M04-05-S1, M05-01;
- Panel I: L05-C-03, L05-07, L03-02, L03-01, F18-11, F18-03, F18-08-S1, G10-01;
- Panel J: G17-02, G17-03, M01-04, M01-03, M01-02, M04-04, M04-02, L09-10, L09-06-S1, L12-05, L12-03;
- Panel K: G16-04, M04-05-S1, M07-07, M07-03, M04-02, L06-05, L0902, L0601, L05-07, L05-02, L05-04, L05-03, L01-05, L01-02.

Three additional regional panels (Panels A, B and D) from the FOCUS Project (Bouroullec et al., 2016) have also been used in this study since they intercept the TB (Fig. 4.2.1). These three panels are shown in Appendix A3. They have not been updated using the results of this study. Below is the list of wells that are included for each panel:
- Panel A1: F17-06, F17-05, L02-05, L03-01, L03-03, L03-04, L06-02, M04-04, M04-03, M04-01,(M08-02), M07-03, M07-07 and M07-01;
- Panel A2: F17-06, F17-05, L02-05, L03-01, L03-03, L03-04, L06-02, M04-04, M04-03, M04-01, M07-03, M07-07, M07-08, M07-01;
- Panel B: G13-02, G16-03, G16-04, G16-05, L03-04, L06-03, L09-02, L09-01;
- Panel D: E18-01, E18-07, F16-A-05, F16-04, F16-02, F17-04, F17-09, F17-05, F18-02, F18-01, F18-09-S1, F18-03, F18-08, G16-02, G16-04, G17-03, G17-01, G17-02.

The location maps (Figure 4.2.1) shows the location of each of the regional panels.
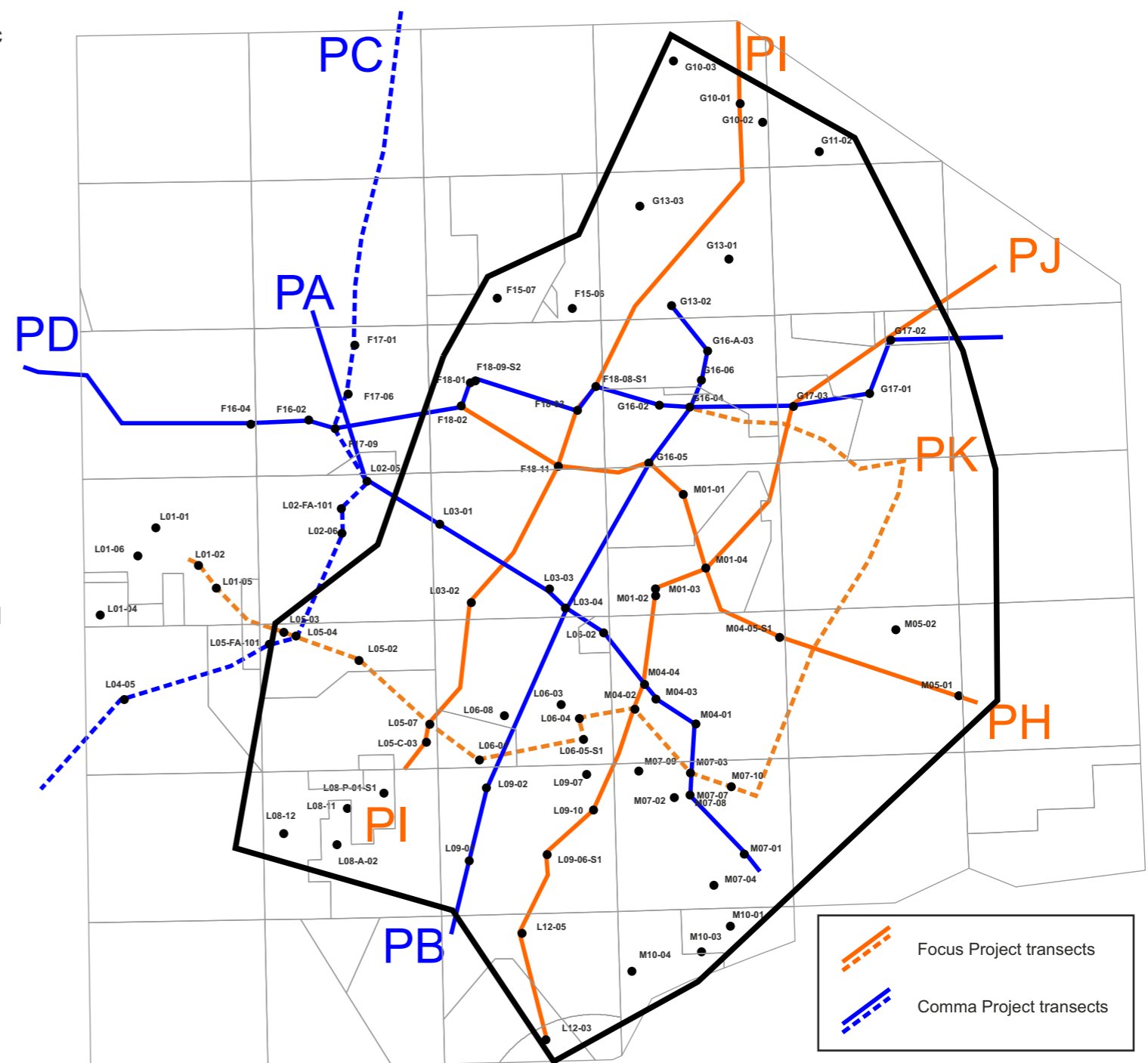
Figure 4.2.1: Location maps of the four regional 2D seismic panels used in this study.

Seismic panel

- Salt body
- Salt feeder
- Salt weld

— Base of Chalk Group (Upper Cretaceous)

Sequence 3 (Upper Jurassic-Lower Cretaceous)

Sequence 2 (Upper Jurassic)

Sequence 1 (Upper Jurassic)

— Top of Lower Triassic (Lower Germanic Trias Group)

Zechstein (Lower Germanic Trias Group)

- / Fault
- Onlap
- Truncation
- Downlap

Stratigraphic correlation panels

- Sand-rich interval
- S3 / S2 / S1 Shale-rich intervals
- — Top of Sequence 3

M-------
L-------
K10-------
K-------
J20-------
J10-------
J-------
Intra-Sequence 3 stratigraphic markers

G— Base of Sequence 3

F10-------
F-------
D-------
C-------
B-------
A-------
Intra-Sequence 2 stratigraphic markers

— Base of Sequence 2
— Base of Sequence 1

Salt body

Cored interval

- / Fault
- Onlap
- Truncation
- Downlap

Figure 4.2.2: Legend for seismic panels (Figures 4.2.3 to 4.2.7) and correlation panels (Figures 4.3.1 to 4.3.4).
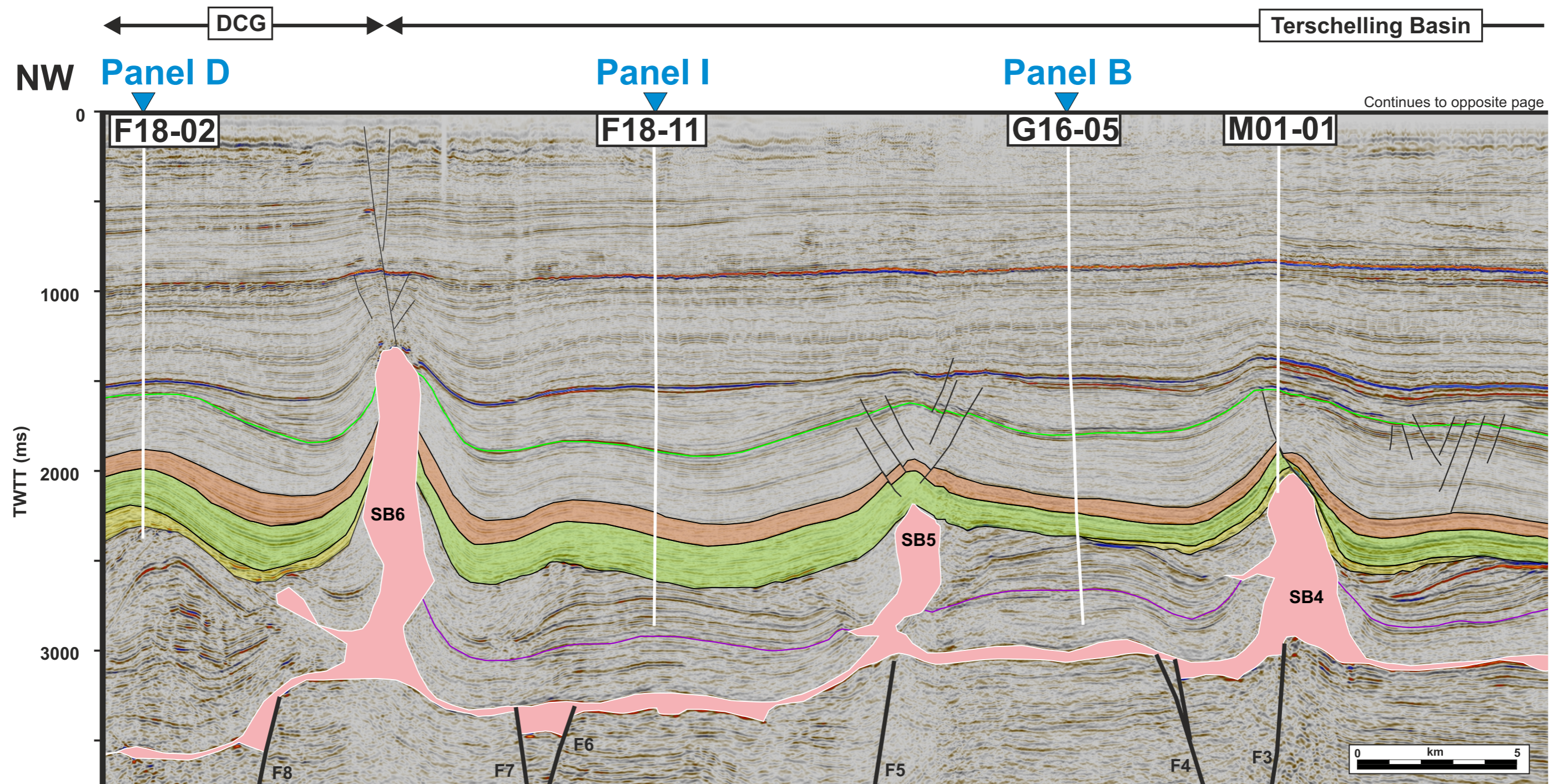
Figure 4.2.3: Interpreted seismic section H is trending NW-SE and is located across three structural provinces, namely from NW to SE, the Dutch Central Graben (DCG), the Terschelling Basin and the Ameland Block. This seismic section is 90 km long. It intercepts one wells in the DCG (F18-02), five wells in the TB (F18-11, G16-05, M01-01, M01-04, and M04-05-S1) and one well on the Ameland Block (M05-01). See Fig. 4.2.1 for location map and Fig. 4.2.2 for legend.

Base Zechstein (BZ) configuration
- Dipping from the SE (2,5 sec. TWTT) to the NW (3,5 sec. TWTT);
- Eight large faults (F1-8) define three grabens and one half graben;
- Several salt bodies are located near or above those faults (SB1b, SB3, SB4 and SB5).

Zechstein salt bodies
- Six salt bodies observed (SB1-6) that include two salt pillows (SB1 and SB2) and four salt diapirs (SB3-6);
- All salt diapirs have salt wings on their northwestern sides (SB4-6) or on both sides (SB3);
- Salt diapirs SB3-5 are located below the Upper Jurassic interval (yellow, green and orange zones) and only SB6 pierced higher within the Chalk Group.

46
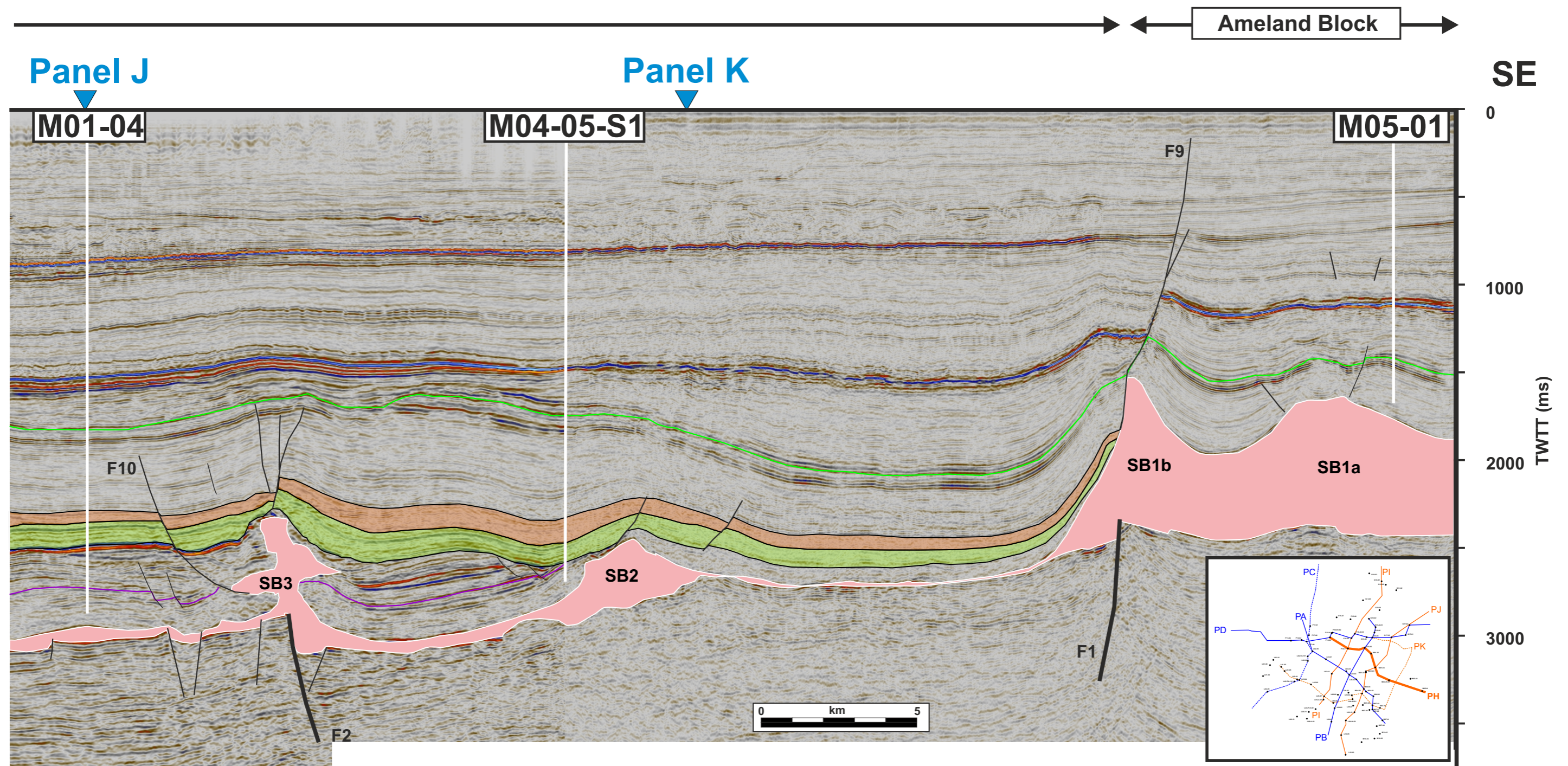
Figure 4.2.3 (continued):

Faults

Several faults are observed in this section mainly above the shallow salt bodies (e.g. SB6).
- Two faults are noticeable, F9 and F10;
- F10 is a growth fault located at the southeastern limit of TB. It is unclear if that fault was active during the Upper Jurassic;
- F9 is a growth fault soling intra-Triassic on the SB3 northern salt wing and was active during the Jurassic and Cretaceous.

Stratigraphy
- The Lower Triassic is over all isopachous except between salt bodies SB1 and SB2 where it is thin and above SB1 where it is missing;
- The Upper Triassic show various thickness changes and internal complexities due to early salt movements. It is locally partially eroded (e.g. at the location of well G16-05) or totally eroded (above and south of SB2);
- Sequence 1 is present south of SB6 and around SB4. It is thin and has a heavily erosional lower surface;
- Sequence 2 thickens toward the NW with local thinning around salt diapirs (e.g. SE of SB4, SB3 and SB6);
- Sequence 3 thickness varies slightly across this section and locally shows effects of salt tectonics (e.g. south of SB3 and north of SB6).
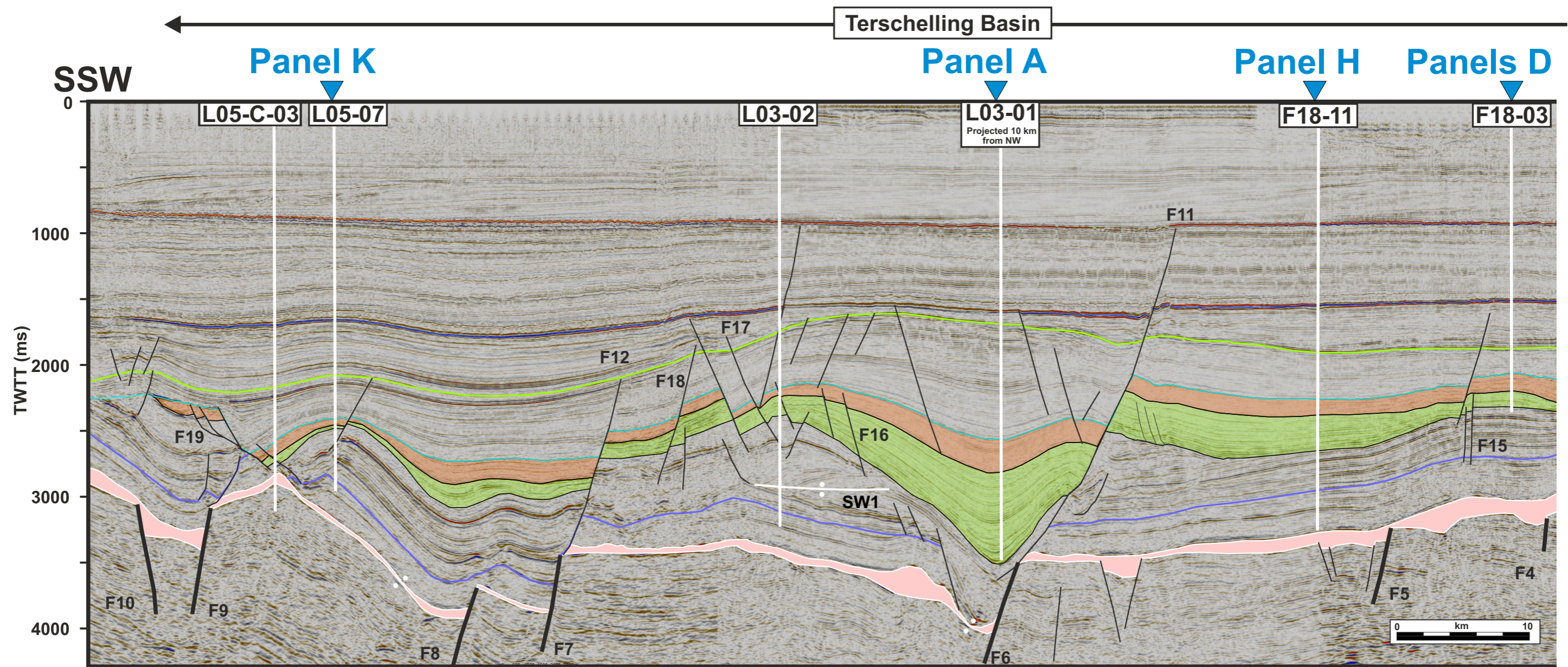
Figure 4.2.4: Interpreted seismic section I is trending NNE-SSW and is located across two structural provinces, namely from NNE to SSW, the Schill Grund Plateau (SGP) and the Terschelling Basin (TB). This seismic section is 109 km long. It intercepts one wells in the SGP (G10-01) and seven wells in the TB (F18-08-S1, F18-03, F18-11, L03-01 (projected), L03-02, L05-07 and L05-C-03). See Fig. 4.2.1 for location map and Fig. 4.2.2 for legend.

Base Zechstein (BZ) configuration
- It varies greatly across this transect from a flat configuration in the north (between wells G10-01 and F18-08-S1), to a faulted (F1-10) and irregular configuration in the TB;
- Fault F1 to F8 dip southward and define half graben with a deepening of the base Zechstein from 3 sec to 3.8 sec (TWTT);
- Faults F9 and F10 define a narrow graben at around 3.3 sec (TWTT.) and are part of the Hantum fault system;
- Note that faults F6 and F7 are located below large shallow growth faults (F11 and F12).

Zechstein salt bodies
- The autochthonous salt is overall thin along this seismic panel, except on the SGP;
- Only four salt bodies (SB1-4) and a salt weld (SW1) are noticeable;
- SB1 and SB3 are two salt pillows that bound to the north and south a small Upper Jurassic basin;
- SB2 is a salt pillow below that same Upper Jurassic basin;
- SW1 is interpreted as a salt weld within the Upper Triassic that separate a north dipping strata below to a south-dipping strata above. It is intercepted by well L03-02 and is interpreted on the composite log as Main Keuper Evaporite Member.
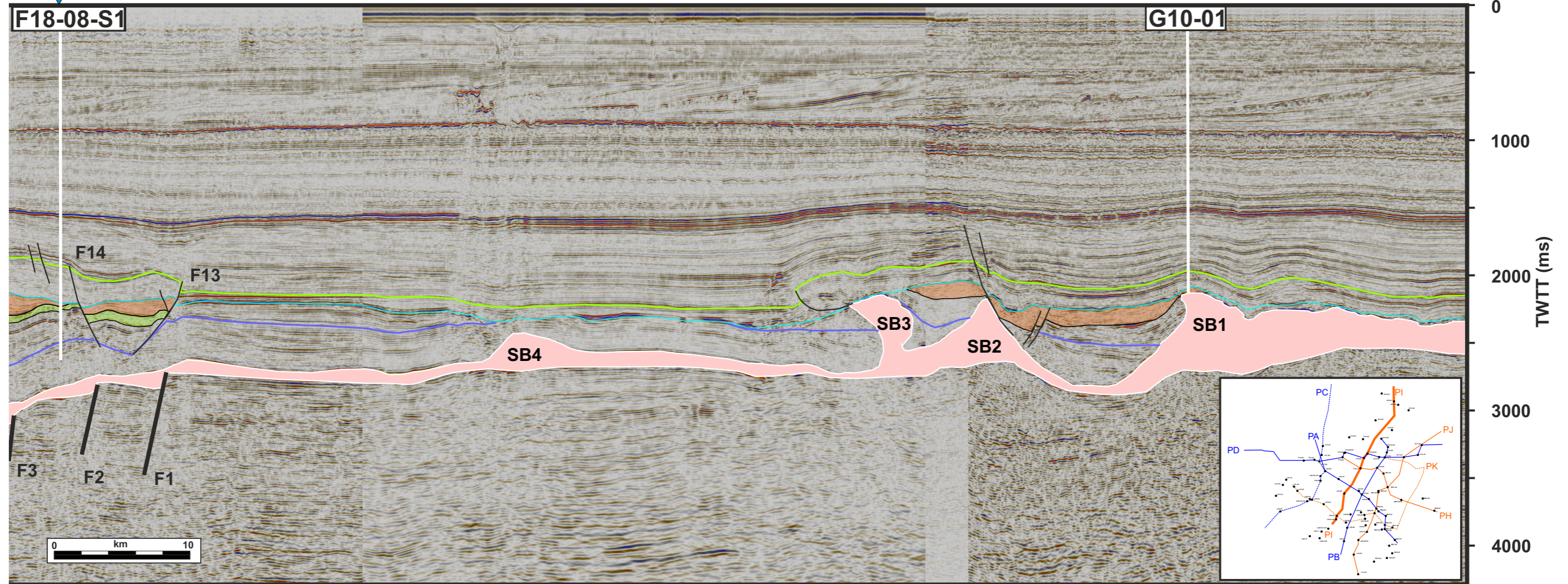
Continues to opposite page

Figure 4.2.4 (continued):
Faults

   Several shallow faults are observed in this section.
- Two large growth fault (F11 and F12) were active during the Cretaceous and Mesozoic (for F11). This fault are controlled by the position of basement faults F6 and F7, respectively;
- Other faults such as F13-19 were also active during the Jurassic with growth wedges observed on their downthrown sides. Note that most faults are soling intra-Triassic except F19 fault systems that sole onto the Zechstein that is elevated here due to the Hantum Fault zone.

Stratigraphy
- The Lower Triassic is over all isopachous but is locally partially eroded on the SGP;
- The Upper Triassic show various thickness changes and internal complexities due to early salt movements, especially in the area between wells F18-11 and L03-02 where it is very thick and show internal wedges, truncation and the presence of an internal salt weld.

Toward the south it become less deformed and more isopachous;
- Sequence 1 is absent along this section;
- Sequence 2 is present only in the TB with a drastic and spectacular thickening in the central part of the basin;
- Sequence 3 also thickens toward the central part of the TB but at a much lower rate than S2 did. S3 also extends farther to the south and the north than S2 did and is even present north onto the SGP where it is preserved within a small (16 km wide) basin south of well G10-01.
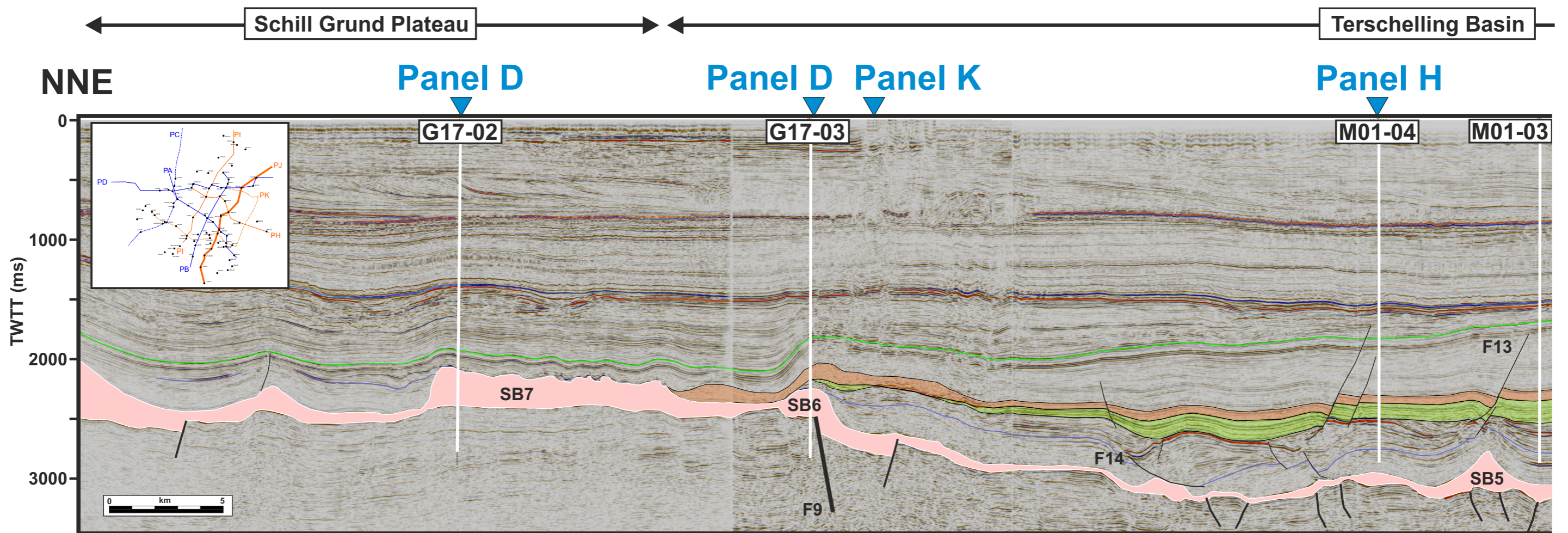
Continues to opposite page

Figure 4.2.5: Interpreted seismic section J is trending NNE-SSW and is located across three structural provinces, namely from NNE to SSW, the Schill Grund Plateau (SGP), the Terschelling Basin (TB) and the Vlieland Basin (VB). Note that the limit between the TB and the VB is approximative since Upper Jurassic strata is present in the inter-basinal area. This seismic section is 130 km long. It intercepts one well in the SGP (G17-02), eight wells in the TB (G17-02, G17-03, M01-04, M01-03, M01-02, M04-04, M04-02, L09-10 and L09-06-S1) and two wells in the VB (L12-05 and L12-03). See Fig. 4.2.1 for location map and Fig. 4.2.2 for legend.

Base Zechstein (BZ) configuration
  - BZ is relatively flat on the SGH and the TB with a gentle slope from the position of well G17-03 to well M01-04. On the southern side of the transect (south of M04-02) it is heavily faulted within the Hantum fault zone;
  - Fault F1 to F9 are the largest fault offsetting the BZ;
  - Two grabens can be defined between F1 and F6 and between F7 (fault array) and F9;
  - Note that the largest fault at the BZ is sitting below a large salt diapir (SB3).

Zechstein salt bodies
  - The autochthonous salt is overall thin within the TB and slightly thicker on the SGP and below the VB;
  - Seven salt bodies (SB1-7) are noticeable;
  - SB1 is a wide autochthonous salt pillow below the VB;
  - SB2 is a salt pillow below the Upper Jurassic;
  - SB3 is a narrow salt pillow that pierced into the Cretaceous and was active during the Upper Jurassic as seen by the stratigraphic thickness variations on both sides;
  - SB4 is salt stock with a narrow stem (feeder) and is located below the Upper Jurassic. It seems that this salt body had a topographic expression during the early part of Seq. 2 deposition;
  - SB5 is a small symmetric salt pillow;
  - SB6 is a salt pillow located above F09;
  - SB7 is similar to SB1 but is located on the SGP.
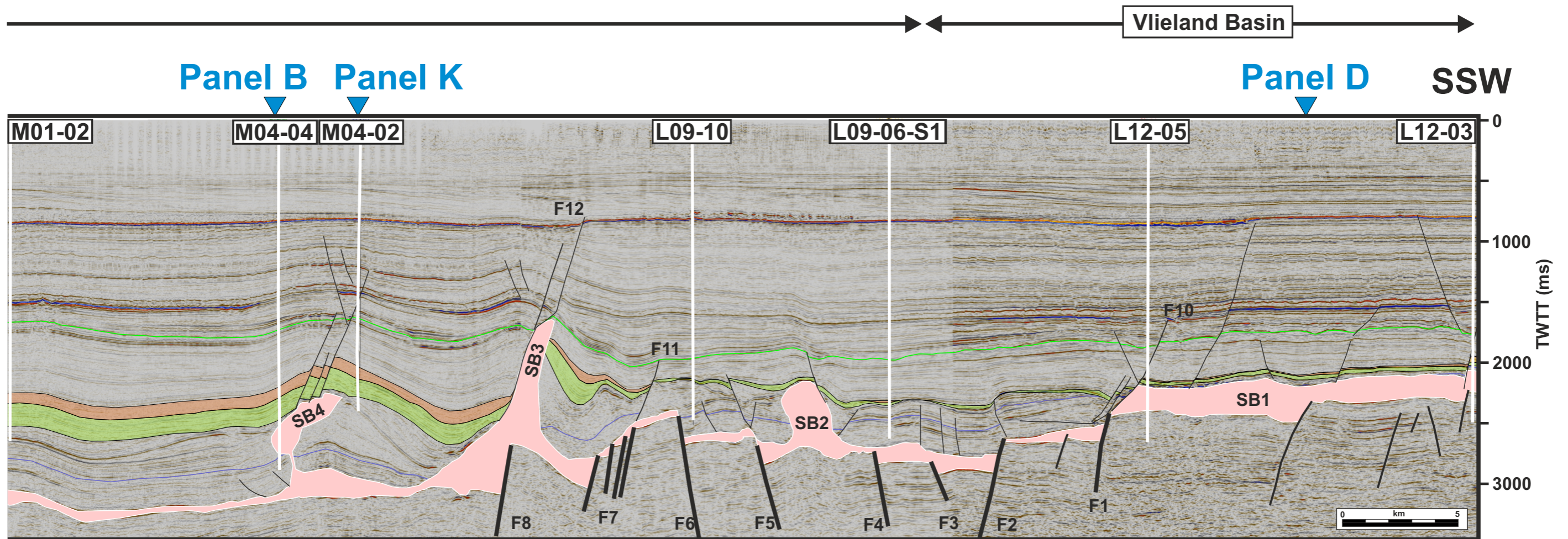
Figure 4.2.5 (continued):
Faults

Several shallow faults are observed in this section.
- A large growth fault (F10) was active during the Cretaceous and Mesozoic and possibly during the Jurassic;
- F11 separate the area of the TB where the Upper Jurassic is thick (north) to the area where is is thinner (south of well L09-10);
- F12 is a set of normal fault that detached on salt body SB3 and was active mainly during the Cenozoic;
- F13 is a growth fault that detaches intra-riassic and was active during the Upper Jurassic;
- F14 is a large low angle growth fault located in the Upper Triassic.

Stratigraphy
- The Lower Triassic is over all isopachous but is locally missing due to erosion or rafting. It is eroded partially and locally totally below the VB and the SGP. In the TB it is locally rafted southward (between G17-03 and M01-04) and northward north of SB3;

- The Upper Triassic show various thickness changes especially in the TB where it locally show large growth stratigraphic wedges such as on the downthrown side of F14 and on the northern side of SB3;
- Sequence 1 is absent along this section;
- Sequence 2 is present in both the TB and VB with a thinner configuration in the south (from L09-10 southward) and in the north (around well G17-03). The central part of the TB has a fairly isopachous S2 which show rapid thickness changes in the southern and northern basin margins (e.g. around SB3);
- Sequence 3 mainly present in the TB but is locally preserved on the VB (e.g. well L012-03). It is quite isopachous overall except in the northern part of the TB where it thickens at the location of the TB basin margin (around G17-03).
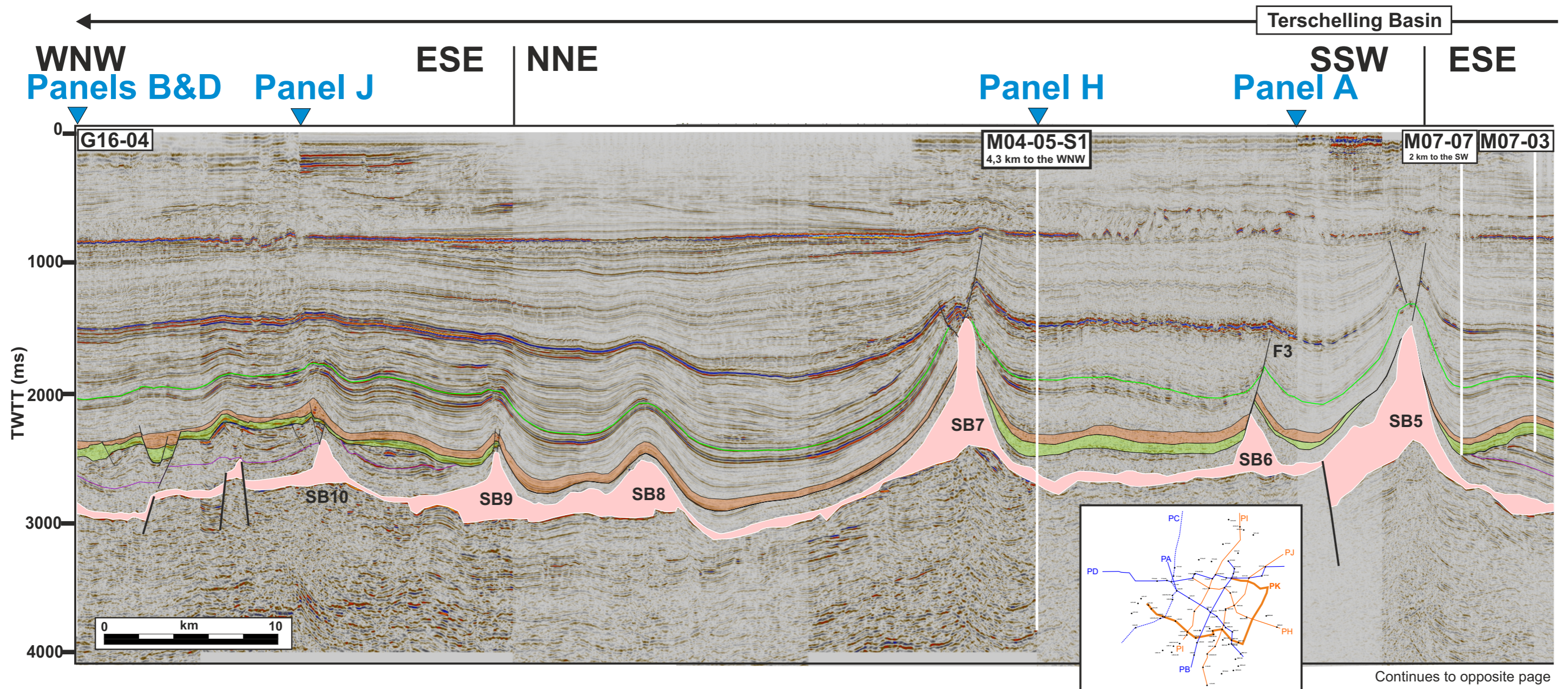
Figure 4.2.6: Interpreted seismic section K is circling around the Terschelling Basin and is used to evaluate the geological variation along the basin margins (northern, eastern and southern margins). It also extends to the southwest to the Dutch Central Graben (DCG). This seismic section is 165km long. It intercepts ten wells in the TB (G16-04, M04-05-S1 (projected), M07-07, M07-03, M04-02, L06-04, L06-05, L09-02, L06-01 and L05-07) and five wells in the DCG (L05-02, L05-04, L05-03, L01-05 and L01-02). See Fig. 4.2.1 for location map and Fig. 4.2.2 for legend.

Base Zechstein (BZ) configuration
- The BZ configuration is highly variable along this profile with most basement faults located in the southern margin of the TB (Hantum Fault Zone) between wells L0604 and L01-02;
- The deepest part of the Zechstein is in the DCG at around 3.5 Sec (TWTT.) and it in average around 3 sec (TWTT) deep in the TB;

Zechstein salt bodies

- The autochthonous salt is overall thin within the TB;
- Ten salt bodies (SB1-10) are not present along this section;
- SB1, SB6, SB8-10 are salt pillows;
- SB2-5 and SB7 are salt diapirs;
- SB5 and SB7 have a triangular shape with a wide base;
- SB2-4 have stock shape with narrow stems. They also have salt wings intra-Upper Triassic or just below the Upper Jurassic;
- Salt bodies, SB2, 5 and 7 are percing above the Upper Jurassic ionto the Cretaceous while SB3 and SB4 are located below the Upper Jurassic yet affect the thickness of the Upper Jurassic interval.
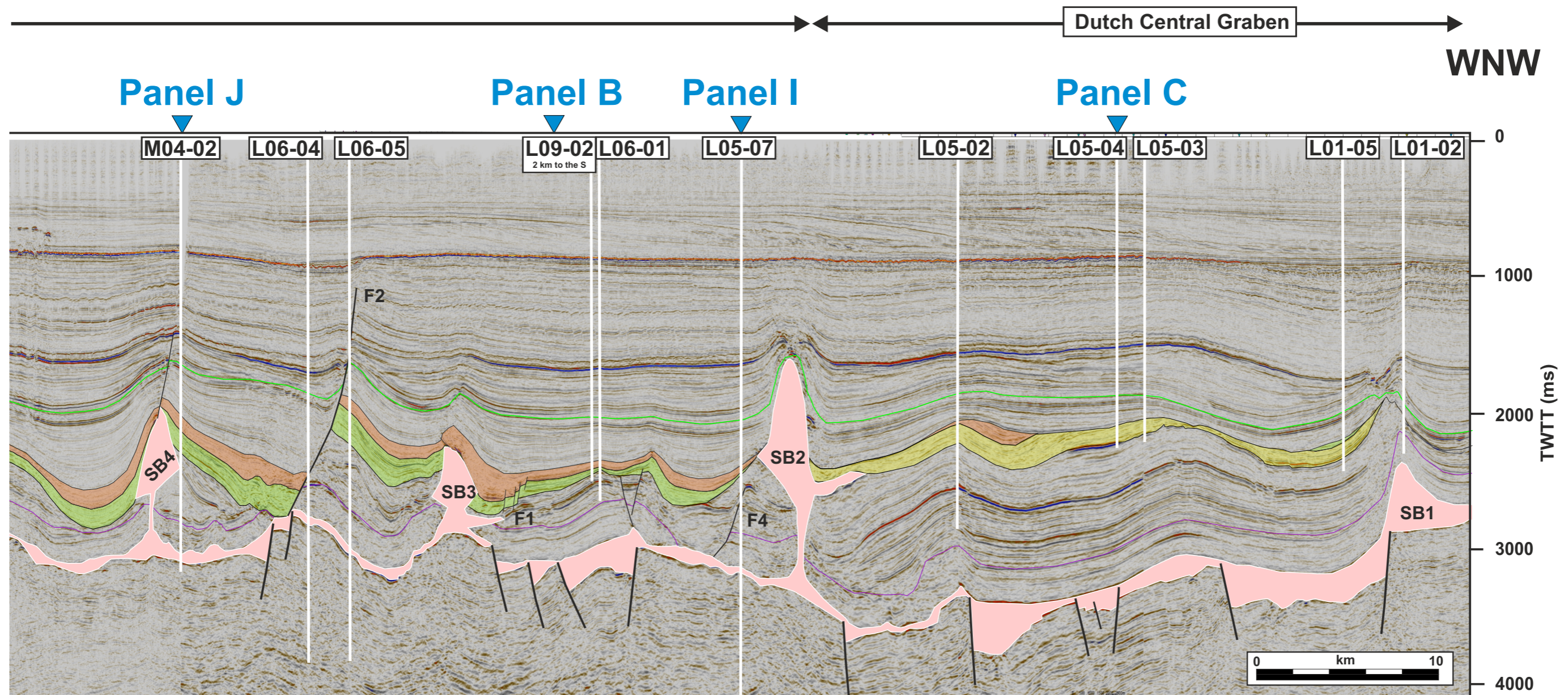
Continues to opposite page

Figure 4.2.6:
Faults

Several shallow faults are observed in this section.
- A series of syn-depositional normal faults (F1 fault set) is present on the western side of SB3 and show significant thickening of S3;
- A large growth fault (F1) was active during the Upper Jurassic, Cretaceous and Mesozoic;
- F3 is a northward dipping growth fault that show significant activity during the Upper Jurassic with S2 and S3 over thickened on the downthrown side of the fault;
- F4 is a intra-Upper Triassic growth fault.

Stratigraphy
- The Lower Triassic is overall isopachous but is locally missing due to erosion or rafting. It is eroded partially in the area to the NNE of well M04-05-S1 where S3 is directly in contact with the lower part of the Lower Triassic. In the TB, between wells L06-01 and L05-07, it is rafted out by a growth fault (F4);
- The Upper Triassic show various thickness and seismic facies changes from highly variable

thickness and more deformed in the TB versus a more isopachous and continuous ion the DCG. Note that the Upper Triassic is absent due to erosion in a large area from salt body SB5 to SB9;
- Sequence 1 is only present in the DCG but is locally eroded by Sequence 3 or by base Chalk Group;
- Sequence 2 is present in three zone. 1) as a small remnant in the DCG (location of well L01-05), 2) in the area between SB2 and SB7, and 3) in the northern basin margin area (from SB9 to well G16-04). The thickness of S2 is highly variable from thin on the southwestern basin margin (well L05-07) and around SB5, to thick in other areas (e.g. area between wells L09-02 and M07-07);
- Sequence 3 is present along most of the section except in the DCG where it is only represented as a remnant below the base Chalk Group at well L05-02. Its thickness varies greatly within the TB due to syn-depositional faulting (e.g faults F1-3) and also due to salt diapirsm (e.g. around SB2-5).

53

B) Base Rijnland Group Subcrop Map
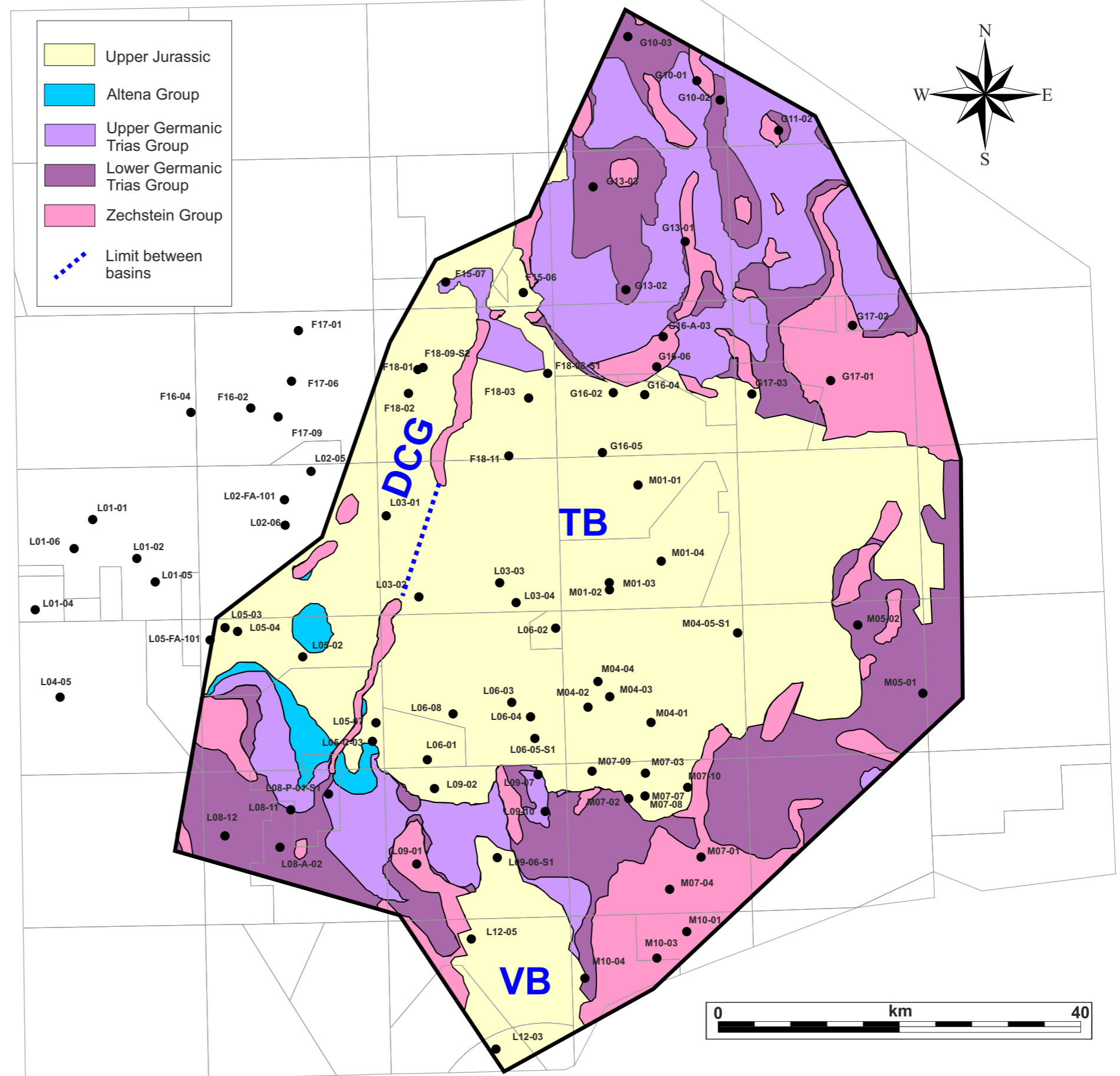
Figure 4.2.7: Base Rijnland Group subcrop map in the study area. On the platfom where no Upper Jurassic is present. The Zechstein, Altena, Lower and Upper Germanic Trias Groups represented as color areas. The Upper Jurassic - Lowermost Cretaceous is show in light yellow and are present in the Terschelling Basin (TB), the Dutch Central Graben (DCG) and in the Vlieland Basin (VB). Note that locally some thin remnant of Upper Jurassic are found (e.g. around well G10-01, L09-10) but are not show on this map since no detail mapping has been done for those satellite zones on the platforms.

C) Salt Bodies Map
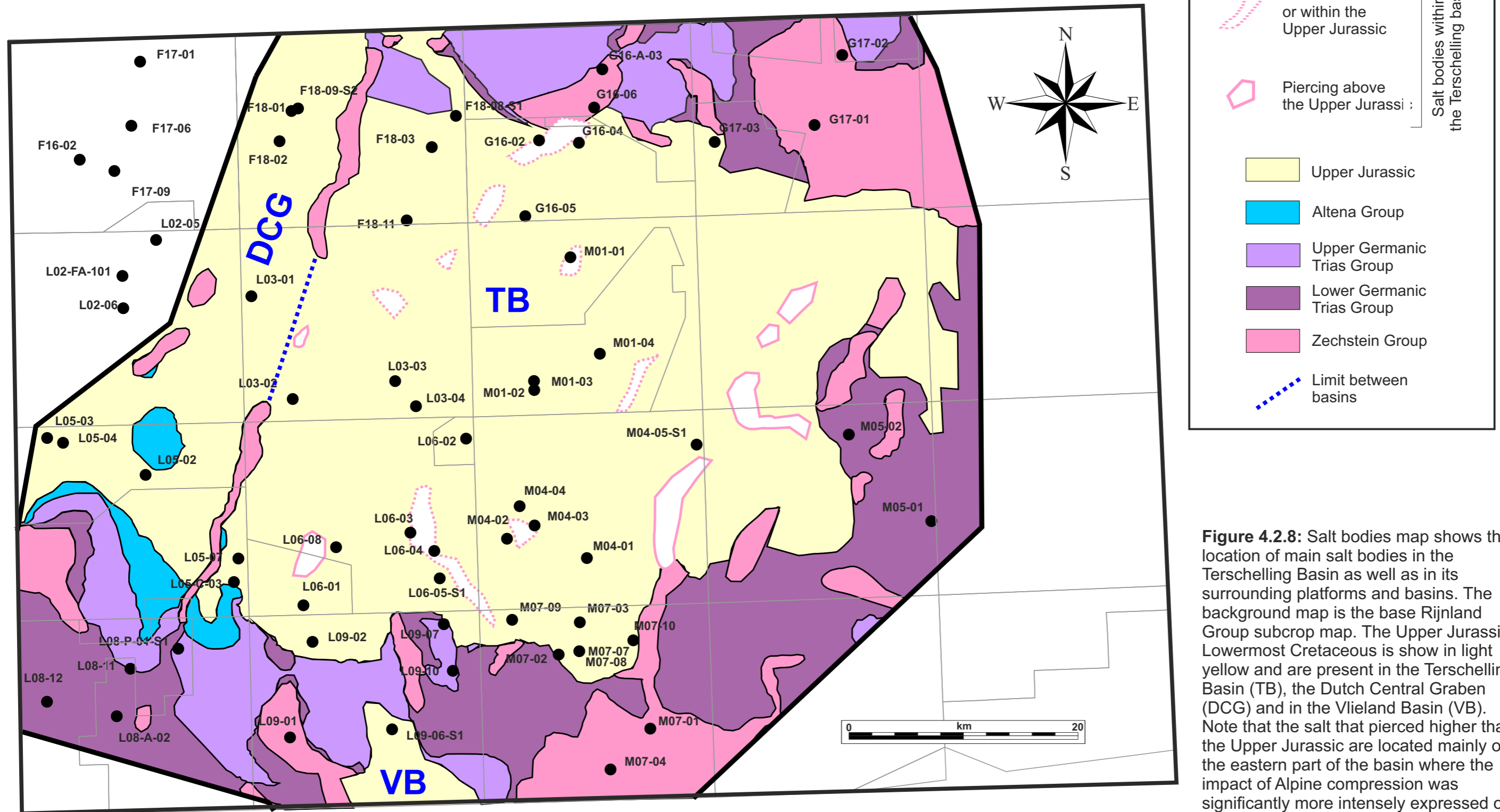
Figure 4.2.8: Salt bodies map shows the location of main salt bodies in the Terschelling Basin as well as in its surrounding platforms and basins. The background map is the base Rijnland Group subcrop map. The Upper Jurassic - Lowermost Cretaceous is show in light yellow and are present in the Terschelling Basin (TB), the Dutch Central Graben (DCG) and in the Vlieland Basin (VB). Note that the salt that pierced higher than the Upper Jurassic are located mainly on the eastern part of the basin where the impact of Alpine compression was significantly more intensely expressed on the salt features. Note also that many salt bodies align themselves along SSW-NNE trends and sometime form salt walls such as in the transitional zone between the TB and the DCG.

55

D) Syn-depositional Faults Map
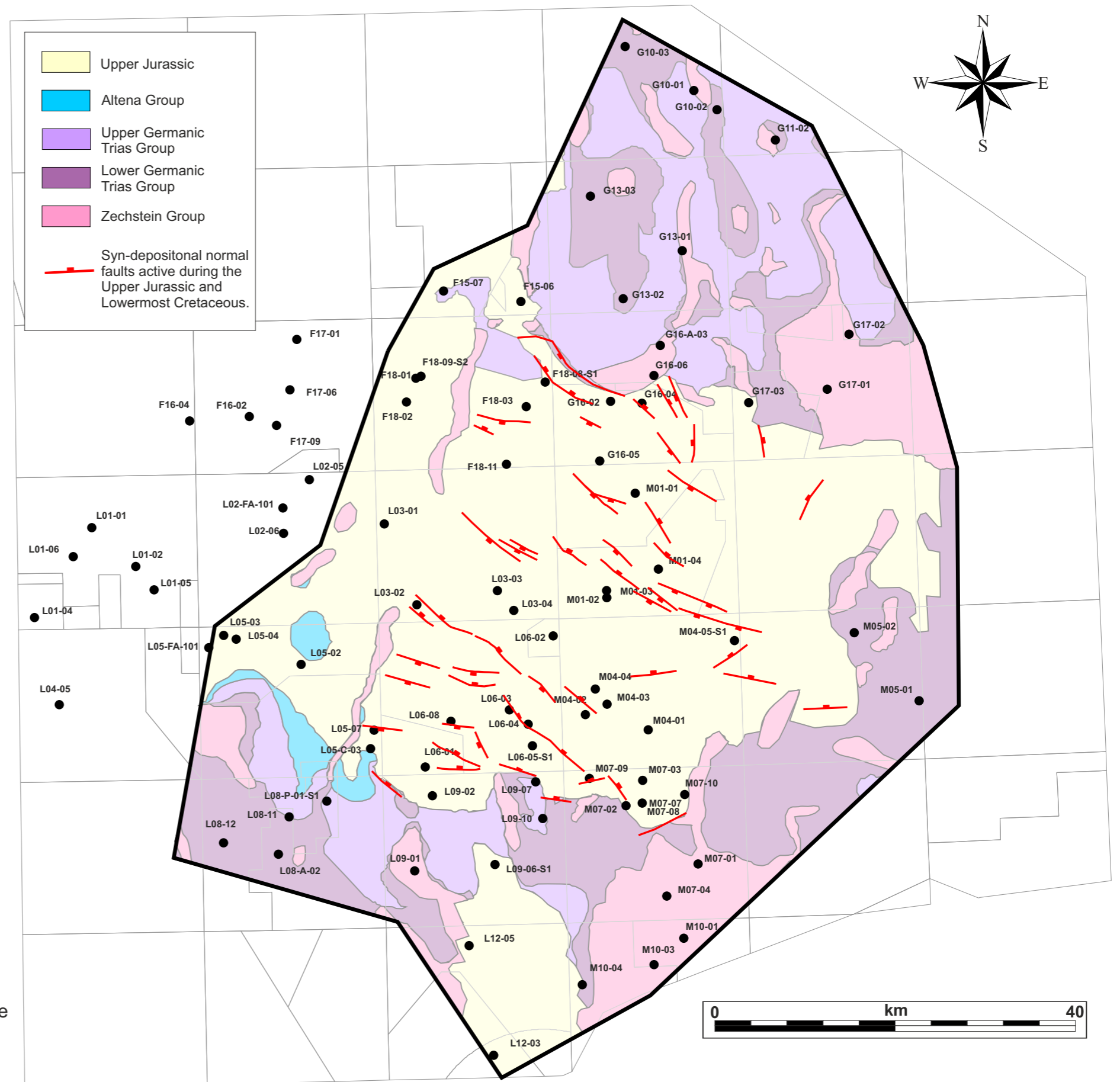
Figure 4.2.9: Syn-depositional faults map. Many faults are present in the study area but only the one active during the Upper Jurassic and the Lowermost Cretaceous are represented here. The Base Rijnland Group subcrop map is shown as background. Note that many faults are aligned along WNW-ESE trends. These trends are also the trends of the Rifgronden and Hantum Fault Zones.

E) Time Structure Maps
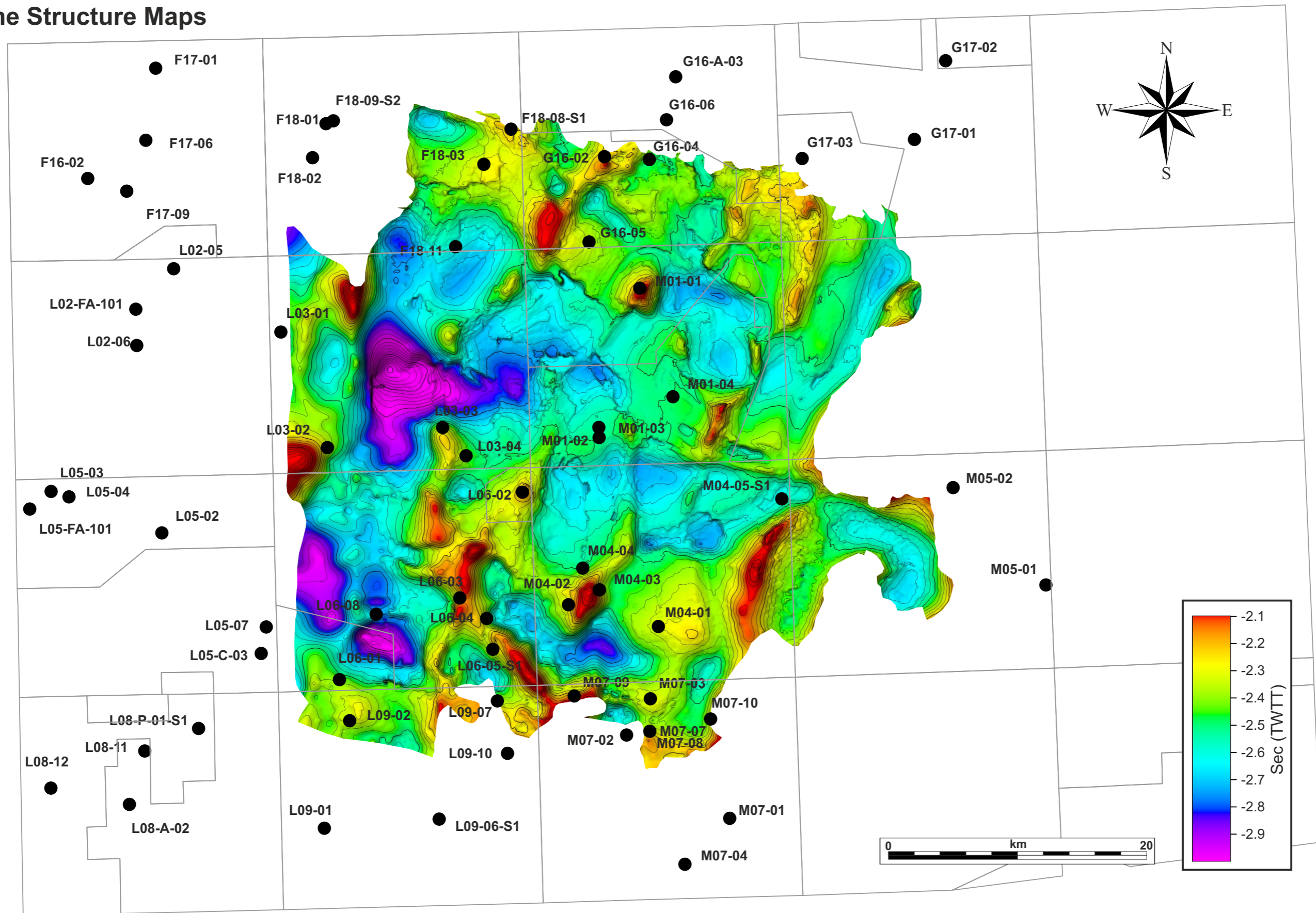
Figure 4.2.10: Time structure map of the base of Sequence 2.
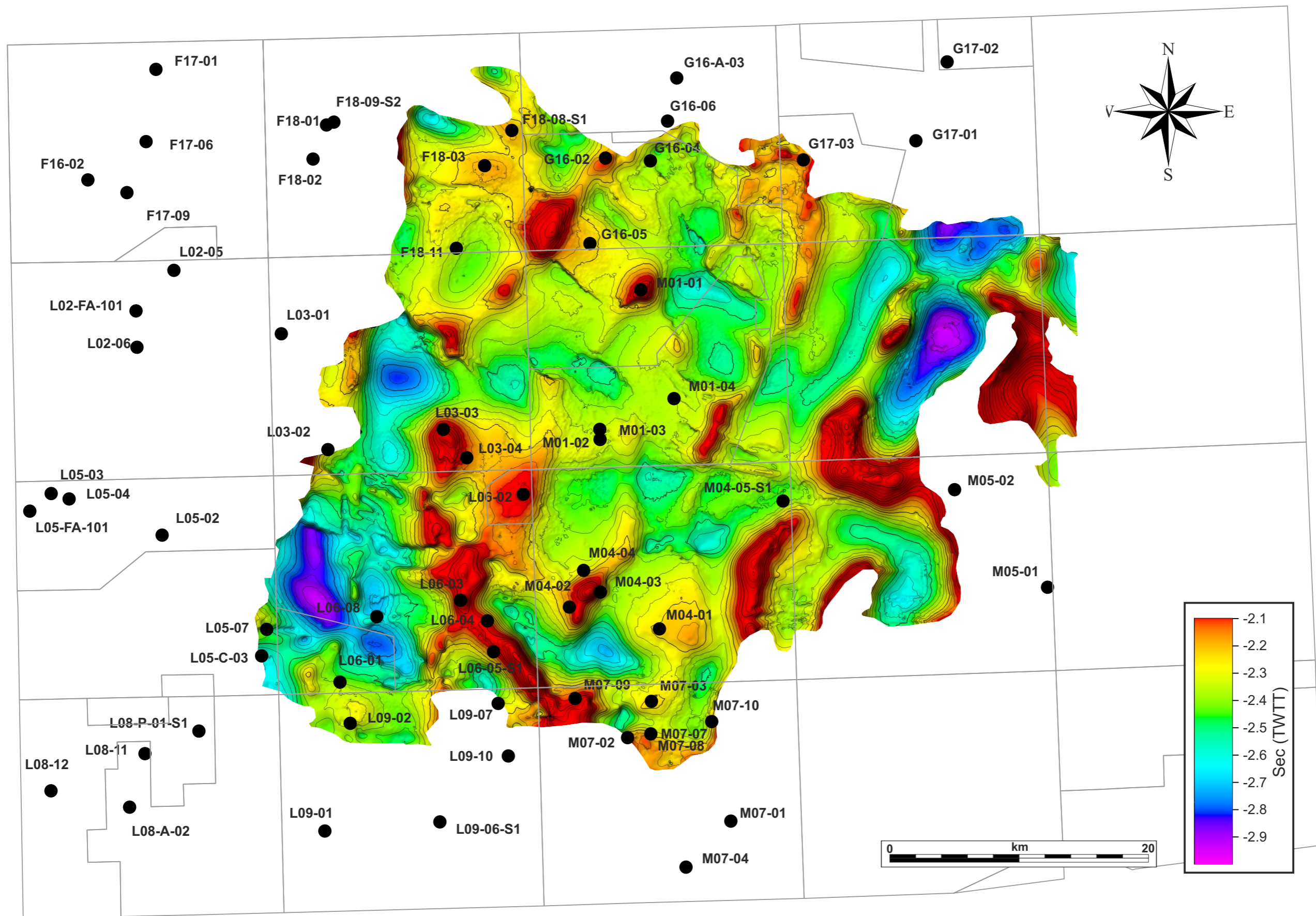
Figure 4.2.11: Time structure map of the base of Sequence 3.
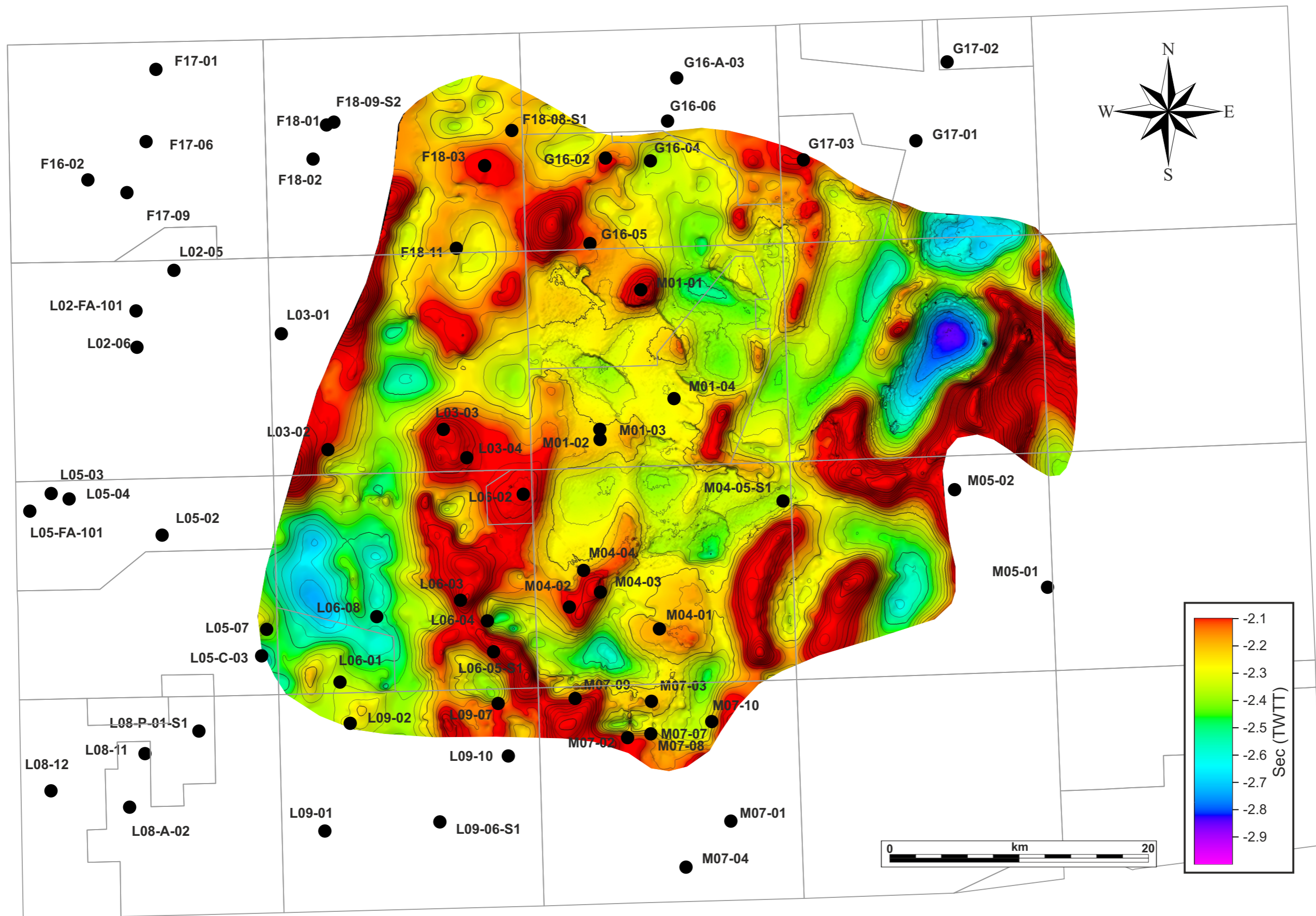
Figure 4.2.12: Time structure map of the top of Sequence 3.

F) Time Thickness Maps
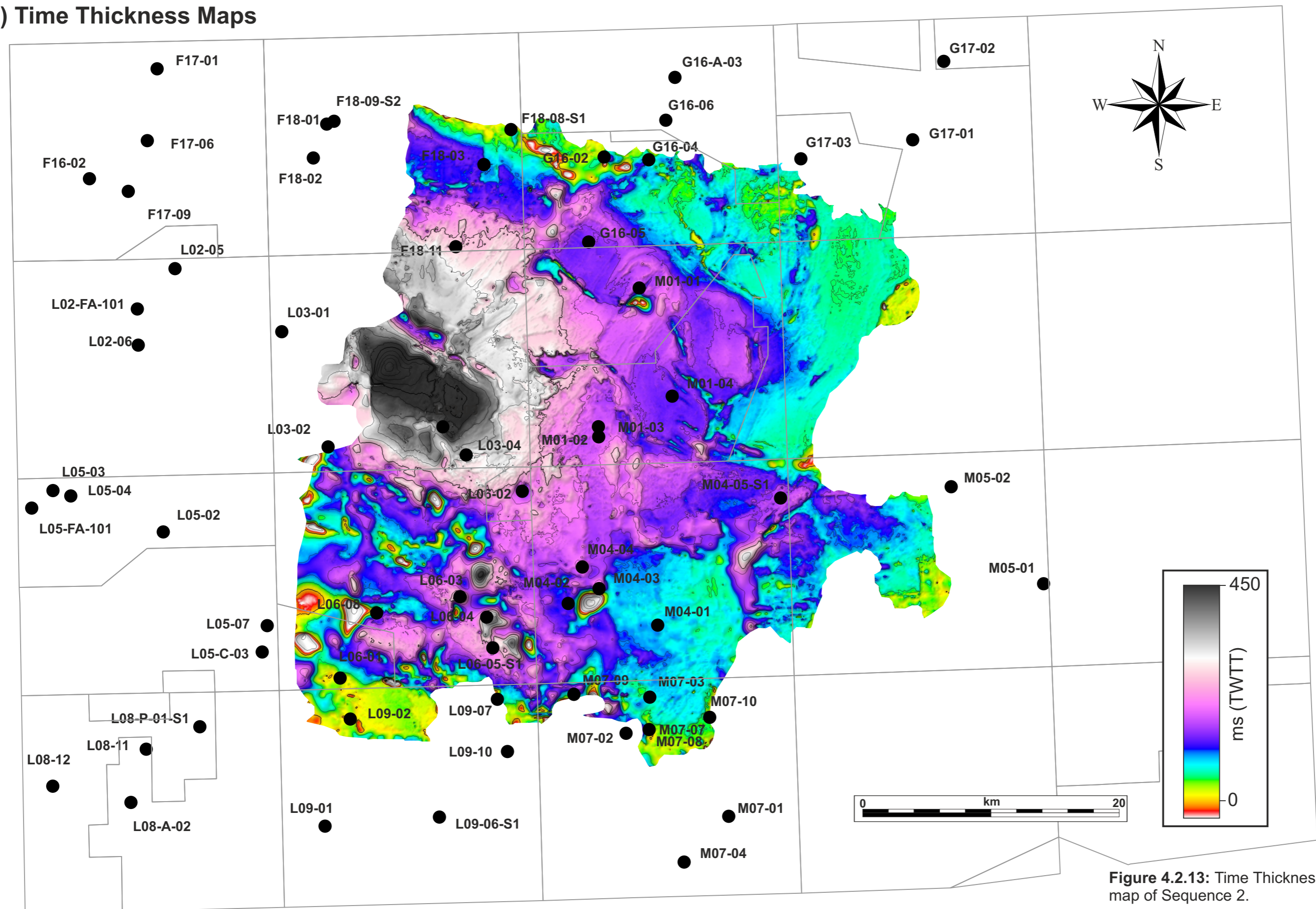
Figure 4.2.13: Time Thickness map of Sequence 2.
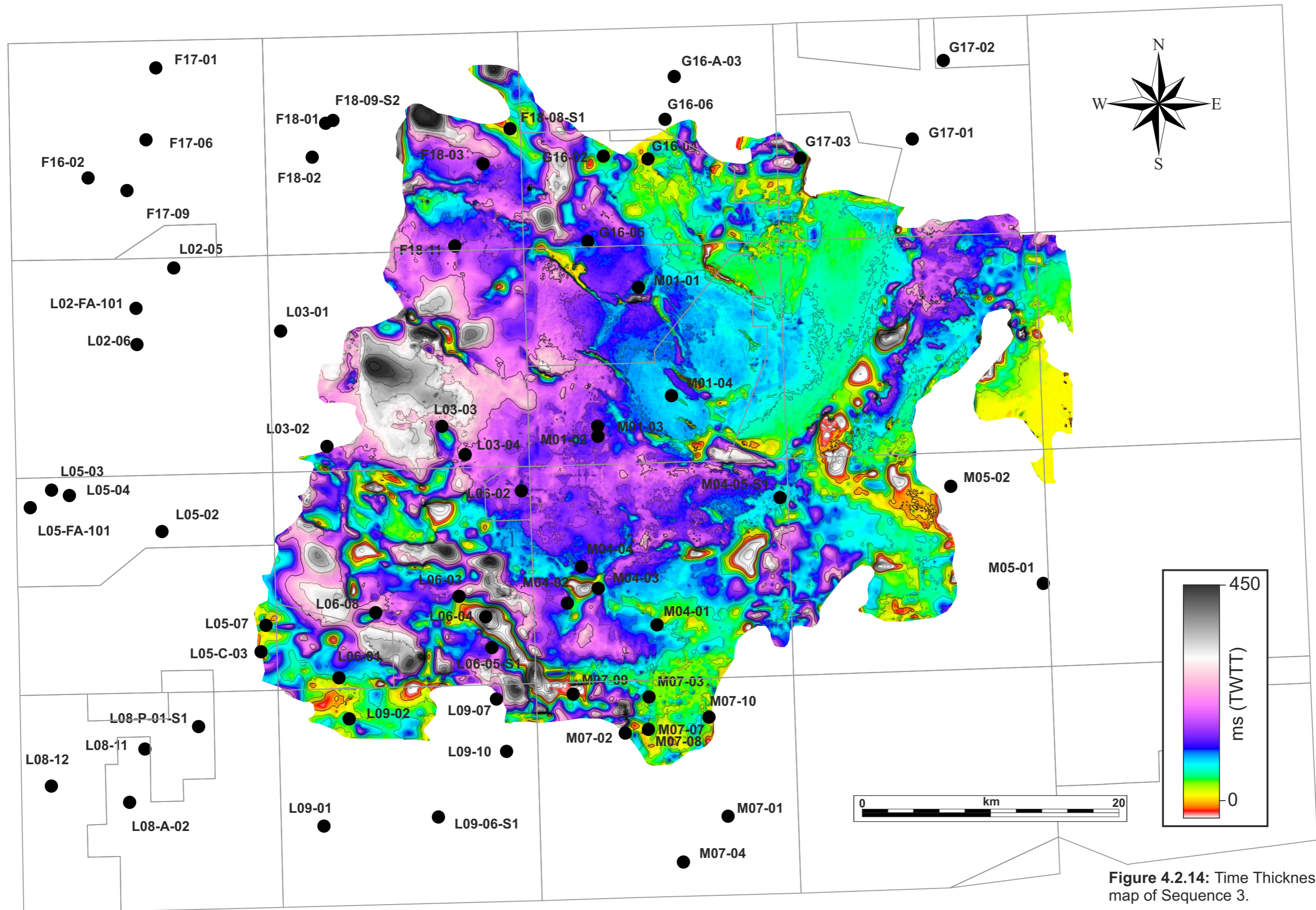
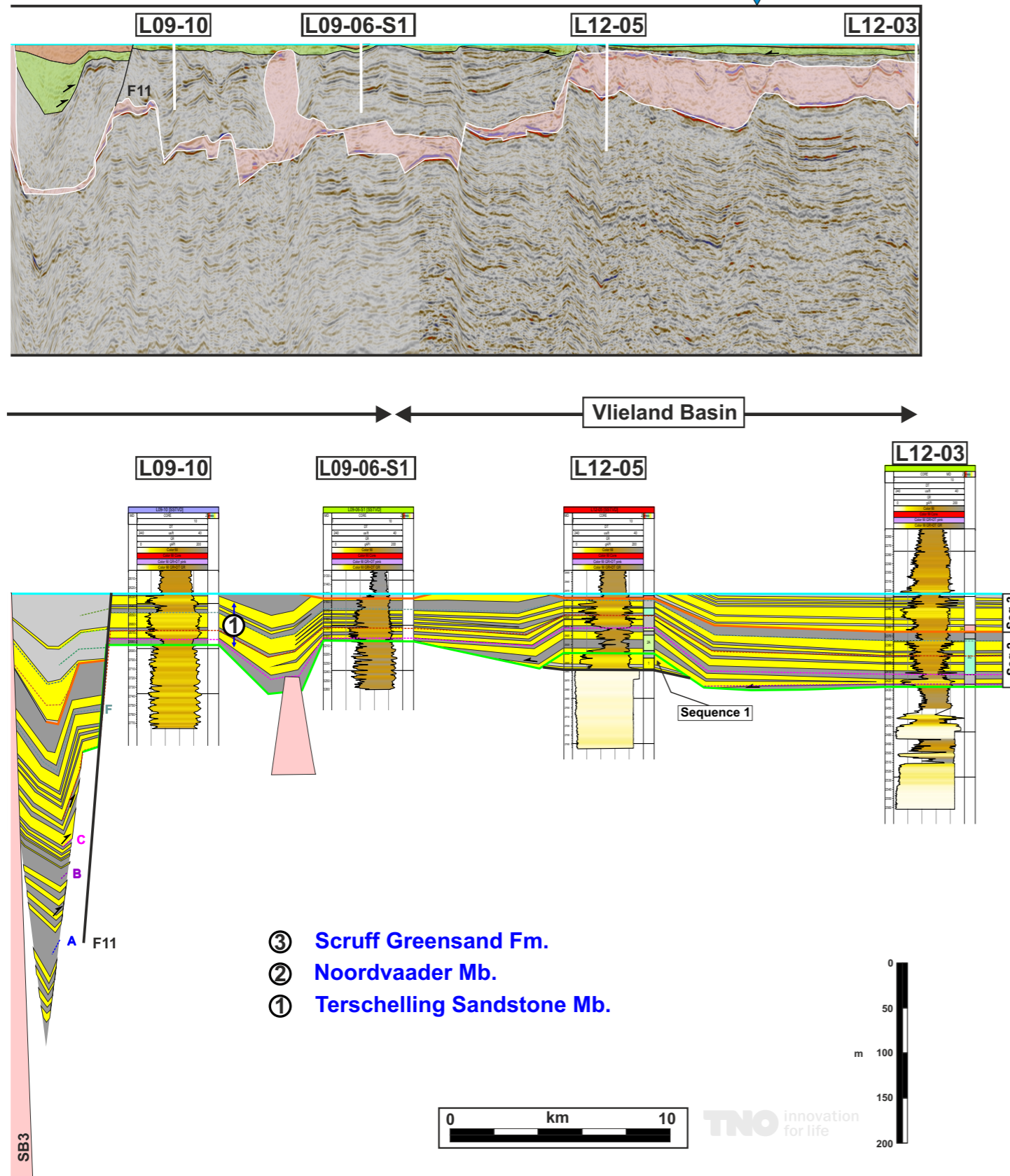**Figure 4.2.14:** Time Thickness map of Sequence 3.
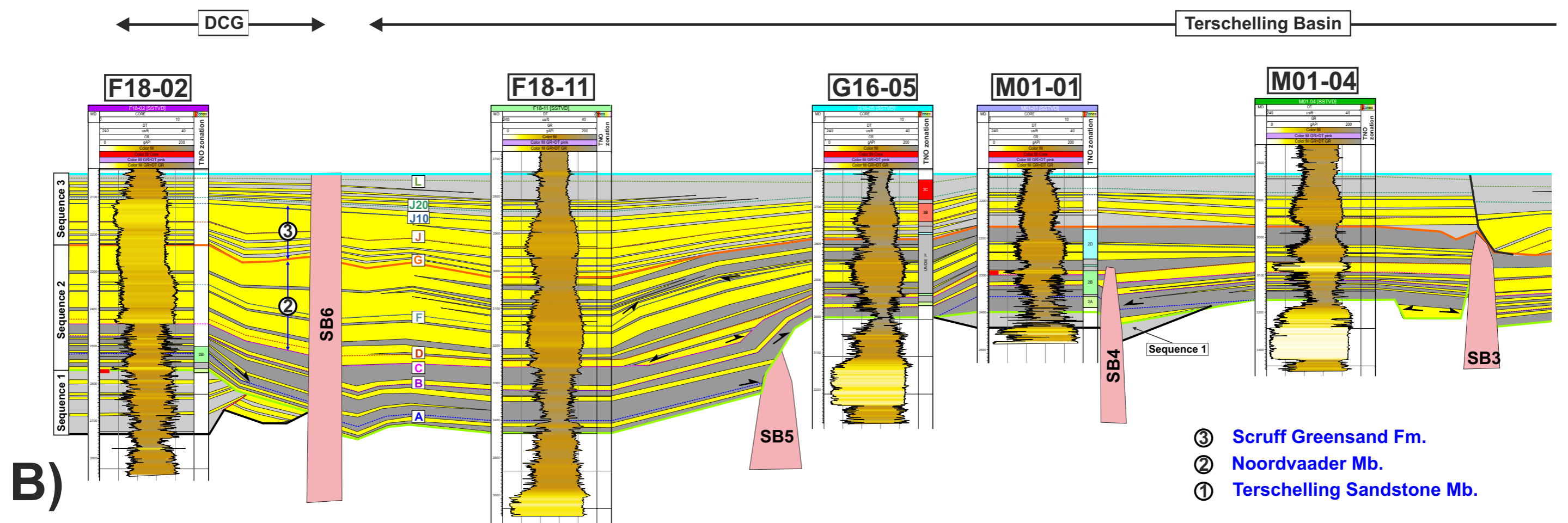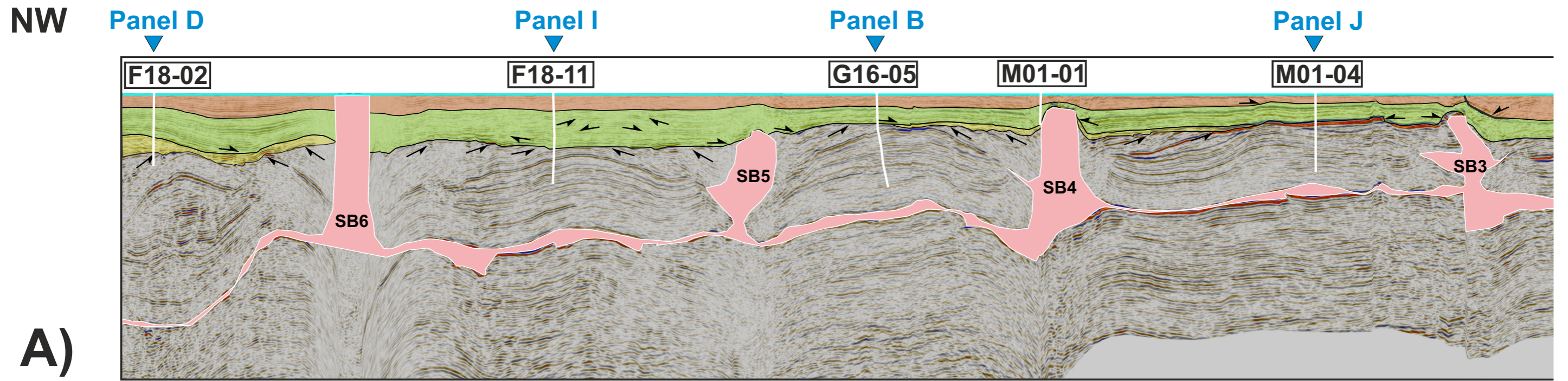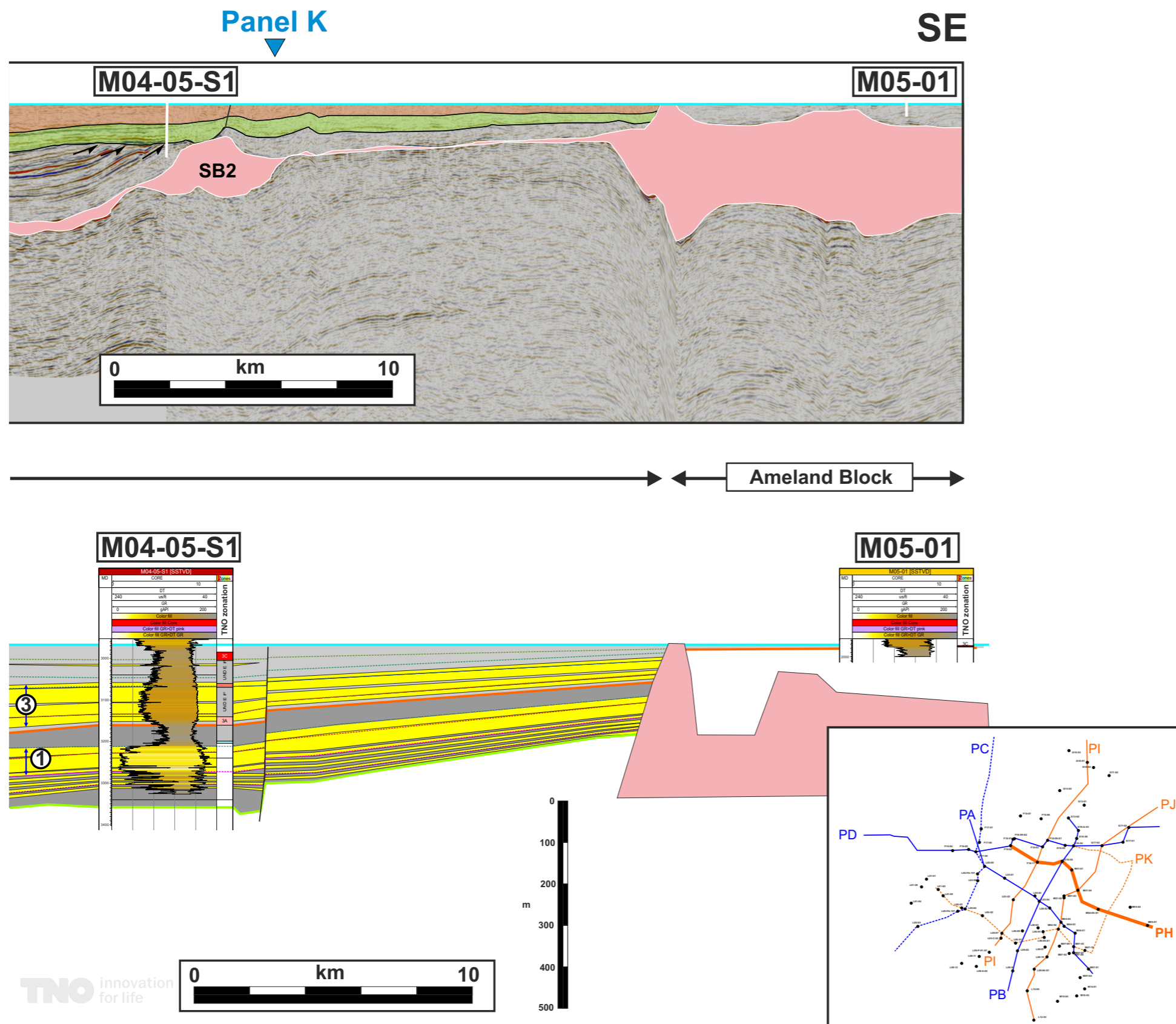
Figure 4.3.1: Stratigraphic correlation for Panel H. See Figure 4.2.1 for location map and Appendix A2 for complete regional panel. A) Flatten seismic on the top Sequence 3. B) Stratigraphic correlation for the Upper Jurassic-Lowermost Cretaceous interval. The section is flattened on the top of S3. TNO zonations (e.g. 2E, 3A) are shown (when available) on the right side of the wells.

Sequence 1:
    S1 is only observed in the northwestern part of the section as well as around salt body SB4. It has a heavily erosional base and cut locally deep into Upper Triassic strata (e.g. south of well G1605). S1 is mainly composed of low net-to-gross strata of the Main Friese Front Mb

Sequence 2:
    S2 overall thins toward the southeast and has its thickest accumulation around well F18-11. The base of S2 is highly erosional and cut into Upper Triassic and S1 strata.
    The lower part of this sequence is composed of low N:G strata of the Oyster Ground Mb. Locally onlaps can be observed at the base of the sequence indicating paleotopography present prior to deposition. The Upper part of S2 is sandier than the lower part and its composed of Noordvaarder Mb (NoMb) strata in the north and central part of the basin (wells F18-02 to M01-04) and Terschelling Sandstone Mb (TeSdMb) in the south and central part of the basin (well M04-05-S1 to G16-05). Note that TeSdMb and NM are time equivalent deposits but have a inverse lateral net-to-gross trend with NoMb getting sandier toward the north and TeSdMb toward the south. Internal onlaps truncations are observed in the area between wells F18-11 and G16-05 in the lower and middle part of the NoMb.

Sequence 3:
    S3 is mainly concordant on S2 and show only rare basal onlap (e.g. north of M01-04). It is the thickest in two area: 1) around F18-11 (similarly to S2) and 2) North of M04-05-S1 where is over thickened due to an interpreted growth fault detaching at the base of S3 onto the upper part of S2, which is muddy (Lies Member). That growth fault is interpreted at this location due to the high angle downlap configuration of S3 strata onto the top of S2 just south of SB3.

SSW

Panel K Panel A Panel H Panels D

L05-C-03 L05-07 L03-02 L03-01 (Projected 10 km from NW) F11 F18-11 F18-03 F18-08-S1

SB4

Terschelling Basin

L05-C-03 L05-07 L03-02 L03-01 (Projected 10 km from NW) F18-11 F18-03 F18-08-S1

F19 F12 F18 F11 F15

③ Scruff Greensand Fm.
② Noordvaader Mb.
① Terschelling Sandstone Mb.

NNE

Schill Grund Plateau
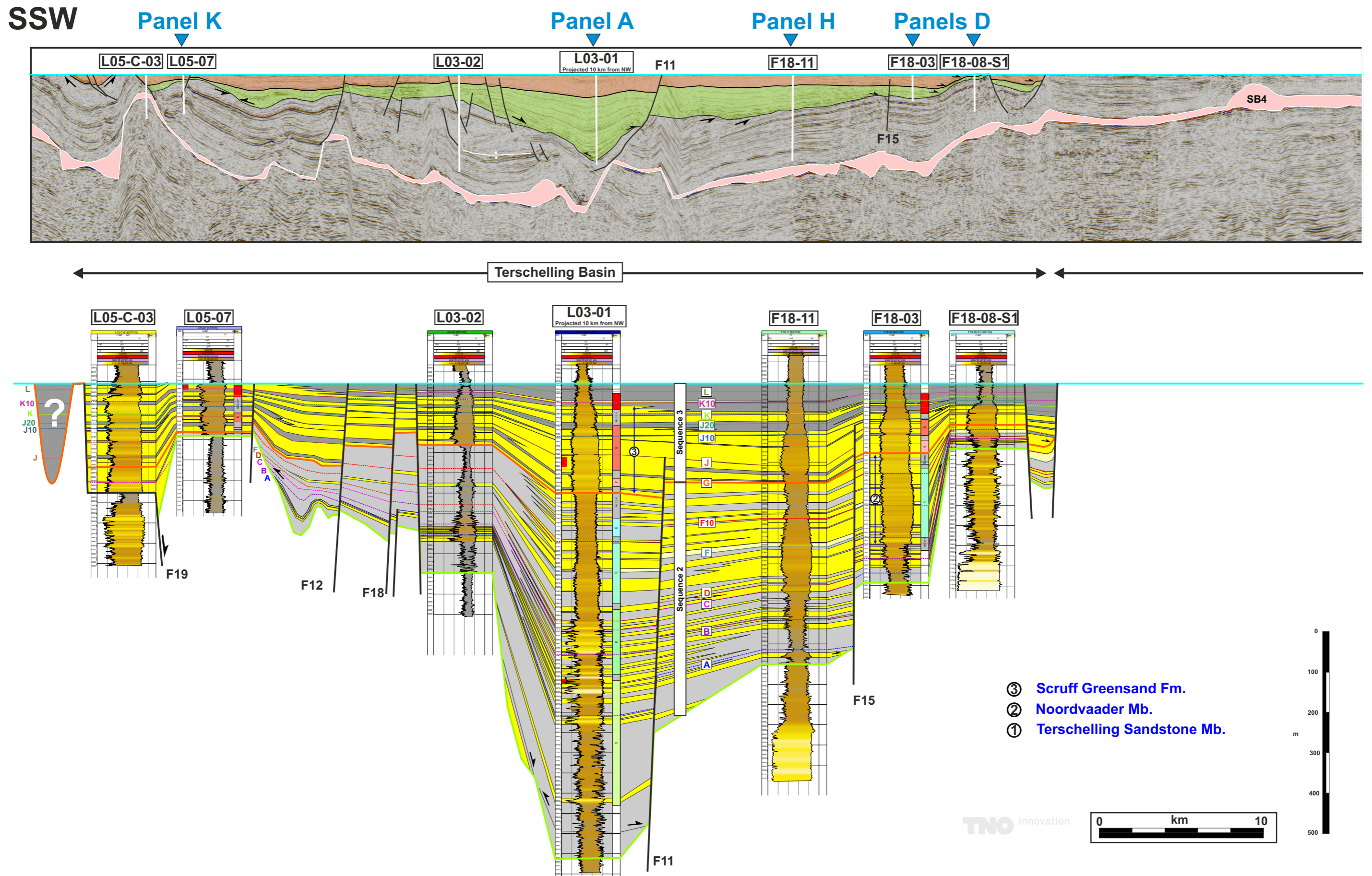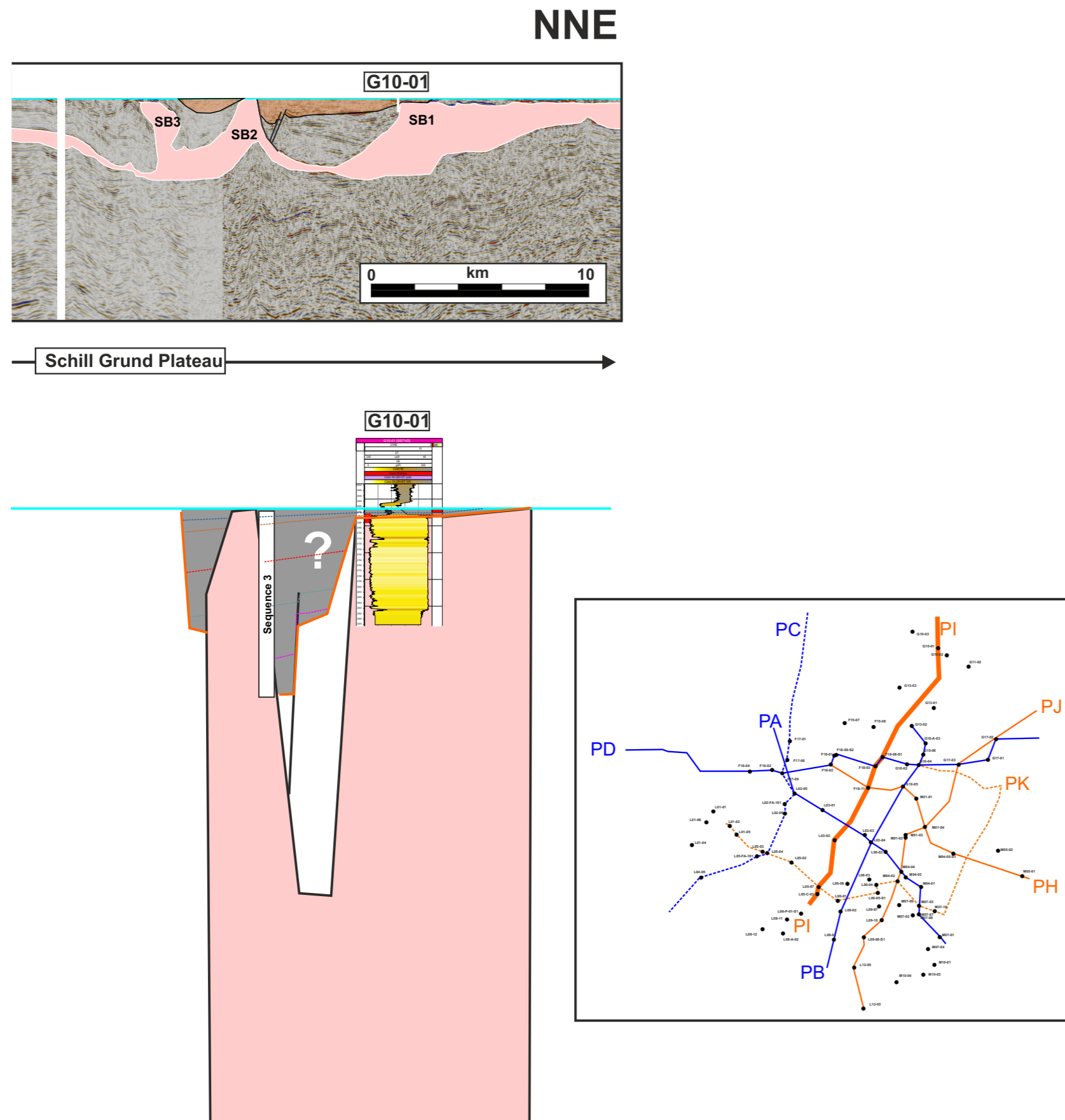
Figure 4.3.2: Stratigraphic correlation for Panel I. See Figure 4.2.1 for location map and Appendix A2 for complete regional panel. A) Flatten seismic on the top Sequence 3. B) Stratigraphic correlation for the Upper Jurassic-Lowermost Cretaceous interval. The section is flattened on the top of S3. TNO zonations (e.g. 2E, 3A) are shown (when available) on the right side of the wells.

Sequence 1:
 S1 is absent.

Sequence 2:
 S2 is only present in the TB where it thickens dramatically from less than 100 m along the southern and northern margins (wells L05-07, L05-C-03, F18-08-S1) to more than 900 m in the basin axis at the location of well L03-01. Note that part of the over thickening at the basin center is accommodated by a large growth fault (F11). Several syn-depositional faults locally thicken S2 (e.g. on the downthrown sides of faults F12, 15, 18 and 19). Note the sandier upper part of S2 in the downthrown side of F19 along the southern basin margin. The fault intercept well L05-C-03 at 3870 m depth and therefore, the lower part of S2 is faulted out and its stratigraphy unclear at this location.
 The basal surface is highly erosional and show stratal onlapping toward the northern basin margin. Onlaps toward the southern basin margin is also observed with a counterintuitive north-directed onlap between wells L03-02 and L03-01 and prominent south-directed onlaps in the area located north of well L05-07. In this area stratigraphic markers A to F are onlapping on the paleo basin margin.
 The lower part of S2 is composed of low net-to-gross trata of the Oyster Ground Member (OyGrMb) that is sandiest at the basin axis. The upper part of S2 is composed of NoMb sandstones in the northern part of the basin that transition southward to lower net-to-gross strata of the Lies Member (LiMb) (e.g. at location of L03-02)

Sequence 3:
 S3 is present in the TB and in a small basin on the SGP (at and south of well G10-01). The nature of this northern remnant Upper Jurassic accumulation is unknown since well G10-01 intercept only the thin basin margin where the strata is muddy. S3 also extends farther south than S2 with some preserved faulted blocks located south of well L05-C-03. S3 is also thicker in the basin center (at well L03-01). Evidence of onpal are only seen along the northern basin margin (around wells F18-03 and F18-08-S1).The Scruff Greensand Formation (ScGrFm) is observed along all of this profile but changes characteristics from south to north. In the south is overall sandy, thick and non-amalgamated (e.g. well L05-C-03). In the basin axis it is sandy in the lower and upper section of S3 an is thick. In the northern basin margin of TB, S3 is only sandy in its lower section and is sand-poor in the upper section.
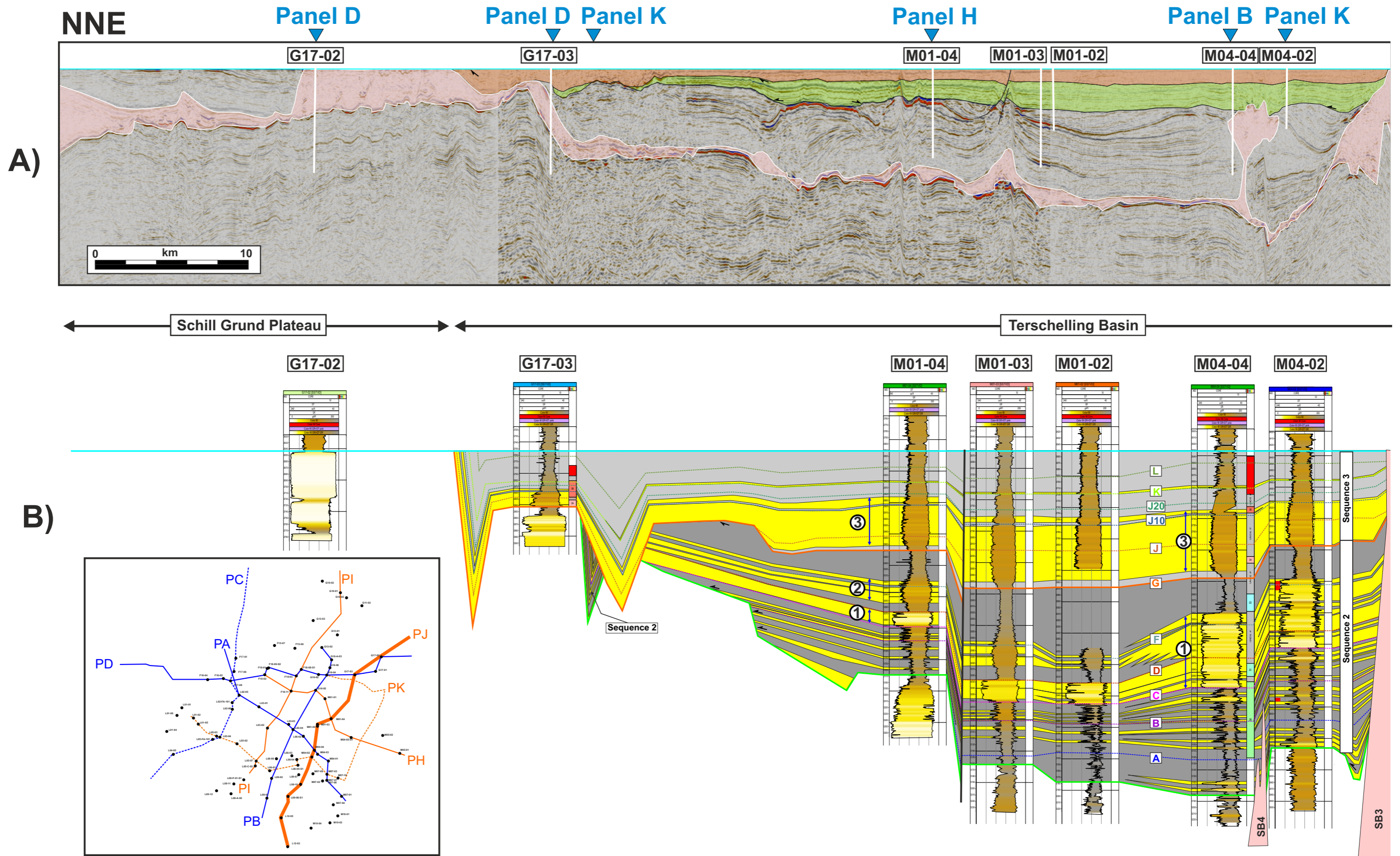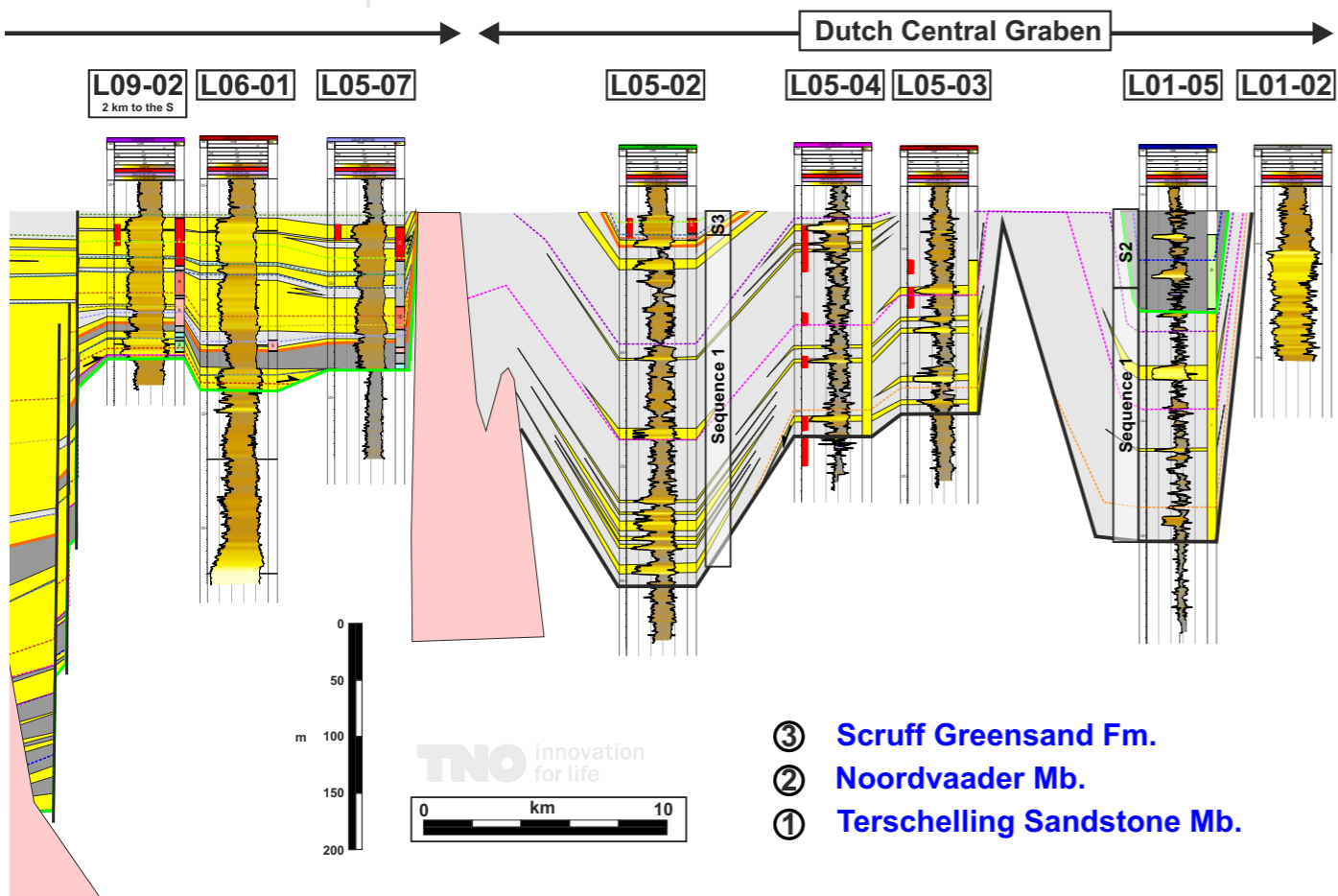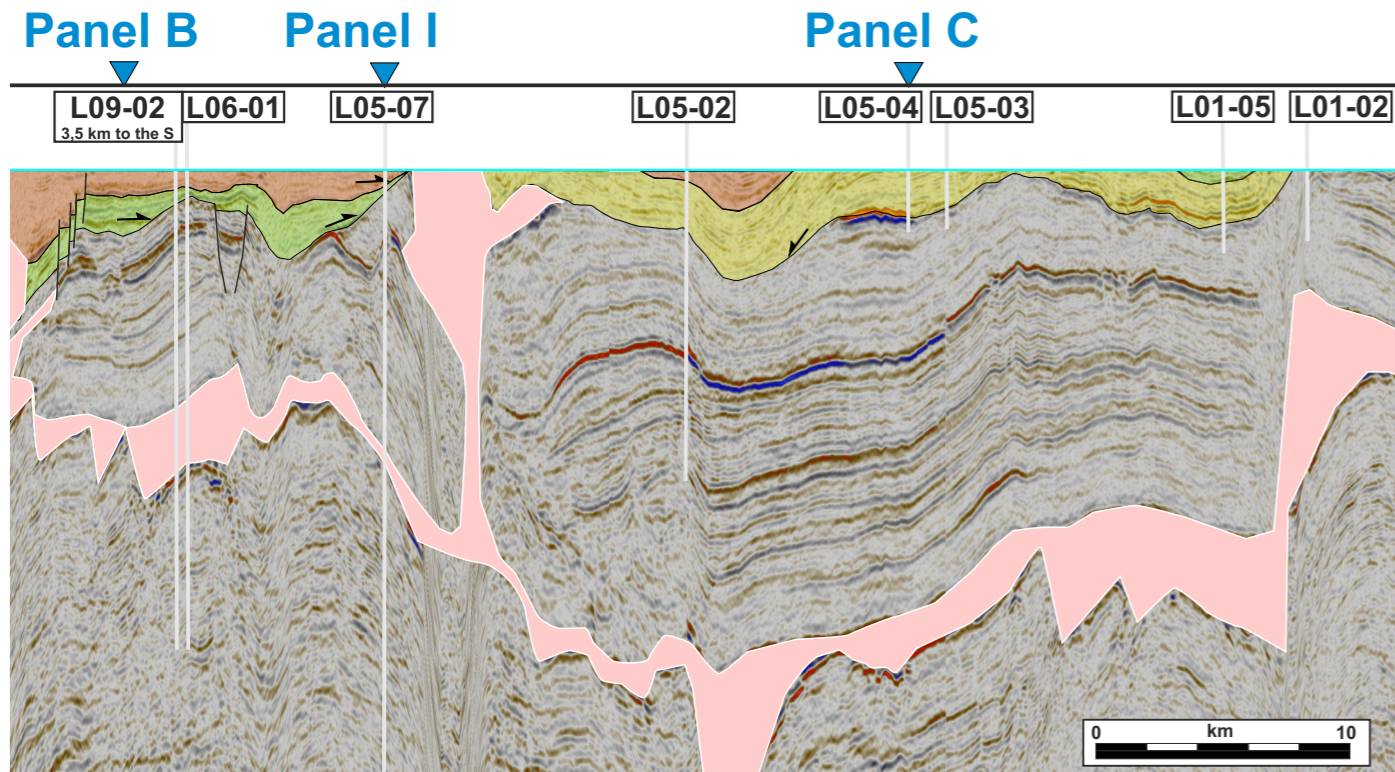
Figure 4.3.3: Stratigraphic correlation for Panel J. See Figure 4.2.1 for location map and Appendix A2 for complete regional panel. A) Flatten seismic on the top Sequence 3. B) Stratigraphic correlation for the Upper Jurassic-Lowermost Cretaceous interval. The section is flattened on the top of S3. TNO zonations (e.g. 2E, 3A) are shown (when available) on the right side of the wells.

Sequence 1:
        S1 is only seen in the Vlieland Basin (well L02-05) where it is thin (15 m) and sandy.

Sequence 2:
        S2 is present in the VB and the TB. In the VB S2 is relatively thin (50 m or less) and thin northward. Basal onlap on older strata is observed in the VB. In the TB, S2 rapidly thickens from the southern basin margin (L09-01) toward the basin center (M04-04, M01-02, M01-03). Toward the north, S2 thin due to basal onlap but also intra Upper Jurassic erosion prior to S3 deposition. (e.g. between M01-04 and G17-03). Note the sharp step at the base of S2 between M01-04 and G17-03 that correspond to the paleo basin margin during the deopistional time of the OyGrMb (Units 2.1 and 2.2, between base Upper Jurassic and stratigraphic markers A and B).
        S2 is relatively sandy in the VB, yet non-amalgamated. In the TB it is sandy in the southern basin margin and in the basin center (TeSdMb). However, in the central part of the basin, the upper part of the TeSdMb transition rapidly to a low net-to-gross interval (LiMb) northward (from well M04-04 to well M01-02). Only the lower part of the TeSdMb can be tracked from well M04-02 to well M01-04.
        A few syn-depositional faults are observed along this section with moderate stratal growth during S2. Salt body also influence the thickness trend of S2 locally. Salt bodies SB3-4 had topographic expression and controlled the deposition of S2 (for SB3-4) and S3 (for SB3).

Sequence 3:
        S3 is present in the VB and the TB. In the VB it is heavily eroded and is only preserved in southern well L12-03, where 45m of relatively sandy strata is present. In the TB S3 is thick in the center part of the basin (well M01-03 and in the northern basin margin where it cut down into S2 and older strata. The lower sandy part of S3 (ScGrFm) in the TB thins toward the basin margins. Note that the TB southern basin margin is bounded by fault F11. It is unclear if this fault was active during the deposition of S2 and S3 due to the amount of post-depositional erosion on the upthrown side of the fault.

③ **Scruff Greensand Fm.**
② **Noordvaader Mb.**
① **Terschelling Sandstone Mb.**

72
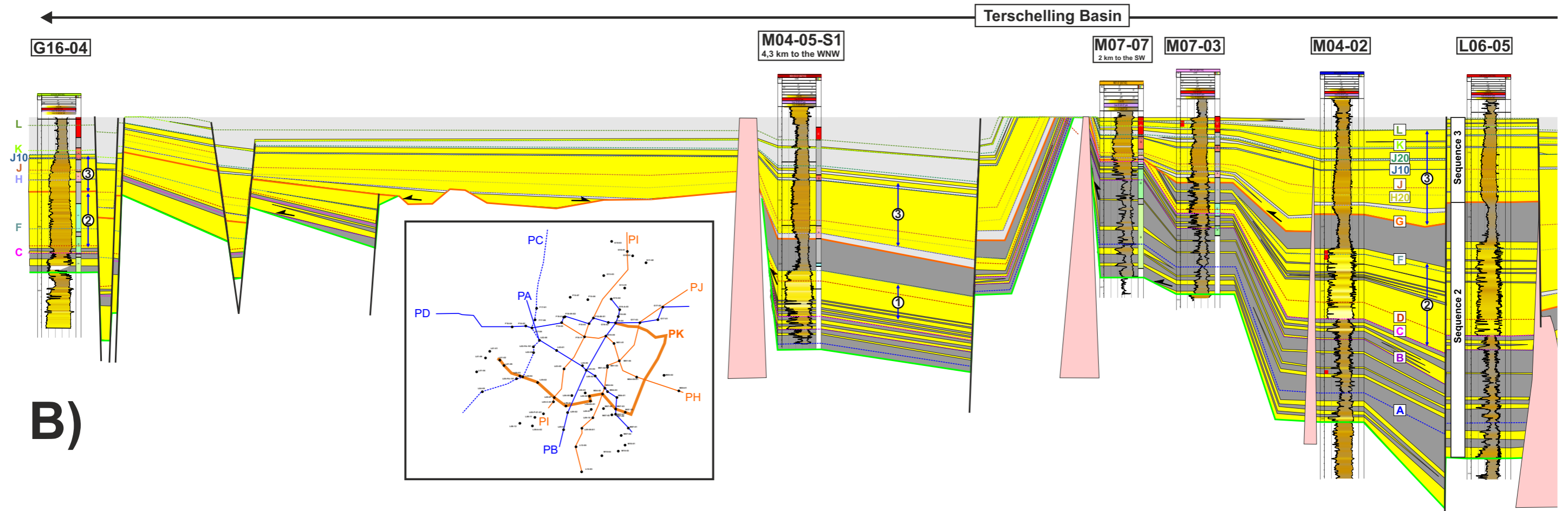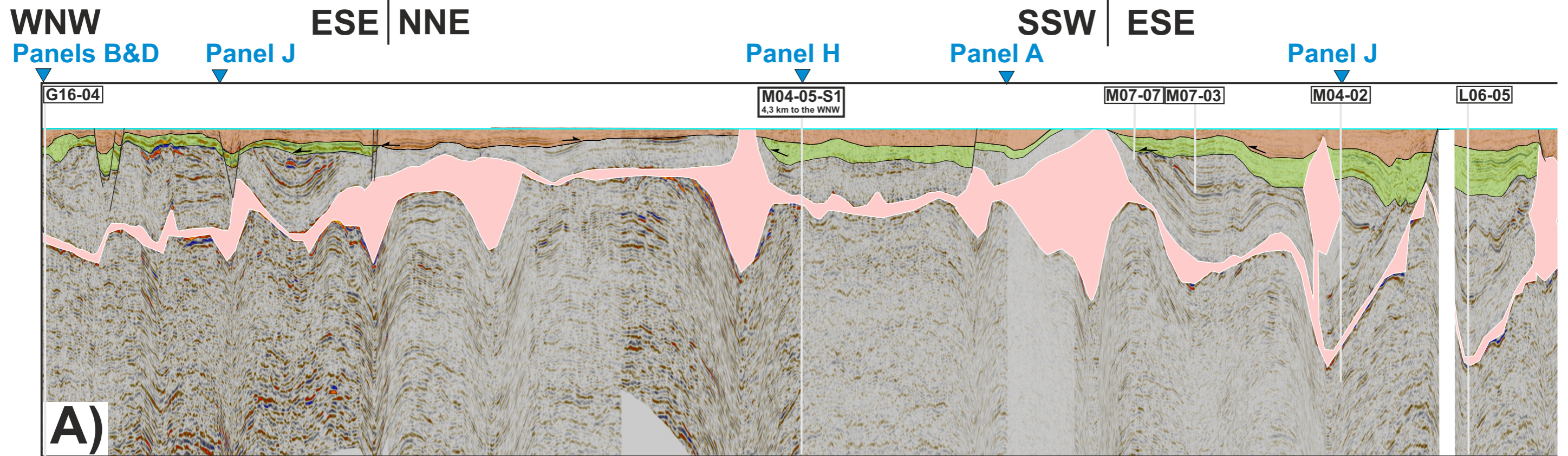
Figure 4.3.4: Stratigraphic correlation for Panel K. See Figure 4.2.1 for location map and Appendix A2 for complete regional panel. A) Flatten seismic on the top Sequence 3. B) Stratigraphic correlation for the Upper Jurassic-Lowermost Cretaceous interval. The section is flattened on the top of S3. TNO zonations (e.g. 2E, 3A) are shown (when available) on the right side of the wells. Note that this panel is circonferential to the TB basin margins and therefore, the stratigraphic correlation observed in this figure need to be evaluated carefully since locally it trends along depositional strike or oblique or along depositional dip.

Sequence 1:

S1 is present in the DCG (wells L05-02 to L01-02) where is thick (200 + m). Some stratal onlap are observed at the base of S1 toward the east.

Sequence 2:

S2 is present in the DCG and the TB. In the DCG it is only observed at the location of well L01-05. In the TB it observed in all wells (except in L06-045 where it is faulted out). On seismic however, a zone of no deposition of S2 is seen northeast of well M04-05-S1.

The base of S2 is erosional and cut locally deep into the Upper Triassic and even the Lower Triassic (e.g. at well M07-07). It is the thickest at the location of well L06-05. Local basal onlap are also observed along this profile.

Sequence 3:

S3 is present in the DCG and the TB. In the DCG it is only observed at the location of well L05-02. In the TB it observed in all wells. It is the thickest in a small syn-depositional graben located between wells L09-02 and L06-05. It onlaps locally onto S2 or older strata

73
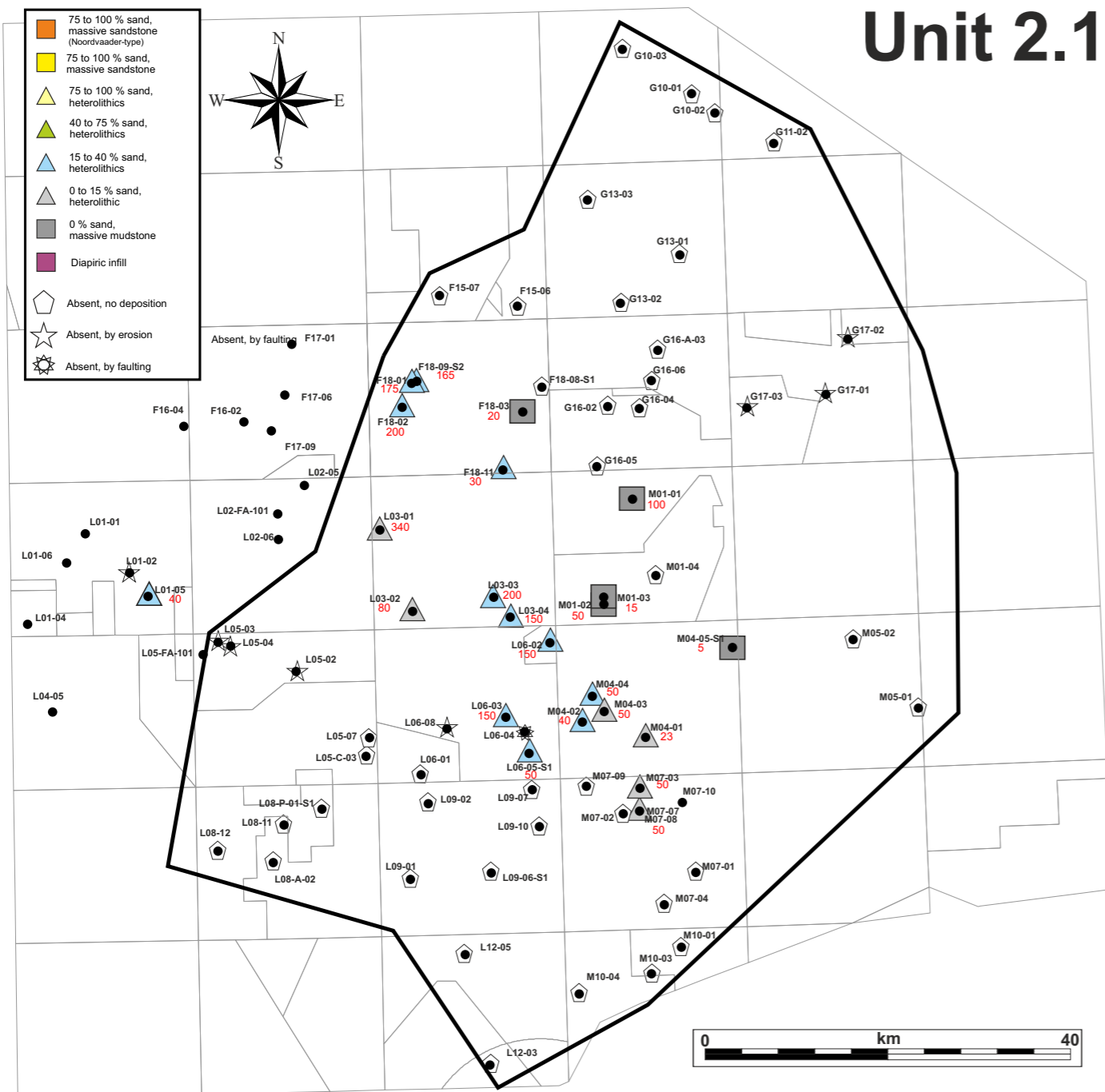
Figure 4.4.1: Lithofacies map of Unit 2.1 (Sequence 2) identified at well locations. The thickness of this unit at well location is also shown (red text) in meters. Chapter 3.5 and Figure 3.5.1 explain in detail how this data was gathered.
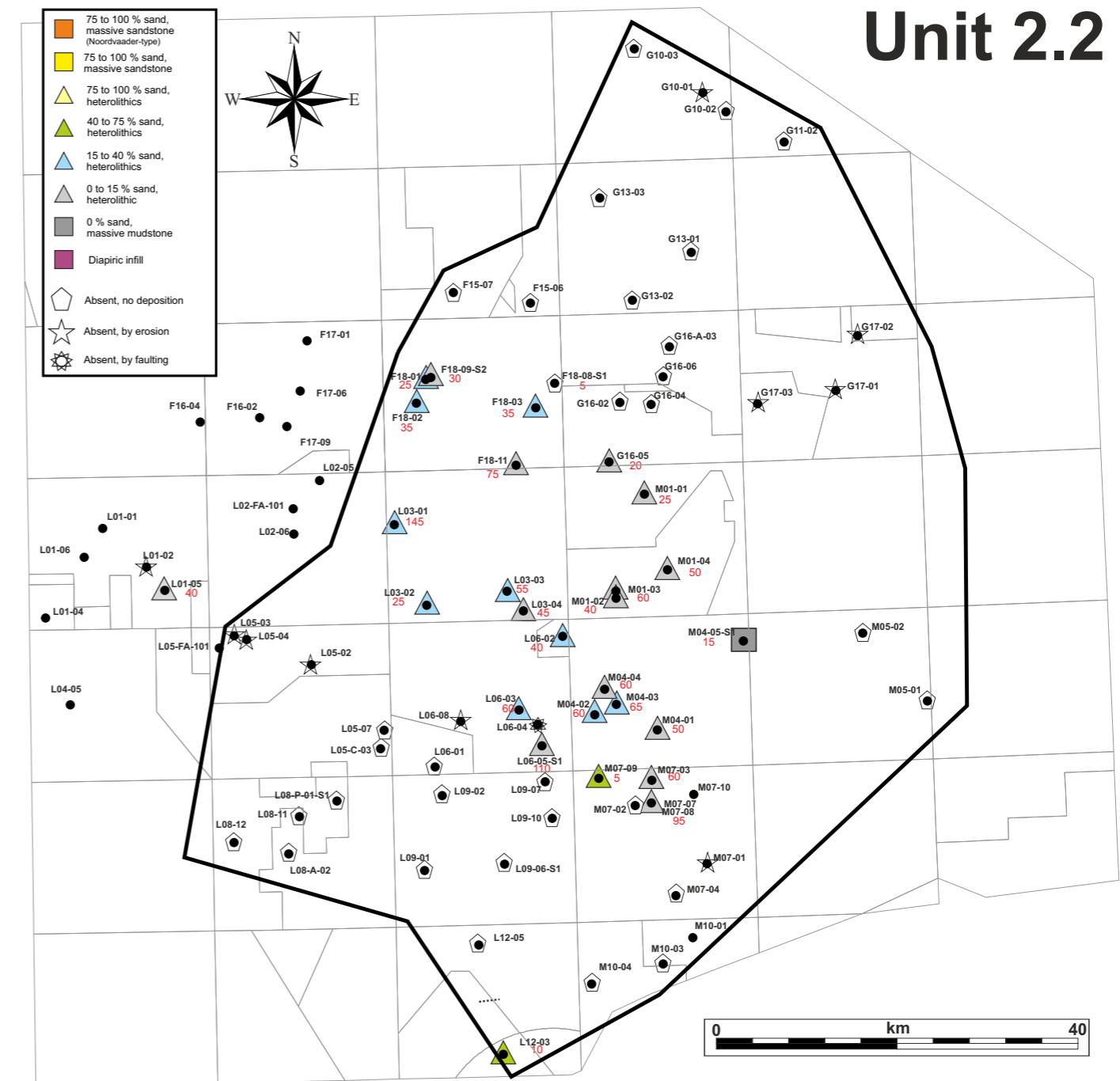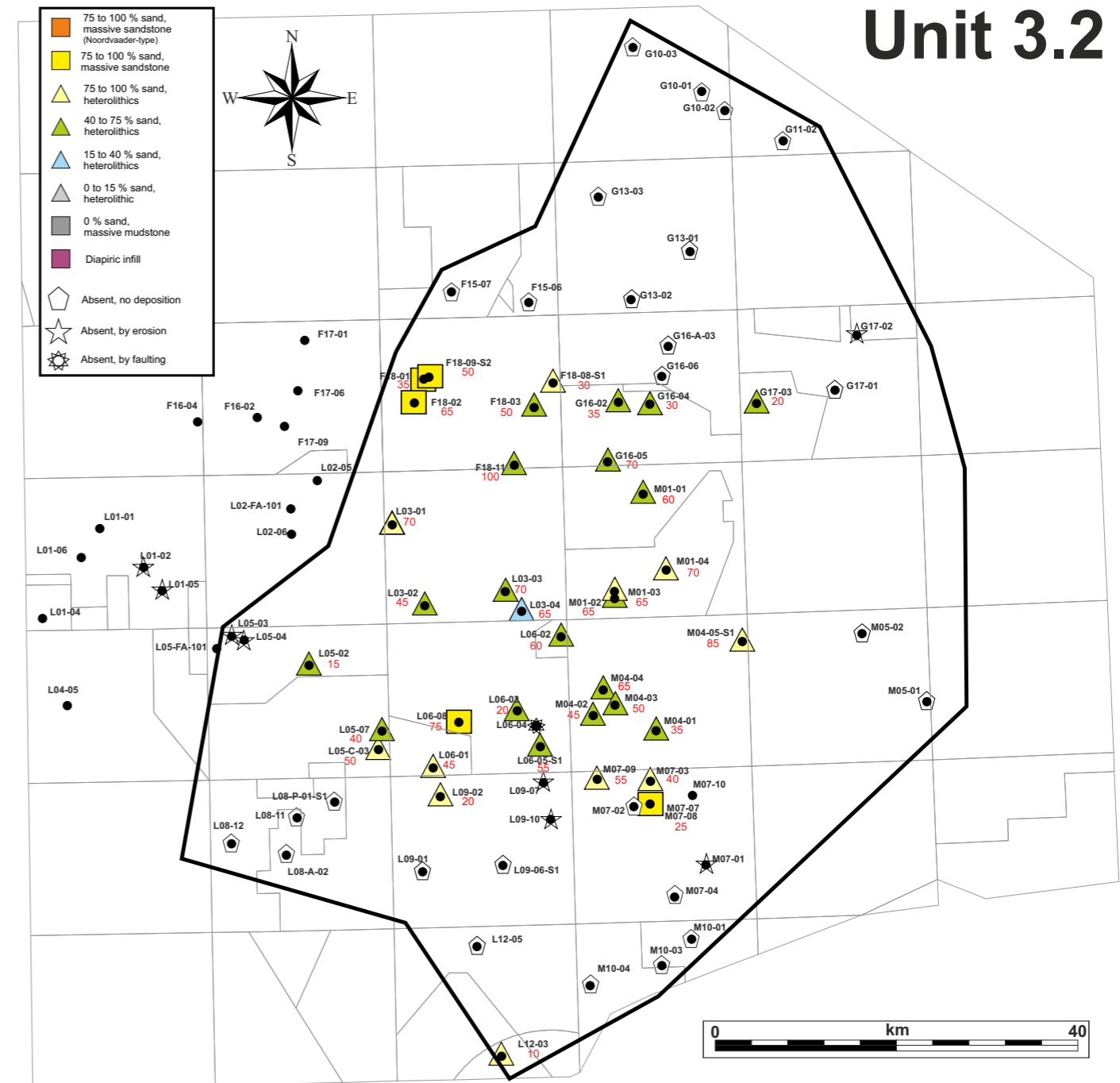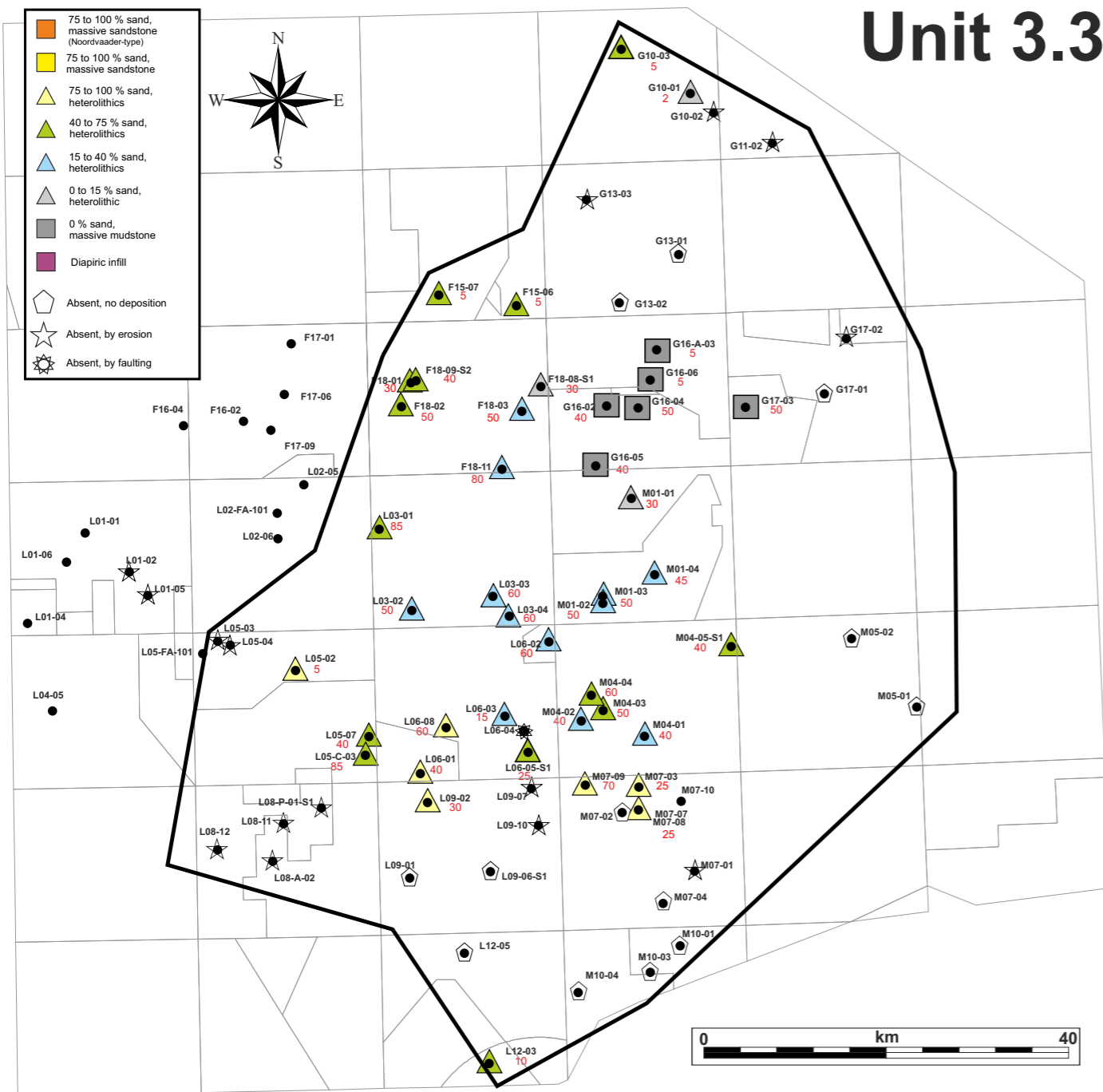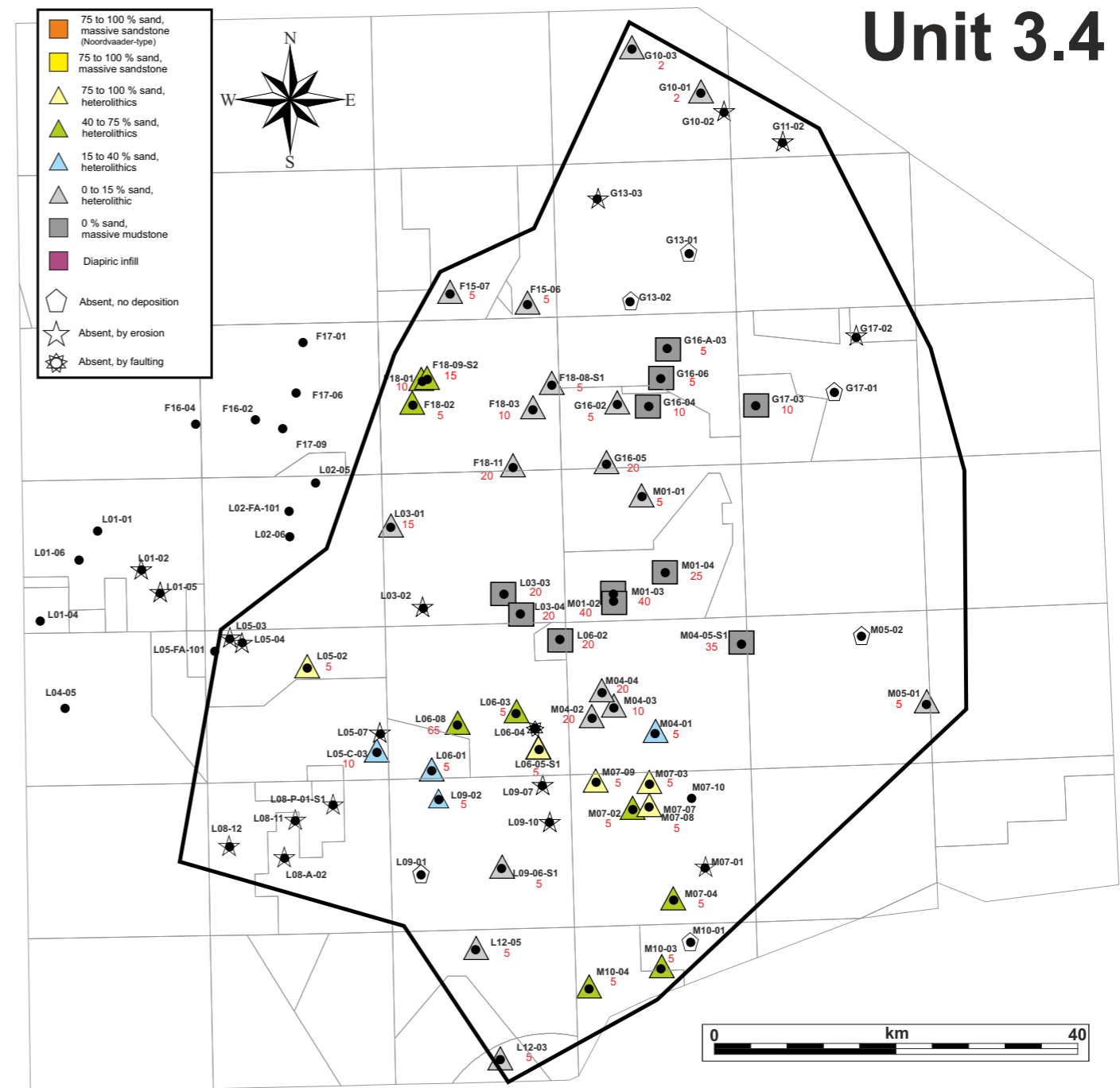
Figure 4.4.2: Lithofacies map of Unit 2.2 (Sequence 2) identified at well locations. The thickness of this unit at well location is also shown (red text) in meters. Chapter 3.5 and Figure 3.5.1 explain in detail how this data was gathered.
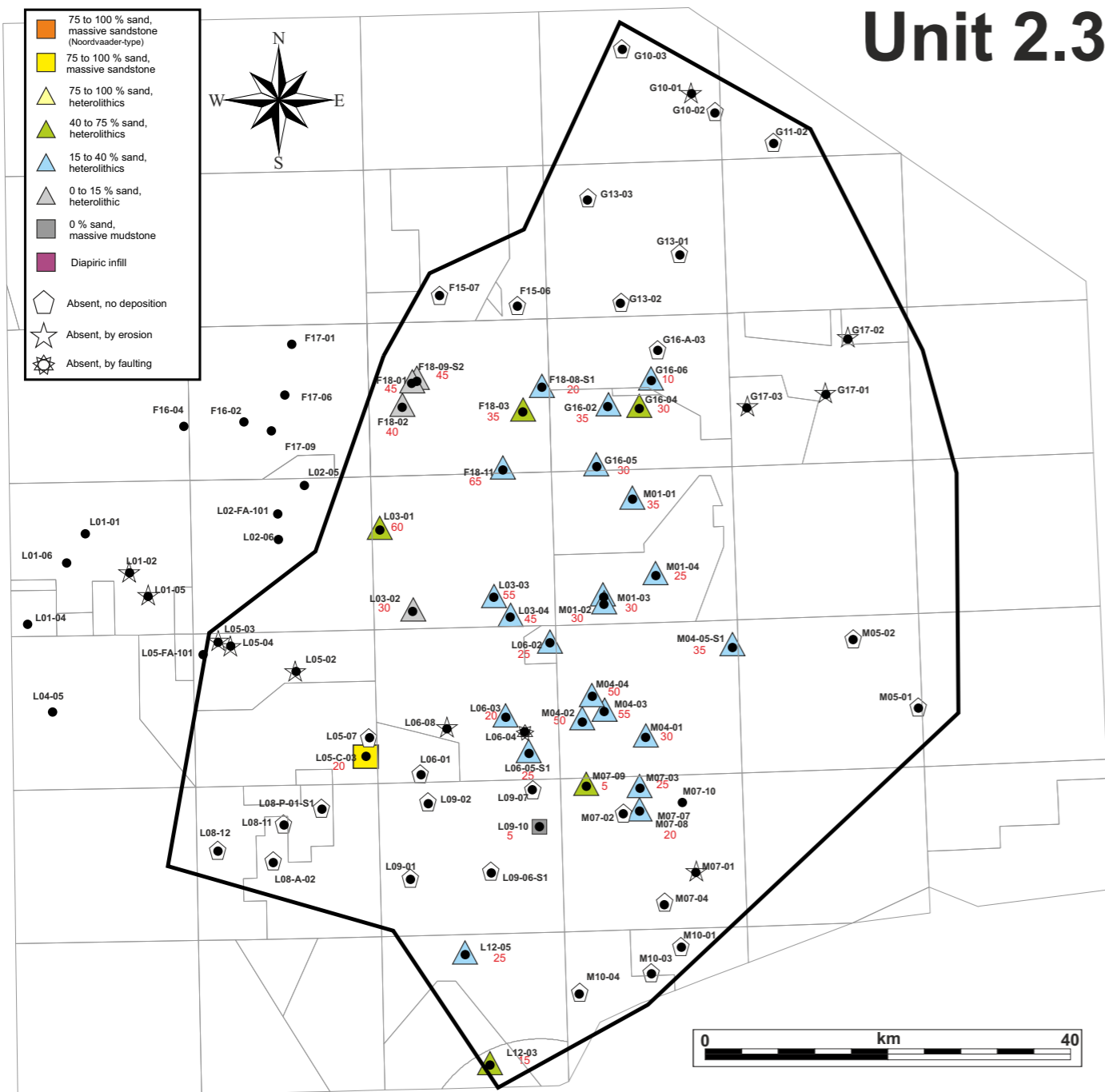
Figure 4.4.3: Lithofacies map of Unit 2.3 (Sequence 2) identified at well locations. The thickness of this unit at well location is also shown (red text) in meters. Chapter 3.5 and Figure 3.5.1 explain in detail how this data was gathered.
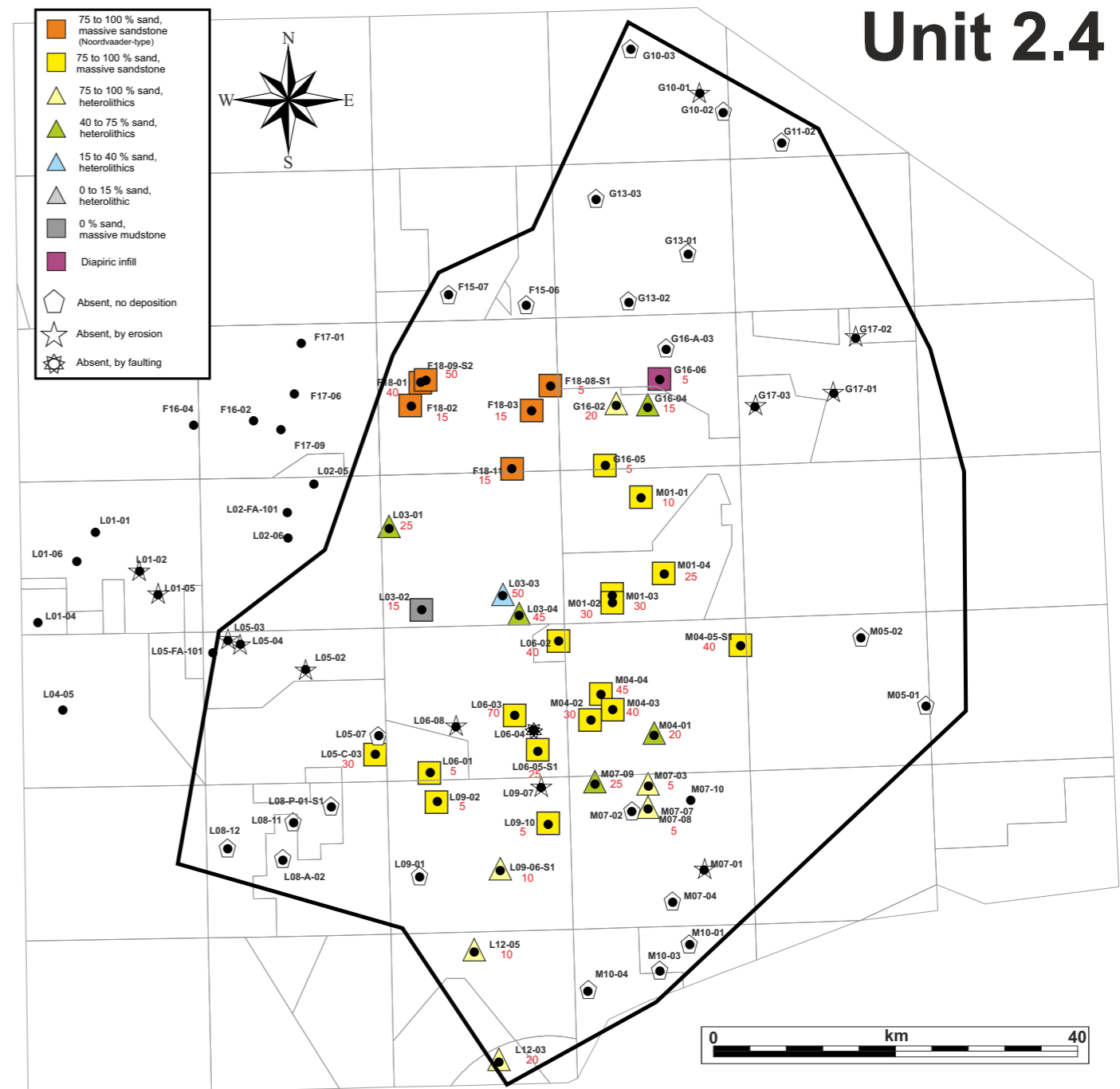
Figure 4.4.4: Lithofacies map of Unit 2.4 (Sequence 2) identified at well locations. The thickness of this unit at well location is also shown (red text) in meters. Chapter 3.5 and Figure 3.5.1 explain in detail how this data was gathered.

Figure 4.4.5: Lithofacies map of Unit 2.5 (Sequence 2) identified at well locations. The thickness of this unit at well location is also shown (red text) in meters. Chapter 3.5 and Figure 3.5.1 explain in detail how this data was gathered.

Figure 4.4.6: Lithofacies map of Unit 2.6 (Sequence 2) identified at well locations. The thickness of this unit at well location is also shown (red text) in meters. Chapter 3.5 and Figure 3.5.1 explain in detail how this data was gathered.
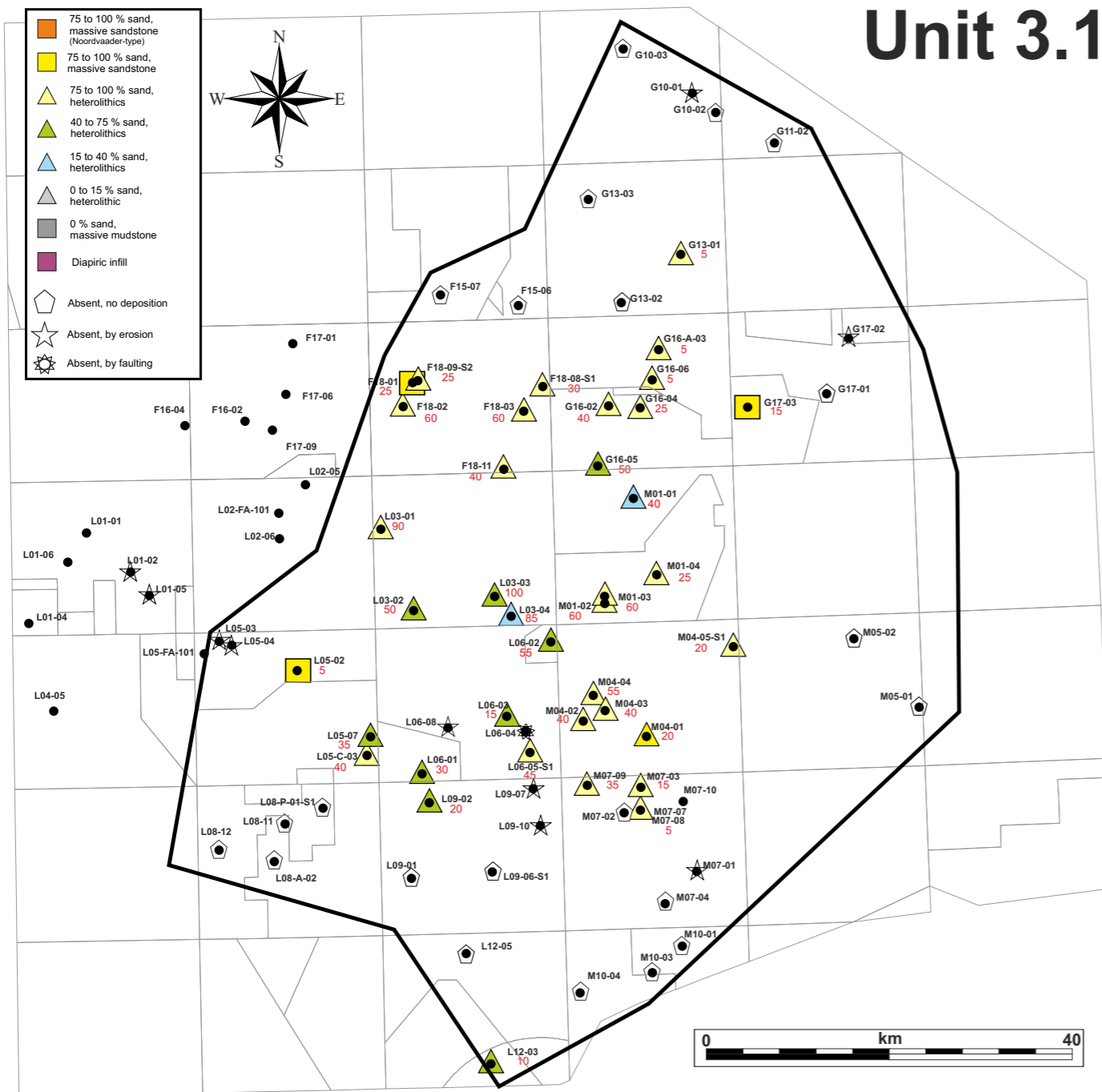
Figure 4.4.7: Lithofacies map of Unit 3.1 (Sequence 3) identified at well locations. The thickness of this unit at well location is also shown (red text) in meters. Chapter 3.5 and Figure 3.5.1 explain in detail how this data was gathered.

Figure 4.4.8: Lithofacies map of Unit 3.2 (Sequence 3) identified at well locations. The thickness of this unit at well location is also shown (red text) in meters. Chapter 3.5 and Figure 3.5.1 explain in detail how this data was gathered.

Figure 4.4.9: Lithofacies map of Unit 3.3 (Sequence 3) identified at well locations. The thickness of this unit at well location is also shown (red text) in meters. Chapter 3.5 and Figure 3.5.1 explain in detail how this data was gathered.

Figure 4.4.10: Lithofacies map of Unit 3.4 (Sequence 3) identified at well locations. The thickness of this unit at well location is also shown (red text) in meters. Chapter 3.5 and Figure 3.5.1 explain in detail how this data was gathered.

5

DISCUSSION

The Terschelling Basin (TB) margins have various configuration depending on the location and the age of the stratigraphy involved. Understanding the geometry and the potential changes in basin margin configuration through time is important since sand-rich deposits that can be reservoir targets, may accumulate along the basin margin but with different facies, stratigraphic architecture and volume depending on the basin margin configuration itself.

In this section we discuss the different types of basin margin observed around the TB. Several characteristics were used to distinguish several end members (Fig. 5.1.2), including:
- the type and age of strata located outside of the basin but in physical contact with the basinal strata (e.g. Permian salt, Triassic clastics),
- the angularity between the marginal basin strata and the basin margin itself (low vs high angle),
- the type of contact such as faulted, non-faulted, or onlapping,
- the stratigraphic growth geometry in the vicinity of the physical basin margin contact (e.g. rim syncline or conduit).
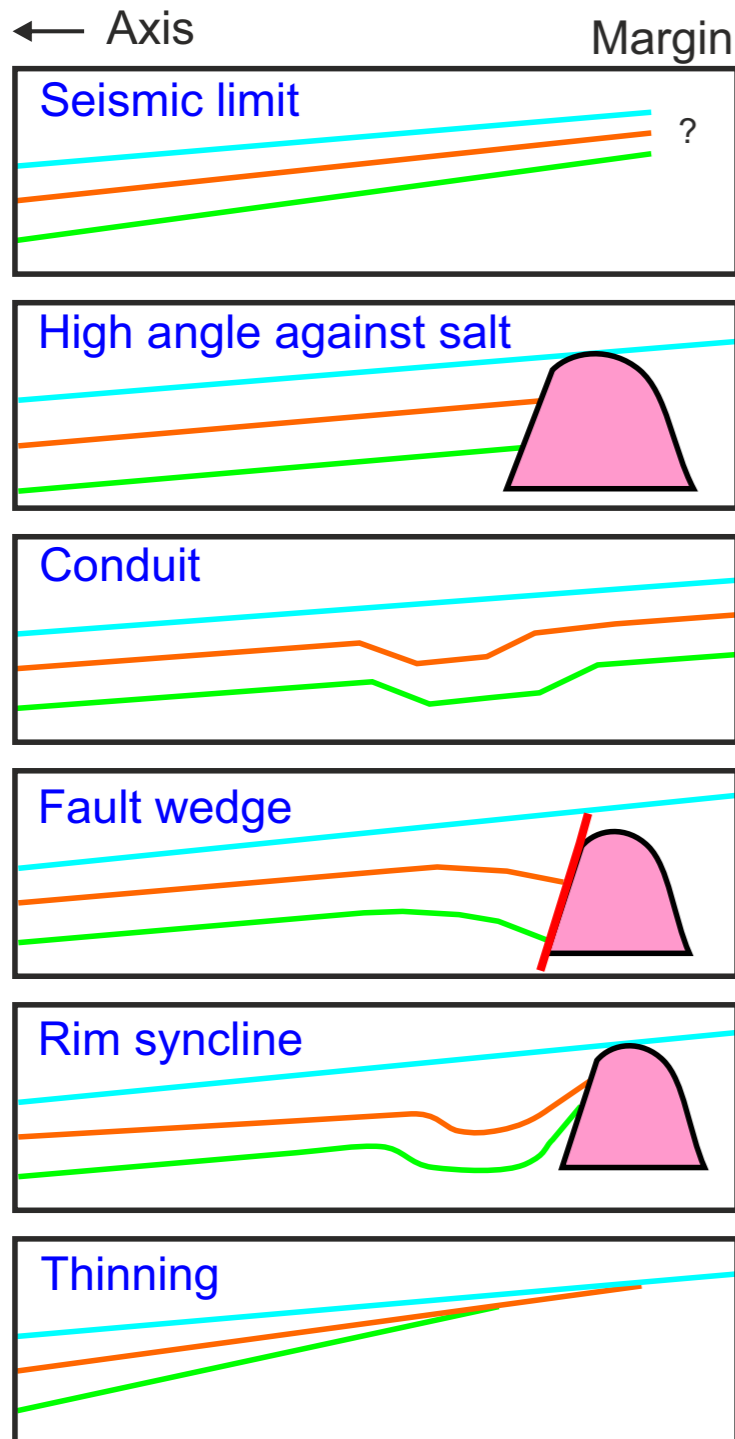
The impact of basin margin geometry on marginal stratigraphy, and other basin parameters, has been studies in deepwater case, using outcrop data (Figure 5.1.2). In Bouroullec et al. (in press) the Grand Coyer Basin in the French Alps was studied to characterize the geometry of deepwater lobes and channelized deposits in the basin axis and along the basin margins. The syn-depositional activity during deposition created various margin configuration from steep to low angle. Several outcrops were characterized using traditional (photopanels, measured sections) and digital (Lidar data) information. Figures 5.1.3-10 show some of the results from the Grand Coyer Sub-Basin margin configuration study (Bouroullec et al., in press) that is very relevant to the discussion regarding the Terschelling Basin margins. Even if the depositional environments defers (shallow versus deep-water), some of the lessons learned from the outcrop study can be used to better predict sandstone occurrences and preservation along the complex basin margins.
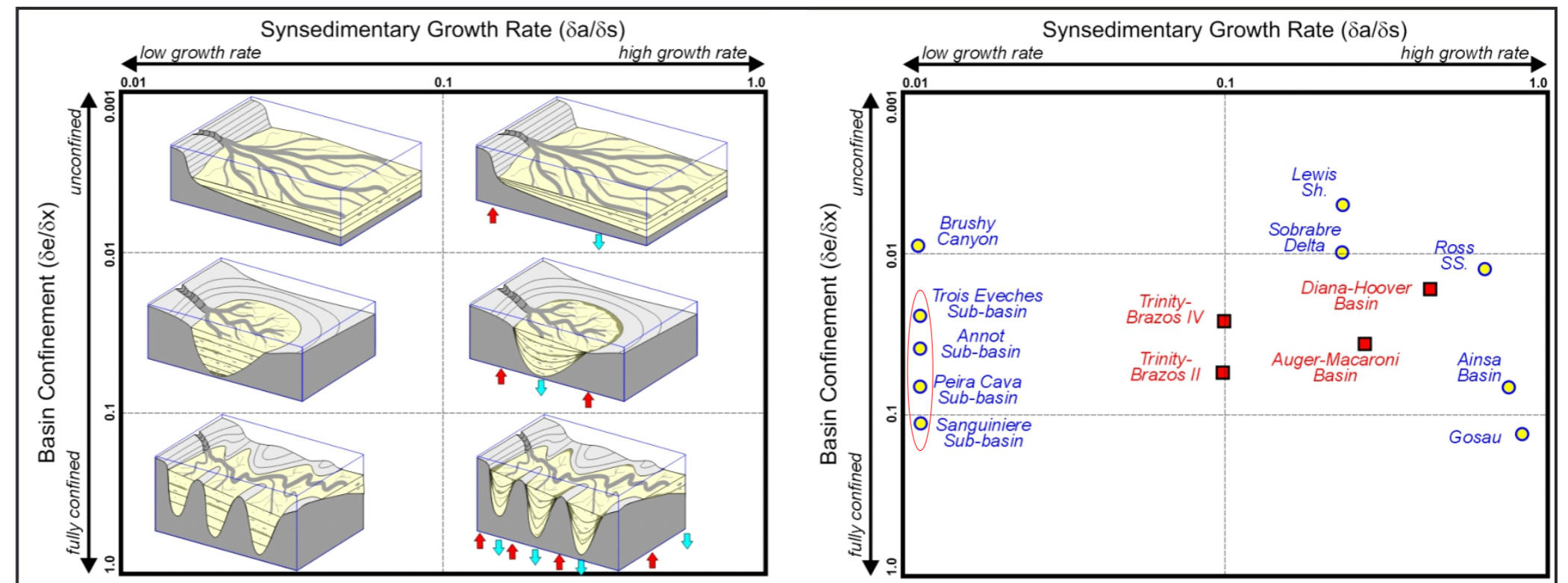
Figure 5.1.1: Type of basin margin configurations observed in the Terschelling Basin during the Late Jurassic - Early Cretaceous.

Figure 5.1.2: Syn-depositional growth in deepwater basins. The Annot sub-basins (red oval) have a low structural growth rate and is moderate to highly confined. Bouroullec et al. (in press).
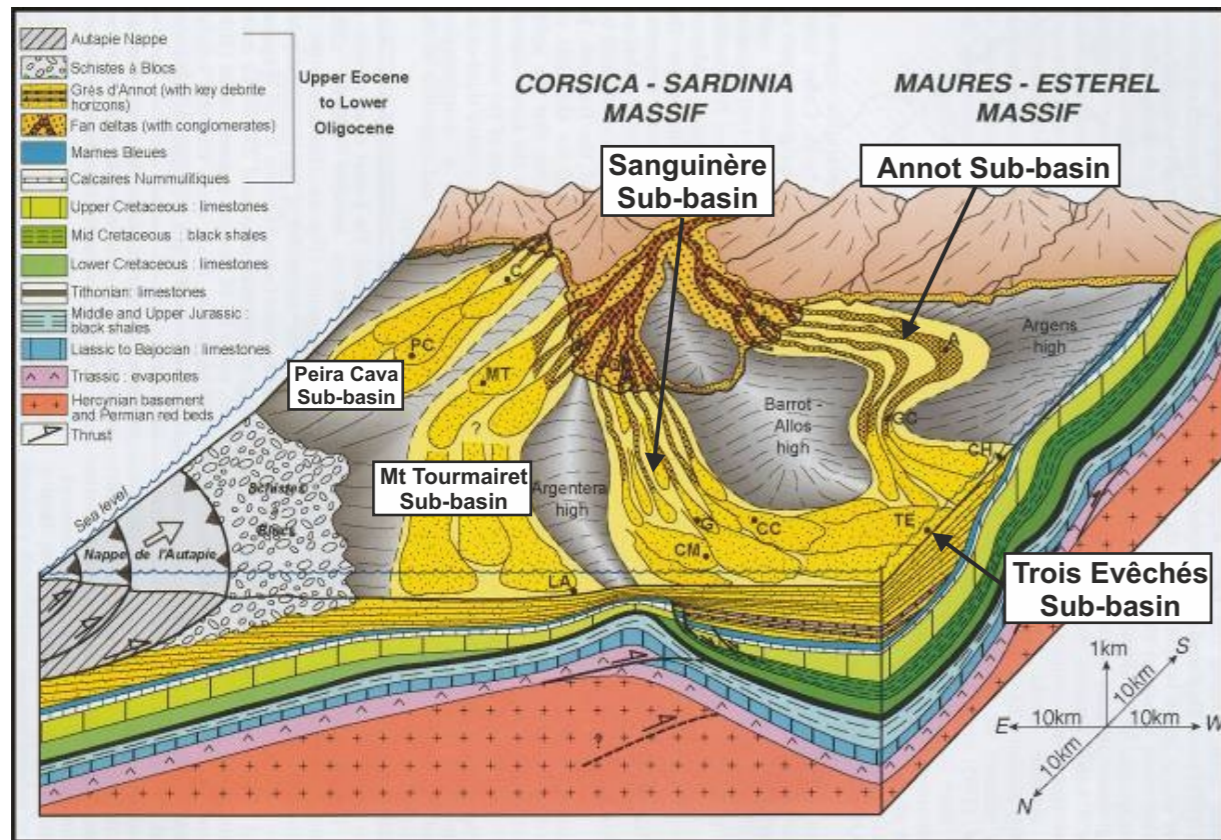
Figure 5.1.3: Schematic paleogeography of the Grès d'Annot system in Early Oligocene time (from Joseph and Lomas, 2004). The paleotopography prior to the deposition of the Grès d'Annot Formation was inherited from early phases of Alpine compression. Ravenne et al. (1987) identified a series of sub-basins trending SE/NW. These sub-basins are partially confined sub-basins linked by channels and bypass surfaces (Pickering and Hilton, 1998). The Grand Coyer inter-basinal conduit is located in the western part of the Annot Basin and links the Annot sub-basin to the Trois Évêchés sub-basin**.** Structural growth during deposition on the Grès d'Annot Formation is minor (Bouroullec *et al.*, 2004).
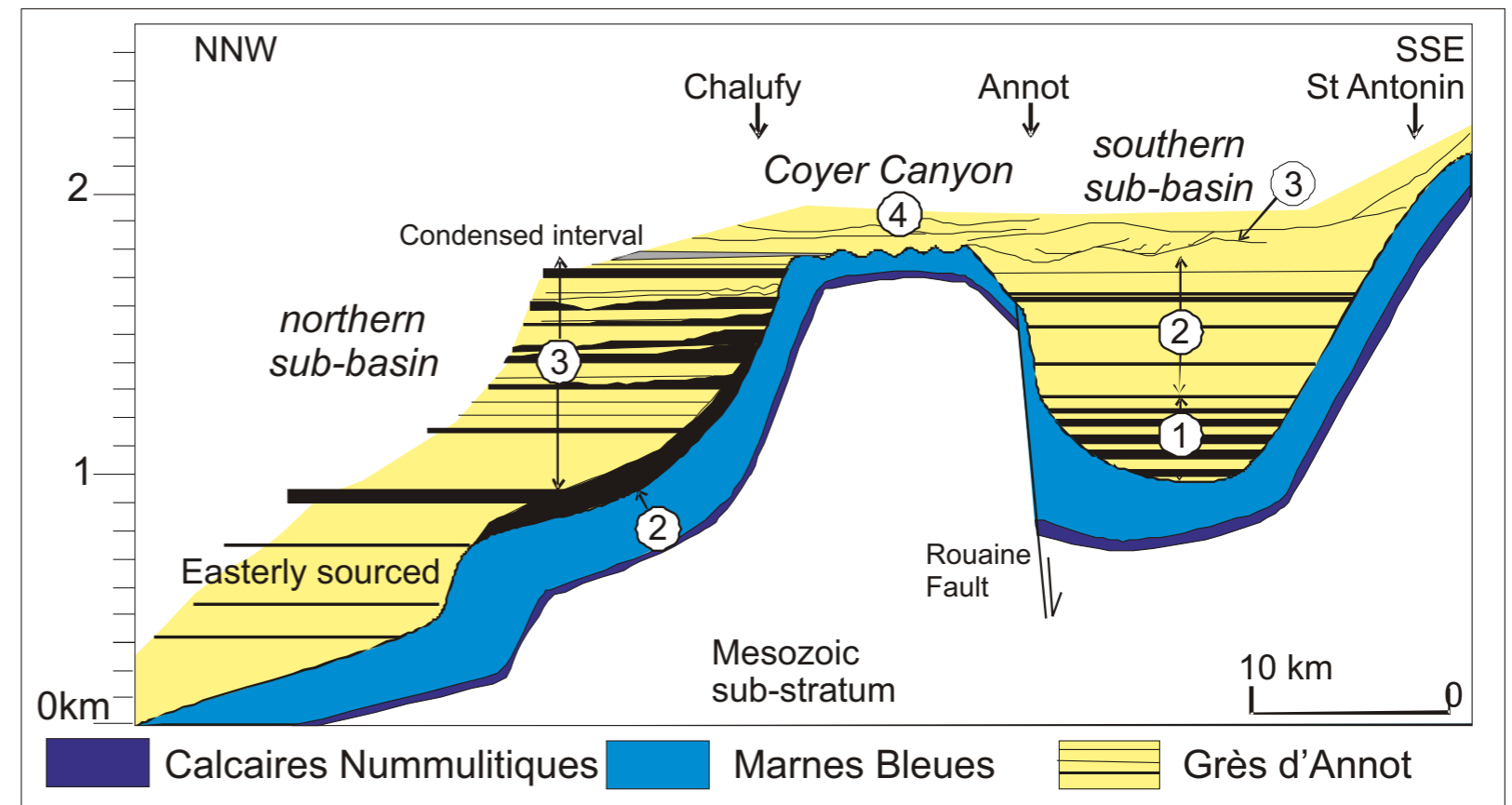
Figure 5.1.5: Cross section through the Grand Coyer conduit (modified from Sinclair and Tomasso, 2002).

Figure 5.1.6: The world-class Chalufy outcrop in the Annot Basin. This exposure show well the low angle onlap of deepwater sandstone units onto the muddy Marnes Bleues basin margin. Photo by R. Bouroullec.

86
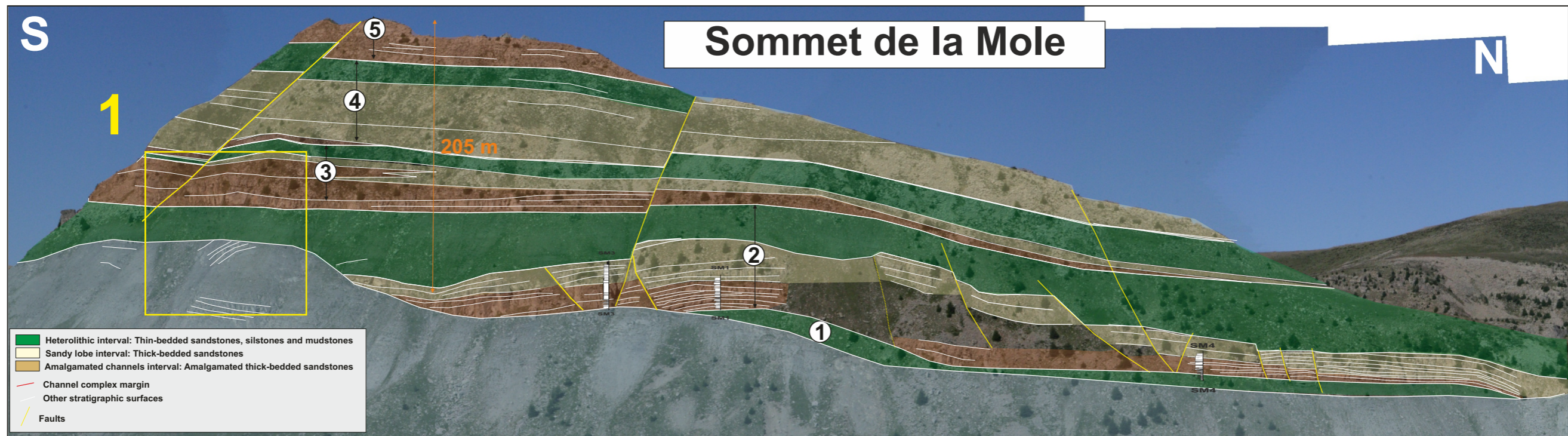
Figure 5.1.7: The Sommet de la Mole outcrop in the Grand Coyer Sub-basin in the Annot Basin. This exposures show a basal step similar to some of the geometry observed in the Terschelling basin at the base of Sequence 2. From Bouroullec et al. (in press).
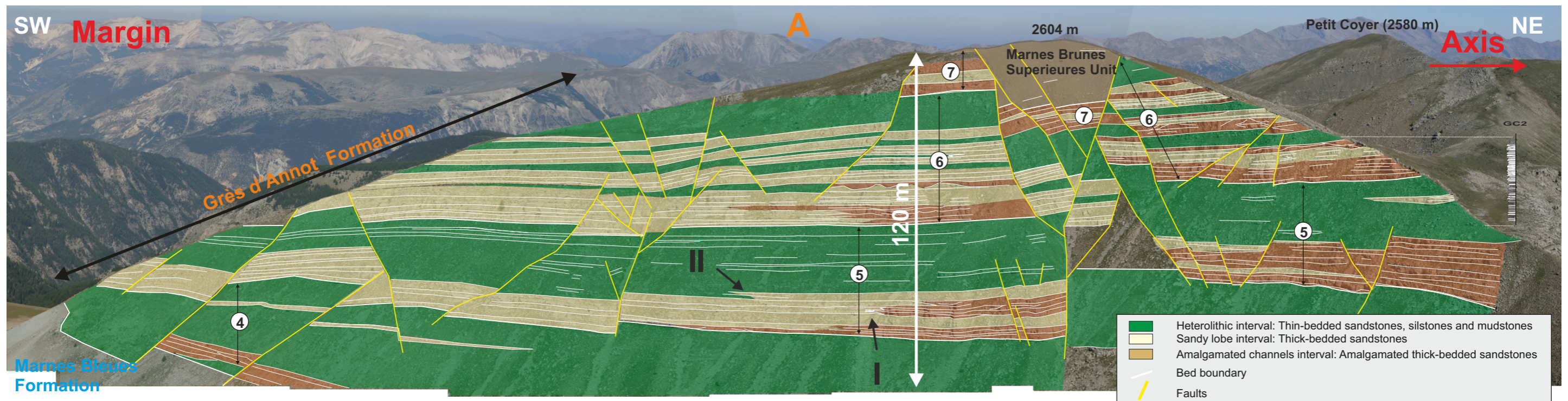
Figure 5.1.8: Interpreted photopanel of the Vallier exposure which represent the low angle basin margin of the Grand Coyer sub-basin. This outcrop shows clearly the lateral facies transition toward the western margin. The thick-bedded coarse-grained sandy channelized strata (brown colored intervals) laterally change to finer grain sand lobes (see **I** as example), which themselves laterally change to more thinly bedded heterolithic intervals (see **II** as example). Cycles 3 has nearly completely lapped out onto the Manes Bleues Formation at the eastern edge of the exposure. All of the faults affecting this outcrop are post-depositional. Note the presence of the upper marl unit (Marnes Brunes Supérieures) within the strike slip flower structure. From Bouroullec et al. (in press).

87
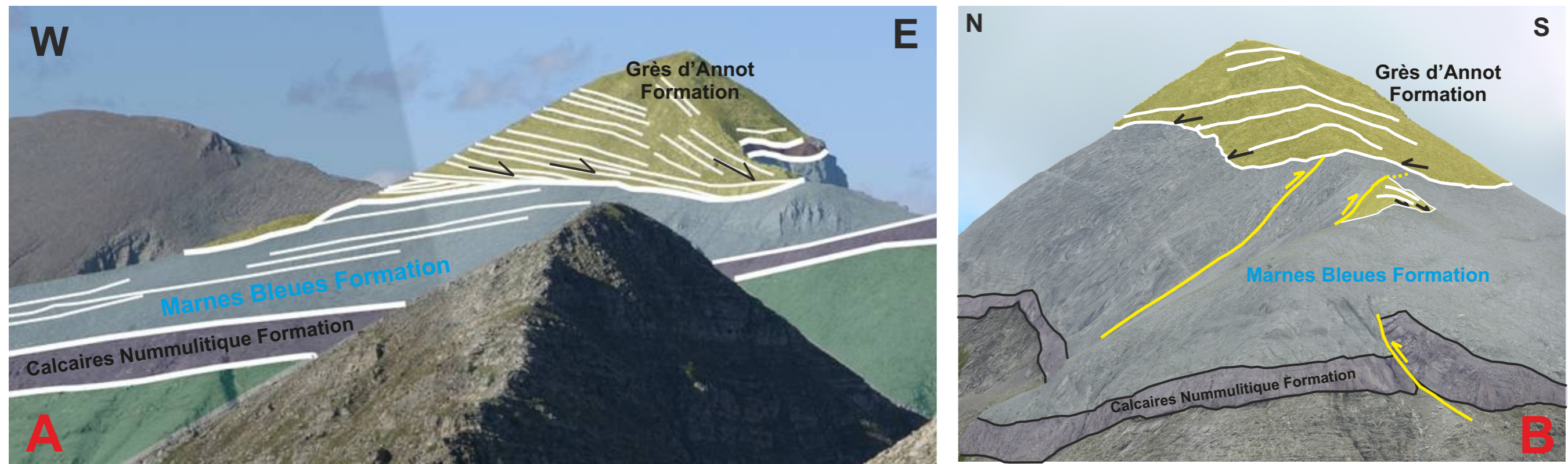
Figure 5.1.9: The Sommet de Frema exposure in the Grand Coyer Sub-basin. **A)** The southern side of Sommet de Frema shows an apparent downlapping of the Annot sands onto the Marnes Bleues Formation. The angle between the Marnes Bleues strata and the Grès d'Annot strata is 25-30 degrees. No thin bedded strata are observed and the thick-bedded sandstones lap directly onto the slope marls. **B)** View toward the east of the Sommet de Frema exposure. This view shows the northern side of the exposure where the Annot sandstones lap at an angle of 35-45 degrees onto the Marnes Bleues. This view also illustrates some pre- and early Grès d'Annot Formation deformation. Some thrusts can be observed that intercepts the Calcaires Nummulitiques Formation and the lower part of the Grès d'Annot Formation. From Bouroullec et al. (in press).
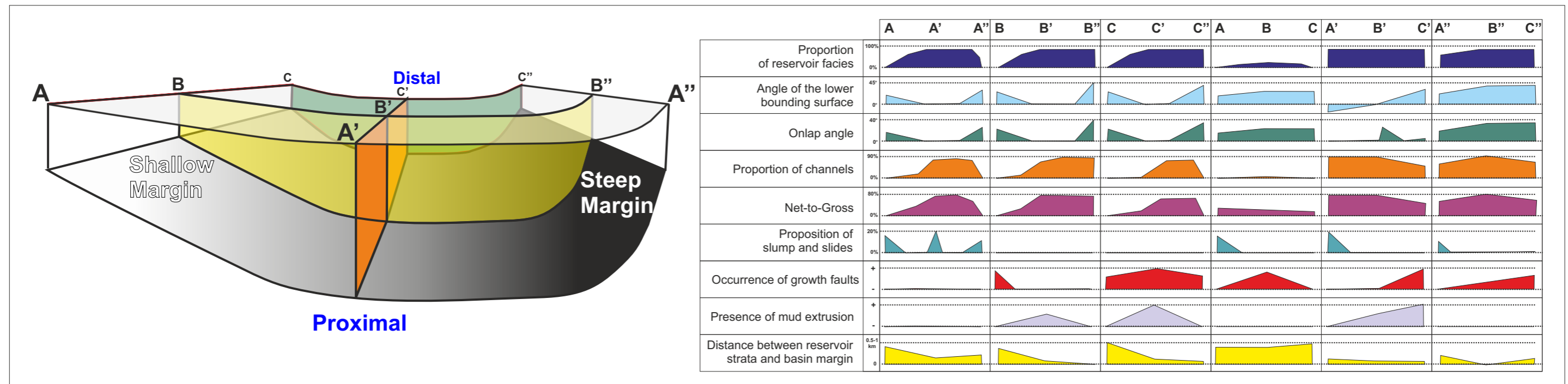
Figure 5.1.10: Schematic basin margin matrix relating basin angle to a series of basin and reservoir parameters. From Bouroullec et al. (in press).

One important fact when discussing the TB basin margins is that they are located at different locations locally between Sequence 2 and Sequence 3 depositional time. Sequence 3 extends farther to the east along most of the basin's eastern margin and locally farther north and south along the northern and southern basin margins (Figure 5.1.11).

This widening of the basin through time also occurred during the deposition of Sequence 2 as seen by the step in S2 time thickness map which correspond is general to the depositional limit of the Oyster Ground Member (Figure 5.1.12). This step and example of the stratal onlaps ca also be seen of Figures 5.1.13 and 5.1.14.
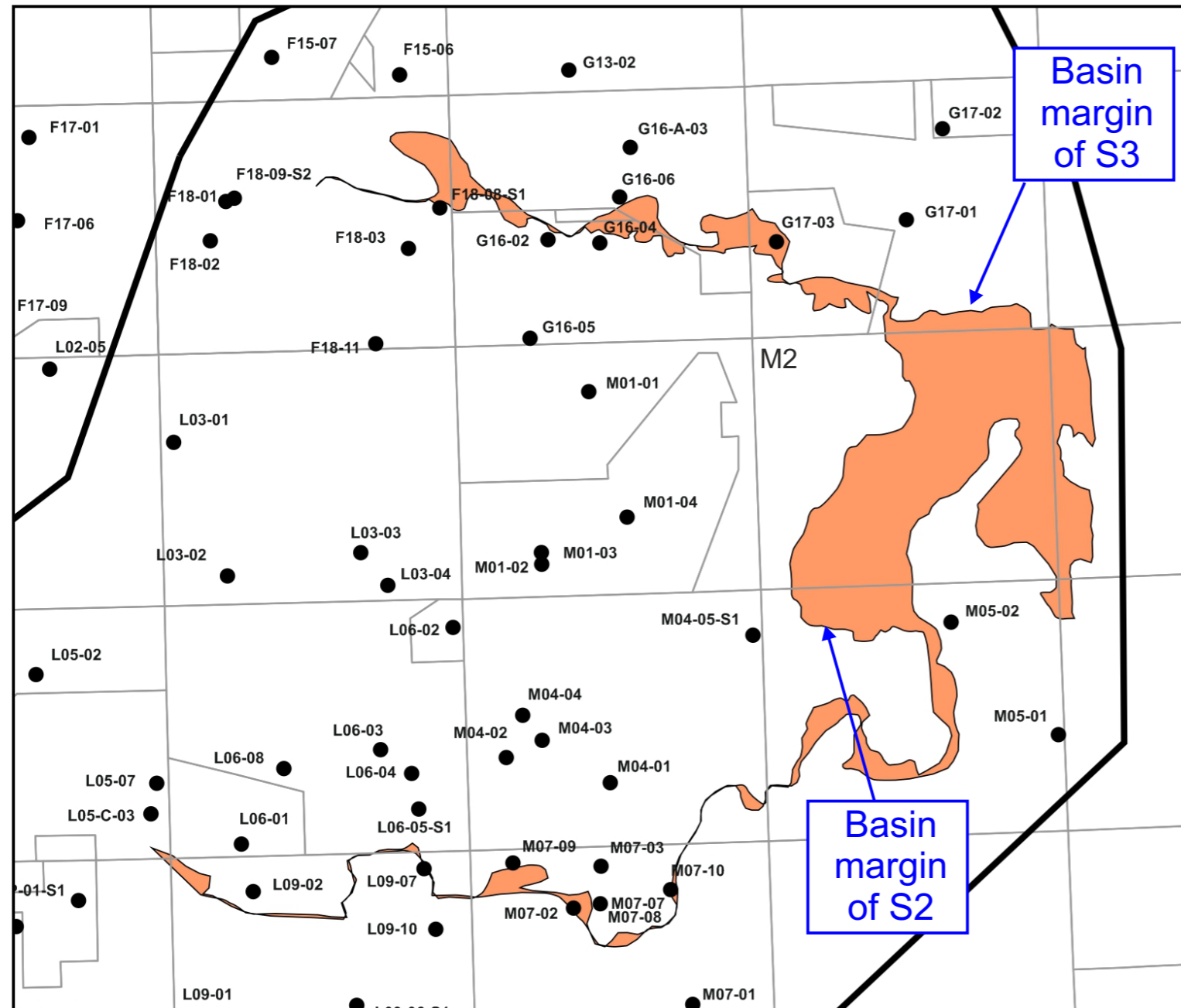
Figure 5.1.11: Areal extent of Sequence 3 when Sequence 2 was not deposited or was eroded prior to S3 deposition. Note the large area in Block M2 when S3 is present but not S2.
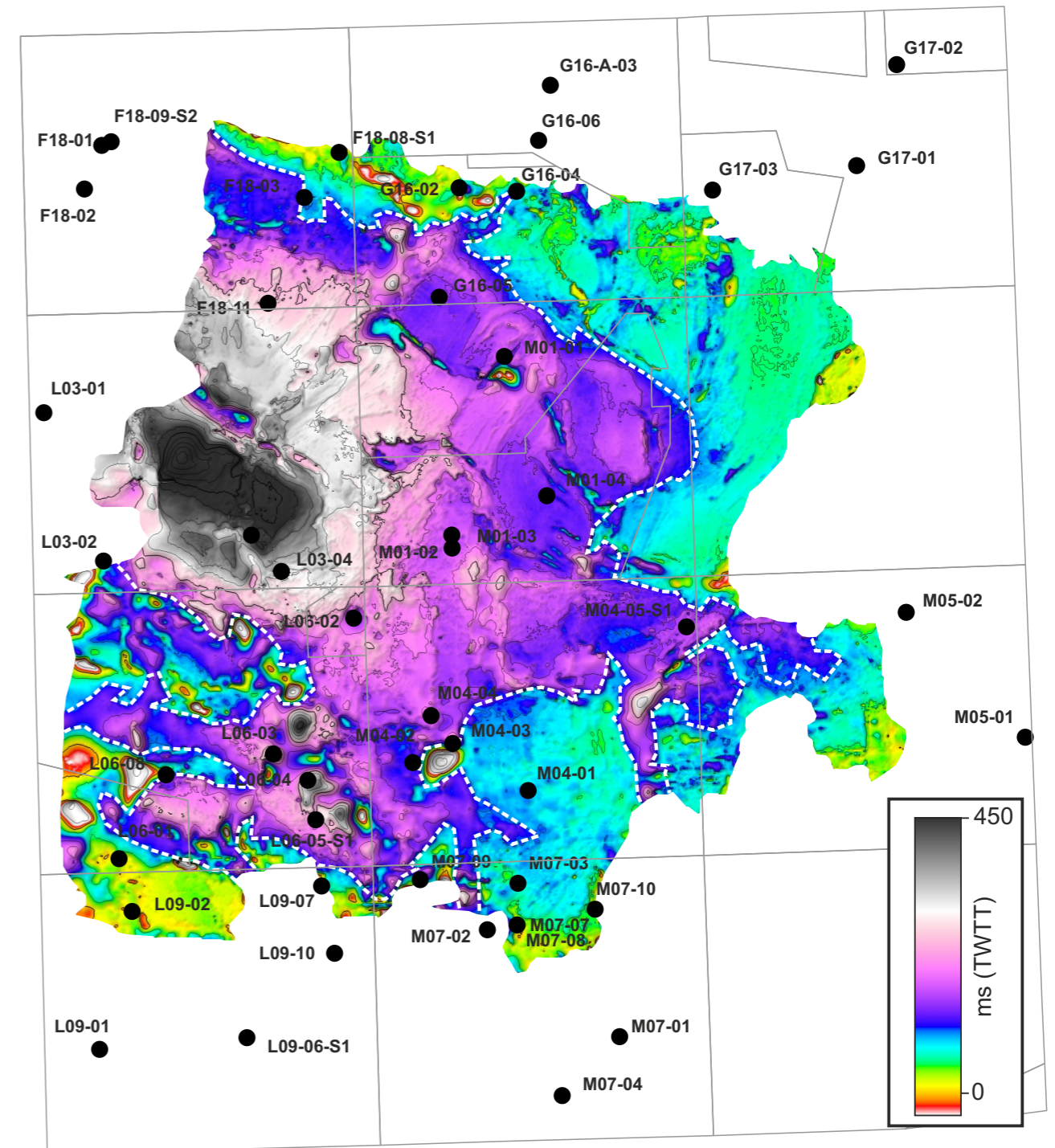
Figure 5.1.12: Time thickness map of S2 showing the marked step in the thickness trend (dashed white line) that represent a pronounced feature at the base of S2 where strata onlap onto (mainly Oyster Ground Mb strata).

89
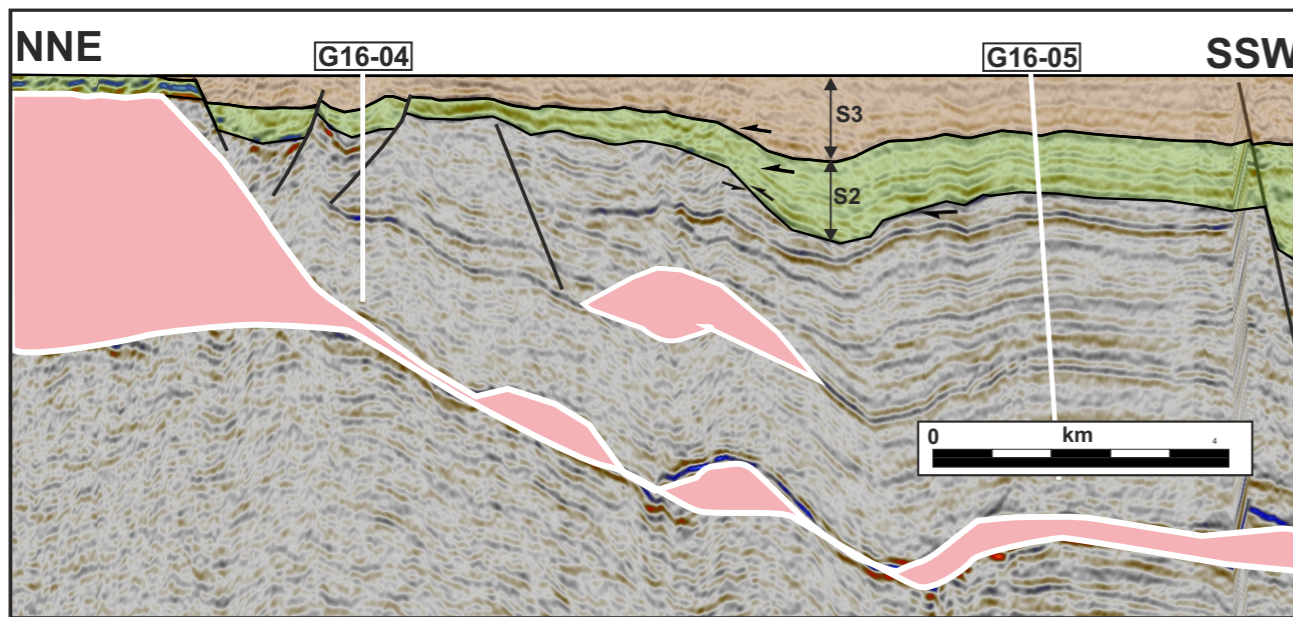
Figure 5.1.13: Seismic example of the intra-S2 basin margin location that is observed on Fig. 5.1.12. This seismic section is an excerpt of regional panel B from the FOCUS Project displayed in the Appendix A3. Note that the step located between wells G16-05 and G16-04 is also present in the lower part of S3. Modified from Bouroullec et al. (2016).
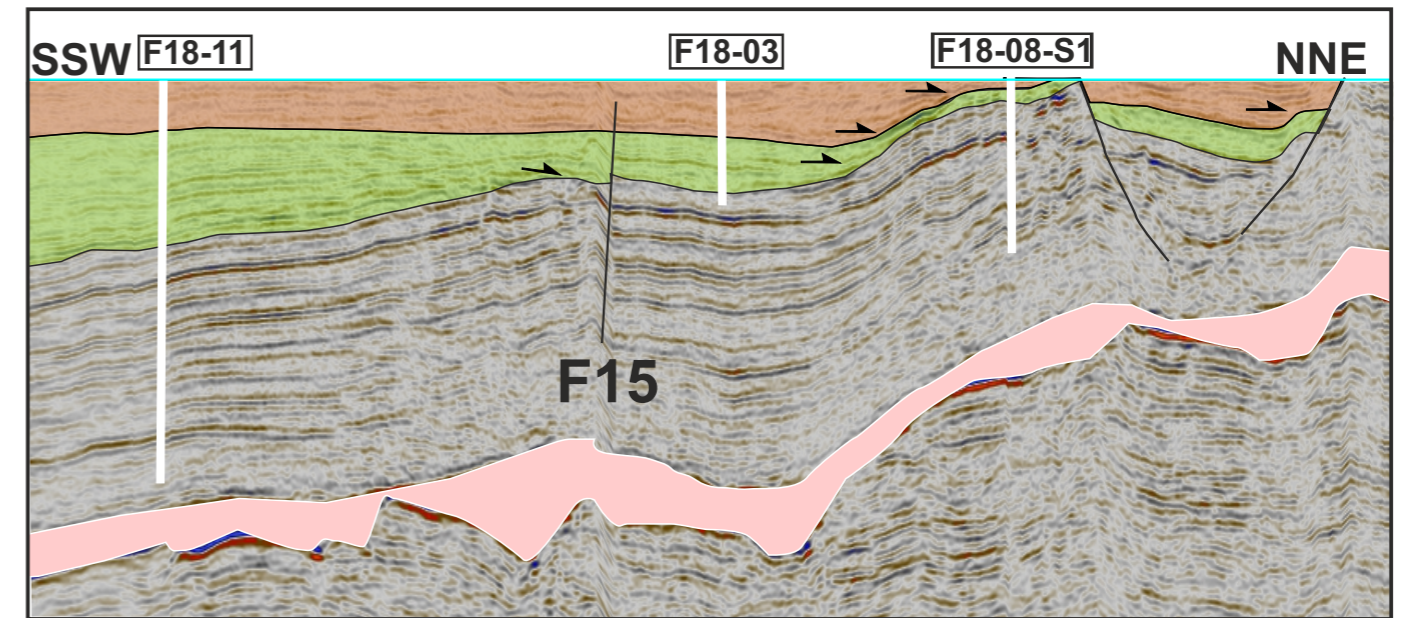
Figure 5.1.14: Seismic example of the intra-S2 basin margin location that is observed on Fig. 5.1.12. This seismic section is an excerpt of regional panel I (Chapter 4.3). Note that the step located between wells F18-11 and F18-03 is a lower angle that the one shown on Fig. 5.1.13. In that section the high angle basin margin is located between F18-03 and F128-08-S1 for the upper part of S2 and S3.

Using the approach shown in Figure 5.1.1, each basin margin (north, east and south margins) have studied and classified for S2 and S3. The results are shown in Figures 5.1.15 & 16 where the margin type is shown as colored lines along the basin margins.

Sequence 2:

For Sequence 2, the basin margin of the Terschelling Basin was 170 km long in the study area, and composed of four basin margin types (Figure 5.1.17):
- thinning: 76 %
- rim syncline: 11%
- conduit: 7%
- fault wedge: 6 %

The predominance of thinning configuration indicate that during most of Sequence 2 deposition, the basin margin was principally low angle and therefore that active structures (faults and salt bodies) along the basin margins were overall moderately active, or at a growth rate equal or slightly higher than the accumulation rate of S2 deposits. The more active basin margin sites (where rim synclines and active syn-deposition faults) for S2 are situated in three blocks, namely G16, M07, L09 and in small zones in block M05 and L05. Figures 5.1.18-26 show some example of those variable basin configurations.

Sequence 3:

For Sequence 3, the basin margin of the Terschelling Basin was 238 km long in the study area, and composed of six basin margin types (Figure 5.1.18):
- thinning: 55 %
- fault wedge: 17%
- high angle against salt   12%
- rim syncline: 7%
- conduit: 2%
- seismic limit   7% (Note that the eastern part of the basin has no 3D seismic coverage (eastern part of block M3). The real basin margin configuration farther east is believed to be thinning type.)

The predominance of thinning configuration still indicate that during most of Sequence 3 deposition, the basin margins were not affected with faults and salt bodies. However, compared with S2 basin margins, S3 show evidence of increased syn-depositional activity in many area with active faults and salt bodies becoming active or increasing their growth compared with S2 times. During this period the basin margins had significant topography in most basin margin blocks except blocks M4 and M5 where stratal thinning is still predominant. Figure 5.1.18-26 show some example of those variable basin configurations.
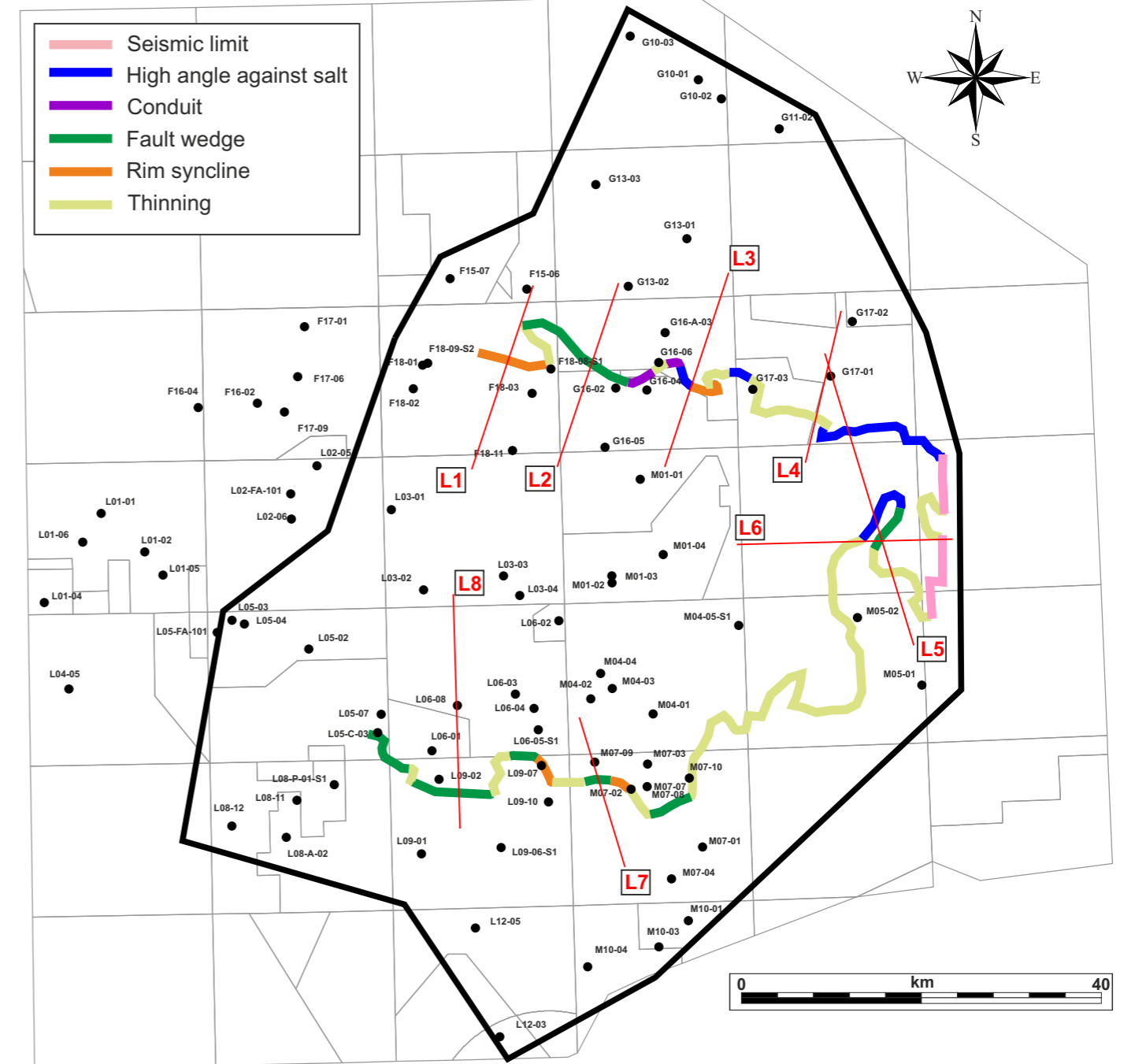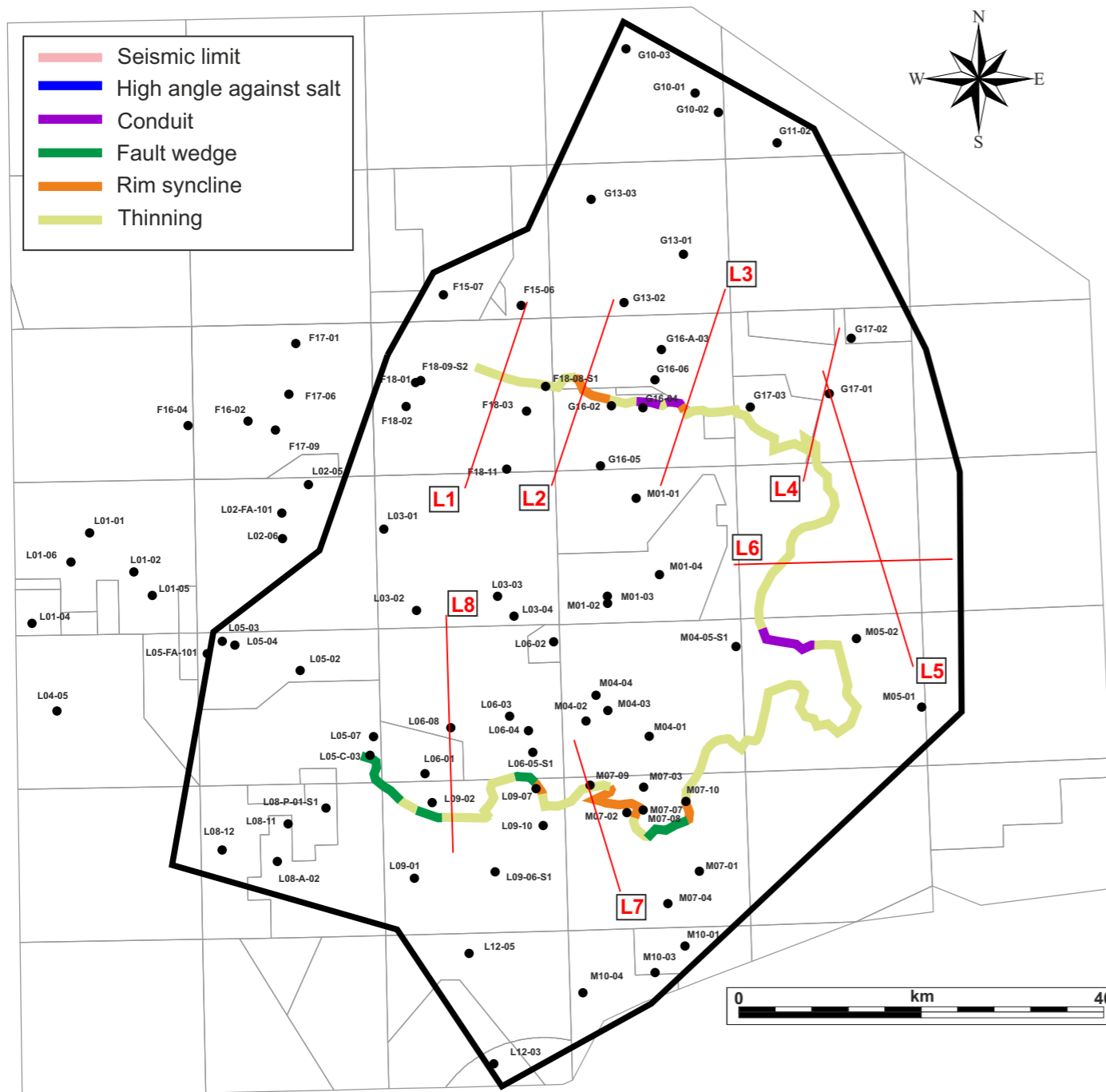
Figure 5.1.15: Terschelling Basin margin types for Sequence 2. Seismic sections L1-8 are shown in Figure 5.1.18-25.

Figure 5.1.16: Terschelling Basin margin types for Sequence 3. Seismic sections L1-8 are shown in Figure 5.1.18-25.
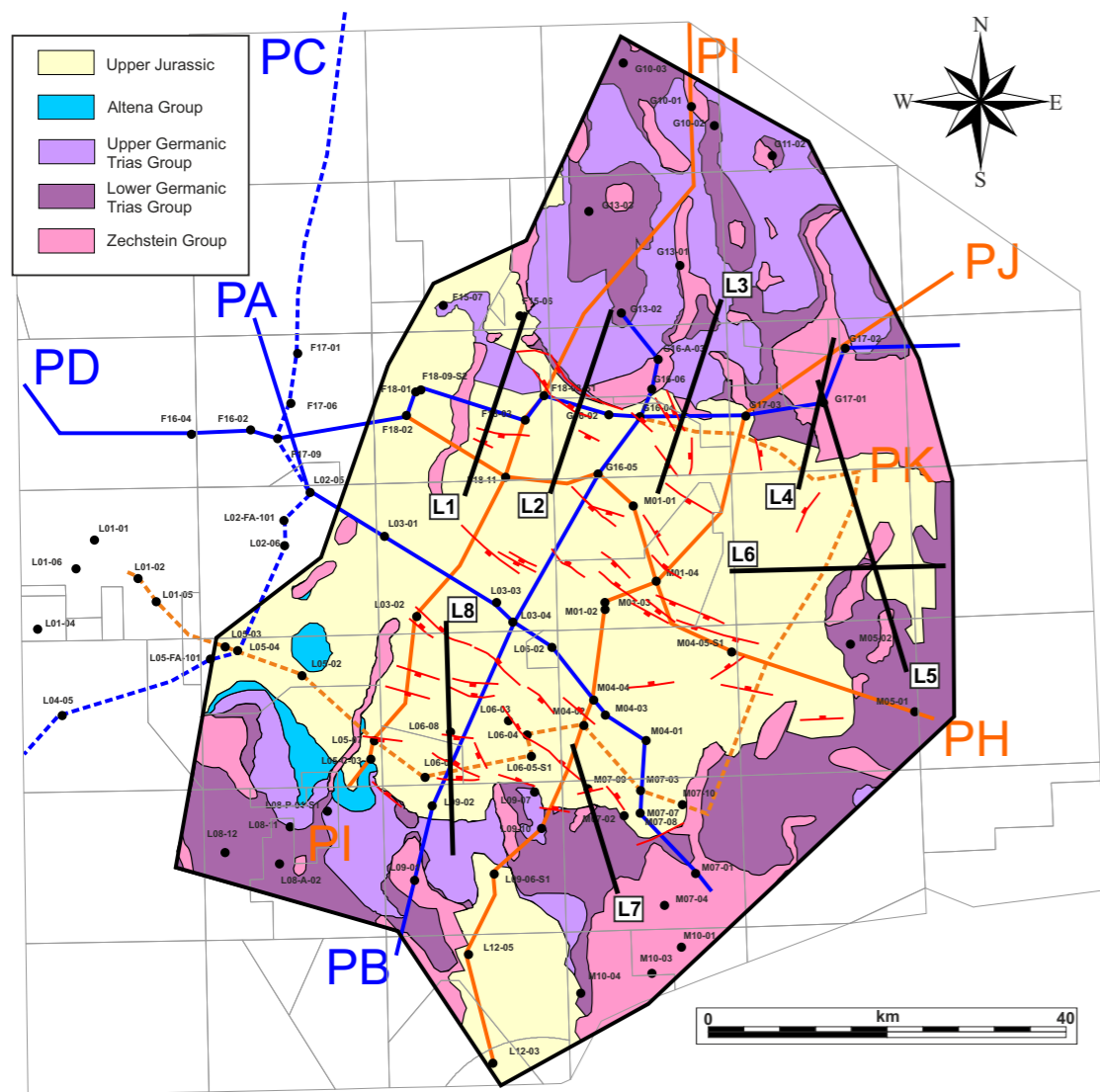
Figure 5.1.17: Location map of the seismic section L1-L08 (black lines) show in the subsequent figures. The regional panels (blue and orange lines) are also shown on this map. The back ground map is the base Rijnland Group subcrop map.

Figure 5.1.19: Seismic section L2.
This section shows the high angle basin onlap of S2 (a) and the faulted configuration for S3. It is unclear if the reverse fault (red fault) was originally a normal growth fault controlling the deposition of S3, but this scenario is believe to be true due to the slight overall thickness increase toward the fault. See Fig. 5.1.17 for location.
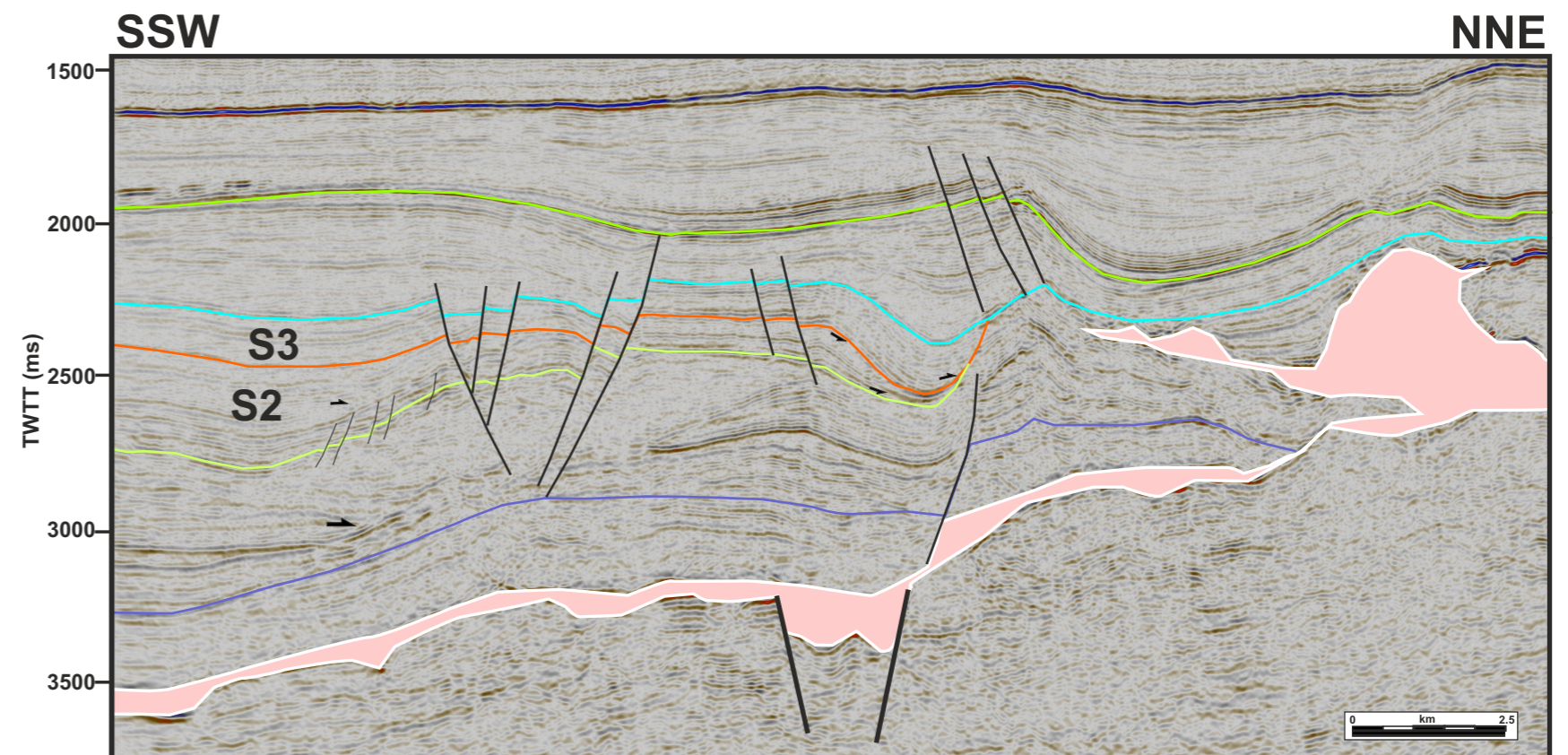
Figure 5.1.18: Seismic section L1. This section shows the low angle basin onlap of S2 and the rim syncline configuration for S3. Note that base S3 erode into S2 close to the basin margin. See Fig. 5.1.17 for location.

92

SSW

NNE
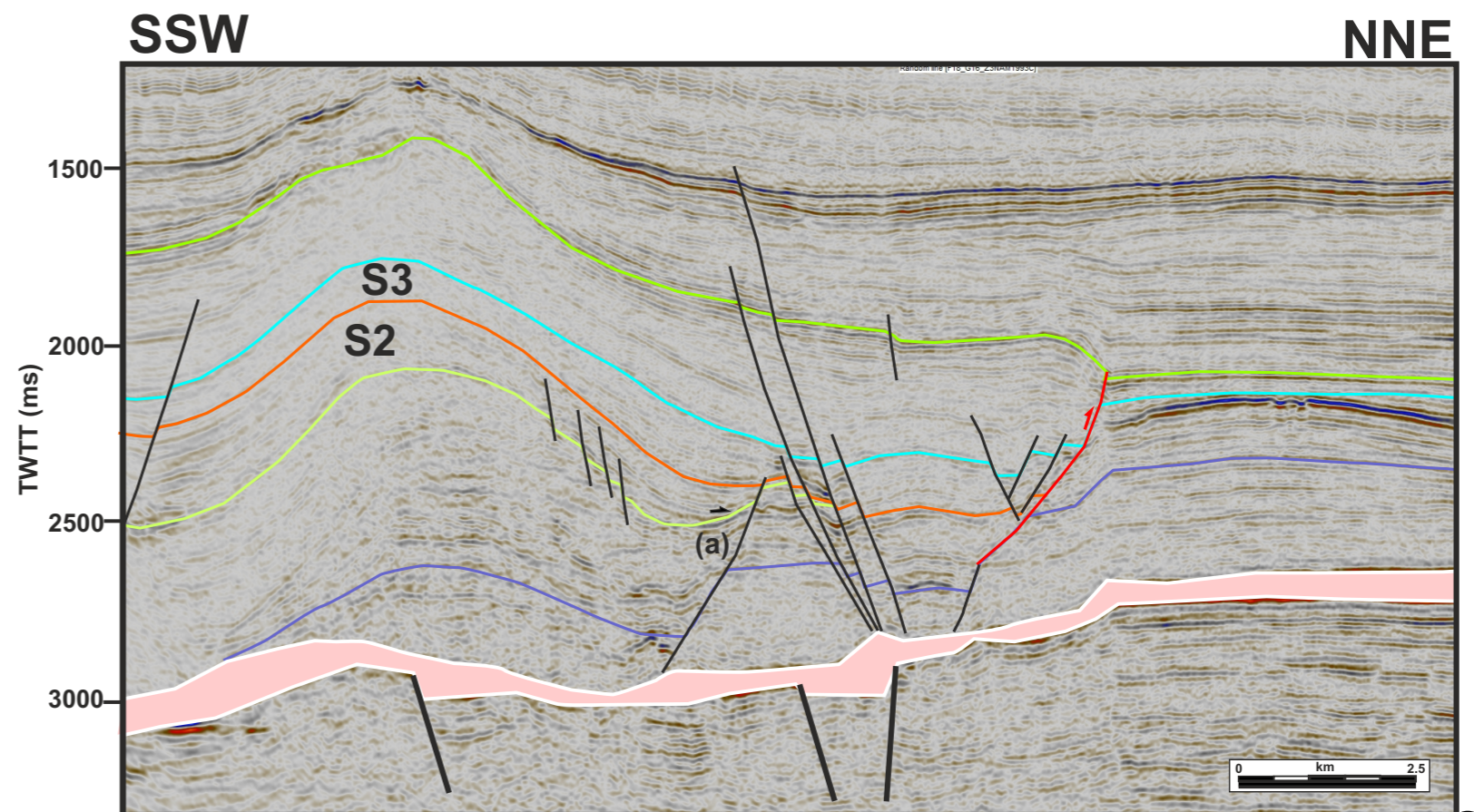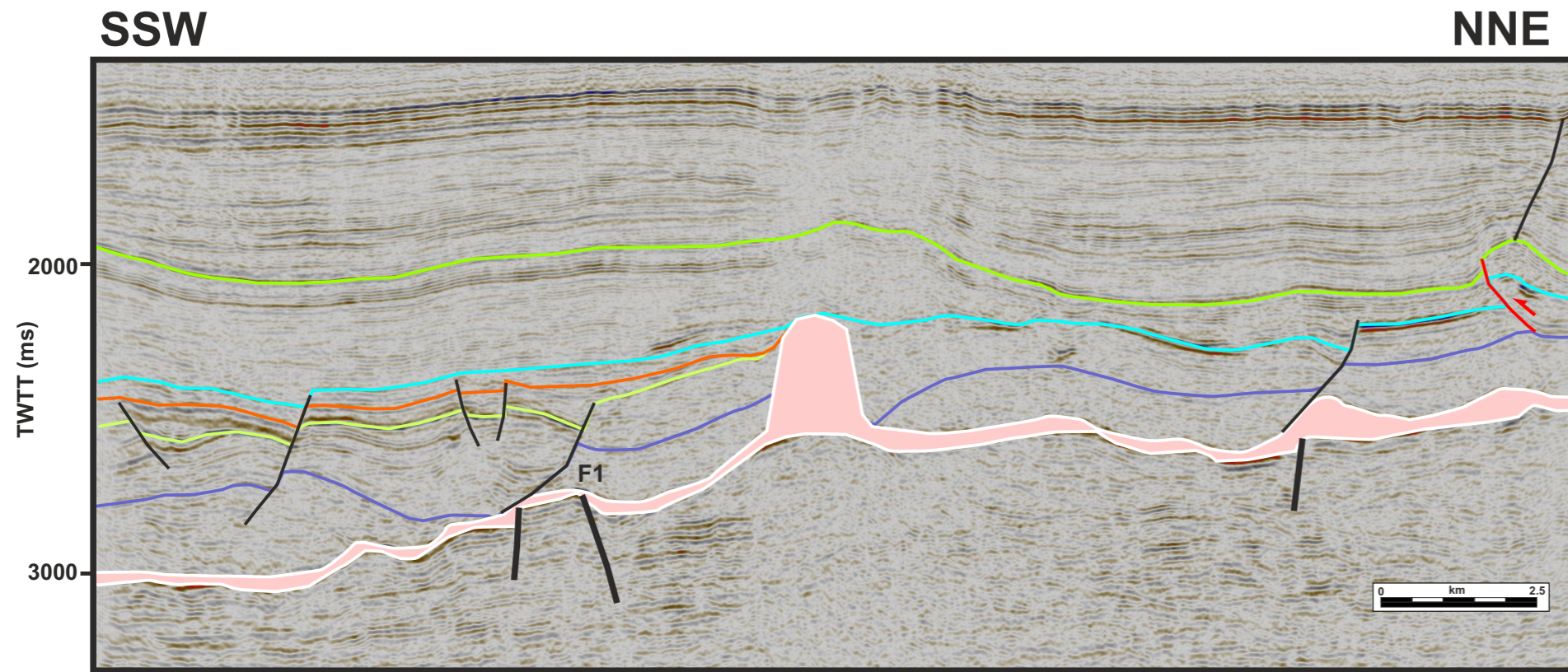
Figure 5.1.20: Seismic section L3.
This section shows the low angle basin onlap of S2 and the small rim syncline configuration for S3. Note that S2 shows low angle onlap at the physical basin margin lap out point but a growth fault (F1) is increasing S2 thickness 3km basinward See Fig. 5.1.17 for location.
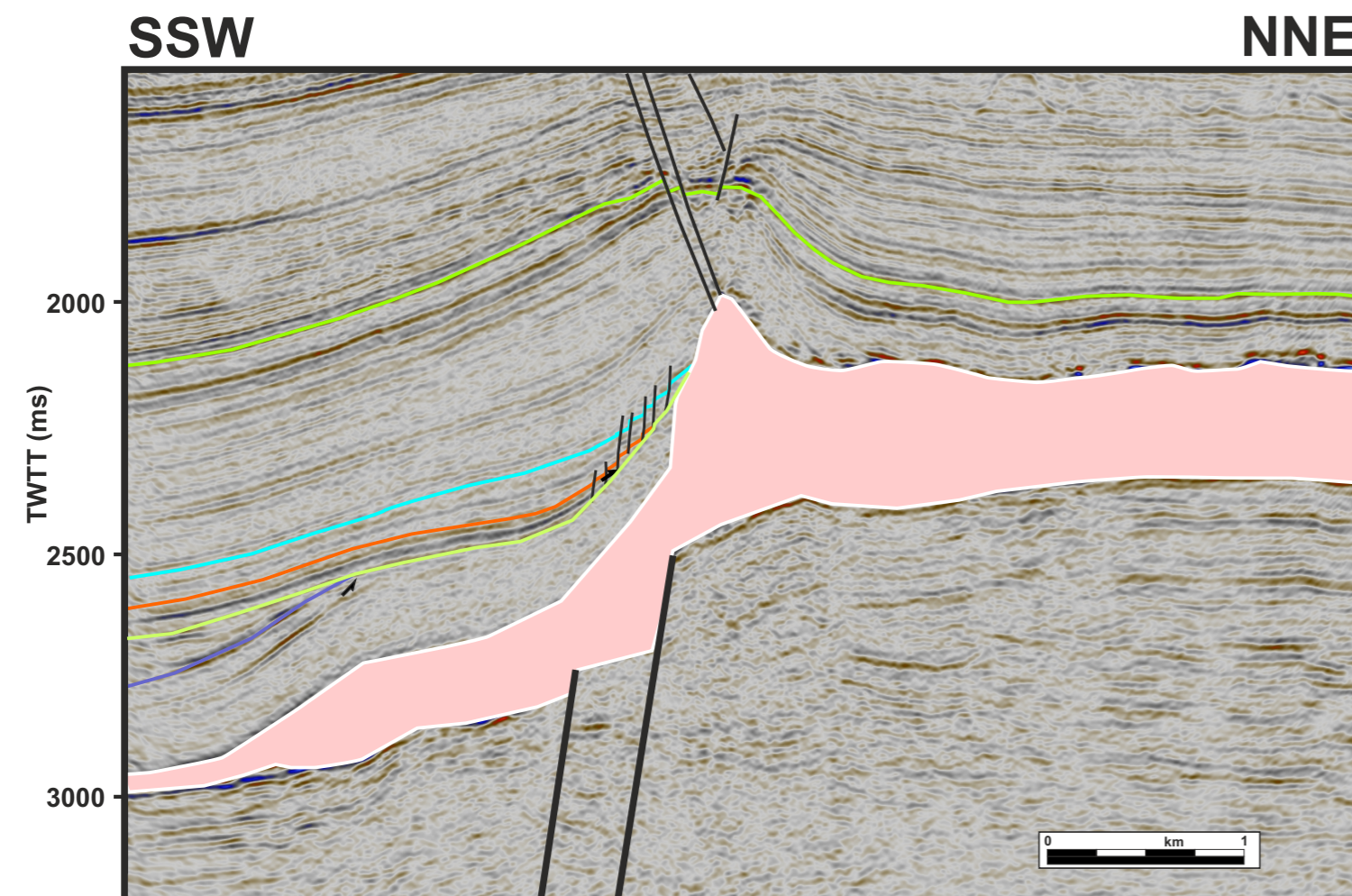
SSW

NNE

Figure 5.1.21: Seismic section L4.
This section shows the low angle, thinning configuration of S2 and S3 at the basin margin. Note the small growth faults detaching at the base of S2 within the lower Triassic. The steepness of the area due to the steep salt and post-depositional deformation created gravitational gliding that deformed the basin margin at this location. See Fig. 5.1.17 for location.
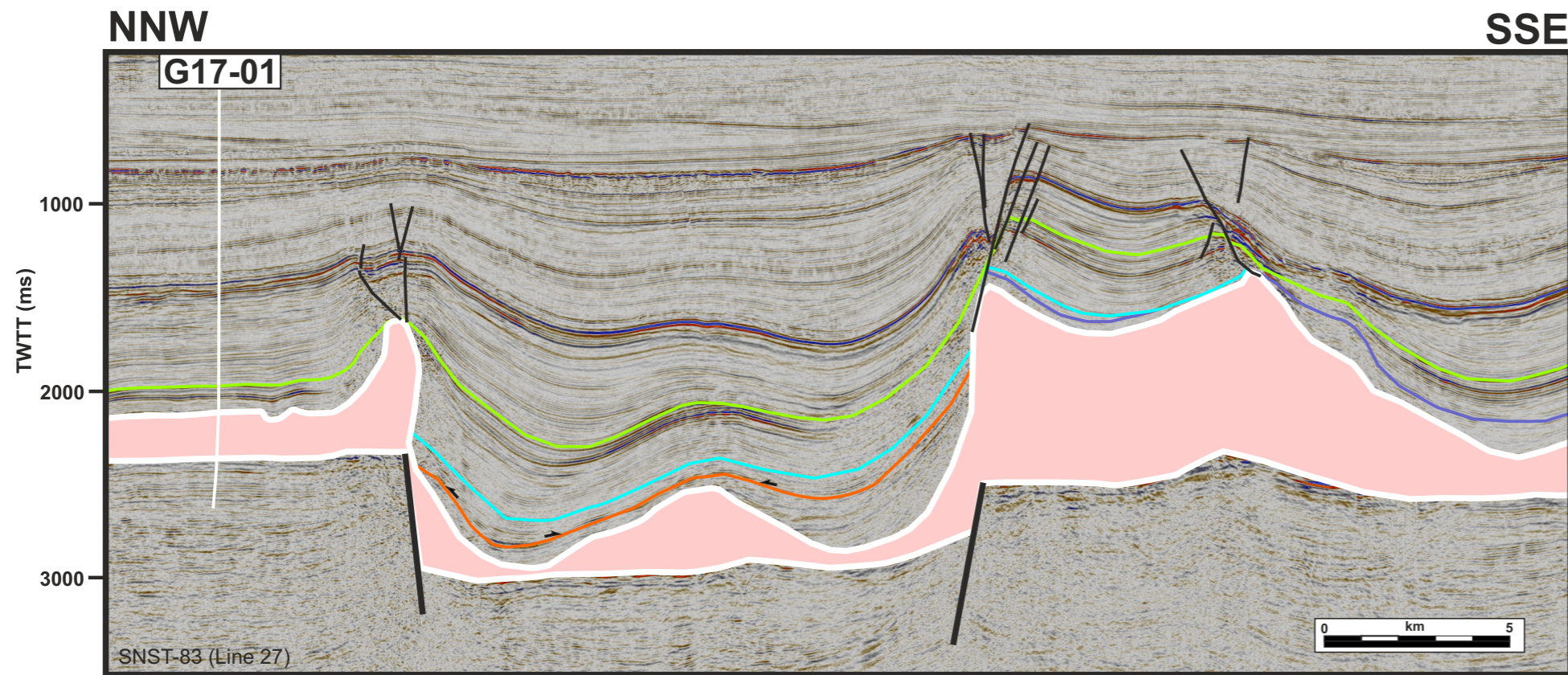
Figure 5.1.22: Seismic section L5.
This section shows the narrow area where S3 extends farther eastward than S2 in the northeastern corner of block M2 (see Figure 5.1.11). In this area S3 onlaps toward the north and the south at high angle against autochthonous Zechstein salt pillows. This configuration indicate that this part of the basin was confined during deposition of S3. This is an important remark since basin confinement can be synonymous of high net-to-gross deposits in many settings (e.g. Grand Coyer Sub-basin, Figure 5.1.9). In addition, the paleogeographic maps for S3 constructed in this project (Figures 5.2.7-10) show that this area is possibly sand-rich for Units 3.1, 3.2. This make this area interesting for future exploration if the other elements such as closures and migration pathway can be favorable. See Fig. 5.1.17 for location.
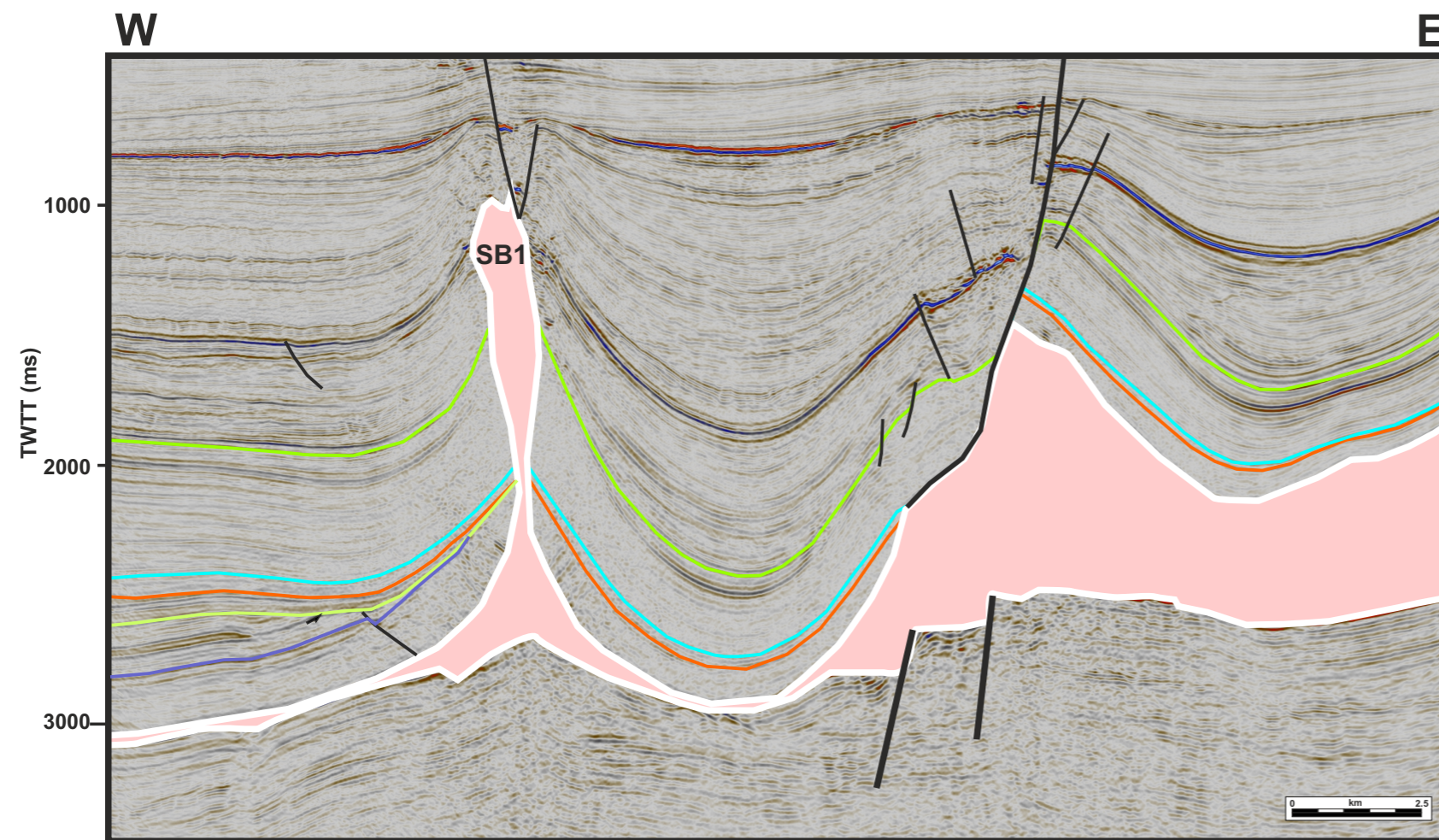

Figure 5.1.23: Seismic section L6.
S2 is only present in the western part of this section where it thins toward salt body SB1. S3 is overall thin at this location. Note that S3 is getting even thinner toward the eastern extremity of the section where no 3D seismic coverage impede farther interpretations. See Fig. 5.1.17 for location.
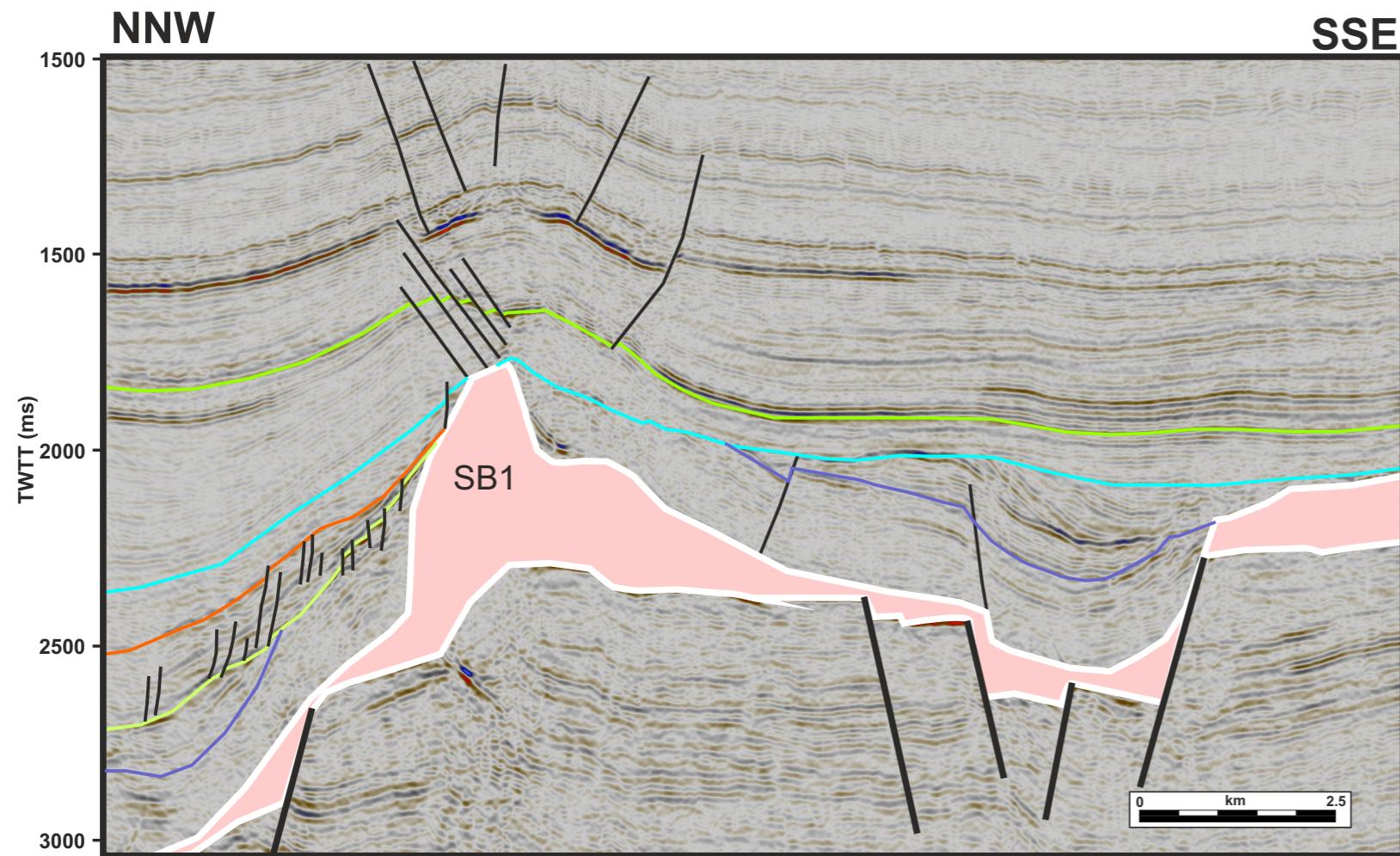
94

Figure 5.1.24: Seismic section L7.
S2 thins rapidly toward the basin margin at this location. This occurred due to stratal thinning but also erosion (S3 cutting into S2). S3 shows a small rim syncline toward the salt body SB1. Numerous small syn-depositional faults dipping toward the NNW are observed at the basin margin location. Such structures are mainly observed with S2 which means that salt movement may have destabilized the basin margin during and and/or after S2 was deposited and prior to S3 deposition. Such geometry can also been seen in the Annot Basin in the French Alps where basin margin syn-depositional deformation can be expressed in the form of syn-depositional faults (Figure 5.1.26), slumps (Figure 5.1.27) and even demobilized upward muddy sediments (mud volcanoes) (Figure 5.1.28). See Fig. 5.1.17 for location.
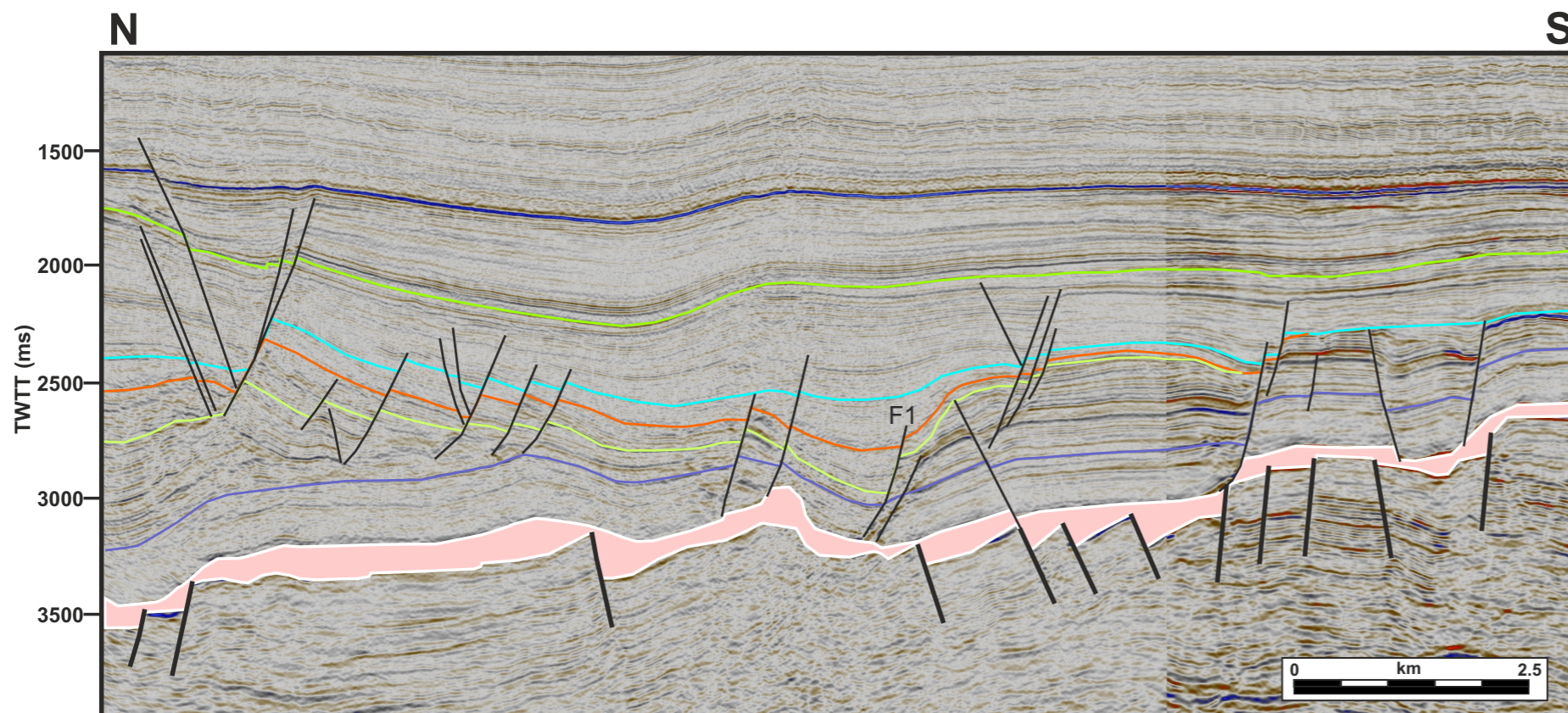

Figure 5.1.25: Seismic section L8.
S2 thins toward the basin margin at this location. As for section L3 (Figure 5.1.20) some large growth fault located away from the basin margin were active during S2 with large stratigraphic wedges observed (e.g. north of Fault F1). S3 thin more rapidly than S2 at the basin margin but may have bee eroded aby Sequence 4 at this location. This type of configuration is also observed in other seismic examples in this part of the basin, such as the southern part of panel I (Chapter 4.3) around wells L05-07 and L05-C-03. See Fig. 5.1.17 for location.
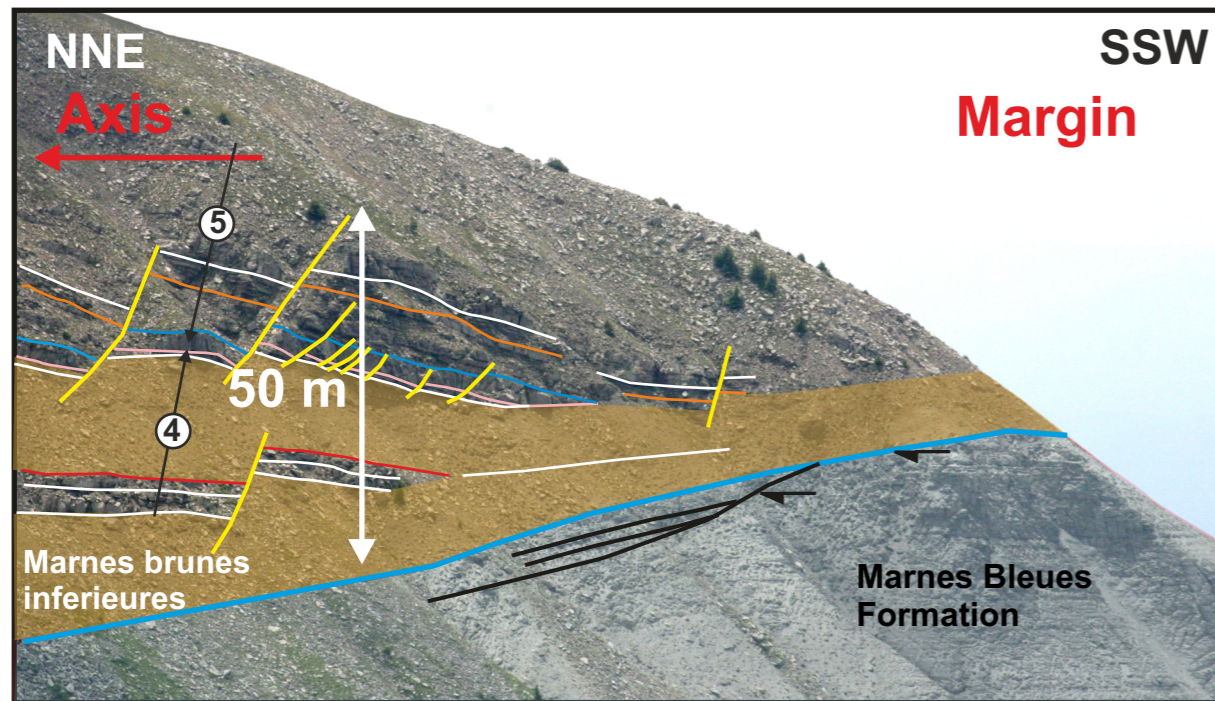
Figure 5.1.26: The Auriac exposure located on the back side of the Baisse du Detroit ridge in the Grand Coyer Subbasin in SE France. This exposure shows a slightly steeper marginal configuration with sandy strata coming closer to the onlap. The thin-bedded marginal facies (green intervals) are used as detachments for small faults (yellow faults). From Bouroullec et al. (in press).
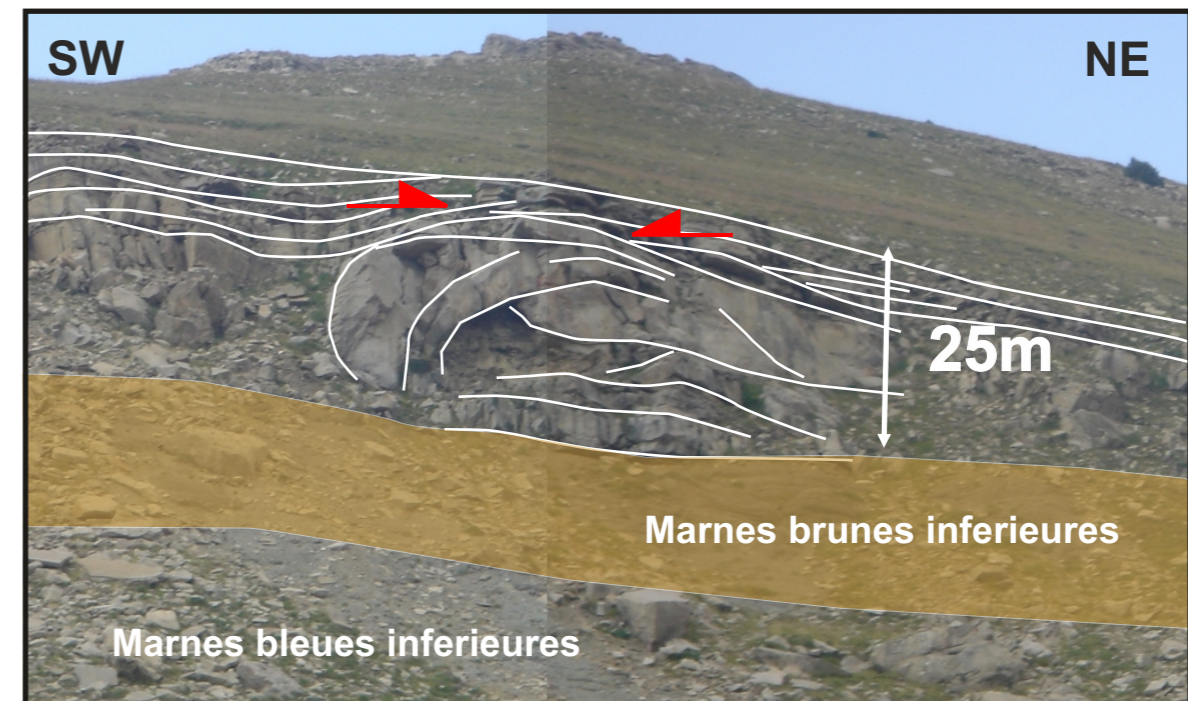

Figure 5.1.27: Large slump at the base of the conduit fill in the proximal western margin of the conduit. The basal detachment is at the top of the muddy Marnes Brunes Inférieures unit. Note the onlap of sediment gravity flow deposits above the structure suggesting a paleotopographic relief post-deformation. From Bouroullec et al. (in press).
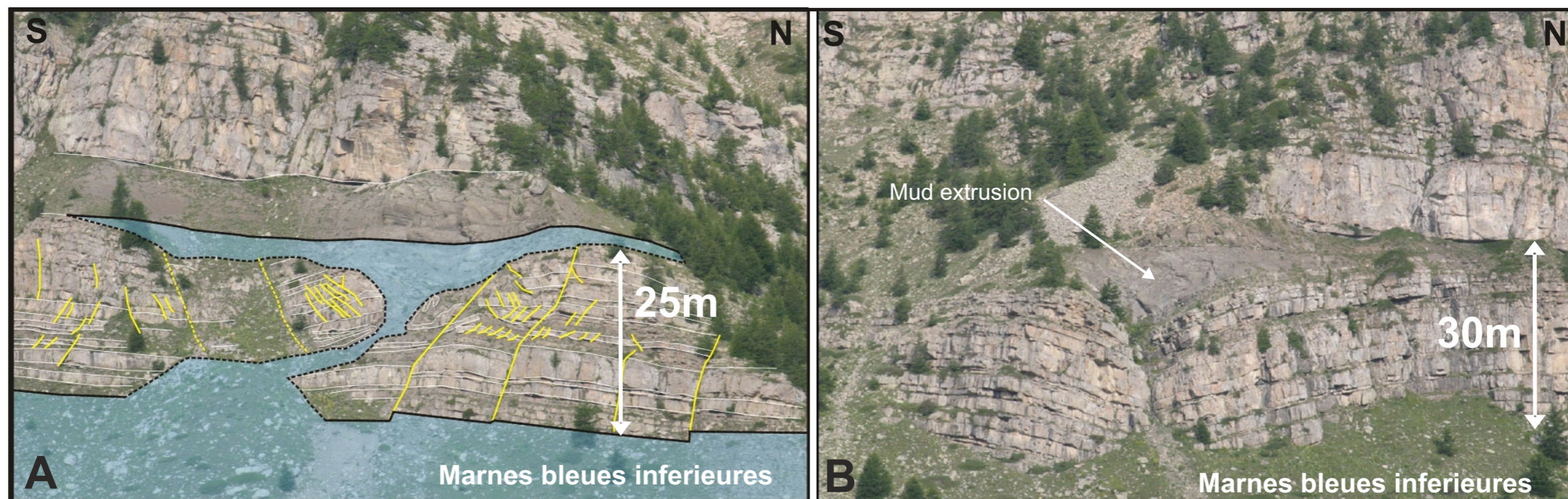

Figure 5.1.28: Mud extrusions in the lower part of the Grès d'Annot at Tete de Mouries exposure. The mudstone injected upward migrated from the Marnes Bleues level. A) The sandy strata rotated downward when the feeder collapsed with normal faults (yellow) accommodated volume change. B) mud extrusion showing the downward rotation of sandy strata resulting from the migration of mud from the Marnes Bleues unit into the Annot Sandstone units. From Bouroullec et al. (in press).

TNO innovation for life

Introduction

Each depositional unit is displayed on one page in two maps: a lithofacies map on the left, displaying the net-to-gross distribution of the depositional unit, and an isopach map, showing the inferred thickness distribution of the depositional unit. The details of the methodology are explained in section 3.5.
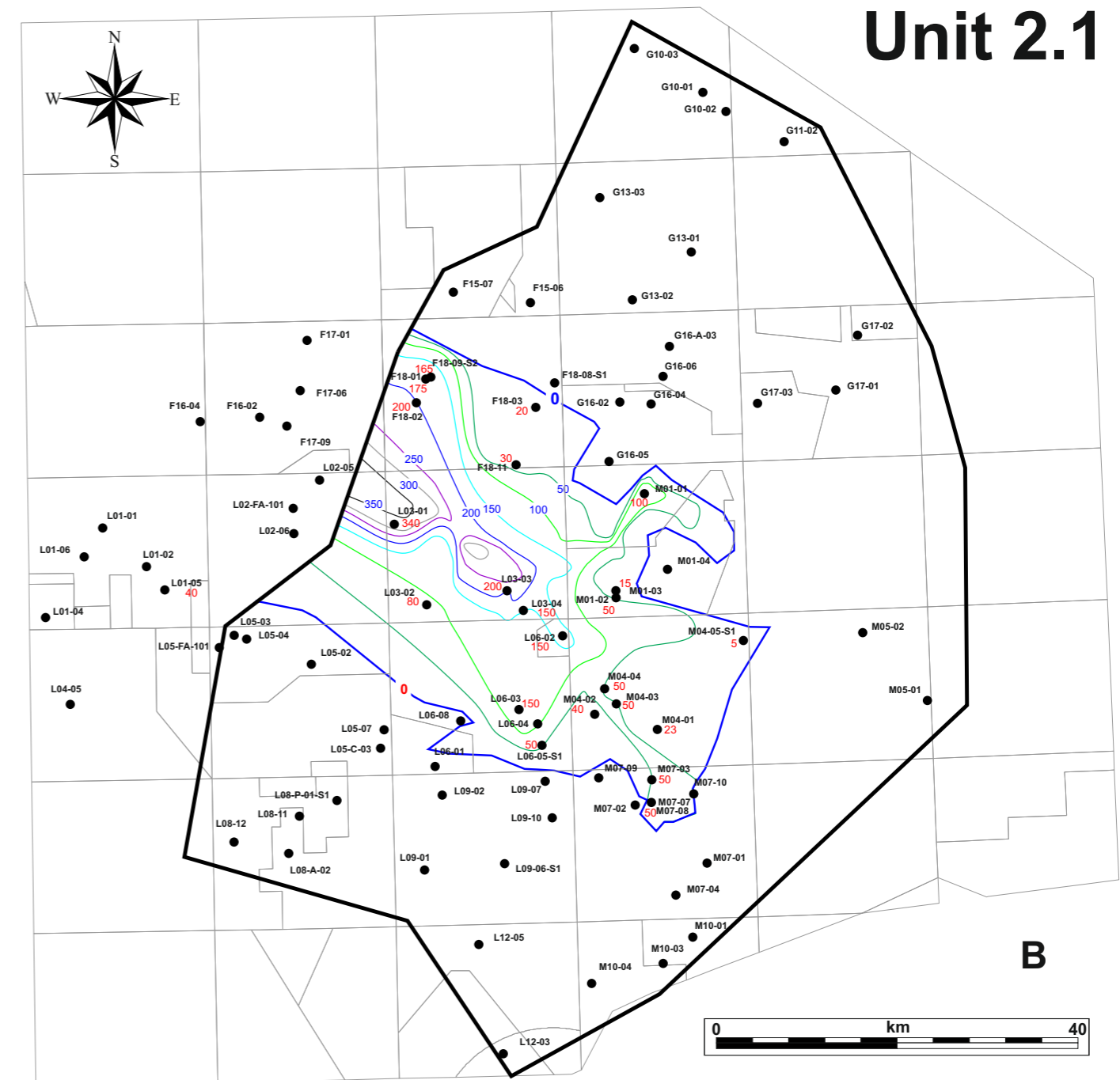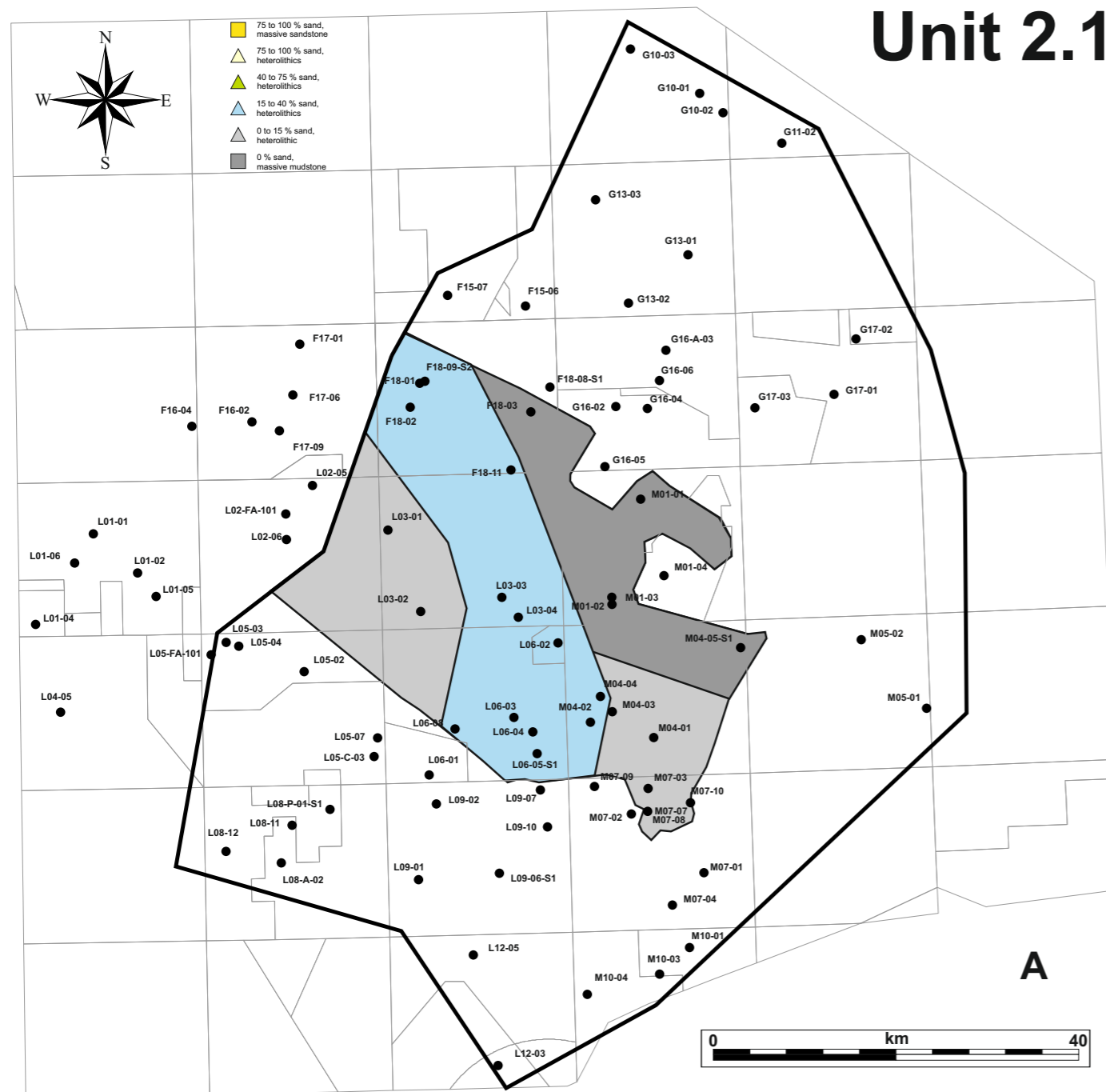

Figure 5.2.1: Lithofacies (A) and isopach map (B) of Unit 2.1

At the onset of Sequence 2, the TB is quite small (Map A). The sediments belonging to Unit 2.1 are dominated by finegrained siliciclastics (A). The palynology results (Figure 4.1.8), indicate that the base of the Upper Jurassic sediment pile shows - weak - marine influence, but the bulk of Unit 2.1 is terrestrial and belongs to the Main Friese Front Member of the Friese Front Formation. Isolotated sandstones occur in the form of channels, such as for instance the fining upward sands at the top of Subzone 2A in well F18-11 and L03-01 (Figure 4.3.2), but these sands are too limited in vertical and horizontal extent to have an expression on the map.

The basin axis is oriented NW - SE (Map B), with wells L03-01 and L03-03 as the main depo centers. Onlap of Unit 2.1 occurs towards both the soutwestern and the northeastern basin margins (Panel I and Panel J, section 4.3). Sequence 1 is not included in the lithofacies maps, because it is only present as isolated pockets in the TB, e.g. in well F18-02 and M01-01 (Panel H, section 4.3). The thick successions of Sequence 1 occuring in Block L01 and L05 belong to the DGB not the TB (Panel K, section 4.3; see also Figure 4.2.7).
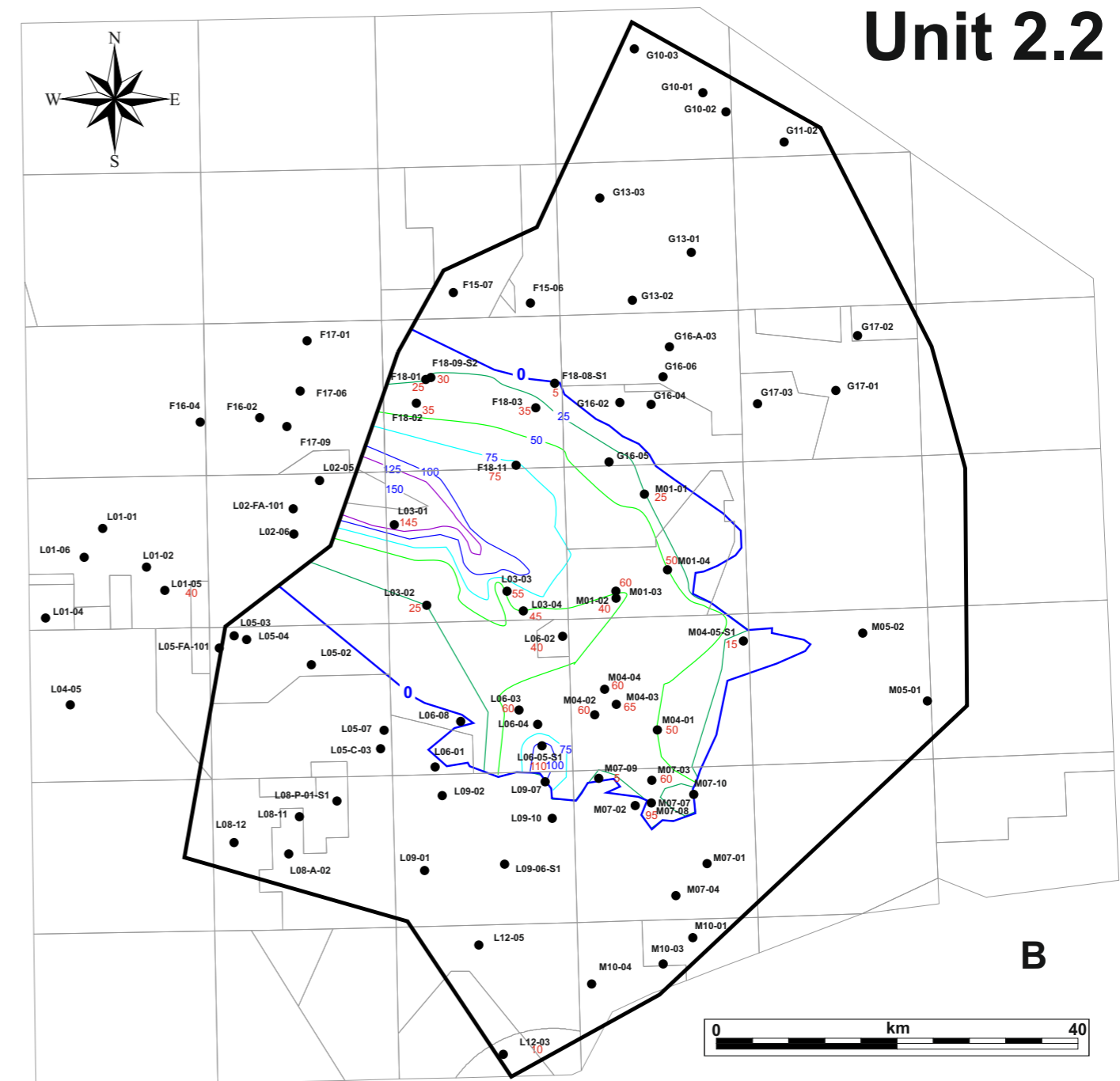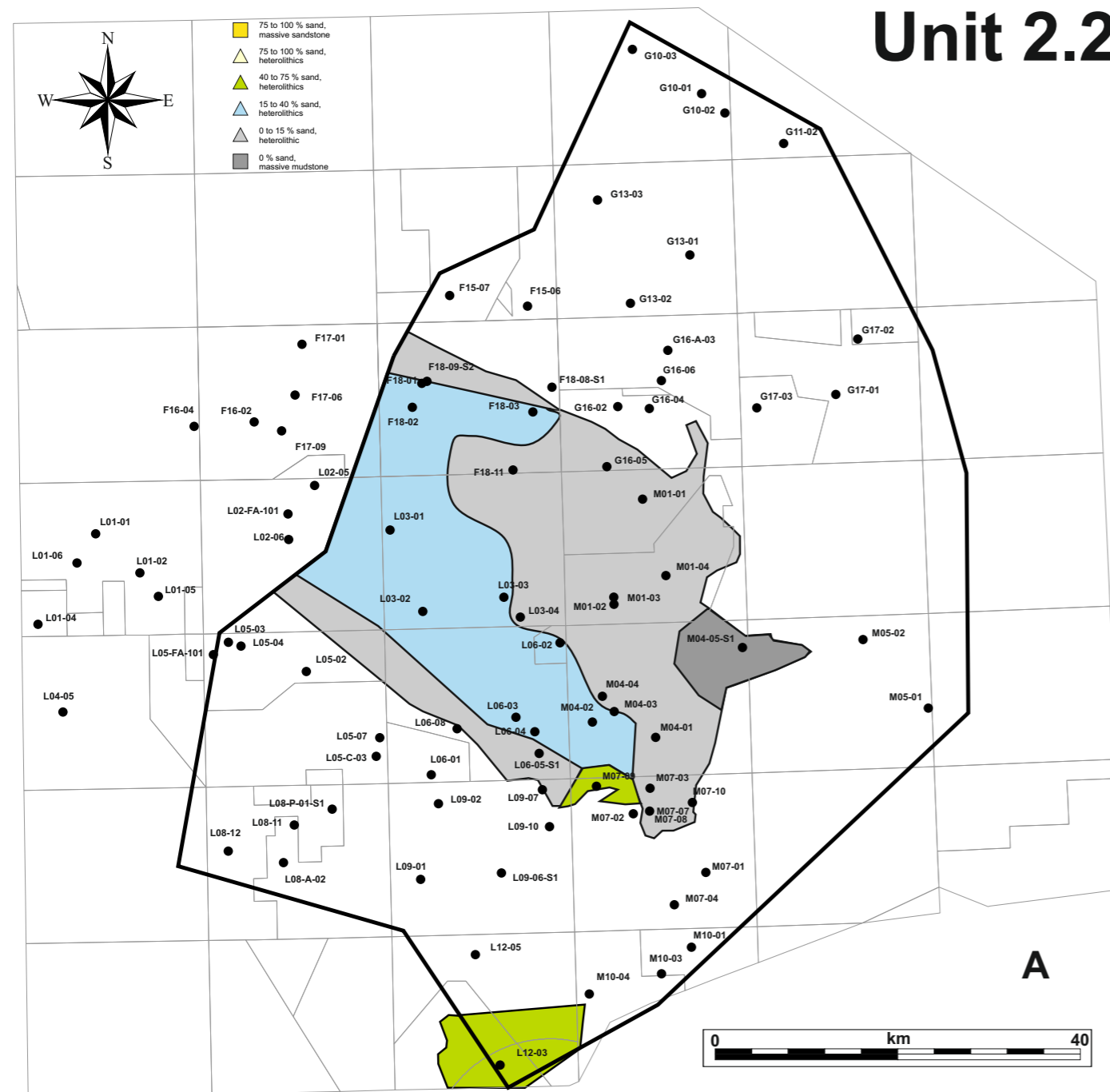
97

Figure 5.2.2: Lithofacies (A) and isopach map (B) of Unit 2.2

The major change occuring in Unit 2.2 is the basin becoming marine. This is expressed in the lithology by the appearance of organic rich mudstones of the Oyster Ground Mb of the Skylge Fm. The basin remains dominated by muddy facies, except for the marginal areas around M07-09 and L12-03 (Map A). The basin axis displays a slightly higher net-to-gross than the areas

alongside it. The depocenter of the TB remains firmly put in the L03 Block in the NW - SE orientation (Map B). Compared to Unit 2.1, the TB expanded a little bit, particularly in the M01 Block and in the L12 Block. Onlap is observed at the basin margins in the SW and in the NE ((Panels I and J of section 4.3).
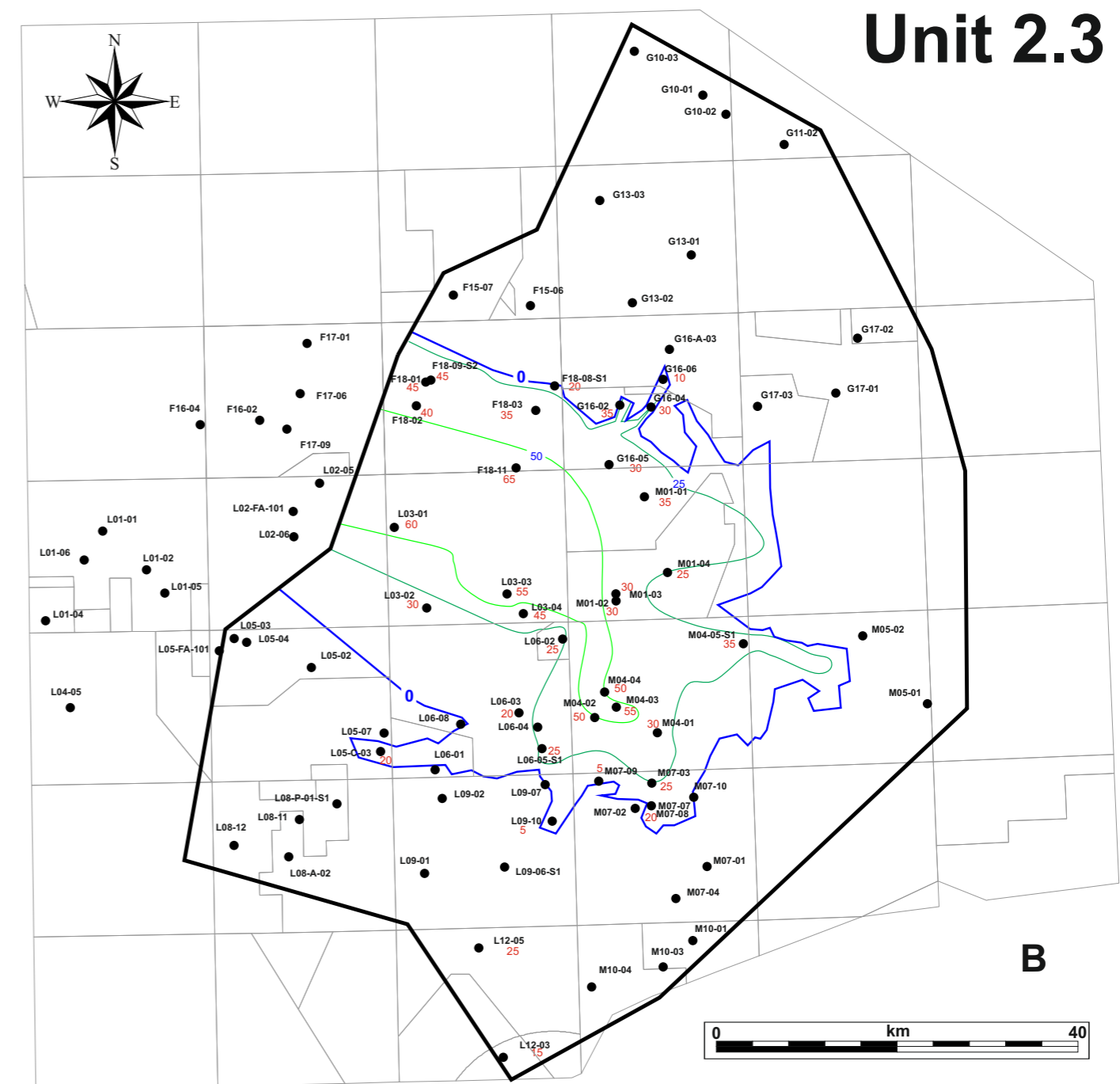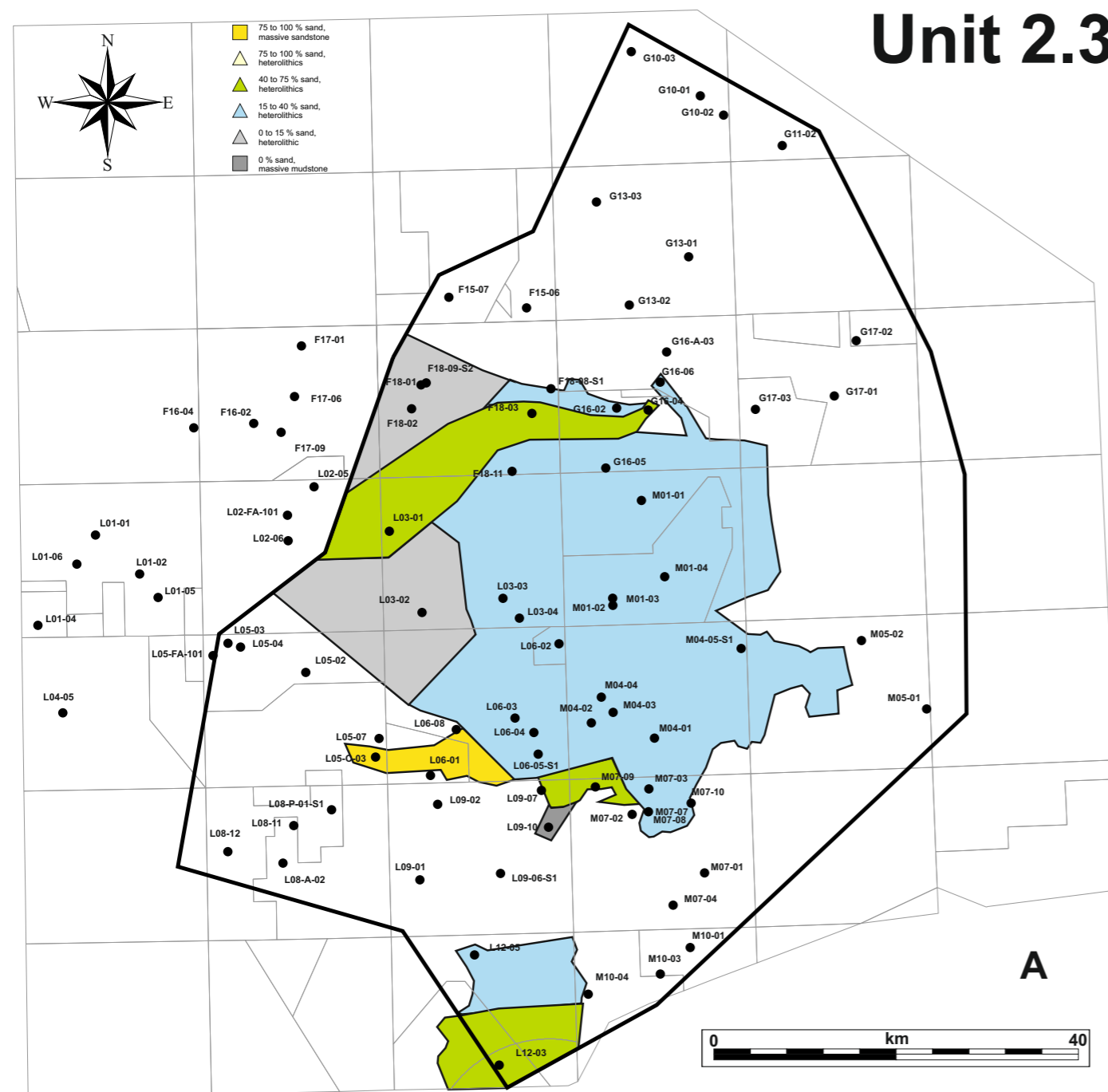
98

Figure 5.2.3: Lithofacies (A) and isopach map (B) of Unit 2.3

The whole of Unit 2.3 belongs to Oyster Ground Mb (Figure 3.4.1). For the first time, yellow colours, indicating high net-to-gross, appear on the map (Map A). The overall facies does not differ very much from Unit 2.2 (organic rich mudstones intercalating with sandstones), but is overall more sandy. The massive sands occurring in Unit 2.3 in well L05-C-03 (Panel I section 4.3) probably reflect the onset of tectonic activity that is triggering the overall increase in net-to-gross. Concomitant with the increased sand supply, the basin is also expanding, particularly in

Block G16 and M02 onlap occurs (Map B).The overstepping of the basin margin is visualized on Panel J (section 4.3), where Unit 2.3 steps over the margin, NE of well M01-04.

The basin expansion points to a relative rise in sea level. This is corroborated by the deepening trend in Unit 2.3, which is, for example, reflected in the offshore marine facies at the top of Unit 2.3 in well L06-02 (Figure 4.1.9). The basin configuration is also changing in Unit 2.3. The strong NW - SE trend of the former units is fading away (Map B).
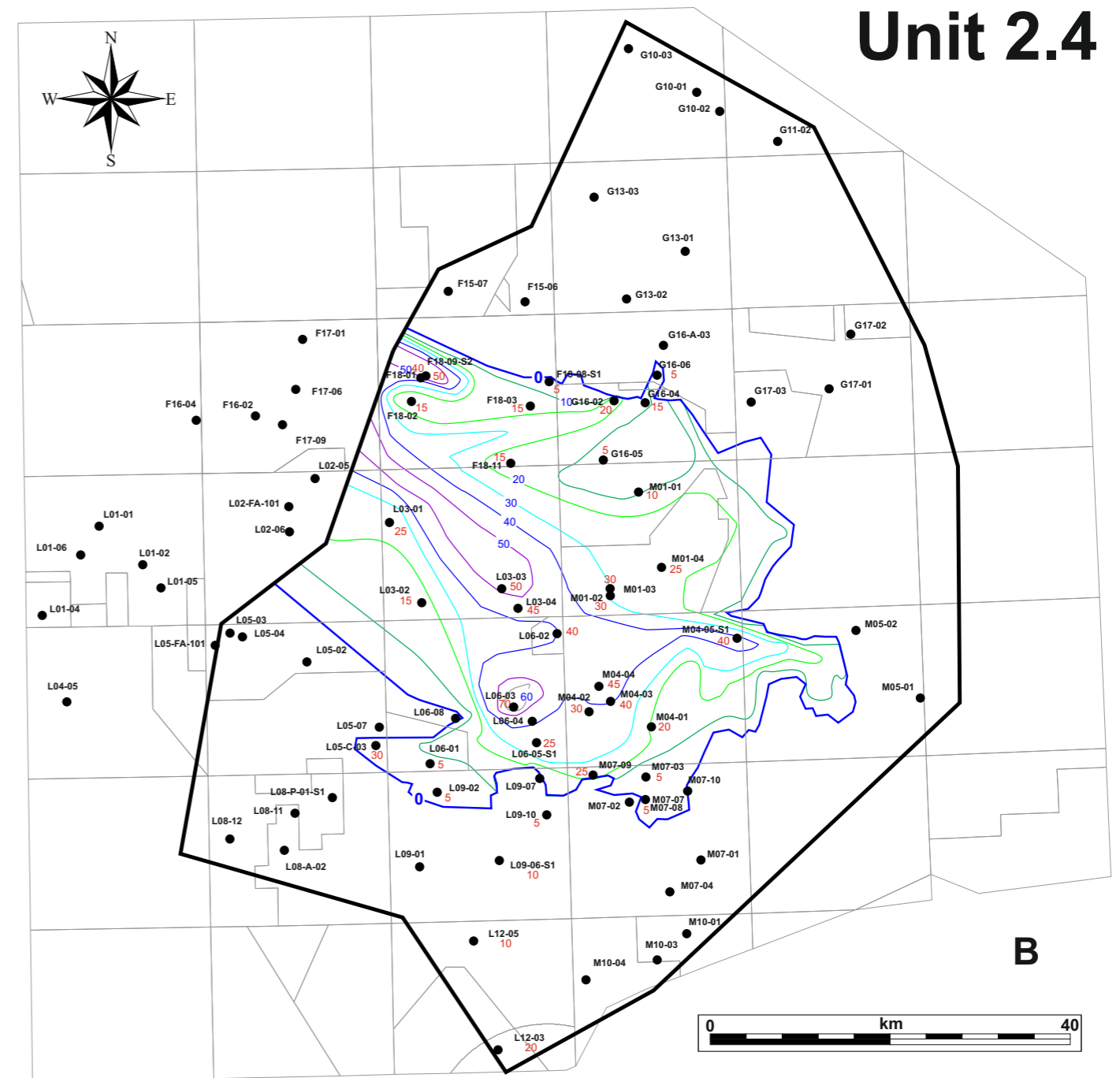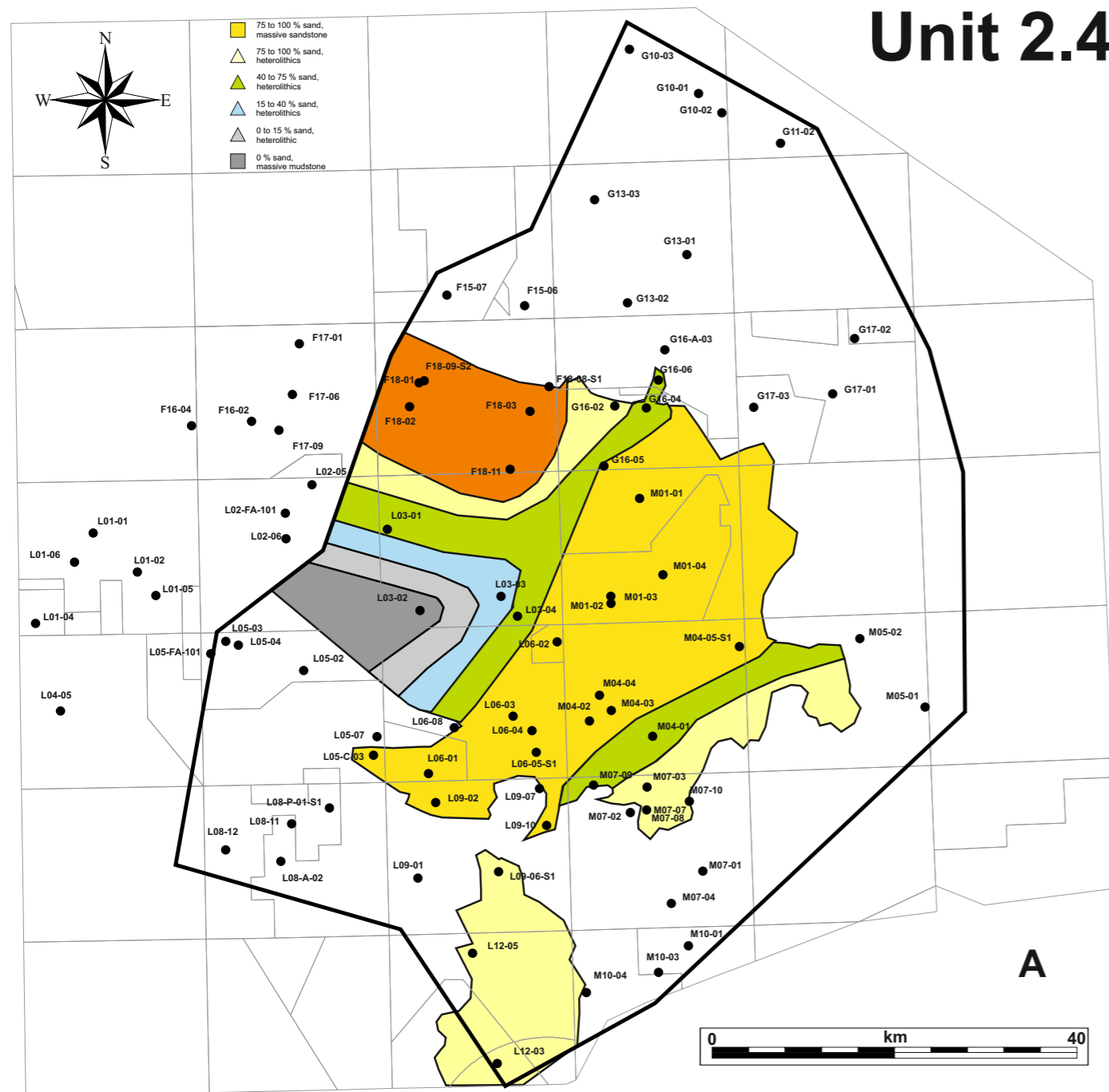
Figure 5.2.4: Lithofacies (A) and isopach map (B) of Unit 2.4

Unit 2.4 marks the most dramatic change that occurs in the Upper Jurassic of the TB. The abundant yellow and orange colours on Map A indicate a sudden increase in net-to-gross that affects the entire basin, except for the deepest part around L03-01. From the northwestern corner, the Noordvaarder Mb of the Skylge Fm makes its entrance. The net-to-gross trend of the Noordvaarder Mb displays a radial pattern (Map A), suggesting more of a point source of the sand, than a broad zone. The source area for the Noordvaarder Mb is inferred to the N and NW of the Fregat Field (F18-FA) in the DCG. This implies that the source consists of a mixture of remobilized Upper Jurassic and older Triassic rocks. The decreasing net-to-gross trend is displayed very well on Panel H (section 4.3).

On the opposite side, in the southeastern corner of the basin, the Terschelling Sandstone Mb appears at exactly the same time: the base of the two sandstone members are synchronous. This can not be attributed to a eustatic sea level lowering only, there has to be tectonic component to the overwhelming synchronous supply of sand. The basin configuration now displays two different directions. The pre-existing NW - SE trend is still present in the L03 Block, although it shifted a little bit towards the NE. In addition, a new WSW - ENE trend appeared in the L06 and M04 Blocks (Map B). This trend mimics the lithofacies pattern of Map A in that area. Note that the Terschelling Sandstone Mb steps over the southern basin margin (Panel J and K, section 4.3).
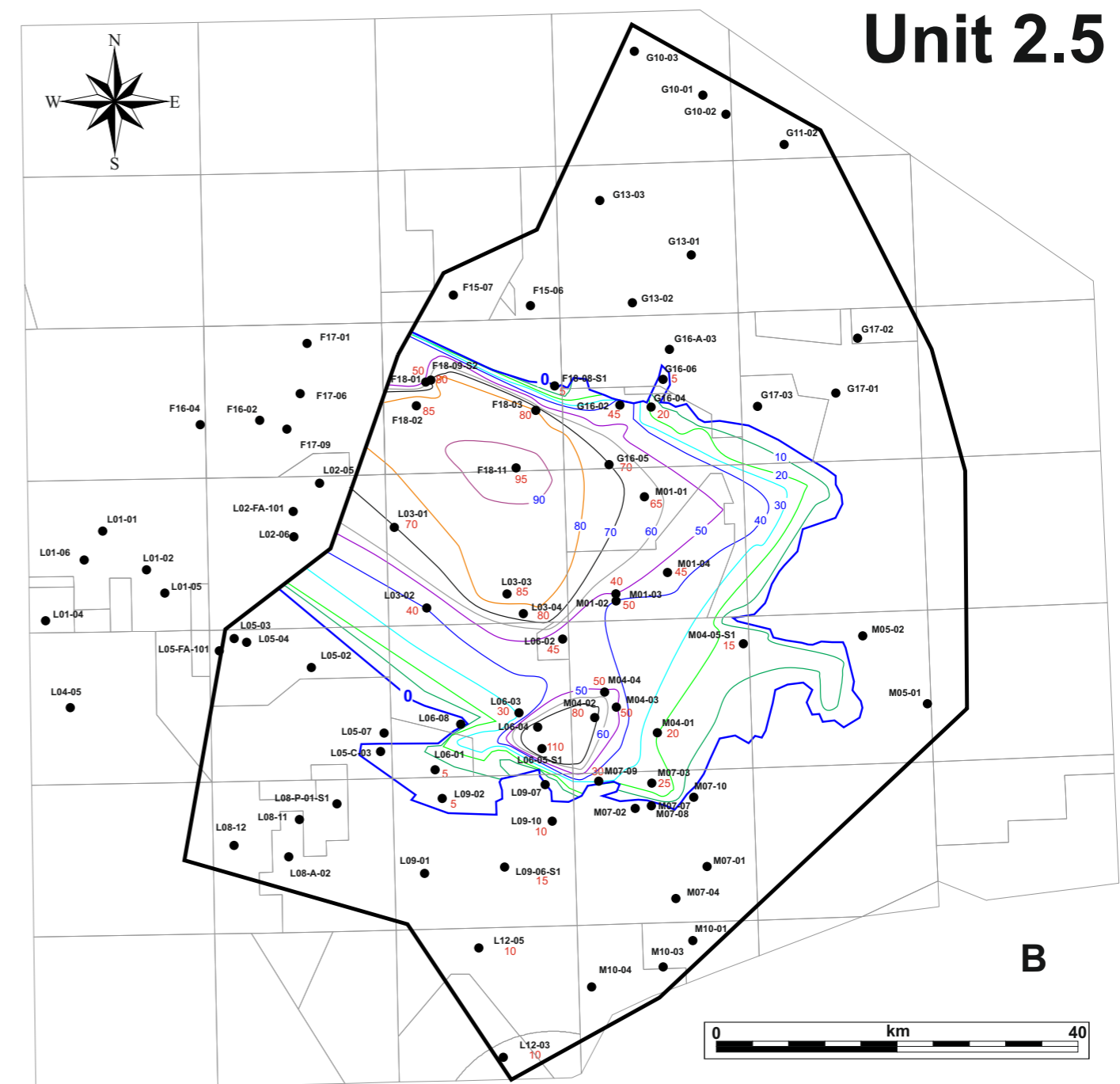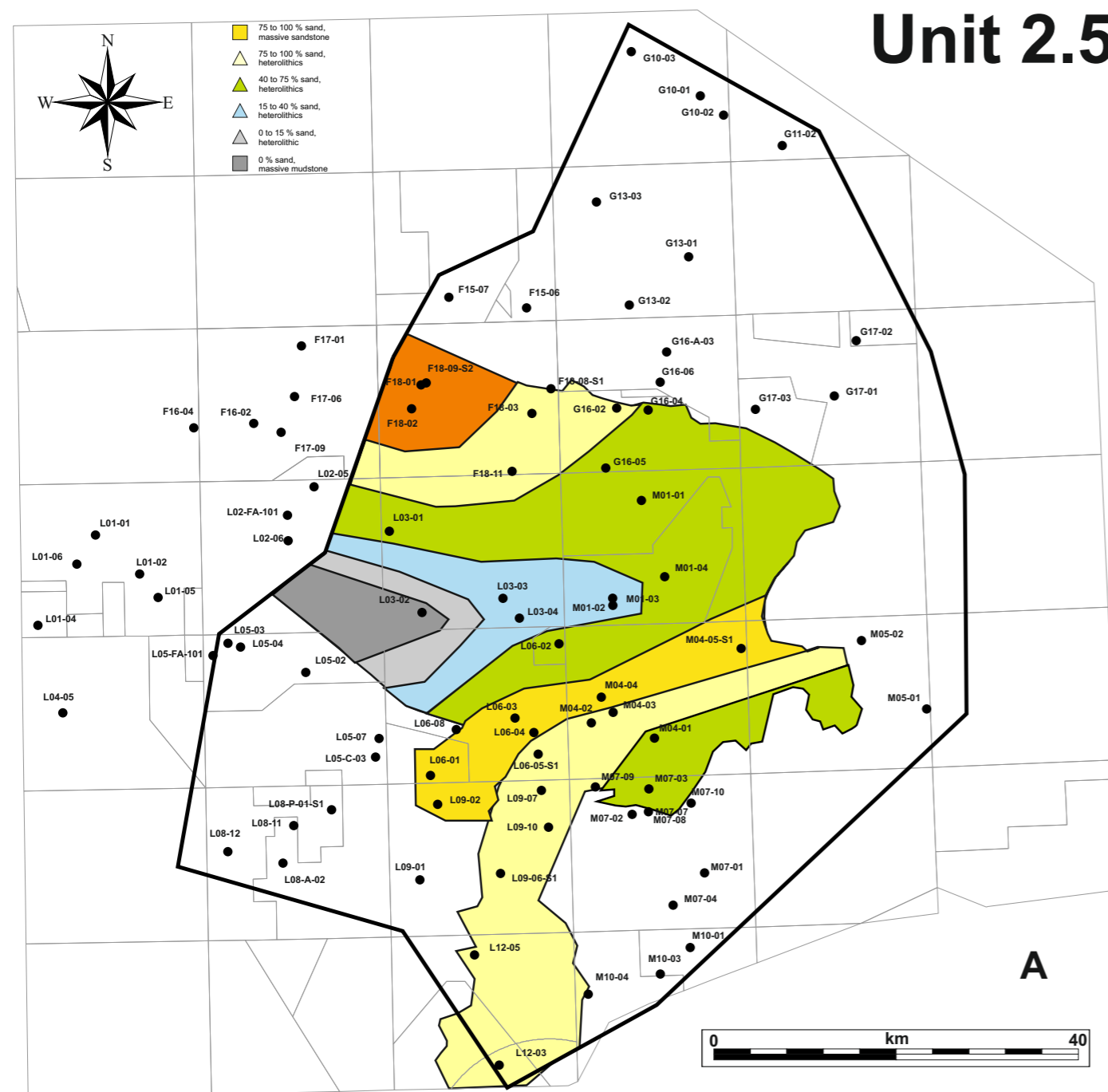
100

Figure 5.2.5: Lithofacies (A) and isopach map (B) of Unit 2.5

The shrinking of the sand-rich areas on the lithofacies map of Unit 2.5 reflects a decrease in the sand supply. The high net-to-gross Noordvaarder Mb is now limited to the F18 source area only and shales out rapidly towards the SE (Panel H, section 4.3). In the southeast, a large arc-shaped pattern appears, with upper Jurassic sediments continuing all the way to L12-03. Again, this pattern mimics the facies distribution of the Terschelling Sandstone Mb and adjacent

sediments. The basin configuration has changed again. The basin now displays two depocenters, one around F18-11 and one around L06-03. These depocenters are related to fault activity: the closely spaced contour lines SW of well L06-03 and NE of well F18-03 indicate active fault movement (Panel I, section 4.3).
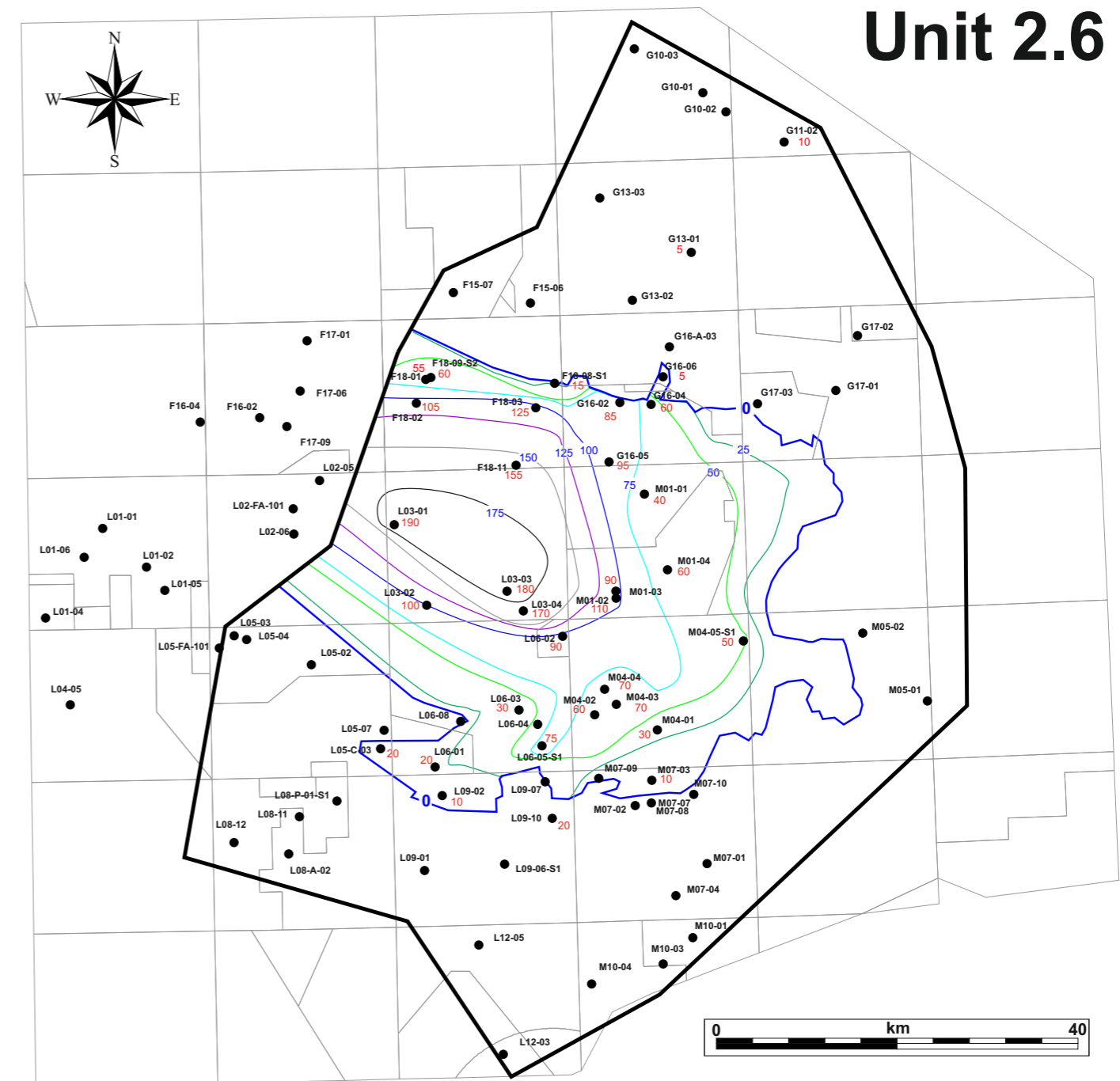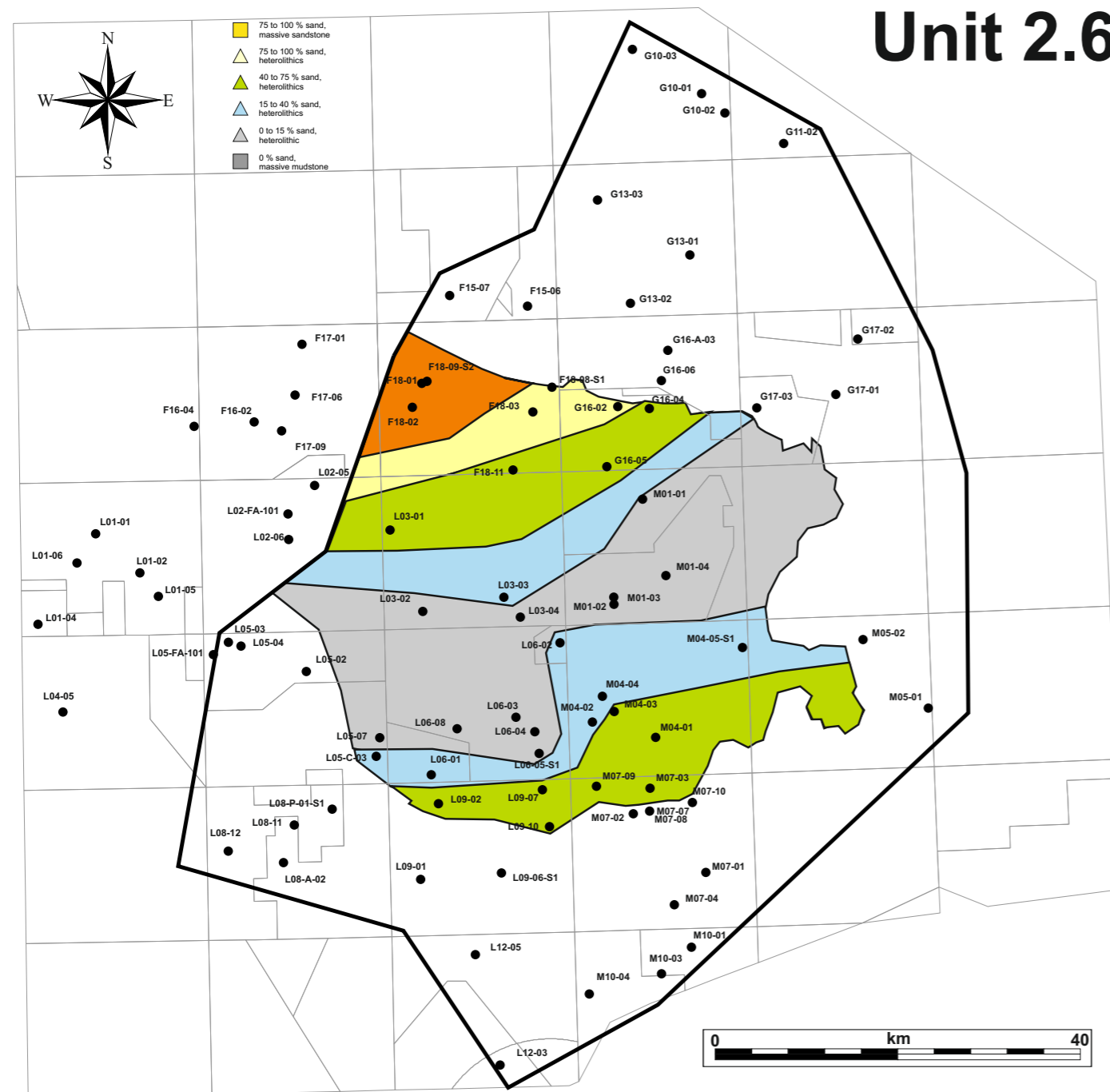
Figure 5.2.6: Lithofacies (A) and isopach map (B) of Unit 2.6

The lithofacies map (A) displays a further decrease in sand content. The fine-grained sediments of Unit 2.6 belong to the Lies Mb of the Skylge Fm. The net-to-gross trend is distributed symmetrical along a WSW - ENE axis, where only in the northwestern corner sand deposition continues uninterruptedly. The muddiest part of the basin lies in the centre of the WSW - ENE axis of the lithofacies map (A). The net-to-gross trend does not reflect the basin configuration, which has become more disk-shaped now (Map B). The former depocenters around L06-03 and F18-11 do not stand out anymore, probably indicating a waning of fault activity in those areas. The regular isopach pattern of Map B further strengthens the idea of homogenous subsidence throughout the entire TB. Note that the basin axis has resumed its original NW - SE orientation.

C

L06-02   L06-03   L12-03   M07-07

B   A'

NE

D

A
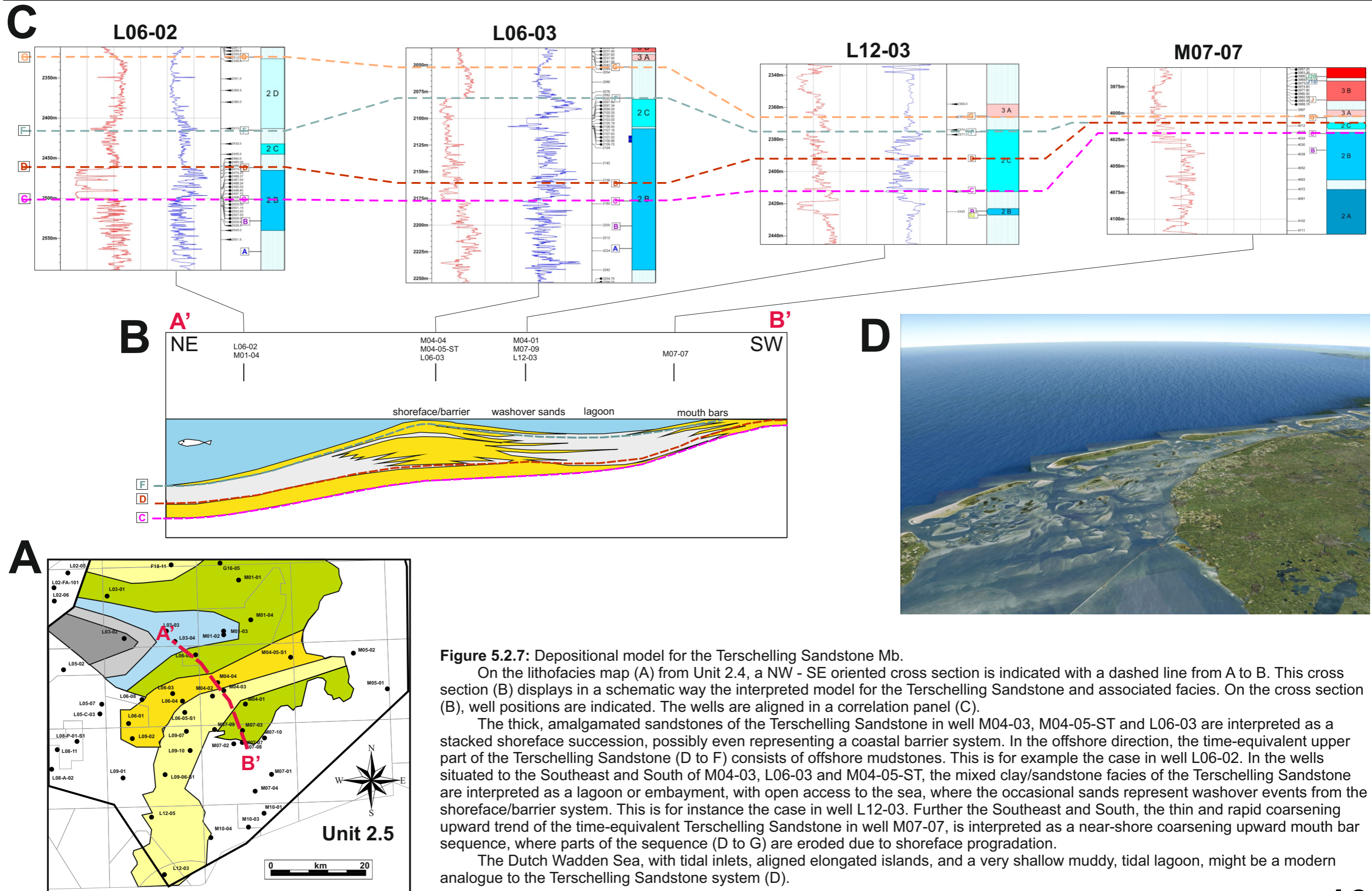
Unit 2.5

Figure 5.2.7: Depositional model for the Terschelling Sandstone Mb.

On the lithofacies map (A) from Unit 2.4, a NW - SE oriented cross section is indicated with a dashed line from A to B. This cross section (B) displays in a schematic way the interpreted model for the Terschelling Sandstone and associated facies. On the cross section (B), well positions are indicated. The wells are aligned in a correlation panel (C).

The thick, amalgamated sandstones of the Terschelling Sandstone in well M04-03, M04-05-ST and L06-03 are interpreted as a stacked shoreface succession, possibly even representing a coastal barrier system. In the offshore direction, the time-equivalent upper part of the Terschelling Sandstone (D to F) consists of offshore mudstones. This is for example the case in well L06-02. In the wells situated to the Southeast and South of M04-03, L06-03 and M04-05-ST, the mixed clay/sandstone facies of the Terschelling Sandstone are interpreted as a lagoon or embayment, with open access to the sea, where the occasional sands represent washover events from the shoreface/barrier system. This is for instance the case in well L12-03. Further the Southeast and South, the thin and rapid coarsening upward trend of the time-equivalent Terschelling Sandstone in well M07-07, is interpreted as a near-shore coarsening upward mouth bar sequence, where parts of the sequence (D to G) are eroded due to shoreface progradation.

The Dutch Wadden Sea, with tidal inlets, aligned elongated islands, and a very shallow muddy, tidal lagoon, might be a modern analogue to the Terschelling Sandstone system (D).
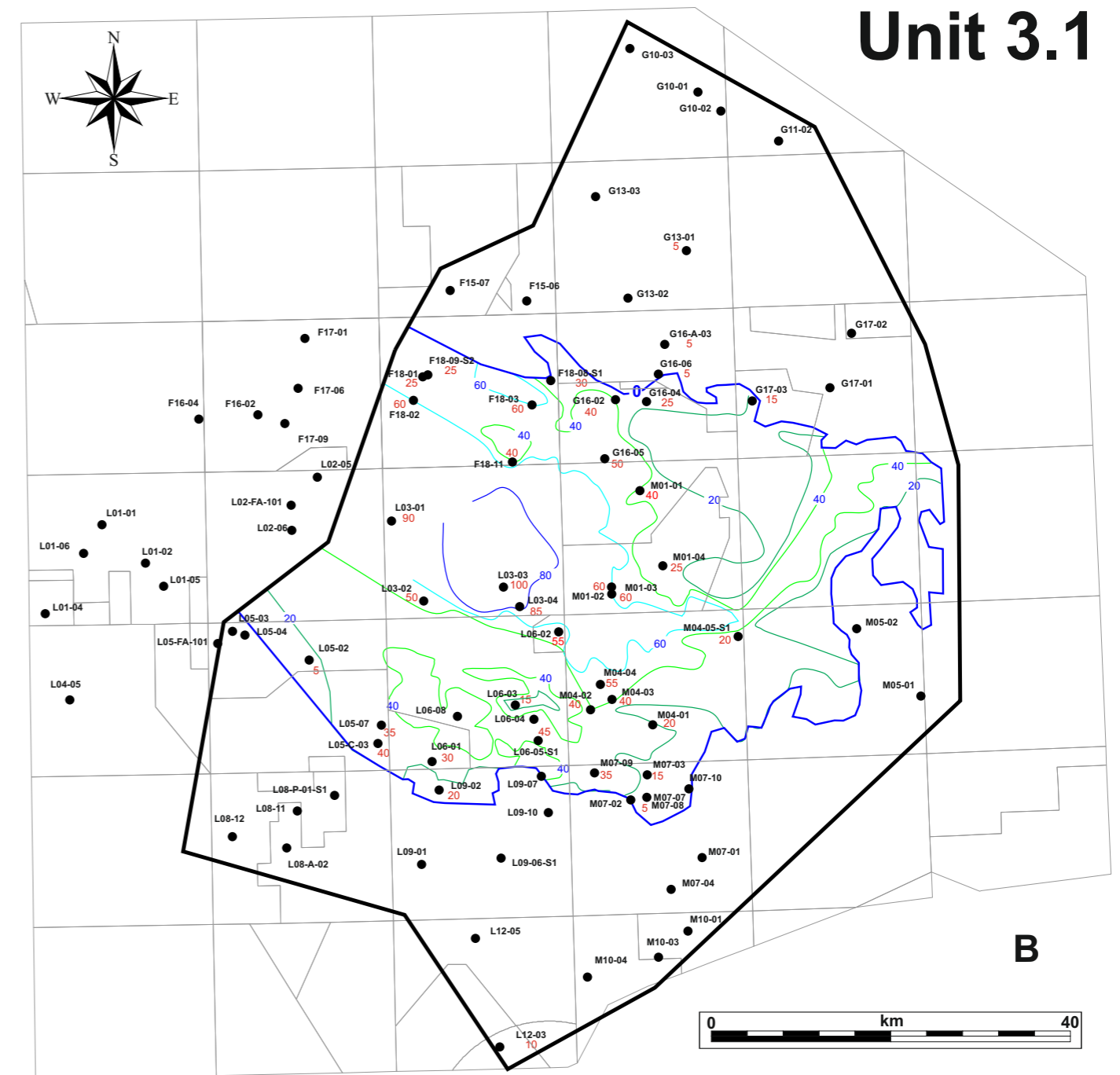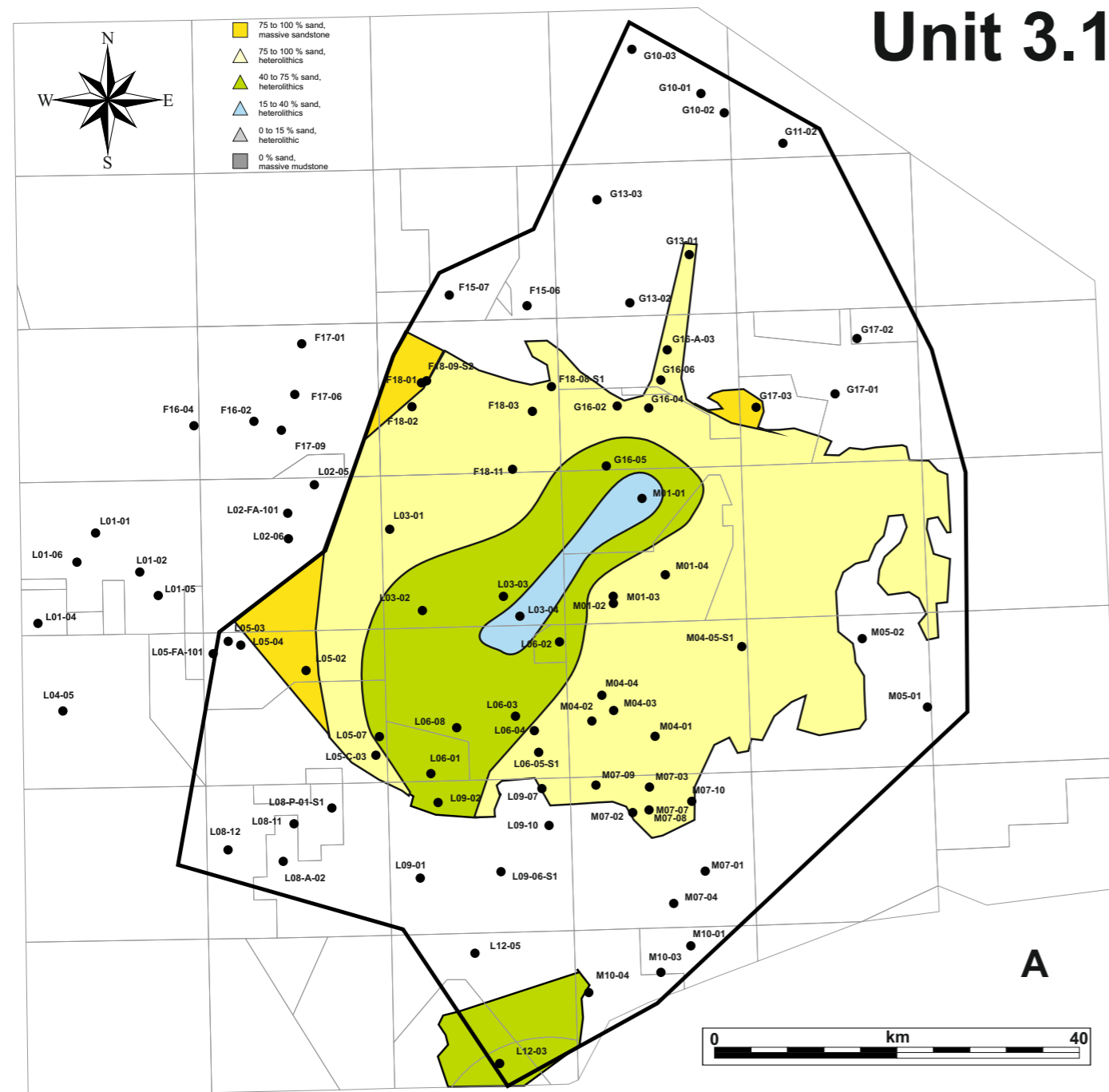
103

Figure 5.2.8: Lithofacies (A) and isopach map (B) of Unit 3.1

On the lithofacies map (A) of Unit 3.1, the yellow colours are back again. Apparently, the muddy phase of Unit 2.6 is succeeded by widespread sand deposition. Only in a narrow SE - NW strip from L03-04 to M01-01 muddy conditions prevail. The vast of sand deposition points to a tectonic origin for the sudden change in lithology. The GR and DT logs display a number of coarsening upward cycles (Panels H, I, J and K, section 4.3), that correlate very well across large distances. Nowhere in the TB clinoforms or any other evidence for prograding deltas are observed. A conspicuous change in the basin configuration is reflected in the isopach map (B).

The contour lines display an irregular pattern. Clearly, the depositional style of Unit 3.1 is aggradational, with sands brought into the basin by marine processes. At the same time, significant uplift occurs in the areas surrounding the TB, as is reflected in the presence of angular clasts in some of the marginal wells, such as M07-07 (Figure 4.1.6). Concomitant with the uplift in the Hinterland, a major transgression occurs, rendering the TB significantly larger than during deposition of Sequence 2 (both Maps A and B).

104
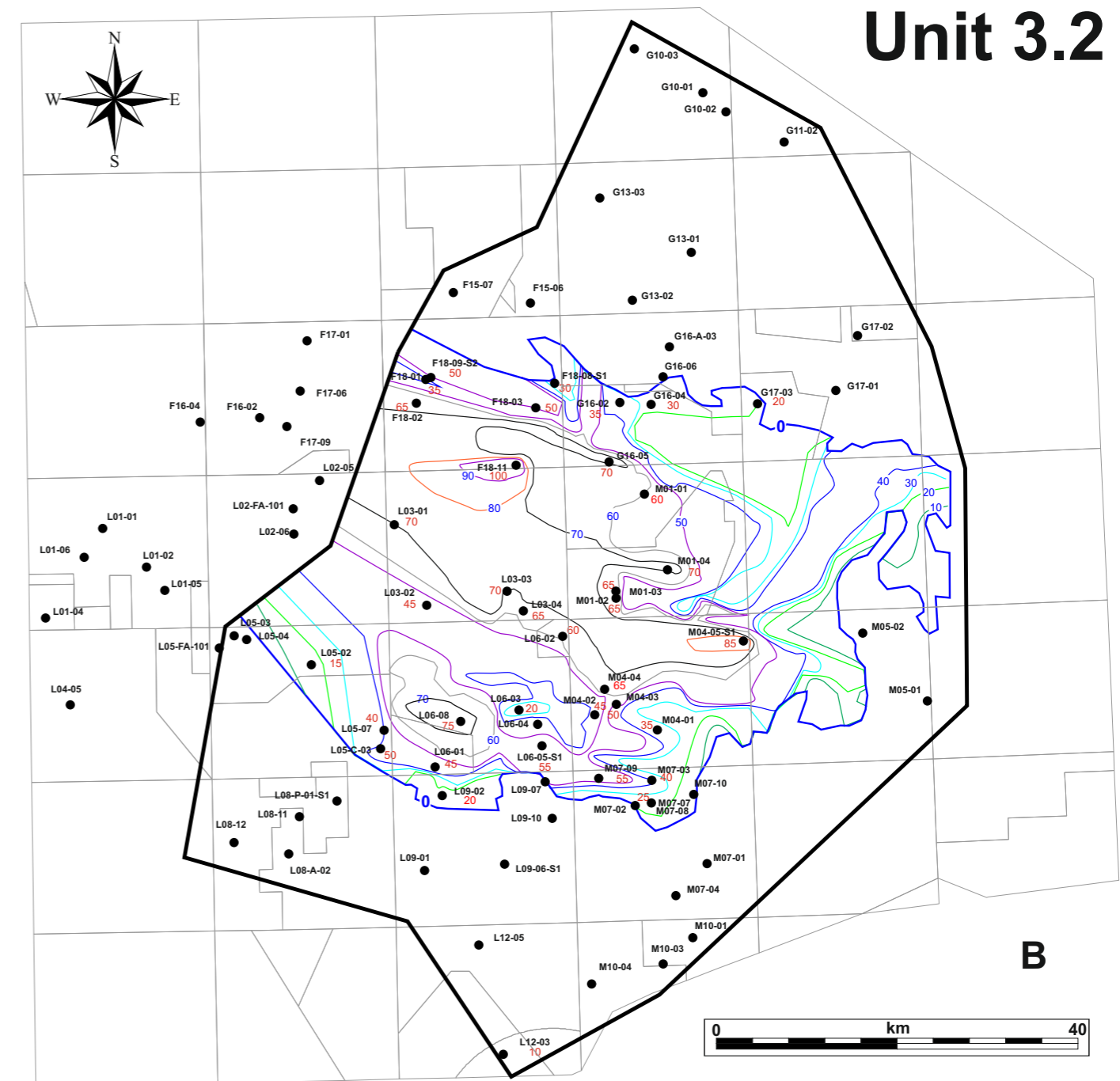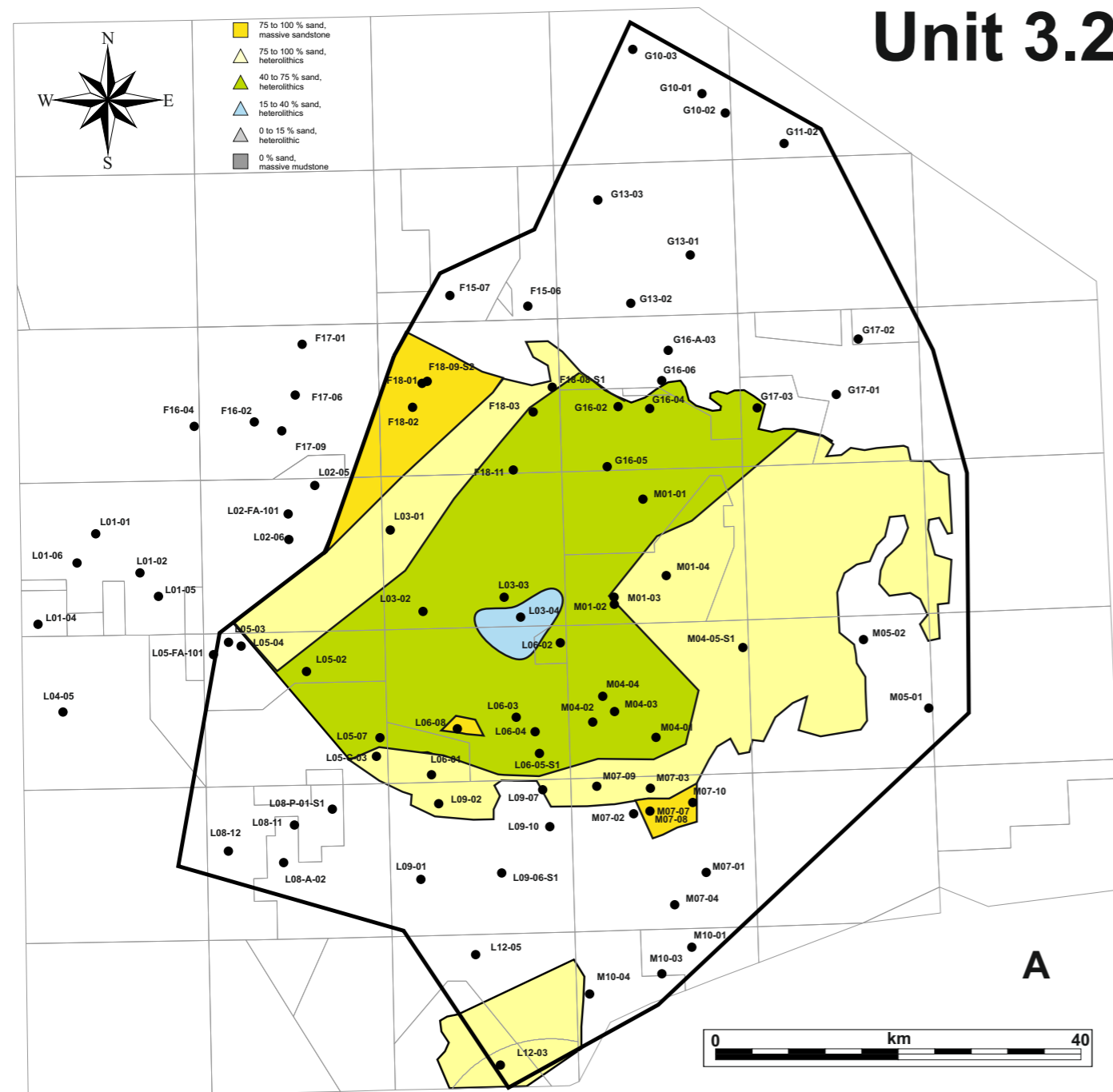
Figure 5.2.9: Lithofacies (A) and isopach map (B) of Unit 3.2

The decrease of yellow in the lithofacies map (A) reflects a lower net-to-gross than the previous Unit 3.1. In general, Unit 3.2 displays either no vertical grain size trend, or a very gradual fining upward (Panels I, J and K, section 4.3). The isopach map (B) displays a rather wild, rugose pattern. The strong variation in thickness across short distances, indicates a lot of vertical

movement within the basin. Especially salt structures are active during deposition of Unit 3.2. An example of an active salt structure is the WNW - ESE trending salt wall Sb3, near wells L06-03 and L06-04. On each side of the structure, rim synclines begin to start develop during this phase (Panel J, section 4.3).

105
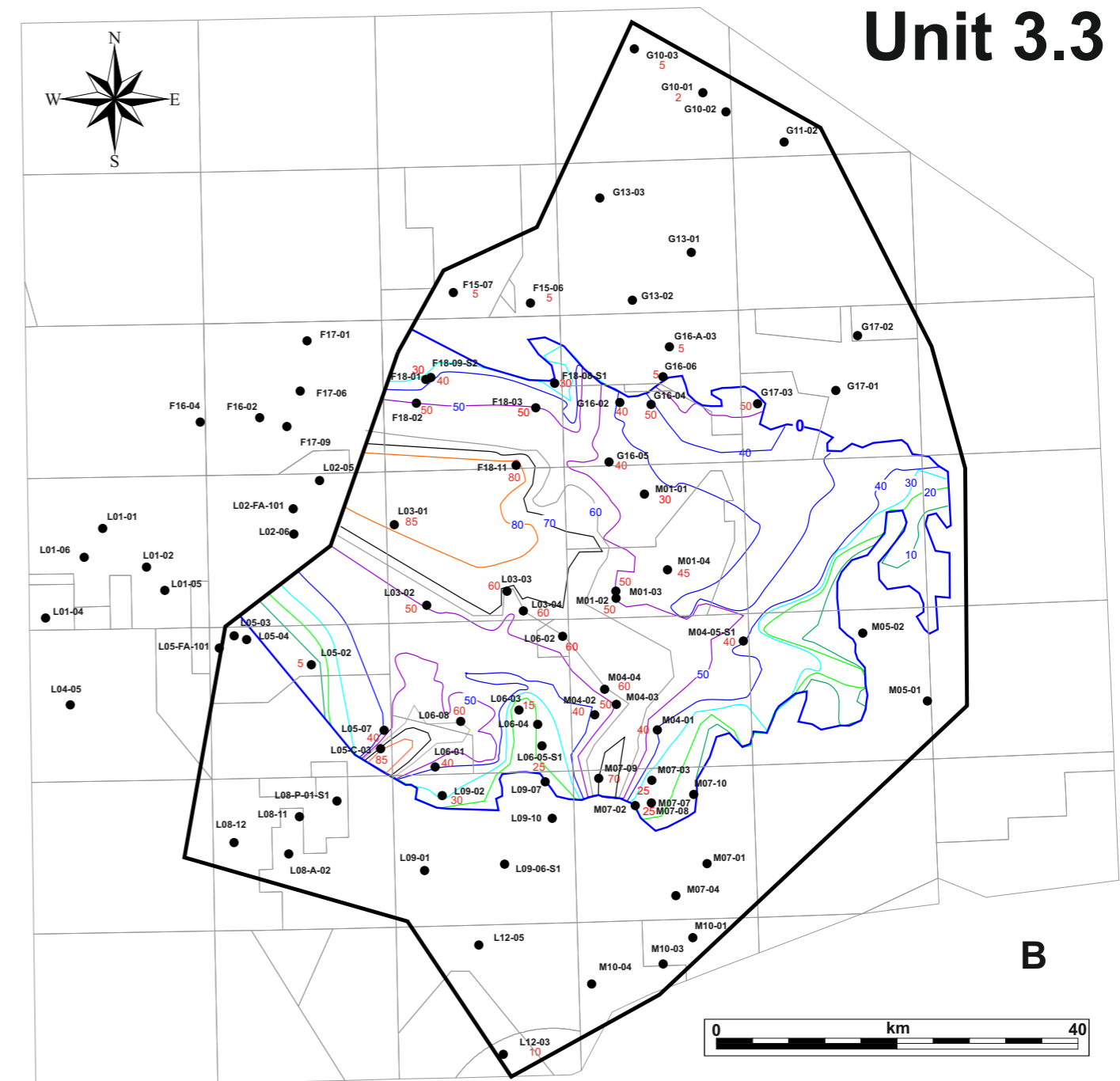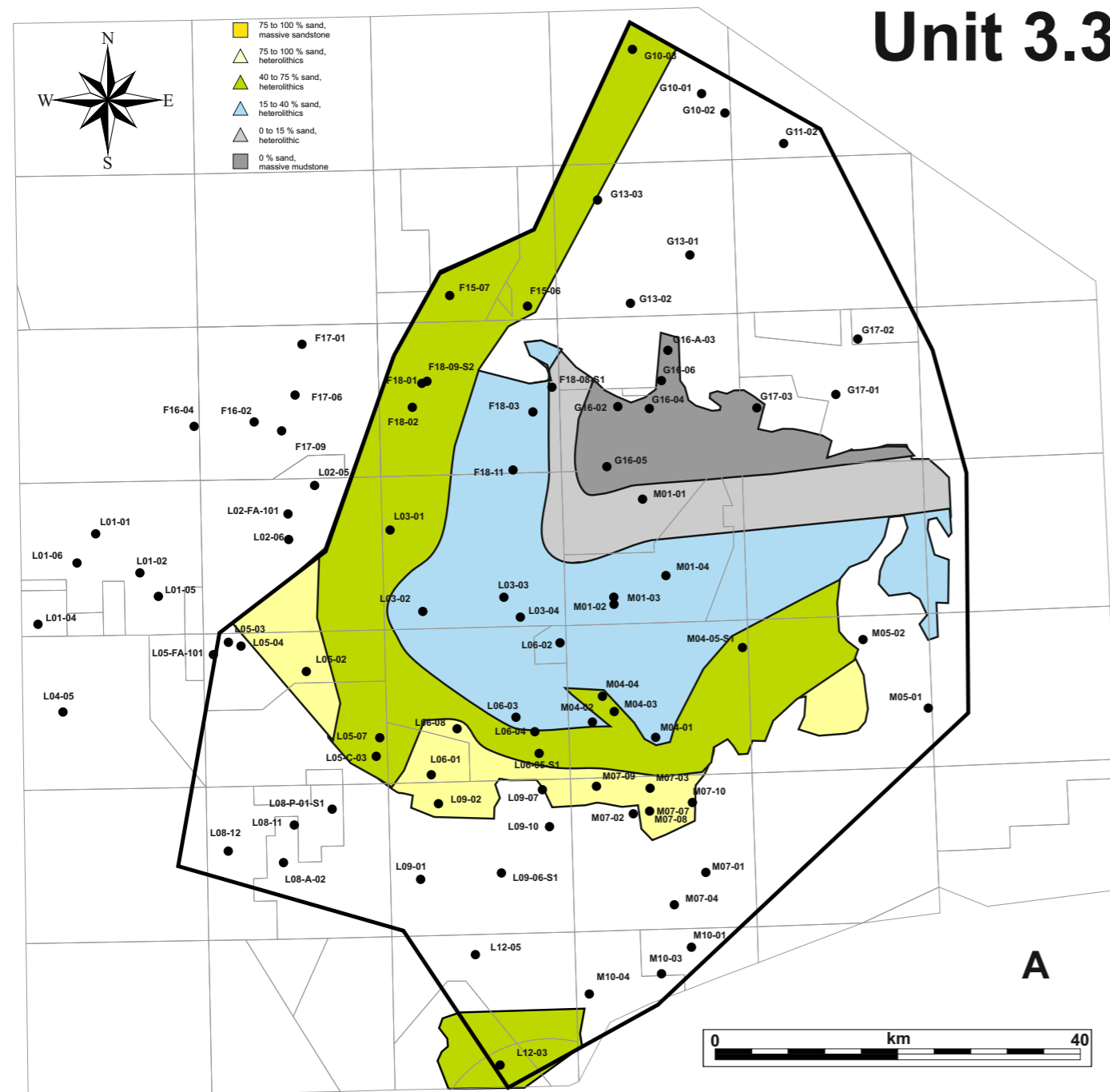
Figure 5.2.10: Lithofacies (A) and isopach map (B) of Unit 3.3

The lithofacies map (A) of Unit 3.3, displays a continuation of the development that set in during Unit 3.2. The basin becomes more and more mud dominated. In most places, a fining upward trend is evident. An exception to the rule is the southern margin of the basin. Here, sandstones dominate the successions (Panel K, section 4.3). It is obvious that the source for the sands of Unit 3.3 are coming from the SW, S and SE. Towards the NE, the net-to-gross decreases rapidly. The isopach map (B) is still rugose, with a more or less WNW - ESE oriented depocenter present near well L03-01. At the southern margin, the contour lines are closely spaced and oriented N - S. This probably indicates erosion and close proximity to the sediment sources.

106
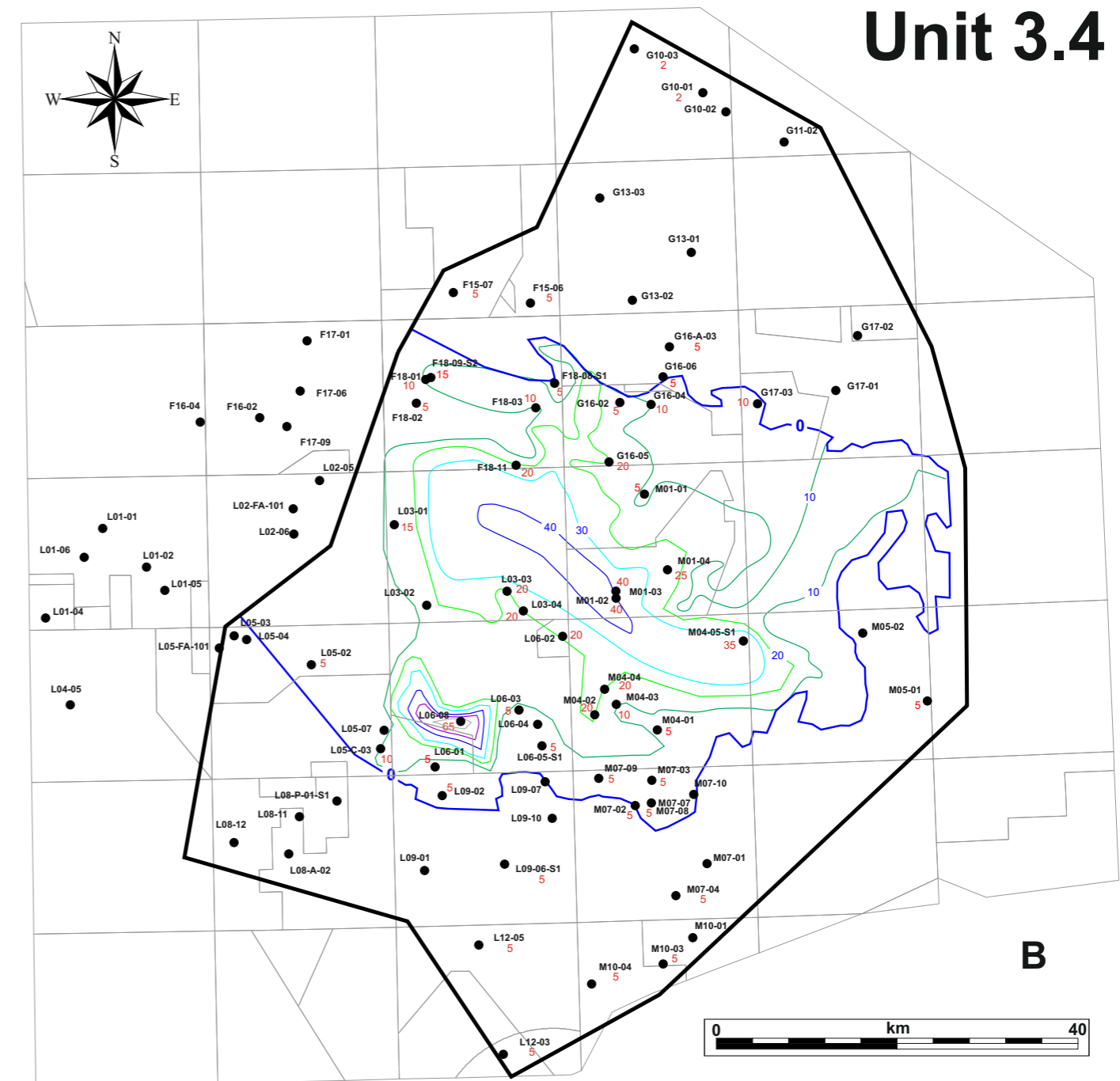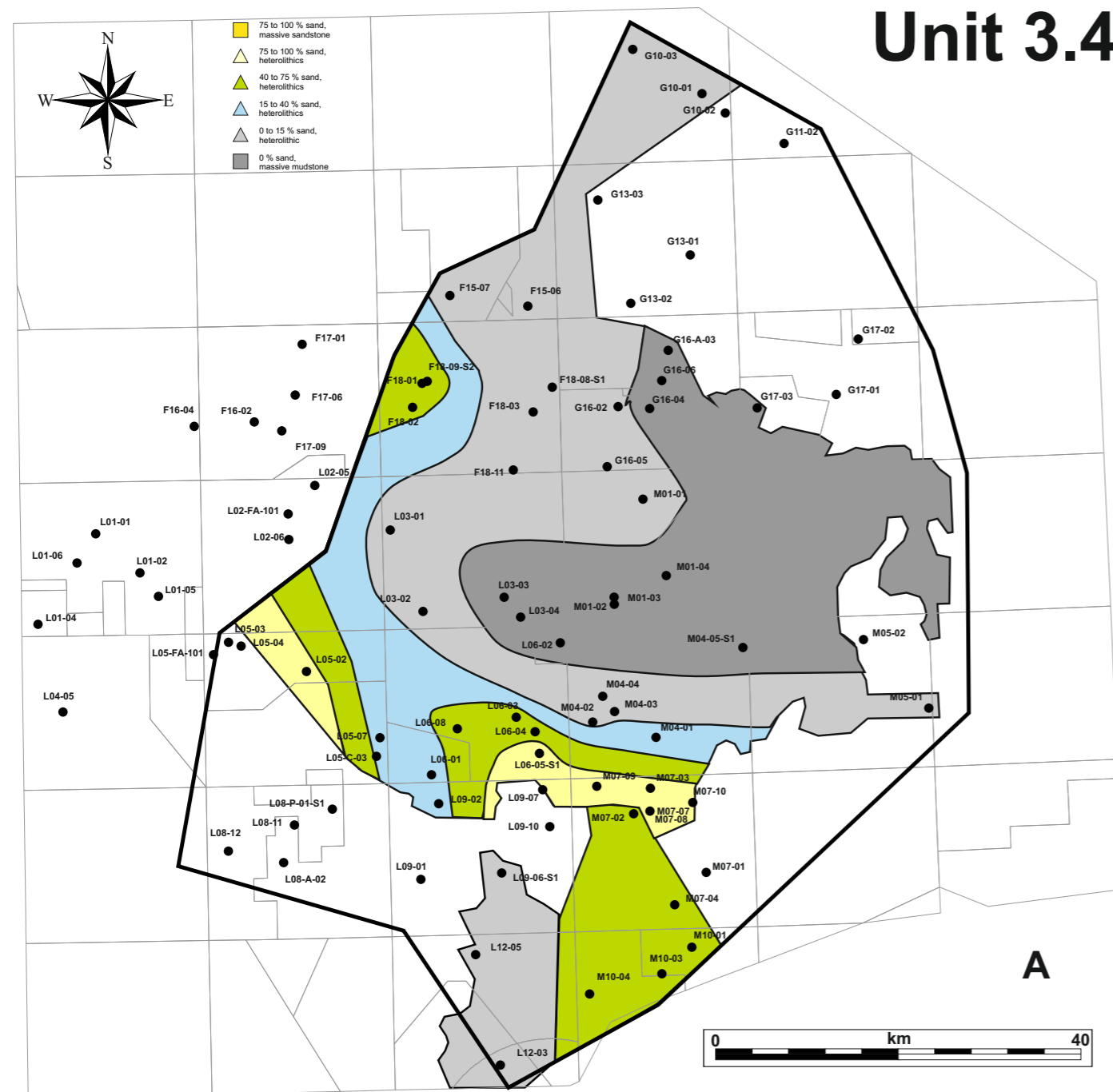
Figure 5.2.11: Lithofacies (A) and isopach map (B) of Unit 3.4

It is obvious from the grey colours on the lithofacies map (A) that Unit 3.4 is dominated by muddy sediments. The highest net-to-gross values are on the southern margin of the basin and decrease rapidly in a northeastern direction, towards Germany. The strong dominance of mud indicate high relative sea levels, pushing back the entry points for sediment far away from study area. Unit 3.4 marks the end of the Late Jurassic rift phase. The muddy sediments of the Schill Grund Mb of the Lutine Formation, are succeeded by the likewise muddy sediments of the Vlieland Shale Formation of the Rijnland Group (not part of this study).

In the area around M07-03 and M07-07, Unit 3.4 remains sandy throughout (Panel K, section 4.3). The sandy ENE - WSW "ridge" from L05-02 to M07-07 indicates that active erosion was still taking place in the vicinity of that area. Probably, small islands were sticking out in the surrounding sea. The basin configuration remains more or less disk shaped (Map B), except for the small mini-basin around L06-08, which is interpreted as fault related stratigraphic wedge (Figure 5.1.25).

107

The tectono-stratigraphy of the Upper Jurassic and lowermost Cretaceous of the TB is complex since it involves active tectonics during deposition that affect regional and local depositional systems in term of types, paleogeographic trends, thickness trends and preservation potential. This discussion focuses of the leassons learned from the basin margin and paleogeographic discussions (Sections 5.1 and 5.2) as well all the key results presented in this report (Chapter 4).

The structural context of the Terschelling Basin (TB) during the Upper Jurassic and Lowermost Cretaceous is of a extensional basin where active normal faulting and salt tectonics locally created high accommodation zones where over thickened sediments were deposited. Later, during the Cretaceous and Cenozoic, several zones were uplifted, especially in the surrounding platform areas, and vast amount of Upper Jurassic and Lowermost Cretaceous were eroded. Even in the TB itself, Upper Jurassic and Lowermost Cretaceous strata were locally eroded in the vicinity of reactivated salt bodies and faults.

The base Rijnland Group subcrop map (Fig. 4.2.7) shows that the TB is surrounded on three sides (north, east and south) by zones composed of older strata than the Jurassic basin fill. The platforms are composed of Permian (Zechstein), Triassic and Lower Jurassic (Altena Group). It is worth noticing that the subcrop interval surrounding the TB are older on the eastern side (mainly Zechstein and Lower Triassic) than on the western side (mainly Upper Triassic and Lower Jurassic).

Several key periods are discuss below to better understand the tectono-stratigraphic evolution of the TB.

A) Sequence 1

Sequence 1 is barely represented in the TB, only well M01-01 has sediments dated as being part of Sequence 1. On seismic (Panel H, Section 4.3) this interval attributed to Sequence 1 is geographically limited to the surrounding zone close to a salt diapir. The other areas where Sequence 1 has been observed in the documents presented in this report are located in the Dutch Central Graben (e.g. Panel H, Section 4.2).

The basin margin for S1 is shown on Figure 5.3.1. The limit between the DCG and the TB is largely defined by the presence of salt walls (Figures 5.3.2) that also seems to delimit the presence of Sequence 1. This can be interpreted in two ways, either (1) S1 was not deposited in the TB (except in small local zones such as around well M01-01, or (2) S1 was deposited in the TB but later eroded, leaving only small remnant such as the M01-01 area. The latter explanation is highly likely since the base of S2 is clearly erosive, cutting down into Lower Jurassic, Upper Triassic and even locally down to Lower Triassic strata.
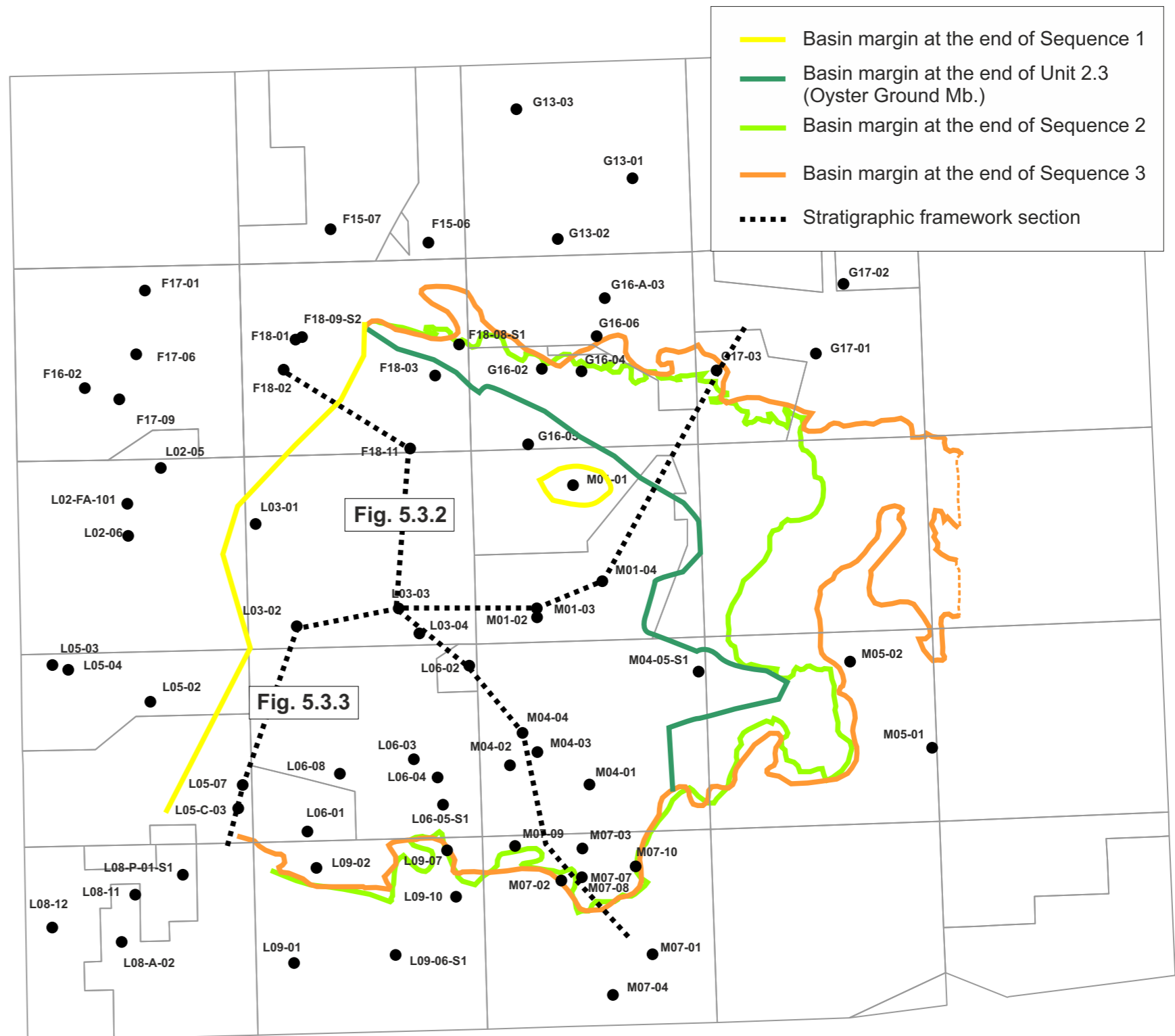

Figure 5.3.1: Basin margin trend map. The color lines are the basin margins for successive stratigraphic unitsocation of the stratigraphic framework sections. Black dashed lines show the position of the stratigraphic framework sections shown in Figures 5.2.2 ad 5.3.3.

B) Lower part of Sequence 2: Main Friese Front Mb and Oyster Ground Mb (Units 2.1, 2.2 and 2.3)

A major change in depositional environment occurred during the deposition of Sequence 2 from continental depositional environments of Unit 2.1 (Main Friese Front Mb) to marine environments at the base of Unit 2.2 (Oyster Ground Mb).

The basin margin at the end of Sequence 2 is displayed as a dark green line on Figure 5.3.1. It follows the boundary between Zone I and II on Figure 5.3.4. This basin margin is formed by a topographic step seen (see Panel I, Section 4.3, between well F18-11 and F18-03, or Panel B (Appendix A3)). Another step in the basin margin configuration is situated between F18-11 and G16-05, where Unit 2.1, going from F18-11 to G16-05, onlaps on the salt body (Panel H, section 4.3) or going from M01-04 to G17-03 (Panel J, section 4.3).

The main depocenter is located in the L03 Block during this period (Figure 5.3.2). Its origin is related to high accommodation related to salt withdrawal and syn-depositional faulting. NW/SE trending faults (such as F11 and F15 on Panel I, Section 4.3) were active during this period. It is important to notice that proportionally sandier sediments accumulated in the deepest parts of the basin (e.g at L03-01 on Panel I (section 4.3) and Figure 5.3.5)

Paleogeographic reliefs were also present within the basin itself, often due to salt bodies present close, or at, the depositional surface (e.g. salt bodies SB3 and SB4 (Panel J, section 4.3; see also Figure 5.3.5).

The paloeogeographic trends during this period are not clear. However, for the upper unit (Unit 2.3), we interpret the main source of sediments entering the basin as being located to the SW. This can be seen in well L05-C-03 that shows thick, amalgamated sandy sediments (Figure 5.3.6; Panel K in section 4.3; Figure 5.2.3) The lithological expression of the sands from Unit 2.3. in L05-C-03, differ from any other sands in the region during this period.

C) Upper part of Sequence 2: Terschelling Sandstone Mb, Noordvaarder Mb and Lies Mb (Units 2.4, 2.5 and 2.6)

This period is represented by a major sedimentary change in the TB with an overall coarsening of the sediments and the introduction of large volumes of sand from various sources around the basin (e.g. Figure 5.2.4). Two geographically different depositional systems were active simultaneously: in the South, the Terschelling Sandstone Mb and in the North, the Noordvaarder Mb. The sandy part of the two depositional systems geographically meet at the base of Unit 2.4 and towards the top of Unit 2.5, but the sandy part of the systems are mostly geographically separated by low net-to-gross basin axis strata (Lies Mb, see M01-02 on Panel J, sSction 4.3)

Three stratigraphic cycles are distinguished in this lower part of Sequence 2, with Units 2.4 and 2.5 being progradational and Unit 2.6 retrogradational (Fig. 5.3.5). The retrogradational trend of Unit 2.6 can be observed by comparing maps shown in Figure 5.2.4 and 5.2.5.

Depositionally, the southern (Terschelling Sandstone Mb) and northern (Noordvaader Mb) systems are different.

The Terschelling Sandstone Mb is a tidally-influenced shoreface depositional system (see core description of L06-02, FOCUS Project, Bouroullec et al., 2016). The coastline trajectory highlighted in Figures 5.2.4 to 5.2.6 is SW/NE to ENE/WSW. This is a very different trend than the one observed in the lower part of Sequence 2 which was NW/SE (Units 2.1 and 2.2, Figure

5.2.1 and 5.2.2). The complete onshore-offshore trend, including back-barrier lagoon, is displayed on Figure 5.2.7 as well as Figure 5.3.5.

The Noordvaarder is more difficult to characterize in term of depositional environment (no core information available in the TB). However, this interval has been interpreted as marine sand deposited in a relatively deep setting (> 20m water depth). Probably, tidal processes were involved to transport large volumes of sand into the deep environment, comparable to the present-day English Channel or Dutch near-shore setting. The source area of the Noordvaarder is postulated to be located to the North and Northwest of TB. Its initial depositional trend is curved during the deposition of the progradational units 2.4 and 2.5 (Figures 5.2.4 and 5.2.5) and becomes straight, in a ESE/WNW orientation, during the deposition of the retrograding Unit 2.6 (Figure 5.2.6). This can be interpreted as showing that the sedimentation is more point sourced during Units 2.4 and 2.5 and became more spread during Unit 2.6. The limited geographic extent of the Noordvaarder towards the south is due to the differential accommodation between the northern basin margin (F15 and F18 Blocks) and the southern axial zone in the L03 Block. The differential accommodation is related to salt withdrawal and fault activity that created the over thickening of Sequence 2 in the L03 Block (see Panel I, Section 4.3).

The depocenter during this period shifted from L03-03 and F18-01 area for Unit 2.4, to F18-11 for Unit 2.5 and then to L03-01- L03-03 area for Unit 2.6 (with up to 200 meters of sediment accumulating (Panel I, section 4.3; Figure 5.2.4 to 5.2.6). This indicate that the tectonic activity (rifting and salt tectonics) played a important role in the thickness trend of this lower part of Sequence 2. As an example, the northern basin margin is locally very steep such as between wells F18-08-S1 and F18-03 (Panel I, Section 4.3), or between wells M04-02 and L09-10 (Panel J, Section 4.3). Zone III (Figure 5.3.4) is also heavily affected by syn-depositional faulting during this period (Panel K, Section 4.3; Panel B, Appendix A3).

D) Sequence 3: Scruff Greensand Fm and Schill Grund Mb (Units 3.1 to 3.4)

Overall the lower two units of S3 are sandier than the upper two units (Figure 5.3.6 and Panel J, Section 4.3).The basin expanded eastward during Sequence 3 (Figures 5.3.1 and 5.3.2), with Zone V reflecting the basin expansion. Zone V is represented by a stratigraphically thick interval (Figure 5.3.3) related to salt migration as evidenced by shallow allochthonous salt bodies present in the southern part of Zone V.

During deposition of the lower two Units (3.1 and 3.2), the basin was confined, with the basin centre located around L03-04 and M01-01 (Figures 5.2.8 and 5.2.9). During the deposition of Unit 3.2 onward, the eustatic sea level increases leading to an overall deepening of the basin, as reflected in the retrogradational trend of the Scruff Greensand Fm (Figures 5.3.5 and 5.3.6). During deposition of the upper two units (3.3 and 3.4) the basin opened towards the NW (Figure 5.2.10 and 5.2.11). This variation from confined to unconfined basin geometry may partially explain the net-to-gross decrease throughout Sequence 3 with sand being trapped exclusively with the basin during for Units 2.1 and 3.2 (Figures 5.2.8 and 5.2.9), and being more regionally distributed along the paleocoastline for Units 3.3 and 3.4 (Figure 5.2.9 and 5.2.10).

The isopach maps (Figures 5.2.8 to 11) display very rugose thickness patterns. These are related to: (1) the presence of paleotopographic features at the base of Sequence 3 (see well M04-05-S1 and G16-04 on Panel K, Section 4.3;Figure 5.1.22). These features locally create confinement, hence the possibility of higher net-to-gross accumulations in those zones (e.g. Zone V in Figure 5.3.4, and specifically in the northwestern corner of the M02 Block, Figure 5.1.16); (2) active faulting (Panel H, I and K, Section 4.3); and 3) active salt structures (Panel J, between M04-02 and L09-10, Panel K, East of L04-02 and West of L05-07, Section 4.3).
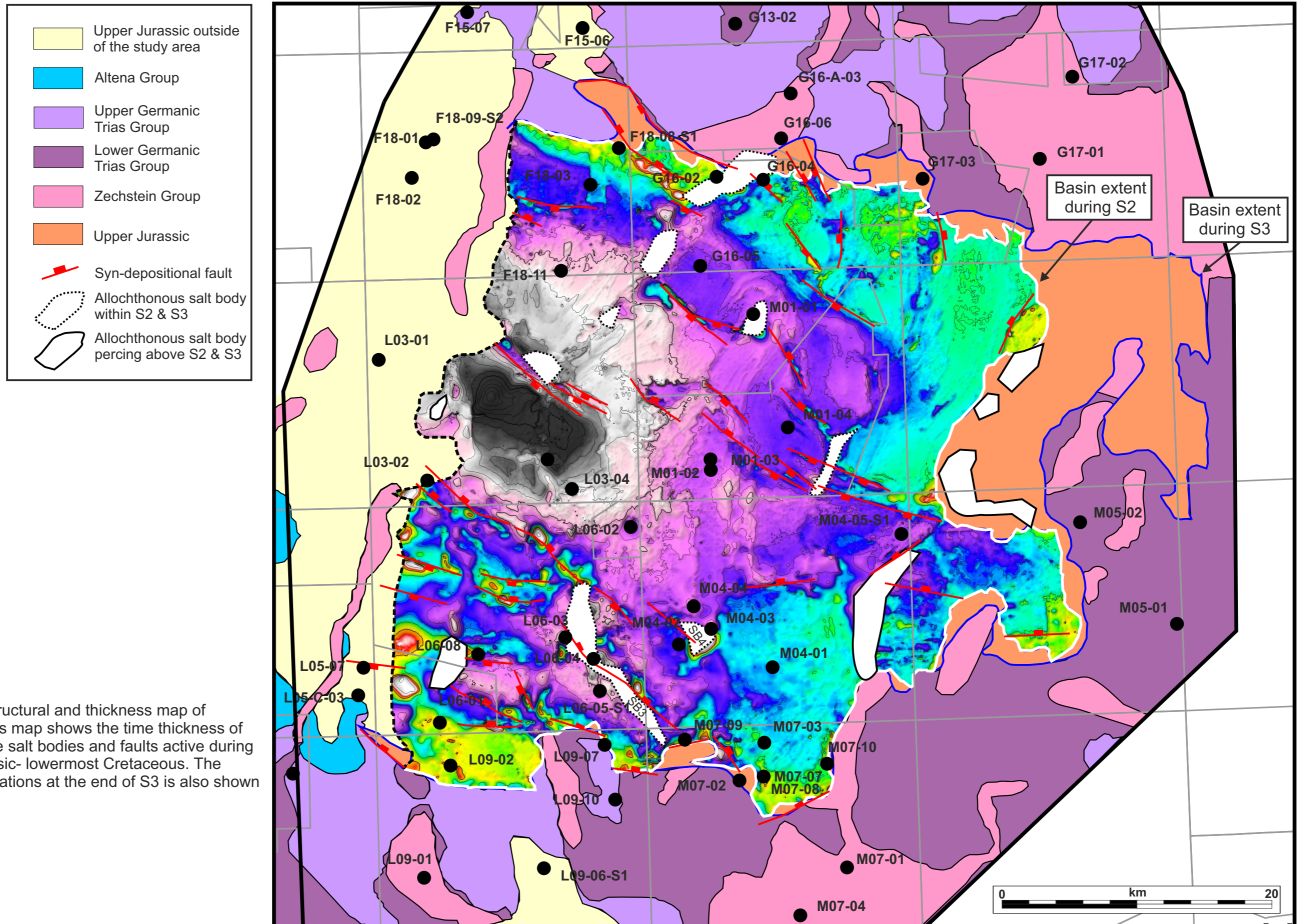
Figure 5.3.2: Structural and thickness map of Sequence 2. This map shows the time thickness of S2 as well as the salt bodies and faults active during the Upper Jurassic- lowermost Cretaceous. The basin margin locations at the end of S3 is also shown (blue line).
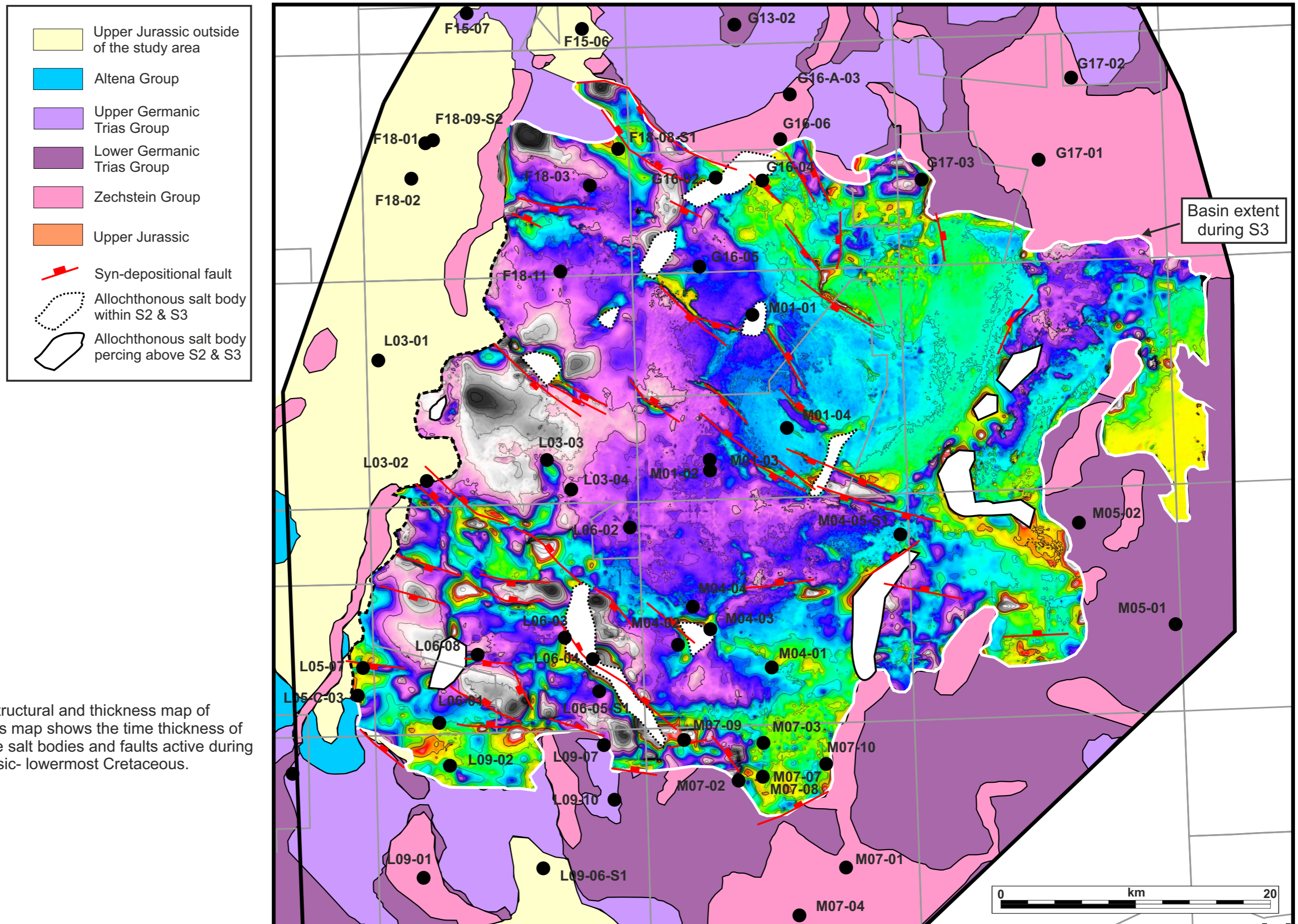
Figure 5.3.3.: Structural and thickness map of Sequence 3. This map shows the time thickness of S3 as well as the salt bodies and faults active during the Upper Jurassic- lowermost Cretaceous.
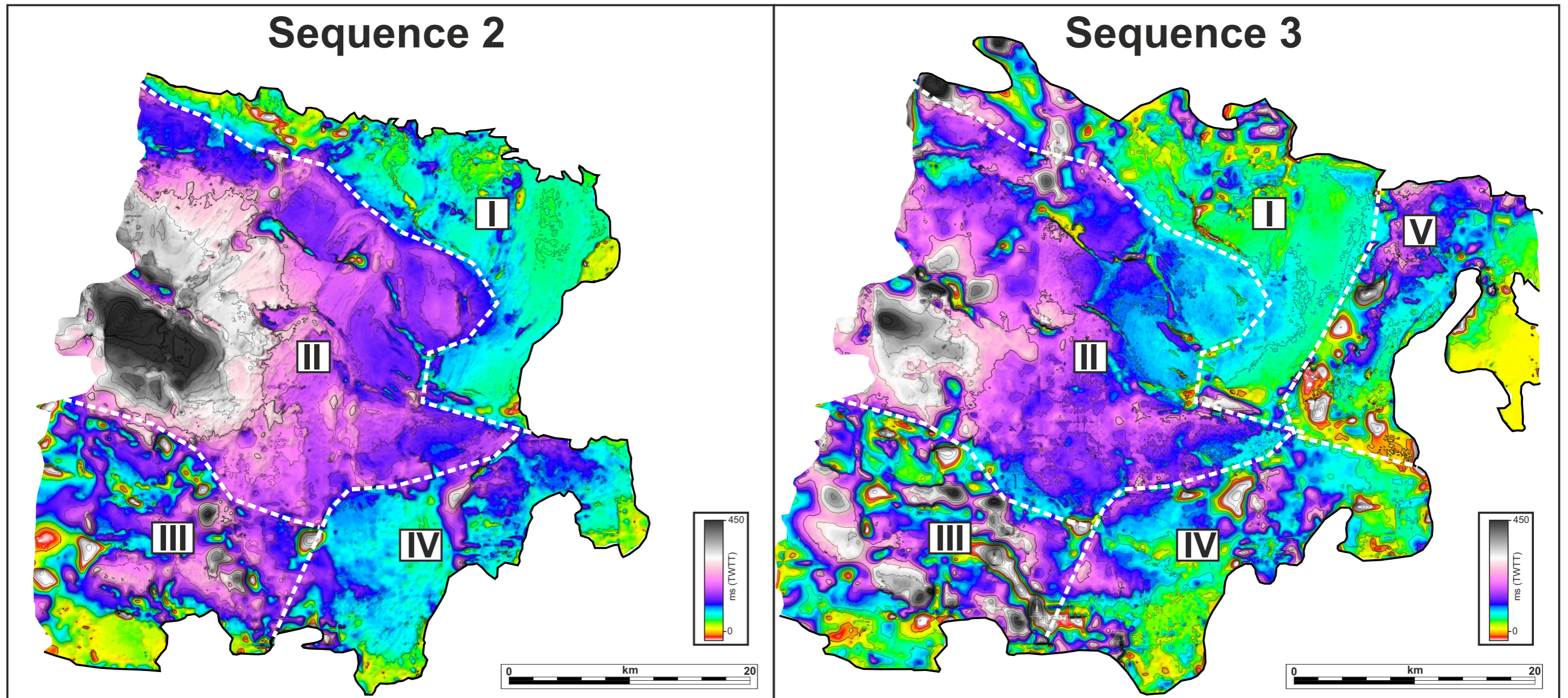
Figure 5.3.4: Time thickness maps of Sequences 2 and 3 in the Terschelling Basin. Sub-zones I to V referred in the text are shown.
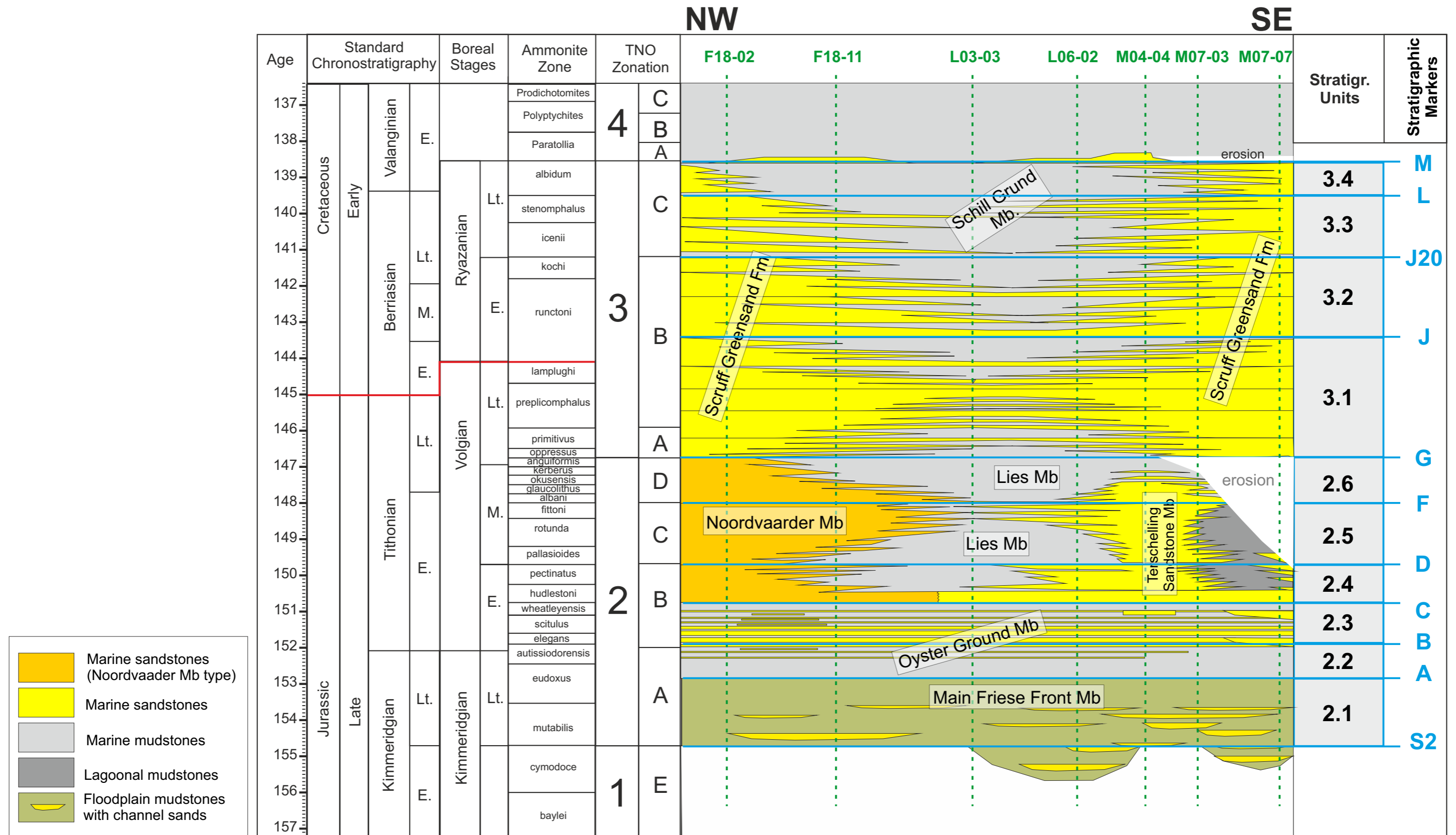
Figure 5.3.5: NW/SE oriented stratigraphic framework of the Terschelling Basin. See text for comments,
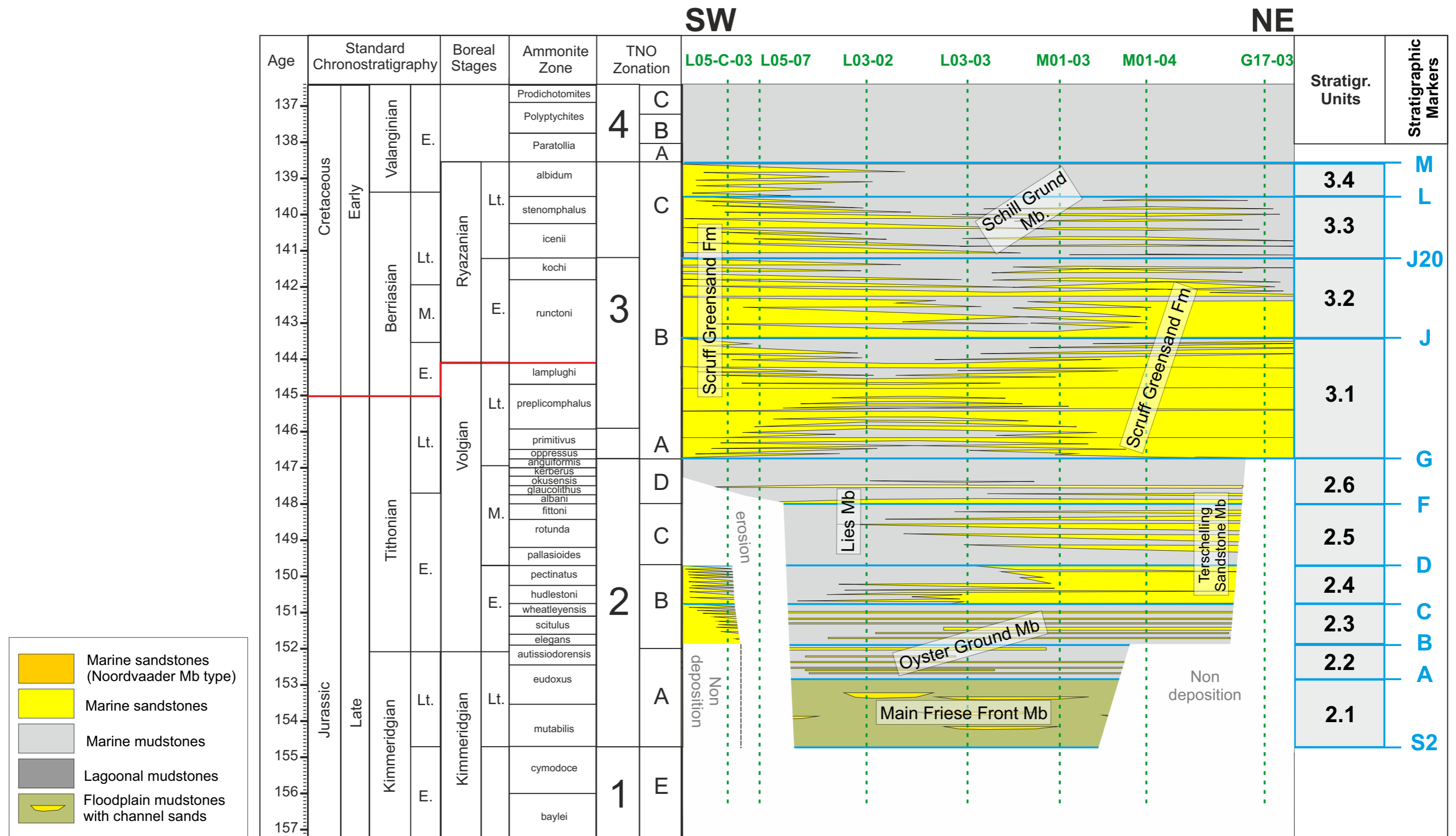
Figure 5.3.6: SW/NE oriented stratigraphic framework of the Terschelling Basin. See text for comments,

CONCLUSION &
REFERENCES

For the first time, the relationship between salt tectonics and sedimentation is investigated in the Terschelling Basin. Throughout the entire Late Jurassic rift phase, the depocenter remains broadly fixed around the L03 Block due to salt withdrawal and sediment loading.

The structural grain of the Late Jurassic Terschelling Basin is demonstrated to be NW – SE. This is observed in the syn-depositional fault trend as well as in the time thickness maps and the isopach maps.

The basin expanded toward the east and northeast throughout the deposition of Upper Jurassic-lowermost Cretaceous. This can be seen by the increase of the depositional area as well as the stepped geometry at the base of the Upper Jurassic.

The basin margins of the Terschelling Basin are classified into five types: (1) high angle against salt, (2) Conduit, (3) fault wedge, (4) rim syncline and (5) thinning. The thinning configurations is the most common but the proportion of actively deformed basin margin increases from S2 to S3.

Sequence 2:

During the deposition of Sequence 2 two sediment sources are identified during the Early and Middle Volgian (151 to 147 Ma). The Noordvaarder Mb in the northwestern part of the Terschelling Basin and the Terschelling Sandstone Mb in the southern part of the basin. The timing of initial sand deposition of the Noordvaarder and the Terschelling Sandstone Members are synchronous. Sequence 2 was deposited during a period of intense rifting with most platforms being zones of sediment transfer rather than deposition.

- The Noordvaarder Mb is interpreted as a tidally influenced sandy offshore system with the locus of deposition in the F18 and F15 blocks.
- The Terschelling Sandstone Mb is interpreted as a costal barrier system with associated lagoons. This depositional system trends SW-NE from blocks L05/09 to M01/M04/G17.

Sequence 3:

During the deposition of Scruff Greensand Formation the study area was subjected to two tectono-stratigraphic cycles, while the regional rifting came to an end.

- During the deposition of the lower part of the Scruff Greensand Formation (Late Volgian to Early Ryazanian, 147 to 141,5 Ma), the basin was confined and sand was entering the basin from multiple locations. This setting is interpreted as being related to syn-depositional deformation along the basin margins and on the surrounding platforms, that led to substantial erosion and increased sediment supply.
- During the deposition of the upper part of the Scruff Greensand Formation (Late Ryazanian, 141,5 to 138,5 Ma), the basin opened to the NE and sand accumulated along a curved coastline oriented N-S, in the north, to E-W, in the south. Syn-depositional structures (salt and faults) still locally affected the basin during this period, with local erosion on the platforms and topographic highs within the basin.

References

Abbink, O.A., 1998, Palynological investigations in the Jurassic of the North Sea region. LPP Contribution Series, 8: 192 pp.

Abbink, O.A., Mijnlieff, H.F., Munsterman, D.K. and Verreussel, R.M.C.H., 2006, New stratigraphic insights in the "Late Jurassic" of the southern central North Sea Graben and Terschelling Basin (Dutch offshore) and related exploration potential. Netherlands Journal of Geosciences – Geologie en Mijnbouw 85(3): p. 221-238.

Bouroullec. R., Verreussel, R., Geel, K., Munsterman, D., de Bruin, G., Zijp, M., Janssen, M., Millan, I., and Boxerm, T., 2016, The FOCUS Project: Upper Jurassic sandstones: Detailed sedimentary facies analysis, correlation and stratigraphic architecture of hydrocarbon bearing shoreface complexes in the Dutch offshore. TNO Report.

Bouroullec, R., Tomasso, m and Pyles, D., in press, Tectono-stratigraphy of a deepwater inter-basinal conduits, the Grand Coyer sub-basin, Annot Basin, SE French Alps, AAPG.

Bouroullec, R, Cartwright J. A., Johnson, H. D., Lansigu, C., Quemener J-M. and Savanier D., 2004, Syndepositional faulting in the Grès d'Annot Formation, SE France. High-resolution kinematic analysis and stratigraphic response to growth faulting. In Joseph, P. and Lomas. S. A. (eds). Deep-Water Sedimentation in the Alpine Basin of SE France: New perspectives on the Grès d'Annot and related systems. Geol. Soc., London, Special Publ., 221, pp. 241-265.

Bucefalo Palliani, R.B., Mattioli, E. and Riding, J.B., 2002, The response of marine phytoplankton and sedimentary organic matter to the early Toarcian (Lower Jurassic) oceanic anoxic event in northern England. Mar Micropaleontol 46: p. 223–245.

Bucefalo Palliani, R. and Riding, J.B., 2000, A palynological investigation of the Lower and lowermost Middle Jurassic strata (Sinemurian to Aalenian) from North Yorkshire, UK. - Proceedings of the Yorkshire Geological Society, 53 (1): p. 1-16. Manchester.

Costa, L.I. and Davey, R.J., 1992, Dinoflagellate cysts of the Cretaceous System. In: Powell, A.J. (ed.), A Stratigraphic Index of Dinoflagellate Cysts: p. 99-154.

Coward, M.P., Dewey, J., Hempton, M. and Holroyd, J., 2003, Tectonic evolution. In: Evans, D.J., Graham, C., Armour, A. and Bathurst, P. (Eds): The Millenium Atlas: Petroleum Geology of the Central and Northern North Sea. The Geological Society (London), p. 17-33.

De Jager, J., 2007, Geological Development. In: Geology of the Netherlands, Eds Wong, Th., Batjes D.A.J. and De Jager, J. Publ. by the Royal Academy of Art and Sciences (KNAW). ISBN 978-90-6984-481-7.

De Jager, J., 2012, The discovery of the Fat Sand Play (Solling Formation, Triassic), Northern Dutch offshore – a case of serendipity. Netherlands Journal of Geosciences, v. 91, Is. 04, pp 609-619.

Davey, R.J., 1979, The stratigraphic distribiution of dinocysts in the Portlandian (latest Jurassic) to Barremian (Early Cretaceous) of northwest Europe. – AASP Contributions Series, 5B: 48-81. Dallas, Texas.

Davey, R.J., 1982, Dinocyst stratigraphy of the latest Jurassic to Early Cretaceous of the Haldager No. 1 borehole, Denmark. Geol. Surv. Denm. Ser. B, 6: 58pp.

De Jager, J., 2007, Geological development. In: Wong, T.E., Batjes, D.A.J. and De Jager, J. (Eds): Geology of the Netherlands. Royal Netherlands Academy of Arts and Sciences (Amsterdam): p. 5-26.

Doornenbal, H. and Stevenson, A, 2010, Petroleum geological atlas of the Southern Permian Basin area. EAGE, 342 pp.

Duin E.J.T., Doornenbal, J.C., Rijkers, R.H.B. Verbeek, J.W. and Wong, Th,E., 2006, Subsurface structure of the Netherlands - Results of recent onshore and offshore mapping, Netherlands Jopurnal of Geosciences - Geologie en Mijnbouw, 85, 4, pp. 245-276.

Duxbury, S., Kadolsky, D. and Johansen, S., 1999, Sequence stratigraphic subdivision for the Humber Group in the Outer Moray Firth area (UKCS, North Sea). In: Jones, R.W. and Simmons, M.D. (eds) Biostratigraphy in Production and Development Geology. Geol. Soc. Spec. Pub., 152: p. 23-54.

Geluk, M.C., 2005, Stratigraphy and tectonics of Permo-Triassic basins in the Netherland and surrounding areas. Thesis. Utrecht University (Utrecht): 171 pp.

Geluk, M.C., 2007, Triassic. In: Wong, T.E., Batjes, D.A.J. and de Jager, J. (Eds): Geology of the Netherlands. Royal Netherlands Academy of Arts and Sciences (Amsterdam): p. 85-106.

George, G.T. and Berry, J.K., 1993, A new lithostratigraphy and depositional model for the Upper Rotliegend of the UK sector of the southern North Sea. In: North, C.P. and Prosser, D.J. (Eds): Characterization of Fluvial and Aeolian Reservoirs. Geological Society Special Publication (London) 73: p. 291-319.

George, G.T. and Berry, J.K., 1997, Permian (Upper Rotliegend) synsedimentary tectonics, basin development and palaeogeography of the southern North Sea. In: Ziegler, K., Turner, P. and Daines, S.R. (Eds): Petroleum Geology of the Southern North Sea: Future Potential. Geological Society Special Publication (London) 123: p. 31-61.

Glennie, K.W. (Ed), 1998, Petroleum Geology of the North Sea, Basic concepts and recent advances. Blackwell (Oxford): 636 pp.

Gradstein, F.M., Ogg, J.G., Schmitz, M.D. and Ogg, G.M., 2012. The geological time scale 2012, Volume 2, 1144 pp.

Heilmann-Clausen, C., 1987, Lower Cretaceous dinoflagellate biostratigraphy in the Danish Central Trough. Danmarks Geol. Unders. Ser. A (17): p. 1-90.

Herngreen, G.F.W., Kerstholt, S.J. and Munsterman, D.K., 2000, Callovian - Ryazanian ('Upper Jurassic') palynostratigraphy of the Central North Sea Graben and Vlieland Basin, The Netherlands. Mededelingen Nederlands Instituut voor Toegepaste Geowetenschappen TNO, 63: 99 pp.

Heybroek, P., 1975, On the structure of the Dutch part of the Central North Sea Graben. In: Woodland, A.W. (Ed.): Petroleum and the Continental Shelf of North-West Europe. Applied Science Publishers Ltd (London): p. 339-349.

Hoffmann, N. and Stiewe, H., 1994, Neuerkenntnisse zur geologisch-geophysikalischen Modellierung der Pritzwalker Anomalie im Bereich des Ostelbischen Massivs. Zeitschrift geologischer Wissenschaften 22: p. 161-171.

Herngreen, G.F.W. and Wong, T.E., 1989, Revision of the Late Jurassic stratigraphy of the Dutch Central North Sea Graben. Geologie en Mijnbouw 68: p. 73-105.

Joseph, P. and Lomas, S. A., 2004, Deep-water sedimentation in the alpine foreland basin of SE France: New perspectives on the Grès d'Annot and the related systems – an introduction. In Joseph, P. and Lomas. S. A. (eds). Deep-Water Sedimentation in the Alpine Basin of SE France: New perspectives on the Grès d'Annot and related systems. Geol. Soc., London, Special Publ., 221, pp. 1-16.

Kley, J. & Voigt, T., 2008, Late Cretaceous intraplate thrusting in central Europe: Effect of Africa-Europe-Iberia convergence, not Alpine collision. Geology 36: p. 839-842.

Koppelhus, E.B. and Nielsen, L.H., 1994, Palynostratigraphy and palaeoenvironments of the Lower to Middle Jurassic Bagå Formation of Bornhorm, Denmark. Palynology, v.18, p.139-194, pl.1-5.

Krzywiec, P., 2004, Triassic evolution of the Kłodawa salt structure: basement-controlled salt tectonics within the Mid-Polish Trough (central Poland). Geological Quarterly 48 (2): p.123-134.

Lott, G.K., Wong, T.E., Dusar, M., Andsbjerg, J., Mönnig, E., Feldman-Olszewska, A. and Verreussel, R.M.C.H., 2010. Jurassic. In: Doornenbal, J.C. and Stevenson, A.G. (editors): Petroleum Geological Atlas of the Southern Permian Basin Area. EAGE Publications b.v. (Houten): p. 175-193.

References

Munsterman, D.K., Verreussel, R.M.C.H., Mijnlieff, H.F., Witmans, N., Kerstholt-Boegehold, S. and Abbink, O.A., 2012, Revision and update of the Callovian-Ryazanian Stratigraphic Nomenclature in the northern Dutch Offshore, i.e. Central Graben Subgroup and Scruff Group. Netherlands Journal of Geosciences-Geologie en Mijnbouw, 91 (4): p. 555-590.

Partington, M.A., Mitchener, B.C., Milton, N.J. and Fraser, A.J., 1993a, Genetic sequence stratigraphy for the North Sea Late Jurassic and Early Cretaceous: distribution and prediction of Kimmeridgian-Late Ryazanian reservoirs in the North Sea and adjacent areas. In: Parker, J.R. (ed.), Petroleum geology of northwest Europe: Proceedings of the 4th Conference, p. 347-370. London (Geological Society).

Partington, M.A., Copestake, P., Mitchener, B.C. and Underhill, .J.R., 1993b, Biostratigraphic calibration of genetic stratigraphic sequences in the Jurassic-lowermost Cretaceous (Hettangian to Ryazanian) of the North Sea and adjacent areas. In: Parker, J.R. (ed.), Petroleum geology of northwest Europe: Proceedings of the 4th Conference, p. 371-386. London (Geological Society).

Pharaoh, T. C., Dusar, M., Geluk M., Kockel F., KrawczykC., Krzywiec P., Scheck-Wenderoth, M., Thybo H., Vejbæk O. and van Wees, J. D., 2010, Tectonic evolution . in Doornenbal, H. and Stevenson, A. G, eds. Petroleum geological atlas of the Southern Permian Basin area. Houten, the Netherlands, EAGE, p. 25-57.

Pickering, K. T. and Hilton, V. C., 1998, Turbidite Systems of southeast France. Vallis press, 223 pages.

Powell, A.J., 1992, Dinoflagellate cysts of the Triassic system. In: Powell, A.J. (ed.), A Stratigraphic Index of Dinoflagellate Cysts: p. 1-6.

Remmelts, G., 1995, Fault-related salt tectonics in the southern North Sea, the Netherlands. In: Jackson, M.P.A., Roberts, D.G. and Snelson, S. (Eds): Salt tectonics: a global perspective. American Association of Petroleum Geologists Memoir 65: p. 261-272.

Riding, J.B. and Thomas, J.E., 1992, Dinoflagellate cysts of the Jurassic System. In: Powell, A.J. (ed.), A Stratigraphic Index of Dinoflagellate Cysts: p. 7-98.

Riding, J.B., Fedorova, VA. and Ilyna, V.I., 1999, Jurassic and Lowermost Cretaceous dinoflagellate cyst biostratigraphy of the Russian Platform and Northern Siberia, Russia. AASP Contribution 36, p. 3-180.

R**avenne, C., Vially, R., Riché, P. and Trémolière P.,** 1987, Sédimentation et tectonique dans le bassin marin Eocène superieur - Oligocène des Alpes du Sud. Revue de l'Institut Français du Pétrole., Vol. 42, 24 pages.

Roberts, A.M., Yielding, G., Kuznier, N.J., Walker, I.M. and Dorn-Lopez, D., 1995, Quantitative analysis of Triassic extension in the northern Viking Graben. Journal of the Geological Society 152: p. 15-27.

Rosendaal, E., Kaymakci, N., Wijker, D. and Schroot, B.M., 2014, Structural development of the Dutch Central Graben: new ideas from recent 3D seismic. Abstract, EAGE Meeting Amsterdam.

Schroot, B.M., 1991, Structural development of the Dutch Central Graben. In: Michelsen, O. and Frandsen, F. (Eds): The Jurassic in the Southern Central Trough. Danmarks Geologiske Undersøgelse series B 16: p. 32-35.

Sinclair, H. D. and Tomasso, M., 2002, Depositional evolution of confined turbidite basins. Journal of sedimentary research, vol72, iss 4, pp 451-456.

Surlyk, F. and Ineson, J.R., 2003, The Jurassic of Denmark and Greenland: key elements in the reconstruction of the North Atlantic Jurassic rift system. In: Ineson, J.R. and Surlyk, F. (Eds): The Jurassic of Denmark and Greenland. Geological Survey of Denmark and Greenland Bulletin 1: 9-20.

T**orsvik, T.H., Carlos, D., Mosar, J., Cocks, L.R.M. and Malme, T.N.M.,** 2002, Global reconstructions and North Atlantic paleogeography 440 Ma to recent. In: Eide, E.A. (Ed.): Batlas – Mid Norway plate reconstruction atlas with global and Atlantic perspectives. Geological Survey of Norway (Trondheim): p. 18-39.

Underhill, J.R. and Partington, M.A., 1993, Jurassic thermal doming and deflation in the North Sea: implications of the sequence stratigraphic evidence. In: Parker, J.R. (Ed.): Petroleum Geology of Northwest Europe: Proceedings of the 4th Conference. The Geological Society (London): p. 37-345.

Van den Haute, P. and Vercoutere, C., 1990, Apatite fission track evidence for a Mesozoic uplift of the Brabant Massif – preliminary results. Annales Société Géologique de Belgique 112: p. 443-452.

Van Hoorn, B., 1987, Structural evolution, timing and tectonic style of the Sole Pit inversion. Tectonophysics 137: p. 239-284.

Van Adrichem Boogaert, H.A. & Kouwe, W.F.P., 1997, Stratigraphic nomenclature of the Netherlands, revision and update by RGD and NOGEPA. Mededelingen Rijks Geologische Dienst, nieuwe serie, vol. 50, section a - j.

Veiweij J. M., and Witmans, N, 2009, Terschelling Basin and southern Dutch Central Graben mapping and modeling - Area 2A, TNO report, TNO-034-UT-2009-01569

Verreussel, R.M.C.H., Dybkjaer, K., Johannessen, P.N., Munsterman, D.K., Ten Veen, J.H. and Van de Weerd, A., in prep., Late Jurassic basin evolution of the Central Graben area from Denmark and the Netherlands.

Wong, T.E., 2007. Jurassic. In: Wong, T.E., Batjes, D.A.J. and de Jager, J. (Eds): Geology of the Netherlands. Royal Netherlands Academy of Arts and Sciences (Amsterdam): p. 107-126.

Wong, T.E., Batjes, D.A.J. and De Jager, J. (Eds), 2007, Geology of the Netherlands. Royal Netherlands Academy of Arts and Sciences (Amsterdam): 354 pp.

Ziegler, P.A., 1988, Evolution of the Arctic, North Atlantic and western Tethys. American Association of Petroleum Geologists: 198 pp.

Ziegler, P.A., 1990a, Geological Atlas of Western and Central Europe (2nd edition). Shell Internationale Petroleum Maatschappij B.V.; Geological Society Publishing House (Bath): 239 pp.

Ziegler, P.A., 1990b, Tectonic and palaeogeographic development of the North Sea rift system. In: Blundell, D.J. and Gibbs, A.D. (Eds): Tectonic evolution of the North Sea rifts. Oxford Science Publications (Oxford): p. 1-36.